PHD

Fabrication of poly(vinylidene fluoride) hollow fibre membranes

Yeow, May Ling

Award date:
2004

Awarding institution:
University of Bath

FABRICATION OF POLY(VINYLIDENE FLUORIDE) HOLLOW FIBRE MEMBRANES

Submitted by

May Ling Yeow

For the Degree of PhD of the University of Bath

2004

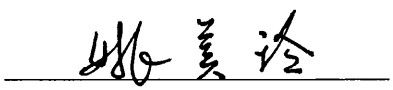

ProQuest LLC
789 East Eisenhower Parkway
P.O. Box 1346
Ann Arbor, MI 48106-1346

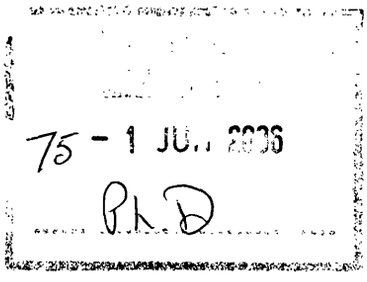
75 - 1 JU

ACKNOWLEDGEMENTS

First and foremost, I would like to express my utmost gratitude to the following parties, for their contribution towards the completion of this study:

- Dr. Kang Li and Prof. Frank C. Walsh for their guidance and advice;
- Dr. Xiao Yao Tan and Mr. Yu Tie Liu for the technical discussions;
- Mr. Hugh Parrot and Mrs. Ursula Potter for developing the SEM photos;
- Mrs. Sally Barker, Ms. Elaine Odgers, Miss Rebecca Norris and Miss Louise Hamblin for their administrative support;
- Mr. Mac Forsyth, Mr. John Bishop, Mr. Fernando Acosta, Mr. Merv Newves and Mr. Robert Brain for their technical support;
- Mr. Andrew Brown and Miss Wan Mahsuri Wan Hashim for their assistance in experimental data collection;
- Department of Chemical Engineering, University of Bath for the studentship award.

Thanks also go to Yuko Aoki, Suxia Liu, Alex Shirley, Brendan Darragh, Hwee Chuan Chua and especially to Bengu Bozkaya for their friendship and support.

My special appreciation is given to my family and Dr. Michael Postlethwaite for their everlasting support.

Finally, I dedicate this work to my grandmother and the memory of my grandfather.

ABSTRACT

The overall aim of this study was to investigate the fabrication of poly(vinylidene fluoride) hollow fibre membranes via phase inversion - immersion precipitation method; followed by the development of a composite hollow fibre membrane via a dip-coating method.

Cloud point technique was used to study the fundamental phase separation behaviour of multicomponent polymer solutions. Four solvents were studied: *N*,*N*- dimethylacetamide (DMAc), 1-methyl-2-pyrrolidone (NMP), *N*,*N*-dimethylformamide (DMF) and triethyl phosphate (TEP). Of these, DMAc was found to be the strongest solvent for PVDF polymer. Morphological study revealed the following: TEP produced symmetrical microporous membrane structures; NMP produced membranes with irregular macrovoids; both DMAc and DMF produced membranes with a short finger-like structure supported by porous substrates.

The influence of additives, namely ethanol, glycerol, lithium chloride (LiCl), lithium perchlorate ($LiClO_4$) and polyvinylpyrrolidone (PVP) [M_w =10 kDa, 40 kDa, 90 kDa, 130 kDa] on the PVDF membrane morphology and performance were studied. Their roles were assessed based on the resulting solution quality (i.e. viscosity, shift of the binodal line, non-solvent tolerance, etc.). With the exception of ethanol, the addition of additives increased the solution viscosity. In terms of membrane morphology, generally PVP was found to promote macrovoid formation; ethanol appeared to sustain the formation of porous substrates; glycerol was found to suppress gelation induced by crystallisation but support some degree of macrovoid occurrence; Li^+ salt enhanced the gelation behaviour. The membrane water permeation flux recorded for the different additives was found to improve in the following order: PVP > glycerol > $LiClO_4$ > ethanol. When combined additives of PVP and water were used, the water permeation flux increased with the amount of water added. An increase in membrane mean pore size was obtained with the addition of $LiClO_4$, however no conclusion could be drawn regarding the membrane pore size distribution. A reduced fibre collapse pressure was recorded with the introduction of solvent (in this case

NMP) in the internal coagulation bath, presumably due to the elimination of inner skin wall, accompanied by a significant increase in the overall cross sectional thickness.

Temperature was found to be the dominating parameter affecting the final PVDF membrane morphology. High temperature suppressed crystallisation but promoted liquid-liquid demixing prior to the nucleation or gelation processes. At high temperature, the distinctive morphology associated with various additives, i.e. polymer globules, island of dense polymer matrix, etc., was collectively substituted with an open cellular porous structure.

Composite hollow fibre membranes with a coating layer of few microns thickness were successfully produced via a 4-step coating procedure (involving pre-treatment, pre-crosslinking, vacuum coating, and finally post-crosslinking) developed in this study. These composite membranes, due to the highly selective nature of the divinyl-PDMS rubbery coating material, demonstrated enhanced oxygen/nitrogen selectivity.

The feasibility of using these PVDF hollow fibre membranes in waste treatment applications was tested using the example of hexene/hexane separation via π complexation with silver ions. The viability of the PVDF composite hollow fibre membranes developed was clearly demonstrated using the example of BTX recovery. In both cases, the potential of these PVDF hollow fibre membranes as a means of separation was demonstrated.

TABLE OF CONTENTS

LIST OF TABLES

LIST OF FIGURES

NOMENCLATURE

D_k	Diffusion coefficient, $m^2.s^{-1}$
l	Membrane thickness, m
M_A	Gas molecular weight, $g.mol^{-1}$
P	Permeability, $cm^3.cm.cm^{-2}.cmHg^{-1}.s^{-1}$
p_f	Feed pressure, Pa
p_p	Permeate pressure, Pa
q_v	Molar flux of viscous flow, $mol.s^{-1}.m^{-2}$
q_s	Molar flux of slip flow, $mol.s^{-1}.m^{-2}$
q_k	Molar flux of knudsen flow, $mol.s^{-1}.m^{-2}$
R	Gas constant, 8.3174 $m^3.Pa.mol^{-1}.K^{-1}$
r	Mean pore radius, m
S_l	Longitudinal shrinkage, %
S_t	Total shrinkage, %
T	Temperature, K
$\overline{v}$	Mean velocity, $m.s^{-1}$
δ_d	Dispersion parameter, $MPa^{1/2}$
δ_p	Polar parameter, $MPa^{1/2}$
δ_h	Hydrogen bonding parameter, $MPa^{1/2}$
δ_t	Total solubility parameter, $MPa^{1/2}$
λ	Mean free path, m
μ	Gas viscosity, Pa.s

CHAPTER ONE
INTRODUCTION

1.0 FOREWORD

Holistically, 'membrane separation' is a widely interdisciplinary subject involving knowledge about material science (to facilitate the necessary material selection, characterisation and evaluation process), accompanied by expertise on membrane fabrication and characterisation (to favour the production of membranes with desirable structural, mechanical, permeation and separation properties), and the final separation processes (which requires comprehensive understanding of the intended applications, i.e. the problems to be solved, transport phenomena entailed, membrane module design, and means of evaluating the specific separation performance). Indeed, the 'membrane' itself remains as the core in any membrane separation process. It is therefore important to understand the relationship between the membrane formation processes and the properties of its precursor polymer solution, as this knowledge can be used advantageously to produce the desirable membrane morphology for the intended applications. This study is aimed at producing poly(vinylidene fluoride) PVDF hollow fibre membranes suitable for the removal or recovery of organic compounds from fluid mixtures.

1.1 BACKGROUND

Volatile organic compounds (VOCs) are defined as compounds that have a high vapour pressure and low water solubility, with vapour pressure less than 760 torr (101.3 kPa) at 20°C. In reality, many VOCs originate from anthropogenic sources such as petrochemical and pharmaceutical industries. The adverse effects of VOC emissions to the hydrosphere and atmosphere are subject of much concern, primarily due to its potential environmental and health hazards as many of these compounds are either toxic or carcinogenic. On the other hand, the presence of some valuable compounds in industrial waste streams make it desirable for them to be recovered and returned to the product streams (Jansen *et al.*, 1994). These compounds include benzene, toluene and xylene (BTX), methyl *tert*-butyl ether (MTBE) and so on.

1.1.1 WASTE TREATMENT TECHNOLOGIES

In general, conventional waste treatment techniques can be broadly divided into *'recovery methods'* such as absorption, adsorption, condensation and cryogenic distillation, or *'destruction methods'* such as direct combustion and catalytic incineration. Each of these techniques has its unique advantages and disadvantages in terms of efficiency, safety, operating and construction costs, space requirement and operability. The choice of a treatment technology depends on a number of factors, including the nature and concentrations of the pollutants to be removed, the targeted removal and recovery efficiency, site-specific characteristics and monetary revenue of the chemicals to be recovered (Simmons *et al.*, 1994).

With increasing awareness of conservation and resource recovery (especially when scarce resources are involved), destructive methods have certainly become less appealing. A classic example of this is thermal and catalytic combustion where the *'pollutants'* are obliterated using supplemental fuel. Another major disadvantage of these processes is the potential generation of hazardous by-products such as phosgene and hydrogen cyanide. In addition, incineration is not suitable for non-flammable solvents such as halogenated hydrocarbons.

Recovery technologies offer the advantages of monetary revenue as it enables the organic compounds to be recovered and / or reused. In this regards, cryogenic distillation has been the dominant technique used especially in olefin/paraffin separations; despite its intensive energy requirement (due to the low relative volatilities of the components) and high capital cost (distillation columns are typically up to 300 feet tall and can contain over 200 trays) (Eldridge, 1993). Other separation technologies such as physical adsorption, physical absorption and chemical sorption have the disadvantage of being a discontinuous process requiring complicated regeneration and disposal. The need for regeneration basically represents the transformation of a pollution problem from one form to another hence reducing its attractiveness. Apart from requiring a huge carbon bed, low boiling hydrocarbons are not adsorbed by carbon due to its weak chemical compatibility, while chlorinated solvents may cause corrosion problems during the steam regeneration cycle.

Meanwhile, biological processes cannot be productively used in many waste treatment processes mainly due to the vulnerability of microorganisms to the presence of high solvent concentration.

In contrast to all of these techniques, membrane technology is commercially appealing due to its higher energy efficiency, lower capital, operating and maintenance costs, compact modular construction, ease of installation and operation, mechanical simplicity and ease of scale-up. More importantly, membrane separation technology enables the valuable compounds to be recaptured in a reusable manner, leaving behind a discharge stream with minor contamination well below the regulatory restriction level (Field, 1996).

1.1.2 POLY(VINYLIDENE FLUORIDE) (PVDF) MEMBRANES

Poly(vinylidene fluoride) (PVDF) polymers, after being commercially introduced in the 1960s, have gained growing recognition as an excellent membrane material primarily for its outstanding thermal stability and chemical resistance. It outweighs many conventional membrane materials such as polysulfone (PSF), polyethersulfone (PESf) and polyacrylonitrile (PAN) as it remains inert to many corrosive materials including halogens, oxidants, inorganic acids (apart from fuming sulphuric acid), as well as aliphatic, aromatic and chlorinated solvents (Lovinger, 1982).

With its exceptional ease of dissolution in common organic solvents such as dimethylacetamide (DMAc), dimethylformamide (DMF) and *N*-methyl-pyrrolidinone (NMP) (Bottino *et al.*, 1991), PVDF membranes can be produced via an immersion induced phase inversion process. This process is by far the most widely employed method in the making of industrial asymmetric membranes due to the simplicity of the process (Kesting, 1991). In contrast, other crystalline polymers with comparable chemical tolerance such as polypropylene (PP) and polytetrafluoroethylene (PTFE) can only be made into membranes via stretching or sintering processes due to their inability to dissolve in common solvents. As a result of these factors, there has been a growing body of research investigating the use of PVDF membranes in various waste treatment applications (Wu *et al.*, 1991; Tomaszewska, 1996; Jian and Pintauro, 1993; Jian *et al.*, 1996, 1997; Kong and

Li, 1999; Li *et al.*, 1999; Mohamed and Matsuura, 2001). In recent years, considerable attention was devoted into studying the formation mechanism of PVDF membranes (Cheng, 1999; Cheng *et al.*, 1999; Young *et al.*, 1999, Wang *et al.*, 1999, Wang *et al.*, 2000a, Wang *et al.*, 2000b), however systematic development of PVDF membranes for intended applications is still lacking. This study aims at developing PVDF hollow fibre membranes for the recovery of organic compounds from waste streams, using olefin/paraffin separation and vapour permeation application as an example.

1.2 Scope Of Work

Macroscopically, the basic principles of the membrane formation process are applicable to all polymers. Microscopically, however, membrane formation process are very much case specific and it can differ greatly between polymers. With concurrent knowledge of the polymer properties, its phase separation behaviour and membrane formation processes, this information can be used in the customisation of membrane morphology for an intended application. In this study, focus is placed solely on the fabrication of poly(vinylidene fluoride) (PVDF) membranes. Feasibility of the PVDF hollow fibre membranes produced as a mean of organic compounds removal and recovery will be studied using the example of hexane/hexane separation and benzene, toluene and xylene (BTX) removal.

1.2.1 Objectives

The specific objectives of this study include:

1. to compare the solution and precipitation bahaviour of PVDF polymer in four organic solvents, i.e *N,N*-dimethylacetamide (DMAc), 1-methyl-2-pyrrolidone (NMP), *N,N*-dimethylformamide (DMF) and triethyl phosphate (TEP) so as to compare the relative solvent power.
2. to study the phase separation and cloud point behaviour of ternary PVDF/DMAc/water system in the absence and/or presence of various additives (i.e. lithium chloride, lithium perchlorate, ethanol and polyvinylpyrrolidone) so as to promote understanding on this subject matter in relation to the asymmetric membrane formation mechanism via phase inversion-immersion precipitation

method. Attention is also given to the effect of polymer concentration, solvent and additive on the solution viscosity.

3. to study the effects of solvents (NMP, DMAc, DMF and TEP), additives (i.e. lithium chloride, lithium perchlorate, ethanol, glycerol and polyvinylpyrrolidone) and temperature on the resulting flat sheet and hollow fibre membrane morphology and permeation performance.
4. to study the viability of PVDF hollow fibres developed as membrane contactor for the separation of hexene/hexane mixtures via the principle of π complexation with silver (Ag^{+}) ions.
5. to develop composite PVDF hollow fibre membranes via vacuum dip coating method using divinyl-polydimethylsiloxane (divinyl-PDMS) modified silicone rubber.
6. to study the feasibility of PVDF composite membranes developed in vapour permeation application for the removal of benzene, toluene and xylene (BTX) from nitrogen gas stream.

1.2.2 THESIS ORGANISATION

This thesis consists of seven main chapters, covering from introduction, literature reviews, materials and methodology, results and discussion, conclusions and recommendations, and finally, references.

A holistic overview on the basic principles of membrane separation technology is provided in Chapter 2. This includes the definition and categorisation of membranes, historical development of membrane separation technology as well as various membrane production methods. The main focal point of this chapter lies in the formation mechanism of synthetic polymeric membranes via immersion precipitation method. Brief descriptions on the fundamental principles of diffusional transport across porous membrane are also included in the chapter.

Chapter 3 focuses on the phase separation behaviour of ternary macromolecular solution of PVDF polymer with various organic solvents (NMP, DMAc, DMF and TEP) and water as

non-solvent. Knowledge and understanding of the phase separation behaviour of the ternary polymer/solvent/non-solvent system contribute towards the successful formulation of a stable dope solution for the subsequent fabrication of asymmetric PVDF membranes using immersion precipitation phase inversion techniques.

In chapter 4, relative solvent strength between NMP, DMAc, DMF and TEP in the formulation of PVDF polymer solution is compared based on ternary phase diagram and polymer precipitation behaviour. The effects of solvents and additives (i.e. LiCl, $LiClO_4$, PVP, ethanol, glycerol) on the morphology of flat sheet membranes at different coagulation bath temperature are disclosed.

The first part of chapter 5 focuses on the effects of various solvents (i.e. NMP, DMAc, DMF and TEP), additives (i.e. LiCl, $LiClO_4$, PVP, ethanol, glycerol) and bath temperature on the hollow fibre membranes morphology. In this chapter, the impact of internal coagulant on the resulting hollow fibre morphology as well as its nitrogen permeation performance are explored. Viability of the PVDF hollow fibre membrane produced as a membrane contactor was tested in the selective removal of hexene from hexene/hexane mixtures via π complexation with silver (Ag^+) ions.

Chapter 6 looks mainly on the development of composite PVDF membrane via vacuum dip coating method, using PVDF hollow fibre membrane as substrate and a modified silicone rubber as coating material. Feasibility of the composite membrane developed is tested for vapour permeation application of BTX removal. A comprehensive review on the development of various membrane technology on these applications, i.e. membrane based olefin/paraffin separation technique and membrane based vapour permeation application will be explicitly discussed in chapter 5 and 6.

Presenting in Chapter 7 is the overall conclusions covering the various important findings from Chapter 3 to Chapter 6, followed by recommendations for future work.

CHAPTER TWO
LITERATURE REVIEW

2.0 FOREWORD

This chapter aims to provide a literature review on the fundamentals of membrane technology, covering the history and development of various membrane making processes, existing theory of membrane formation mechanisms and their relationship with the resulting membrane microstructures and the development of asymmetric membranes in general. Due to the limited number of publication on PVDF specifically, examples using other polymeric materials are referred to with care.

2.1 FUNDAMENTALS OF MEMBRANE TECHNOLOGY

Traditionally, the word *'filtration'* refers to the removal of suspended solids or particles from liquids or gaseous stream. Membrane *'separation'* technology broadens the definition of a conventional filtration process to include the separation of dissolved solutes from liquid streams as well as the separation of gaseous mixtures (Cheryan, 1986).

From a historical point of view, membrane separation technology begun in the mid 19th century after the invention of the first semi-synthetic cellulose nitrate polymer. Meanwhile, systematic studies of gas separation could be traced back to Thomas Graham's studies on the gas permeation of porous membranes that leads to Graham's law of diffusion (Cheryan, 1986; Mulder, 1996, Kesting, 1971; 1985).

Despite the long history, the golden age of membrane technology began after the breakthrough invention of the first integrally skinned cellulose acetate hyperfiltration membranes by Loeb and Sourirajan in the 1960s (Kesting, 1985; Mulder, 1996), which are also known as 'asymmetric membranes'. This invention marked a significant milestone in the development of subsequent membrane separation technology, both academically and commercially. In the last three decades, intensive progress has been achieved over a wide area of membrane technology, from the

fundamentals of membrane formation processes to their final industrial applications. Table 2.1 provides an overview of the various commercial/industrial membrane processes.

Table 2.1 A Summary on Various Commercial Membrane Processes (Mulder, 1996)

Membrane processes	Feed	Permeate	Driving force	Application
Microfiltration	Liquid	Liquid	Pressure (0.5-5bar)	Bacteria and suspensions
Ultrafiltration	Liquid	Liquid	Pressure (2-10bar)	Emulsions and polymers
Nanofiltration	Liquid	Liquid	Pressure (5-20bar)	Bivalent ions and low molecular weight components (microsolutes)
Reverse Osmosis	Liquid	Liquid	Pressure (10-100bar)	Desalination (NaCl)
Gas separation	Gas	Gas	Partial pressure	Gases (O_2/N_2. CO_2/CH_4)
Vapour permeation	Vapour	Vapour	Partial pressure	Organic vapours from air, VOC removal/recovery, gas dehydration
Pervaporation	Liquid	Vapour	Partial pressure	Dehydration of organic solvents
Electrodialysis	Liquid	Liquid	Electrical potential	Chlorine production, heavy metals and salt recovery
Membrane contactor	Liquid	Liquid	Concentration	Volatiles organic compounds from water
	Gas	Liquid	Partial pressure	Removal of vapours (SO_2, NOx, NH_3, PAC's)
Diffusion dialysis	Liquid	Liquid	Concentration	Acid and base recovery

2.1.1 DEFINITIONS AND CLASSIFICATIONS OF MEMBRANES

A membrane in its simplest sense is an interface separating two phases that is capable of selectively restricting the movement of one or more components between the two phases.

A membrane can be classified in a number of ways. Firstly, it can be categorised based on the nature of the material it is made of, i.e. biological or synthetic materials. Further to that, synthetic membranes can be sub-divided into two main categories: polymeric and inorganic. In this study, our focus is placed solely on synthetic polymeric membranes. Cellulose acetate (CA) was widely used in the early days of membrane making due to its vast availability and low cost. Many commercially available membranes nowadays are made of synthetic polymers such as polysulfone (PS), polyethersulfone (PES), polyetherimide (PEI), polyacrylonitrile (PAN). In recent years, there has been an increasing demand for membranes with greater chemical and thermal tolerance, which led to the emergence of poly(vinylidene fluoride) (PVDF), polytetrafluoroethylene (PTFE) and polypropylene (PP) membranes.

Membranes can be grouped according to their structure, i.e. symmetric or asymmetric. From a morphology point of view, a symmetric membrane has a homogeneous structure throughout the entire membrane thickness. This homogeneous structure can be of dense or porous nature. Asymmetric membranes, on the other hand have a heterogeneous structure, comprised of a porous cross sectional structure with a thin skin on the surface. This thin skin can be integrally formed during the membrane formation process. Alternatively, the thin dense layer could be made of a different polymer material that is deposited in-situ during the membrane fabrication process or via an independent coating procedure. This type of asymmetric membrane is called a composite membrane.

Furthermore, membranes can be defined according to their geometry (flat sheet and tubular membranes) and configuration (plate-and-frame, spiral wound, etc.). Commercial flat sheet membranes have been widely available in various types, sizes

and configurations for many years. Basically, the popularity of flat sheet membranes is attributed to ease of fabrication and high reproducibility. Tubular membranes offer the advantage of high packing density and ease of upscale. Such membranes can be further classified based on the diameter: hollow fibre (diameter < 0.5 mm); capillary (0.5 mm < d < 5 mm) and tubular (diameter > 5 mm) (Mulder, 1996). The growing recognition of commercial hollow fibre membranes is well supported by the launch of various commercial hollow fibre membranes.

Indeed, the *'membrane'* remains as the core of all membrane separation process. However, different applications impose specific requirements on the membrane material and morphology. In summary, there is no one universal membrane type/structure that can meet all separation needs. For instance, in a process where a sorption-diffusion mechanism plays a major role (such as gas separation, pervaporation and pervaporation), the choice of membrane material is based on the selective sorption and diffusion properties of the membrane material. In these types of processes, the impact of membrane morphology on the overall separation performance is limited to the flux but not the selectivity. For the selectivity and permeability of the membrane, however, the material determines the efficiency of the separation process. For application where the separation mechanism is based on the size of the species to be separated (such as microfiltration and ultrafiltration applications), the porosity and pore size of the membrane determine the overall filtration efficiency.

In conclusion, membrane science is clearly a very widely interdisciplinary subject involving a huge variety of topics. Strathmann (1986) commented that a *'membrane'* could be better described in terms of what it actually does rather than what it is. One must be aware of the fact that some distinctions between various membrane separation processes remain arbitrary and are still evolving with use (Cheryan, 1986).

2.1.2 FABRICATION OF POLYMERIC MEMBRANES

Phase inversion, sintering, stretching and track etching are the four important methods used in the fabrication of synthetic membranes. Each method will produce membranes with different pore properties as summarised in Table 2.2 (Mulder, 1996). The final membrane morphology and pore properties depend greatly on the properties of the membrane material and process conditions. Brief descriptions of these membrane fabrication methods will be presented in the following paragraphs.

Table 2.2 Membrane pore properties prepared via various methods (Mulder, 1996)

Process	Porosity	Pore size distribution
Phase Inversion	High	Narrow/wide
Sintering	Low/medium	Narrow/wide
Stretching	Medium/high	Narrow/wide
Track-etching	Low	Narrow

A. SINTERING

This technique is widely used in the commercial production of inorganic membranes, as well as symmetric polytetrafluoroethylene (PTFE) and polypropylene (PP) membrane due to the low solvent solubility of these polymers. It involves the compression of powder containing particles (such as metal, metal oxides or polymer powders) of a given size, followed by sintering at a suitably elevated temperature. Membranes produced using this method normally have pore size larger than 1 μm, with relatively low porosity in the range of 10 to 20%.

B. STRETCHING

This is another method of producing microporous symmetric membranes. A partially crystalline polymeric material (such as polypropylene (PP), polyethylene (PE) or polytetrafluoroethylene (PTFE)) is stretched perpendicular to the direction of the extrusion, which results in the formation of small cracks with uniform pores ranging from 0.1 to 3 μm. This method is only suitable for highly hydrophobic crystalline polymeric materials and produces membranes with approximately 90% porosities.

C. TRACK ETCHING

In this method, a polymer film (e.g. polycarbonate and polyester films) or foil (e.g. polycarbonate) is subjected to high-energy particle radiation (metal ions) in the direction perpendicular to the material, followed by film etching (via immersion in an acid or alkaline bath). As a result, cylindrically shaped pores with narrow pore size distributions (i.e. ranging from 0.02 μm to 10 μm) could be obtained; with membrane porosity mainly determined by the radiation duration while the membrane pore size is determined by the etching time.

D. PHASE INVERSION

Phase inversion is the most widely used technique in the production of commercial polymeric membranes (Kesting, 1971; 1985; Mulder, 1996; Nunes and Peinemann, 2001). Phase inversion is defined as a demixing process where the initially homogeneous polymer solution is transferred in a controlled manner from liquid form to a solid state/matrix (Kesting 1971; 1985). Properties of the resulting membrane are related to the material selection and the condition of the initial phase transition process (Mulder, 1996; Strathmann, 1986).

Phase inversion can be induced in several ways, namely (a) thermally induced phase separation (TIPS); (b) air casting of polymer solution (also known as controlled evaporation of solvent from a three component system); (c) precipitation from vapour phase and (d) immersion precipitation. These will be explained in the following paragraphs.

(a) Thermally induced phase separation (TIPS)

This method is based on the phenomenon that solvent quality decreases with the decrease in solution temperature. Demixing is induced by the change in the temperature at the interface of the polymer solution. The remaining solvent is removed by mean of extraction, evaporation or freeze drying.

(b) Air casting of polymer solution

Phase separation is induced by controlled evaporation of solvent from a three components system comprises of a polymer dissolved in a mixture of a volatile solvent and a less volatile non-solvent. As the volatile solvent evaporates, polymer solubility decreases and hence results in phase separation.

(c) Precipitation from the vapour phase

Phase separation is induced through the penetration of a non-solvent vapour into the polymer solution. With the increase in the concentration of non-solvent in the polymer dope, phase separation begins to take place.

(d) Immersion precipitation

The freshly cast or extruded membrane is immersed in a non-solvent coagulation bath whereby phase separation is induced by the exchange of solvent in the polymer solution with the non-solvent from the coagulation bath.

Methods (b), (c) and (d) are sometime collectively known as the **diffusion induced phase separation (DIPS)** as the phase separation is induced by the diffusional mass exchange between solvent and non-solvent. However, of the above-mentioned four methods, TIPS and immersion precipitation are the two most commonly employed techniques in the preparation of polymeric membranes. In this study, our focus is placed solely on the phase inversion via immersion precipitation method as will be discussed in chapter 4 and chapter 5. Principles and theories of membrane formation via phase inversion - immersion precipitation process will be discussed in the following section 2.2 with the aid of an isothermal ternary phase diagram.

2.1.3 Preparation of Composite Membranes

A composite membrane is essentially a heterogeneous membrane comprising of two (or more) different layers that are made of different materials. Composite membrane can be produced using the following techniques: (a) dip-coating; (b) interfacial polymerisation (c) in-situ polymerisation and (d) plasma polymerisation. Among the

methods mentioned above, dip coating has gained high popularity primarily for its ease of operation, especially in the making of flat sheet membranes. The major challenge in the fabrication of composite membranes lies in the deposition of a thin, defect free, homogeneous selective polymer layer onto the porous substrate. Optimisation of the individual substrate and coating layer has been the focal point of composite membrane research (Kimmerle *et al.*, 1988; 1991). A new composite membrane preparation method has been developed in this study, using modified silicone rubber and poly(vinylidene fluoride) hollow fibre substrate, as will be discussed in chapter 6.

2.2 PHASE INVERSION – IMMERSION PRECIPITATION PROCESS

The development of an integrally skinned asymmetric membrane via the phase inversion method (Loeb and Sourirajan, 1962) is indeed a breakthrough in the membrane field, which has greatly facilitated the advancement of various industrial membrane separation processes. Following this, much research has been carried out in an attempt to rationalise the relationship between the asymmetric membrane structure with its formation process (Kesting, 1971; Rosenthal *et al.*, 1971; Strathmann *et al.*, 1971, 1975; Frommer *et al.*, 1970, 1971; Frommer and Lancet, 1972, Frommer and Messalem, 1973; Strathmann *et al.*, 1975; Broens *et al.*, 1980; Wijmans *et al.*, 1983). A detailed description of a comprehensive membrane formation mechanism is still lacking. Also, knowledge on phase separation phenomena in concentrated polymer solution is still not very well comprehended. This is in part due to the highly complex nature of the membrane formation mechanism involving phase equilibrium transformation of a concentrated macromolecular solution, both thermodynamically and kinetically, all within a very short time frame.

Prior to any discussion on the complicated ternary phase diagram involving three components polymer/solvent/non-solvent system, it is important to understand some fundamental principles of phase rules and phase equilibrium. These will be presented in the following section 2.2.1.

2.2.1 PHASE RULES AND PHASE EQUILIBRIUM

A homogeneous system is one with uniform properties throughout its volume; this uniformity can either be the same throughout the system or at least varies continuously from one point to another. On the other hand, a heterogeneous system consists of two or more distinct homogeneous regions that are separated from one another by surfaces or interfaces at which sudden changes in physical, and perhaps chemical properties occur. For a system to be in heterogeneous equilibrium it must be in thermal, mechanical, and chemical equilibrium; these three conditions must apply not only within each phase but also between the phases.

System equilibrium can be divided into (a) true equilibrium, (b) meta-stable equilibrium and (c) apparent equilibrium. True equilibrium is a state of ultimate stability with the system remaining in the same thermal, mechanical and chemical equilibrium state regardless from which direction the system is approached. Meta-stable equilibrium can be described as a state where a system is in thermal, mechanical and chemical equilibrium; this is not the most stable state possible but it is stable almost indefinitely in the absence of any external disturbance. It is virtually impossible to distinguish between a system in true and meta-stable equilibrium without approaching the system. Finally, a system in apparent equilibrium is one that is approaching an equilibrium position so slowly that the changes remain undetectable (Ferguson and Jones, 1966).

2.2.2 ISOTHERMAL TERNARY PHASE DIAGRAM

The state and equilibrium composition of a three components polymer solution system during a phase separation process can be depicted in a ternary phase diagram, as shown in Figure 2.1. The corners of the triangle represent the three essential components, i.e. polymer (3), solvent (2) and non-solvent (1). Any point within the triangle represents a mixture of these three components.

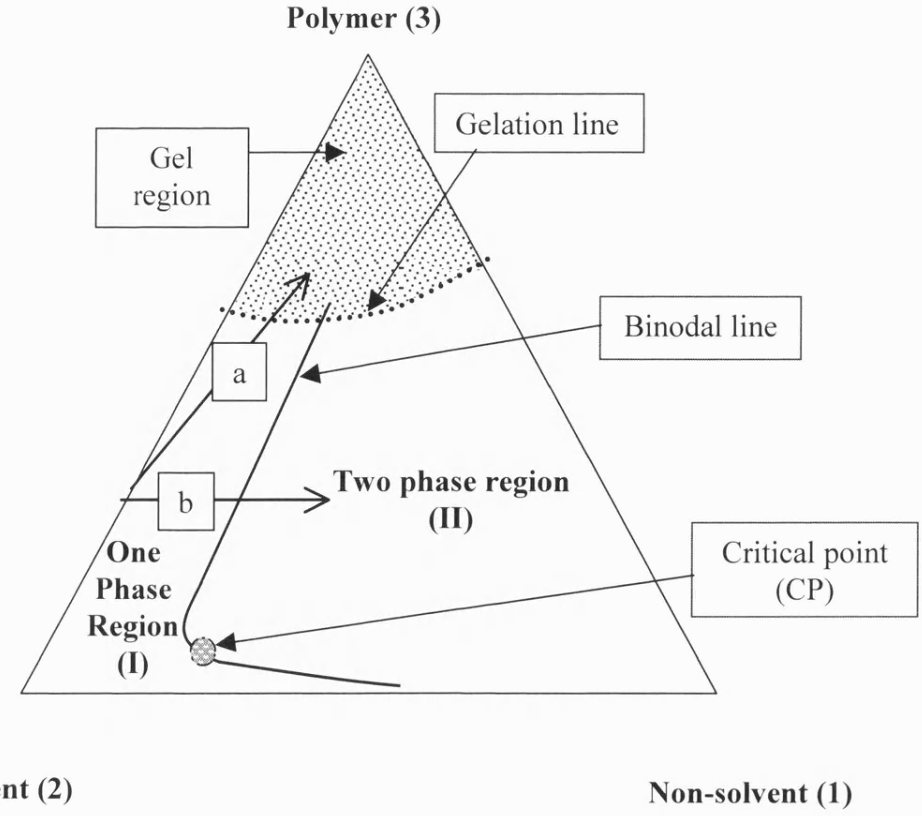

Figure 2.1 Illustration of an isothermal ternary phase diagram of a three components polymer / solvent / non-solvent system

The three components system can be broadly divided into two main compartments, i.e. a stable one-phase region (I) and a two-phase region (II), separated by the binodal line. The location of the binodal line can be obtained experimentally by cloud point measurements or by measuring the light scattering of the polymer solutions of varying compositions using differential scanning calorimeter (DSC). Alternatively, it can be calculated if the thermodynamic interaction parameters of the system are known (Wienk *et al.*, 1996).

Although the one phase region is thermodynamically continuous, the initially low viscosity liquid becomes increasingly viscous as the localised polymer concentration increases and eventually reaches such high values that the system can be regarded as a solid, as indicated by shaded 'gel region' in Figure 2.1. This process is called 'gelation' (labelled as arrow 'a' in Figure 2.1 and Figure 2.2). The gelation process can be described as the formation of ordered agglomerates due to the decline in the

thermodynamic quality of a polymer solution, which may be caused by solvent loss, temperature drop or even the introduction of non-solvent. In addition, the formation of ordered structures is also a direct indication of the ability of the semi-crystalline macromolecules (such as polyvinylidene fluoride) to crystallise in the time available (Wijmans *et al.*, 1983; Wienk *et al.*, 1996; Matsuyama *et al.*, 1999). For most semi-crystalline polymers, gelation is often initiated by the formation of micro-crystallites, which are small ordered regions comprised of nuclei from the crystallisation process. Due to their crystalline nature, these gels are thermo-reversible. Mulder (1996) discounted gelation as a phase separation process due to its ability to develop in a one phase homogeneous system, but defined gelation as the formation of three-dimensional network by chemical and physical crosslinking.

Also, the solvent and non-solvent exchange that takes place during the process of immersion precipitation results in a localised compositional change. The initially homogeneous one phase system approaches the binodal line and enters the two phases region via a compositional pathway known as liquid-liquid (L-L) demixing (as shown by arrow 'b' in Figure 2.1).

Further to the illustration in Figure 2.1, the three component polymer system could be more comprehensively divided into three main regions, i.e. (i) a stable one-phase region located between the solvent/polymer axis and the binodal line; (ii) a meta-stable region (shaded) located between the binodal line and spinodal line, and (iii) an unstable region located between the spinodal and the non-solvent/solvent axis, as illustrated in Figure 2.2. At any point along the binodal line (which is essentially the frontier of the two-phase region), the three-component system separates into two distinct liquid equilibrium phases, i.e. a polymer rich phase (α) and a polymer-lean (β) phase that are connected by a tie line, via the L-L demixing process. Critical point (CP) is the meeting point of binodal and spinodal line, which plays a crucial role in determining whether the polymer-rich or polymer-lean (polymer poor) phase forms a new phase. For most high molecular weight polymers (Mw > 104g/mol), CP is normally located at a polymer concentration of less than 5 vol.% (Pinnau, 1991).

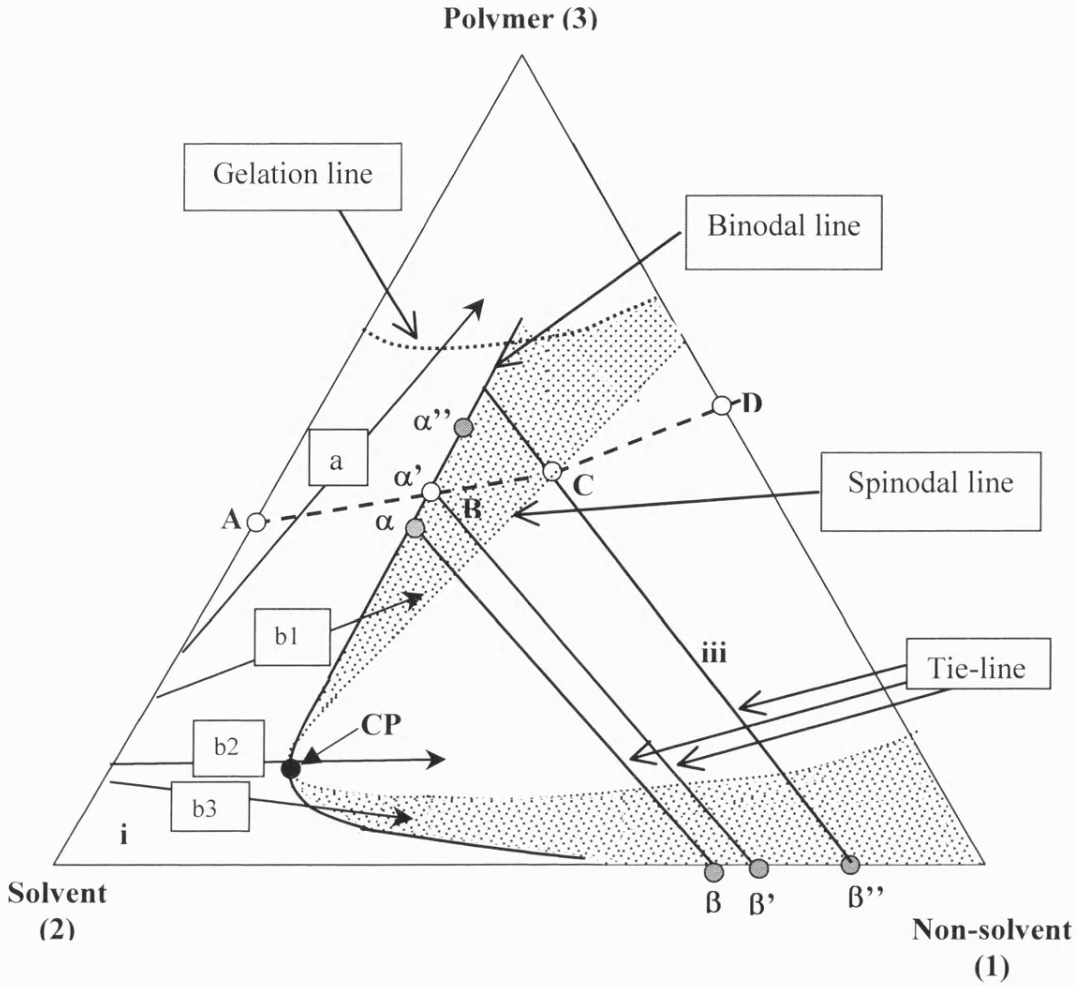

Figure 2.2 Illustration of the various phase separation pathways of a three components polymer / solvent / non-solvent system

In general, L-L demixing is the dominating phase separation process for solution with low and medium polymer concentration (typically less than 10%) with variable non-solvent content. Meanwhile, gelation (and crystallization) often dominates the phase separation process at high polymer concentration and low non-solvent content. For a polymer solution of moderately high concentration (between 10-20%), both L-L demixing and gelation or crystallisation are thermodynamically feasible. However, the fast process of L-L demixing would normally surpass the kinetically slower gelation process. The reverse is often true with an increase in polymer concentration due to the presence of a localised polymer super saturation phenomena, which can enhance the rate of nucleus formation for crystallisation.

2.2.3 COMPOSITIONAL PATHWAYS

As shown in Figure 2.2, phase separation phenomena of polymer solution can take place via four elementary composition pathways as schematised by arrows a, b1, b2 and b3. Composition path 'a' designates the direct solidification of polymer, such as thermo reversible gelation, vitrification (glass transition) and crystallization, which result in dense membrane structure such as that in skin formation (Stropnik, 2000). Composition path 'b1', 'b2' and 'b3' are collectively known as L-L demixing. More specifically, two kinetic pathways of L-L demixing have been identified, i.e. nucleation and growth (NG) (also known as *delayed demixing*) and spinodal decomposition (SD) (also known as *instantaneous demixing*).

For a one phase homogeneous solution that crosses the binodal boundary and enters the meta-stable region between the binodal and spinodal curves (regions ii), phase separation will take place by nucleation and growth (NG) (path b1 and b3). If the average polymer concentration in the meta-stable region at the point of phase separation is smaller than that of the critical point, the polymer-rich phase will nucleate (path b3). On the other hand, if the average polymer concentration in the meta-stable region at the point of phase separation is greater than that of the critical point, nucleation of the polymer-lean phase will take place (path b1).

Thus, at low polymer concentrations, nucleation and growth of the polymer-rich phase leads to low integrity polymer agglomerates. Nucleation and growth of the polymer-lean phase at high polymer concentration in the upper meta-stable region results in a closed cell morphology. In this case, the polymer lean phase will nucleate and the polymer rich phase will continue to grow in concentration until glass transition of the system is reached locally and vitrification of the solution takes place. It is generally believed that the microporous substructure of asymmetric membranes originates from nucleation and growth of the polymer-poor phase (Smolders, 1980; Wienk *et al.*, 1996).

Meanwhile, for a polymer system that enters the unstable two-phase region directly (path b2) without going through the meta-stable region (i.e. from region i → region

iii), phase separation takes place instantaneously via spinodal decomposition. This will result in a regular and highly interconnected structure.

The above composition paths b1, b2 and b3 represent the general aspects of liquid-liquid phase separation phenomena and their relationship to the evolution of membrane structures from initially stable polymer solutions. Now, considering a typical precipitation pathway of a polymer solution system with initial composition A that forms porous asymmetric membrane with final composition D: point B along the path (on the binodal frontier) indicates the concentration at which the first polymer precipitates. At any point along the binodal line (which is essentially the frontier of the two-phase region) the three-component system separates into two distinct phases, i.e. a polymer-rich phase (α) and a polymer-lean (β) phase, connected by the tie line. With a three-component polymer system moving further towards the non-solvent axis (as solvent non-solvent exchange proceeds), the polymer-rich phase become more viscous due to the solvent loss during the precipitation process. When it reaches point C (also known as the solidification point) the solution viscosity becomes so high that the precipitated polymer can be regarded as a solid. Further solvent loss brings the system to point D, where the polymer-rich phase (R) and polymer-lean phase (L) are in equilibrium (here, R represents the membrane while L represents the membrane pores filled with the non-solvent).

Due to the presence of macromolecules, three-component systems in the two-phase region are often slow to separate into the polymer rich and polymer lean phase and enter metastable state, hence system equilibrium is never truly reached. This is also in part due to the rapid precipitation of polymer during an immersion precipitation process, hence hindering the system from reaching the polymer-lean/polymer-rich phase equilibrium. As the structural network of polymer chains is continuously formed, free movement of the polymer chains is further restrained. It is important to recognise that the phase diagram is only a thermodynamic description of the overall phase distribution in equilibrium, the actual membrane structure is ultimately controlled by the kinetic factors, which dominate the distribution of the two phases, i.e. polymer rich and polymer lean phase.

A number of mathematical models have been developed based on the Flory-Huggins solution theory (Flory, 1953) to quantitatively address the thermodynamic aspect of the ternary polymer (P)-solvent (S)-non-solvent (NS) system during the phase separation process (Cohen *et al.*, 1979; Altena and Smolders, 1982; Yilmaz and McHugh, 1986a; 1986b; 1988; Reuvers et al., 1987a; 1987b; Kang *et al.*, 1991; Tsay and McHugh, 1990; 1991; Cheng *et al.*, 1994; Boom *et al.*, 1994; Sandeep *et al.*, 2001; Karode and Kumar, 2001). From a thermodynamic point of view, these models involve the construction of a complete ternary polymer-solvent-non-solvent phase diagram as well as its relationship with the formation mechanism and the resulting membrane structure. Meanwhile, the kinetic aspect of the modelling engages the building of a diffusion equation that can be mathematically used to describe various fluxes and changes in concentration profiles during the actual precipitation processes.

Four main assumptions commonly adopted in these published models include (a) instantaneous local equilibrium, (b) zero polymer dissolution in the coagulation bath (c) equality of solvent flux across the interface, (d) equality of non-solvent flux across the interface. Many of the earlier models are predominantly confined to describing the short evaporation step prior to the non-solvent quenching step, which is in fact an optional step in obtaining asymmetric membrane structure (Yilmaz and McHugh, 1986a; 1986b). Many of these models compared the calculated binodal curves with experimental cloud point measurements by considering only the concentration dependency of the solvent - non-solvent (S-NS) interaction parameters, while polymer – solvent (P-S) and polymer – non-solvent (P-NS) parameters were considered to be constant.

In other cases, P-S interaction parameters were also taken into consideration, but P-NS interaction parameters were still ignored. Yilmaz and McHugh (1986a; 1986b; 1988) considered all three interaction-parameters of P-S, S-NS and P-NS. Meanwhile, Sandeep *et al.* (2001) applied an improved algorithm to the Reuver's model (Reuver *et al.*, 1987a; 1987b) for the solution of the governing equations describing ternary mass transfer during the quench-period in the formation of

immersion precipitation membranes. Kang *et al.* (1991) explored the importance of diffusion coefficient of non-solvent coagulation medium as a crucial parameter in controlling the membrane morphology, which is directly related to non-solvent tolerance estimated from the pseudo-ternary phase diagram as well as polymer solution viscosity. Coagulation medium with high diffusion coefficients produced membranes with defect free smooth surface and macrovoid free cross section. Details development of these models can be found in the references cited (Cohen *et al.*, 1979; Altena and Smolders, 1982; Yilmaz and McHugh, 1986a; 1986b; 1988; Reuvers *et al.*, 1987a; 1987b; Kang *et al.*, 1991; Tsay and McHugh, 1990; 1991; Cheng *et al.*, 1994; Boom *et al.*, 1994; Sandeep *et al.*, 2001; Karode and Kumar) and are beyond the scope of this study.

The final membrane structures depend strongly on the local distribution of the polymer-rich phase at the point of solidification. Upon immersion in non-solvent coagulation medium, fast solvent depletion occurs instantaneously at the interface, resulting in a drastic increase in local polymer concentration (a condition that favours gelation process that is responsible for the actual skin formation). Generally, the higher polymer concentration before nucleation in the skin sets in, the higher polymer super saturation, hence the more numerous and the smaller the structural units will be. Solvent out-flow and non-solvent in-flow will encounter a greater diffusion barrier due to the skin formation. As a result of this, beneath the skin layer, phase separation will take place at a lower polymer concentration, i.e. dominated by the L-L demixing process. Indeed, the final membrane structures depend strongly on the local distribution of the polymer-rich phase at the point of solidification.

The porous sublayer of asymmetric membranes can be further subdivided into two distinctive morphologies, i.e. spongy structures and finger-liker cavities. It is believed that these membrane morphologies are directly related to the composition pathway of the homogeneous one-phase solution and their entry to the two phases region (Nunes and Peinemann, 2001). It is a well-known fact that larger finger-like cavities are formed from rapidly precipitating solution, often accompanied by the following signature characteristics: high porosity, high flux but low solute rejection.

This type of membrane normally has a skin on both sides and is widely used in low-pressure ultrafiltration processes. On the contrary, a porous spongy structure is a result of a slow precipitation process, typically with low flux but significant rejection performance. This type of membrane is generally used in high-pressure reverse osmosis processes. This membrane also has a skin on the topside, with gradual increase in pore size in the substructure progressing from the top to the bottom surface.

2.3 FORMATION OF MACROMOLECULE SOLUTIONS

The first major task in the fabrication of asymmetric fabrication via the phase inversion method is to dissolve the polymer in a suitable solvent. One of the most persistent difficulties that limit the successful casting of asymmetric membranes is the lack of a predictable and systematic method in solvent selection (Klein and Smith, 1972). Proper selection of solvent is crucial in maintaining high polymer chain mobility, which is directly influenced by both polymer-solvent and polymer-polymer interactions. A poor or weak solvent cannot accommodate many polymer molecules due to the low polymer affinity. Hence, polymeric molecules will tend to aggregate in a poor solvent as their concentration increases, and beyond a certain concentration there will appear to be phases, i.e. a phase of dilute solution and a phase of concentrated solution. This phenomenon is called 'phase separation'; its occurrence can be predicted from the free energy of mixing (Doi, 1996). In contrast, polymer molecules dissolve easily in a good solvent resulting in a uniformly distributed polymer configuration.

2.3.1 POLYMER SOLUBILITY

Dissolving a polymer is a slow process (especially for material with very high molecular weight), and can be broadly described as a two-stage process. Firstly, solvent molecules slowly diffuse into the polymer to produce a swollen gel. In cases dominated by strong interactions between polymer molecules (i.e. strong polymer-polymer interactions, such as crosslinking, crystallinity or strong hydrogen bonding), this may be all that happens. If these forces can be overcome by introducing strong polymer-solvent interactions, the second stage of solution can then proceed whereby

the swollen gel gradually disintegrates into a true solution (Billmeyer, 1984). A cross-linked polymer does not dissolve but only swells upon interaction with the solvent, with its degree of swelling inversely proportional to the level of crosslinking. As a result of this, lightly cross-linked polymers will swell extensively when they come into contact with a solvent. However, the absence of solubility does not necessarily imply crosslinking. Another main hindrance to polymer solubility is the degree of crystallinity, especially for non-polar polymers. This type of polymer does not dissolve easily except at temperatures near their crystalline melting point. Polymer crystallinity decreases as the melting point is approached, and the melting point is habitually depressed by the presence of solvent, hence in practice solubility can often be achieved at temperatures significantly below the melting point (Morawetz, 1975).

Polymer solubility behaviour could be adequately described using Hildebrand values (Billmeyer, 1984; Burke, 1984), despite the fact that solubility theory was originally developed for small molecular weight, amorphous (non-crystalline), linear polymers based on the thermodynamics of polymer solutions. Inevitably, the complex solute-solvent solubility relations involved in macromolecular system have resulted in behavioural deviation from ideal solution (that is classically associated with a finite heat of solution) even in cases with negligible heat of mixing between polymer and solvent molecules. In fact, polymer solutions are often characterised by their large positive excess entropy of dilution (Morawetz, 1975). The accuracy in forecasting the polymer solubility behaviour can be improved by assigning three parameters to each liquid, i.e. hydrogen bonding, polar forces, and dispersion forces. It is a well-known fact that materials having similar solubility parameters have high affinity for each other (Flory, 1953; Morawetz, 1975; Elias, 1984; Billmeyer, 1984). It has been reported that amorphous polymers are usually soluble in solvents having δ values within 1.8H (Hildebraand units) of the polymers (Burke, 1984). For example, a total of 8 out of 46 organic solvents were identified which were screened to be good solvents for PVDF using the Hansen solubility parameters, as tabulated in Table 2.3 (Bottino *et al.*, 1991).

Table 2.3 Hansen Solubility Parameter of Common Solvents for PVDF polymer (Bottino *et al.*, 1991)

	Dispersion parameter (δ_d)/MPa$^{1/2}$	**Polar parameter (δ_p)/MPa$^{1/2}$**	**Hydrogen bonding parameter (δ_h)/MPa$^{1/2}$**	**Total solubility parameter (δ_t)/MPa$^{1/2}$**
N, N-dimethylacetamide (DMAc)	16.8	11.5	10.2	22.7
N, N-dimethylformamide (DMF)	17.4	13.7	11.3	24.8
Dimethylsulfoxide (DMSO)	18.4	16.4	10.2	26.7
Hexamethyl phosphoramide (HMPA)	18.4	8.6	11.3	23.2
N-methyl-2-pyrrolidone (NMP)	18.0	12.3	7.2	22.9
Tetramethylurea (TMU)	16.8	8.2	11.1	21.7
Triethyl phosphate (TEP)	16.8	11.5	9.2	22.3
Trimethyl phosphate (TMP)	16.8	16.0	10.2	25.3

Solubility parameter values of PVDF polymer published in various literatures are compiled in the following Table 2.4. (Total solubility parameter values can be calculated using Hansen relation, i.e. $\delta_{t,P}^2 = \delta_{d,P}^2 + \delta_{p,P}^2 + \delta_{h,P}^2$).

Table 2.4 Summary on the solubility behaviour of PVDF polymer

Source	**Method**	**Dispersion parameter (δ_d)/MPa$^{1/2}$**	**Polar parameter (δ_p)/ MPa$^{1/2}$**	**Hydrogen bonding parameter (δ_h)/MPa$^{1/2}$**	**Total solubility parameter (δ_t)/MPa$^{1/2}$**
Bottino *et al.*, 1991	Solubility test	17.2	12.5	9.2	23.2
Burke, 1984	Solubility test	17.0	12.1	10.2	23.2*
Hansen, 1970	Contact angle	13.7	10.6	8.2	19.2

Note: *calculated based on Hansen relation: $\delta_{t,P}^2 = \delta_{d,P}^2 + \delta_{p,P}^2 + \delta_{h,P}^2$

2.3.2 POLYMER-SOLVENT INTERACTIONS

Polymer-solvent interactions in macromolecular solutions can be calculated based on solution viscosity, solution turbidity, non-solvent tolerance, various cohesion parameters and the Lewis-acid-Lewis-base characteristics of polymer and solvent (Kesting, 1985). In general, solution viscosity increases with increased molecular weight (as the chain length increases) as well as solution concentration (due to the greater polymer-polymer and polymer-solvent interaction as more polymer molecules are now present).

When comparing two polymer solutions of identical concentration, the solution viscosity gives a direct indication of their respective solvent strength with a good solvent producing lower solution viscosity. The presence of a strong solvent often results in the ascendancy of polymer-solvent interactions while marginalizing intermolecular contact between polymers. Under such circumstances, an increased solution concentration results in tighter molecular coiling hence causing each coil to have less contribution to the overall viscosity. On the other hand, polymer-solvent interaction is only slightly greater than polymer-polymer interaction in a weak solvent, hence intermolecular contacts are not so strongly forbidden.

The growth of polymer networks (as a result of increased solution concentration) is directly responsible for the increase in solution viscosity. Solution turbidity is another strong indication of solvent power whereby a clear solution indicating well-dispersed particles, i.e. the finer the dispersion, the stronger the polymer-solvent interactions, hence the stronger the solvent. In addition, solutions made of stronger solvents often demonstrate greater tolerance for non-solvent. This is clearly demonstrated in phase separation and cloud point experiments (as will be discussed in chapter 3).

2.4 MEMBRANE CHARACTERISATION

The separation performance of asymmetric polymeric membranes is directly associated with the overall membrane morphology. Information about the pore size, shape, density and distribution are therefore of importance to both membrane

manufacturers and users, so as to allow a meaningful prediction of membrane performance with significant levels of confidence (Singh *et al.*, 1998). These predictions could only be carried out based on known membrane characteristics, which can be characterised based on permeation and structural related parameters (Mulder, 1996).

The gas permeation test, bubble point technique, mercury intrusion, mercury porosimetry, and solute transport are among the few well established techniques for the determination of membrane pore statistics. Meanwhile, various electron microscopic techniques such as scanning electron microscopy (SEM), atomic force microscopy (AFM), transmission electron microscopy (TEM) and scanning tunnelling microscopy (STM) have been developed for visual examination of membrane surfaces and cross sectional structures, as well as pore morphology. Detailed principles of the above mentioned membrane characterisation methods can be found in many textbooks and papers (Kesting, 1971; 1985; Capannelli *et al.*, 1983; Smolders and Vugteveen, 1985; Nakao; 1994; Mulder, 1996). In the following sections, brief descriptions of some of the membrane characterisation methods will be presented, with specific emphasis placed on the various electron optics and gas permeation methods.

2.4.1 Membrane Pore Size Distribution

First of all, it is important to acknowledge that it is impossible to obtain a single uniform pore size for asymmetric membranes prepared via phase inversion method. Instead, a distribution of pore sizes is often observed. The bubble point technique involves the displacement of a liquid from wetted membranes using a purified gas. The bubble point is a determination of the minimum pressure at which a wetting liquid is pressed out of the membrane pore system and forms a steady bubble chain, which corresponds to the maximum pore size. Both cumulative and differential pore size distribution of a membrane can be obtained by measuring the flux of the displacing permeate gas as a function of pressure. This method has the advantage of being a non-destructive method as no pre-treatment is required.

Mercury porosimeters is in fact an extension of the bubble point technique, based on the physical principle that a non-reactive, non-wetting liquid (i.e. mercury) will not penetrate membrane pores until sufficient pressure is applied to force its entrance. The relationship between the applied pressure and the pore size into which mercury will intrude is given by Washburn equation, $PD = -4\gamma\cos\theta$ where P is the applied pressure, D is the pore diameter, γ is the surface tension of mercury (480 dyne cm^{-1} or 0.48N/m) and θ is the contact angle between mercury and the wall of the membrane pore (usually around 141.3°).

As pressure is applied, the largest pores will be filled with mercury; followed by the smaller pore as the pressure increases until finally a maximum intrusion value is reached, i.e. when all pores are filled. A sigmoid shaped cumulative curve can be generated based on the relationship between the applied pressure and the volume of mercury filled pores. As pressure increases, the instrument senses the intrusion volume of mercury by the change in capacitance between the mercury column and a metal sheath surrounding the stem of the sample cell. As the mercury column shortens, the pressure and volume data are continuously acquired and displayed by an attached personal computer. (http://www.quantachrome.com/Porosimetry.htm, 1999). It is important to note that the mercury porosimetry method assumes capillary pores. Also, the high pressure required to force the mercury into the membrane pores (especially the smaller ones) might damage the membrane pore properties.

Molecular weight cut off (MWCO) is a number expressed in Dalton indicating that 90% or more of a species with a molecular weight larger than the MWCO will be retained. The method is given by the smallest molecular mass of macro-solute with retention coefficient of greater than 90% under controlled conditions, as recommended by the Standardisation Committee of ESMTS (Gekas, 1988). It is important to note that MWCO is not a direct membrane characterisation method and it is only significant with reference to a specific experimental condition. Also, the MWCO method is useful in the characterisation of reverse osmosis (RO) membrane but is not as meaningful in the characterisation of microfiltration and ultrafiltration membrane due to the higher MWCO value (Wagner, 2001). Apart from the

molecular mass of the retained species, macro-solute retention is strongly influenced by factors such as interaction between the macro-solutes within the membrane, concentration polarization, operating time, etc.

For ultrafiltration membrane topped with a thin layer of dense skin, thermoporometry and permporometry can be used to characterise the membrane pore size distribution. Thermoporometry method is based on the calorimetric measurement of solid-liquid transitions, whereby a solid-liquid thermodynamic equilibrium is assumed. Cumulative pore size distribution curves can be obtained from the melting curve (as a function of the degree of undercooling) measured using a differential scanning calorimeter (DSC). It has been reported that membrane pore size characterised using the thermoporometry method is considerably larger than those obtained from solute transport analysis and measurement made from electron microscope images (Kim *et al.*, 1994). Permporometry method is based on the blockage of pores by means of a condensable gas, with the simultaneous measurement of a gas flux through the membranes, similar to the principle of capillary condensation in adsorption-desorption (Mulder, 1996). As opposed to the thermoporometry method, the permporometry method measures only the active pores that are actually responsible for the membrane performance.

2.4.2 Gas Permeation Method

Gas permeation test is one of the most widely used methods in the characterisation of membrane pore properties (Yasuda and Tsai, 1974; Kong and Li, 2000) partly due to its ease of operation. A major advantage of gas permeation method is that the test is carried out in the dry state as opposed to the use of wetted membranes in the bubble point technique. Hence, no pre-treatment (which might introduce unnecessary alteration to membrane properties) is required. The following diagram (Figure 2.3) illustrates the differences between the gas permeation through dry (i.e. gas permeation method) and wetted (i.e. bubble point technique) microporous membranes as a function of pressures (Reichelt, 1991).

With reference to Figure 2.3, the dashed horizontal line represents the flow profile of a dry membrane that is independent of the feed pressure (as shown by section D1). Meanwhile the solid line curve represents the flow profile of a wet membrane with feed pressure. Section W1 illustrates that all the liquid filled pores are impervious at low pressure. As the pressure increases, the pores open one after another and gas permeation become noticeable. The pressure at which the first flow through gas bubble can be detected is called the bubble point pressure (section W2). At high pressure, the flow curve through the dry membrane is asymptotically reached, as shown by section W3.

Membrane characterisation using the gas permeation method is based on the transport principles across porous membranes, which has been extensively studied (Kamide *et al.*, 1982, Rogers, 1985; Włosek-Szydłowska and Straszko, 1987, Pinnau *et al.*, 1988; Kimmerle *et al.*, 1991; Blume *et al.*, 1991; Leeman *et al.*, 1991). Table 2.5 summarises the equations used for gas permeation across porous membrane media depending on the microscopic membrane pore size (r) and the mean free path (λ) of gas/vapour molecules.

Preferential diffusion of one component over the other could be attributed to the interactions between the membrane material and the molecules to be separated. As the pore size decreases to the point where the majority of the collisions are between the gas and the pore walls, the lighter molecules pass through the membrane faster than the heavier molecules. This process, known as Knudsen diffusion, however, does not provide high degree of separation. When the diameter of the pores approaches the diameter of the larger molecules in a mixture, only the smaller molecules will pass through. This process of molecular sieving provides a lower pressure purified stream of the smaller molecules. Due to the lack of accurate information on the complicated and irregular membrane pore sizes, shapes and structures, a number of assumptions were made by individual researcher for the ease of analysis based on their membrane systems. Kamide *et al.* (1982) concluded that slip flow could not be ignored in a membrane with small pore size (i.e. mean diameter < 35 nm). Based on these principles, Kong (2000) proposed a new

improved gas permeation method for membrane characterisation, whereby both standard normal (Gaussian) and log normal distribution functions were used to represent the membrane pore size distribution of PVDF hollow fibre membranes fabricated.

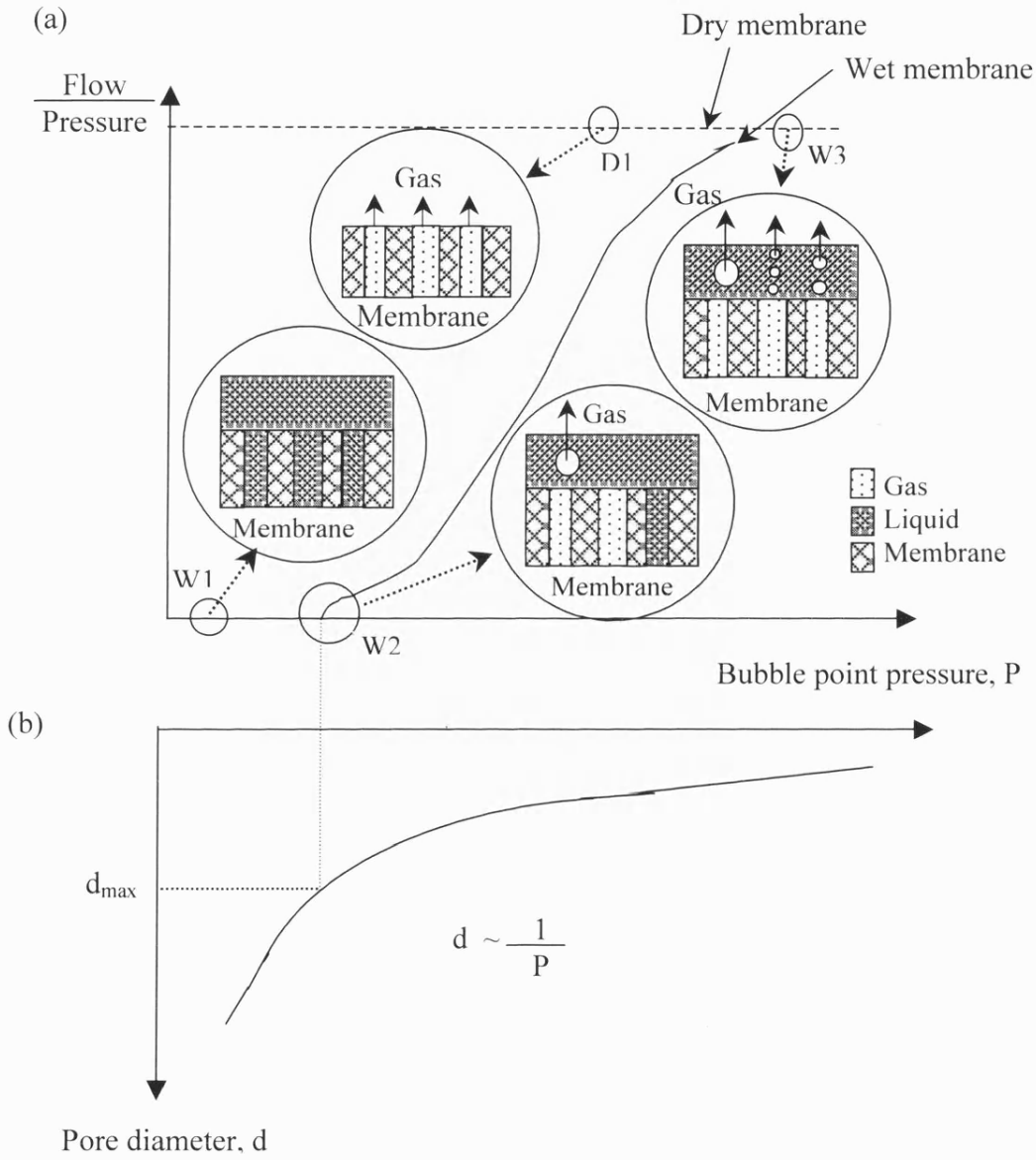

Figure 2.3 Schematic diagrams showing (a) the principles of gas flow through dry and wet membranes; (b) the relationship between pore diameters and pressure (Reichelt, 1991).

Table 2.5 Overview on membrane pore sizes with corresponding diffusion flow

Pore size (r)	Permeation flow	Molar flux (q)	Equation
r>>λ	Viscous flow	$q_v = \frac{(p_f - p_p)}{16\mu . RT . L} . (p_f + p_p) r^2$ (Hagen-Poiseuille equation)	(2.1)
r~λ	Slip flow	$q_s = \frac{r}{M_A \bar{\nu} L} \frac{(p_f - p_p)}{2}$; where $\bar{\nu} = \sqrt{\frac{8RT}{\pi M_A}}$	(2.2)
r<<λ	Knudsen diffusion	$q_k = \frac{D_k}{L} \frac{(p_f - p_p)}{RT}$; where $D_k = \frac{2}{3} r \sqrt{\frac{8RT}{\pi M_A}}$	(2.3)

where r is the membrane mean pore size; λ is the mean free path, being defined as $\lambda = \frac{RT}{\sqrt{2} . \pi\sigma^2 . p_i}$; other notations are listed in nomenclature.

2.4.3 Various Electron Microscope Techniques

A number of electron microscopic techniques have been employed in the study of membrane characterisation, namely scanning electron microscopy (SEM), atomic force microscopy (AFM), transmission electron microscopy (TEM) and scanning tunnelling microscopy (STM). Of these, SEM is undoubtedly the most popular electron microscopic device used in membrane characterisation, primarily for its ease of operation and depth of focus. It reveals the membrane cross sectional structure, which provide quick insight into the membrane formation process. Unfortunately, because of its limited resolution, SEM is incapable of analysing detailed skin morphology (Bessieres *et al.*, 1996).

In recent years, AFM is becoming a popular tool in membrane characterisation (Fritzche *et al.*, 1992; Bottino et al., 1994; Singh *et al.*, 1998; Khulbe *et al.*, 1996; Bessieres *et al.*, 1996, Khayet *et al.*, 2002). Among the many advantages it offers include its ability to image the non-conducting sample both in air and in liquid. Also, there is no requirement for tedious processes of sample preparation, as needed by SEM and TEM. Moreover, the tedious specimen preparation could result in membrane morphology alteration and artefacts (Bessieres *et al.*, 1996).

A number of studies have been dedicated to compare the differences between these electron microscopic methods (Fritzche *et al.*, 1992); some even include comparisons with membrane pore properties obtained using gas permeation method (Shih *et al.*, 1990) and solute transport studies (Singh et al., 1998; Bessieres et al., 1996). Fritzche *et al.* (1992) used contact and non-contact AFM and SEM to investigate the surface structure and morphology of 30-kilo Dalton (kDa) membranes of different materials. In their study, it was found that membrane pores with diameters in the range of 12-20 nm were revealed by AFM but SEM failed to discern any pore structure. Also, on 100 kDa polyethersulfone membranes, pore dimensions obtained by AFM were larger than those obtained by SEM which could be due to the alteration of membrane pore properties as a result of the solvent exchange procedure used in the drying process of SEM sample preparation.

Chahboun *et al* (1992) compared microfiltration and ultrafiltration membranes using STM, AFM and SEM techniques. It was concluded that AFM allows direct measurement of pore density but with limitation at high magnifications. Bottino *et al.* (1994) used AFM to study the surface of UF and MF ceramic membranes, whereby AFM was able to provide more information on both size and shape of Al_2O_3 particles constituting the selective skin layer as well as the skin surface roughness. For microfiltration membranes, however, AFM results were found to be similar to those obtained by conventional SEM. Mean pore sizes measured by AFM were about 3.5 times larger those calculated from solute transport (Singh *et al.*, 1998). Using AFM Nanoscope III, Khayet *et al* (2002) was able to analyse both the internal and external surfaces information of PVDF hollow fibres, as well as

measuring the pore size and nodule size from the line profiles on the AFM images with a scan size 0.1μm x 0.1μm at a 5μm range.

In this study, scanning electron microscope (SEM) is used extensively to characterise morphology of the asymmetric and composite PVDF membranes produced. An improved gas permeation method proposed by Kong (2000) will be used in the analysis of hollow fibre membrane pore statistics.

CHAPTER THREE

A STUDY ON THE PHASE SEPARATION AND VISCOSITY BEHAVIOUR OF POLY(VINYLIDENE FLUORIDE)

3.0 FOREWORD

Basic knowledge about polymer science, related to macromolecular solution systems is essential in understanding polymer/solvent/non-solvent interactions. This knowledge provides a great insight into the relationship between membrane formation processes and its precursor macromolecular solution, hence making it possible to engineer the system to produce desirable membrane morphologies for the intended applications. In this chapter, the phase separation behaviour of isothermal ternary PVDF/solvent/water systems is studied; the knowledge is then extended and applied in the formulation of a stable polymer dope for membrane preparation in the later stages.

3.1 POLY(VINYLIDENE FLUORIDE) AS COMMERCIAL MEMBRANE MATERIAL

As mentioned in Section 1.1.2, PVDF outweighs many other conventional membrane materials such as polysulfone (PSF), polyethersulfone (PESf) and polyacrylonitrile (PAN) primarily for its exceptional chemical resistance. It remains inert to many corrosive materials including halogens and oxidants, inorganic acids (apart from fuming sulphuric acid), as well as aliphatic, aromatic and chlorinated solvents. Its chemical resistance superiority makes it an outstanding membrane material especially in waste treatment applications where harsh chemicals are commonly involved (Wu *et al.*, 1991; Tomaszewska, 1996; Jian and Pintauro, 1993; Jian *et al.*, 1996, 1997; Kong and Li, 1999; Li *et al.*, 1999; Mohamed and Matsuura, 2001). In summary, the popularity of PVDF polymer as a membrane material is intrinsically attributed to the high carbon-fluorine dissociation energy in its monomer unit ($-CH_2F_2-$), as shown in Figure 3.1.

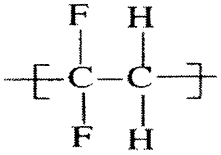

Figure 3.1 Monomer unit of poly(vinylidene fluoride) (PVDF)

Another major advantage of PVDF polymer as compared to polypropylene (PP), polyethylene (PE) and polytetrafluoroethylene (PTFE) is its ease of dissolution in common organic solvents including dimethylacetamide (DMAc), dimethylformamide (DMF) and *N*-methyl-pyrrolidinone (NMP) (Bottino *et al.*, 1991). As a result of this, PVDF membranes can be produced via the immersion precipitation phase inversion process. As discussed in Section 2.1.2, this is is by far the most widely employed method in the making of industrial asymmetric membranes due to the process simplicity (Kesting, 1971). In contrast, other crystalline polymers with comparable chemical tolerance such as polypropylene (PP) and polytetrafluoroethylene (PTFE) can only be made into membranes via stretching or sintering due to their inability to dissolve in the above-mentioned common solvents.

3.2 POLYMER CRYSTALLINITY

The polymer crystallisability is intimately related to its structural regularity, hence any substituent atoms or groups present on the polymer backbone chain have to be sufficiently small for them to have an orderly structure, even if they are irregularly spaced (Flory, 1980; Billmeyer, 1984). X-ray diffraction could be used to detect the polymer crystallinity by revealing the sharp features associated with regions of three-dimensional order, as well as the more diffuse features characteristic of molecularly disordered substances such as liquids (Flory, 1981; Billmeyer, 1984).

The popularity of crystalline polymers is a result of their many desirable properties, including being a stronger, tougher and stiffer polymer material with better solvent and chemical resistance than their non-crystalline counterparts (Billmeyer, 1984). From a membrane science point of view, however, the crystalline state is the densest state of polymer aggregation whereby a perfect crystallite is virtually impermeable due to the lack of free volume. As a result of this, active transport can only take place in the amorphous region (Kesting, 1985; Mulder, 1996). According to Bitter (1984), the diffusion coefficient across semi-crystalline polymeric membrane can be described as a function of its crystallinity as $D_i = D_{i,o}\left[\frac{\psi_c^n}{B}\right]$ (whereby ψ_c is the fraction of crystallinity, B is a constant and n is an exponential factor with n<1).

However, the permeation resistance due to polymer crystallinity is considered negligible at low level of crystallinity, i.e. ψ_c <0.1, which is the case for most semi-crystalline polymers (Mulder, 1996).

Semi crystalline polymers, such as PVDF polymer, have been reported to exhibit more complicated phase separation behaviour than the amorphous polymer (Wienk *et al.*, 1996). Knowledge of the polymer crystallinity and its resulting membrane morphology are important in providing a basis of understanding about membrane permeability and selectivity, as well as its various chemical and mechanical properties (Kesting, 1971). Growth of polymer crystallinity has a detrimental effect to the final membrane transport properties as it decreases both the free volume of the amorphous region available for species transport and increases the membrane tortuosity (Kesting, 1971). In general, it is beneficial to suppress the polymer crystallinity in the membrane formation process so that the superior characteristic (i.e. excellent thermal and chemical resistance) of a semi-crystalline polymer could be maximised at the smallest expense of permeation properties.

3.3 ISOTHERMAL PVDF / SOLVENT / NON-SOLVENT TERNARY SYSTEM

Research and development of PVDF membranes has been actively pursued by a number of researchers, primarily focused on the effect of various preparation parameters on fundamental membrane morphology via the phase inversion process (Uragami *et al.*, 1980; Bottino *et al.*, 1986; 1988a; 1988b; 1991; Deshmukh and Li, 1998; Wang *et al.*, 1999; 2000; Kong and Li, 2001). However, the mechanism of PVDF membrane formation is rarely discussed in the abovementioned literatures.

Due to its crystallinity, the phase inversion behaviour of PVDF polymer is more complicated than amorphous polymers such as polysulfone (PSf) and polyethersulfone (PESf) (Wienk *et al*, 1996). However, despite the extensive use of PVDF / DMAc / water system in the fabrication of asymmetric PVDF membranes (Wu *et al.*, 1991; Tomaszewska, 1996; Kong and Li, 1999; 2001; Li *et al.*, 1999; Mohamed and Matsuura, 2001; Deshmukh and Li, 1998; Wang *et al.*, 1999; 2000), no information on the phase separation behaviour of the polymer solution system

was reported in these articles. Information of such a nature is extremely useful in providing important thermodynamic and kinetic information on the membrane making process (Lau *et al.*, 1991). It is therefore very important to study and understand its phase inversion behaviour, and utilise such information in membrane preparation processes.

In recent years, a number of articles related to the phase separation behaviour of PVDF polymer system has emerged recognising the importance of such information. (Soh *et al.*, 1995; Young *et al.* 1999; Cheng, 1999; Cheng *et al.*, 1999; Hong and Chou, 2000). Phase behaviour of PVDF/DMF/1-octanol system, i.e. liquid-liquid phase separation and their crystallisation boundaries were computed over a wide temperature range (300K-460K) based on Flory-Huggins theory (Soh *et al.*, 1995). Matsuyama *et al.* (1999a, 1999b) investigated the phase separation of PVDF/DMF system induced by penetration of non-solvent from the vapor phase using a phase diagram.

Phase behaviour of crystalline PVDF polymer was studied based on a PVDF / DMF system using 1-octanol (soft non-solvent) and water (harsh non-solvent) as non-solvent over a temperature of 25°C to 80°C (Young *et al.* 1999; Cheng, 1999; Cheng *et al.*, 1999; Hong and Chou, 2000). Cheng (1999) demonstrated the shift of PVDF/DMF system gelation boundary in accordance with the increase in solution temperature. As temperature increases, a greater amount of octanol was required to induce gelation behaviour, hence resulting in a shift of gelation boundary. The normally inaccessible amorphous phase boundary for PVDF was calculated by Young *et al.* (1999) using Flory-Huggins interaction parameters and was found to match the experimentally obtained crystallisation data reported (Cheng, 1999; Cheng *et al.*, 1999). The gap between gelation boundary and binodal line was minimised as temperature increased, with gelation line moving closer towards the binodal line but still remaining parallel to the initial gelation boundary. This knowledge was extended in the study of PVDF membrane formation mechanism, providing a basis for the optimisation of membrane structure, using both equilibrium thermodynamic and diffusion kinetic theory. Scanning electron micrographs of PVDF film membranes obtained confirmed the dominance of the gelation process at low temperatures leading to crystalline structures. At elevated temperature, this is

overtaken by liquid-liquid demixing processes whereby a more open and porous membrane structure was obtained.

The relationship between phase separation behaviour and gelation kinetics for poly(vinylidene fluoride) / tetra(ethylene glycol)dimethylether (PVDF/TG) solutions was studied by Hong and Chou (2000) using time resolved light scattering and the gelation kinetic analysis. According to the authors, two distinct gelation pathways could be identified based on the gelation temperature. At temperature above spinodal temperature, the gelation process dominates with pure crystalline nucleation. However, for gelation below spinodal temperature, crystalline nucleation and liquid-liquid demixing are both kinetically feasible hence could lead to a more porous structure.

Here, we study the precipitation curves of PVDF Kynar® K-760 polymer, using four different solvent systems, i.e. *N,N*-dimethylacetamide (DMAc), 1-methyl-2-pyrrolidone (NMP), *N,N*-dimethylformamide (DMF) and triethyl phosphate (TEP), whereby water is used as non-solvent. Also included in this report is the effect of three additives, i.e. ethanol, lithium perchlorate ($LiClO_4$) and polyvinylpyrrolidone (PVP, Mw=10 kDa) on the phase inversion behaviour of PVDF / DMAc system, again using water as non-solvent. Finally, the cloud points of 10 wt%, 15 wt% and 20 wt% PVDF / DMAc system were investigated using ethanol, glycerol and water as the non-solvent.

3.4 Materials and Methods

3.4.1 Materials

Commercial grade poly(vinylidene fluoride) (PVDF) pellets, i.e. Kynar®K760 [Elf Autochem] were used as the sole membrane material in this study. Solvents used include *N,N*-dimethylacetamide (DMAc) [99.9+%, HPLC grade] and 1-methyl-2-pyrrolidone (NMP) [99+%, spectrophotometric grade], *N,N*-dimethylformamide (DMF) [99.8%, ACS reagent garde] and triethyl phosphate (TEP) [99%, GC grade]. Ethanol [reagent grade], lithium perchlorate ($LiClO_4$) [99+%, ACS reagent grade] and polyvinylpyrrolidone (PVP) [99.9+%, M_w =10 kDa] were used as additives. Ultra pure water, ethanol [reagent grade] and glycerol [Fw=92.09, 99%] were used

as non-solvent. All chemicals were purchased from Sigma Aldrich and used as received. PVDF polymer pellets were pre-dried at 50 °C prior to use.

3.4.2 Preparation of Polymer Solution

Polymer solution with concentration up to 20 wt% was prepared by dissolving the polymer pellets using four different solvents, i.e. DMAc, DMF, NMP and TEP respectively. Pre-dried polymer pellets were weighed using an electronic balance [Precisa 2200C, accuracy ± 0.005 g] and then poured into a Scott's bottle, pre-rinsed with solvent, followed by the addition of measured amount of solvent and additives, whenever applicable. The mixture was then shaken rigorously to ensure a thorough wetting of polymer pellets, and to prevent the formation of polymer lump. The mixture was then left rotating on a mechanical rotator [Stuart Scientific Roller Mixer SRT2] for 48 hours at 20 °C. Dissolution of polymer solution with concentration greater than 10wt% was enhanced by leaving the mixture in a 50 °C isothermal water bath-mechanical shaker [Grant OLS-200] with shaking motion set at 50 per minute, for a period of 24-hour.

3.4.3 Measurement of Solution Viscosity

Solution viscosity was measured using Bohlin Rheometer Measuring System 4/40 [Bohlin], at 30 s delay time and various operating temperature. This equipment uses the Ramp Stress Test Method, whereby a gradually increasing ramped stress (0.07892 Pa – 6.662 Pa) was applied onto the sample solution, and the induced shear rate was continuously monitored. The viscosity of the sample solution was calculated based on the ratio of these two parameters, i.e. shear stress versus shear rate. Viscosity measurements were made on 15 wt% PVDF polymer solutions in four different solvent systems (i.e. DMAc, DMF, NMP and TEP). A viscosity profile was also generated for PVDF / DMAc solutions of varying polymer concentrations (i.e. 10 wt%, 15 wt% and 20 wt%) over the temperature range of 20 °C – 70 °C. The effect of additive on solution viscosity was studied based on the presence of 2 wt% and 6 wt% of additives (ethanol, $LiClO_4$ and PVP M_w = 10k) in 15 wt% PVDF / DMAc solution. These results will be discussed in Sections 3.5.4 and 3.5.5.

3.4.4 MEASUREMENT OF CLOUD POINTS

Cloud point data for PVDF polymer solutions in four different solvent systems, i.e. DMAc, DMF, NMP and TEP, was measured up to 20 wt% polymer concentration by means of a titration method. Polymer solutions were poured into a sealed Quickfit® round flask and immersed in a water bath at controlled temperatures of 25 °C and 70 °C, respectively. The non-solvent used, i.e. ultra pure water [ELGA MAXIMA] was slowly added into the polymer solution, with a magnetic stirrer constantly agitating the solution until the first appearance of turbidity was detected using experimental set-up as illustrated in Figure 3.2.

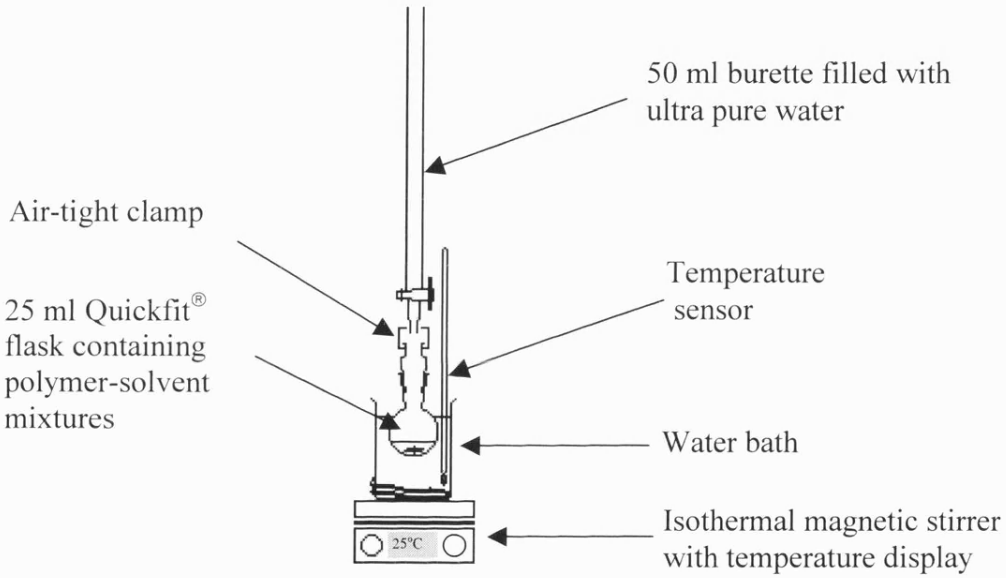

Figure 3.2 Experimental arrangement for cloud point measurements

The effects of ethanol, lithium perchlorate ($LiClO_4$) and polyvinylpyrrolidone (PVP, M_w = 10k) as non-solvent additives on the phase inversion behaviour of PVDF / DMAc system were also studied using water as non-solvent. In these cases, two concentrations (i.e. 2 wt% and 6 wt%) of additives were added into the PVDF / DMAc polymer solution. Similarly, ultra pure water [ELGA MAXIMA] was added slowly into the polymer solution, with a magnetic stirrer constantly agitating the solution until the first appearance of turbidity was detected. The cloud points of 10 wt%, 15 wt% and 20 wt% PVDF / DMAc system were investigated using ethanol,

glycerol and water as the non-solvent, following the same procedure mentioned above.

Extra care was taken throughout the study to avoid spurious effects caused by localised precipitation, especially at higher polymer concentration. When the first persistent sign of polymer precipitation was observed, the precipitated solution was kept in isothermal water bath and was subjected to constant agitation overnight. Further addition of non-solvent was performed only after the solution become homogeneous again. If the turbidity persisted (or solution showed sign of gelation), the volume of non-solvent added was recorded as the coagulation value. Three independent titrations were taken for each polymer concentration so as to minimise the error.

3.5 Results And Discussions

Thorough phase separation study was carried out on PVDF / solvent / water systems using four different solvents, i.e. DMAc, DMF, NMP and TEP. The aim was to gain understanding of the phase separation behaviour of these ternary systems. It is believed that information of such nature is crucial in the formulation of a stable polymer dope for membrane preparation purposes. Isothermal ternary phase diagrams were produced for various PVDF / solvent / water systems with and without the presence of additives as will be discussed in the following chapters.

3.5.1 Effect of Solvents on PVDF / DMAc / Water Phase Diagram

Solvent plays a very important role in determining the final outcome of membrane structure and performance (Bottino *et al.*, 1991; Klein and Smith, 1972). A good solvent is essential in formulating a uniform polymer solution, and to obtain the membranes with narrow pore size distribution, or even good mechanical strength. Out of the eight good solvents for PVDF polymers identified by Bottino *et al.* (1988), four are tested in this PVDF phase inversion studies, including N,N-dimethylacetamide (DMAc), N,N-dimethylformamide (DMF), N,N-methylpyrrolidone (NMP), and triethyl phosphate (TEP). In this study, it is found that PVDF polymer dissolved fairly easily in DMAc, DMF and NMP; however it did

not easily dissolve in TEP. The effect of individual solvent power on the solution viscosity will be discussed in section 3.5.4.

Precipitation point curves of PVDF in these four solvents system (i.e. DMAc, NMP, DMF and TEP) using water as non-solvent are presented in Figure 3.3. As noted by Lau *et al.* (1991), this miscibility region can be considered as a measure of the system's resistance or tolerance to polymer precipitation by the non-solvent (in this case, water). In short, the stronger the solvent power, the greater amount of non-solvent is required to disturb the system equilibrium and to induce the polymer precipitation. Here, the solvent power could be ranked in the order of DMAc > NMP > DMF > TEP, as suggested by the width of the one phase homogenous gap shown in the ternary phase diagram (Figure 3.3). Since DMAc is the strongest solvent of PVDF polymer used (as confirmed by the highest amount of water required to induce polymer precipitation), it is used for further investigating the effect of additives on the phase inversion behaviour of PVDF polymer solution in the subsequent experiments. The benefit of using a strong solvent has been explained in section 2.3.2, which includes a better and more uniform dispersion of polymer molecules. Apart from that, the use of a strong solvent also enhances the non-solvent tolerance of a polymer system. This is important due to its direct association with the final membrane void volume and skin thickness, which is proportional to the final non-solvent concentration within the phase inversion casting solution (Kesting, 1985).

It is important to note that the end point of the titration differ remarkably between low concentration and high concentration polymer solutions. When polymer concentration is low, the solvent-solute effect (i.e. strong interactions between solvent and macromolecule) dominates the solution behaviour, while macromolecule-macromolecule interaction remains negligible. Under such circumstances the titration end point is designated by the presence of persistence solution turbidity that could be detected visually. At high polymer concentration, the growing interaction between macromolecules starts to interfere (alongside the interactions between solvent and macromolecule) and could result in different phase separation behaviour. Under such circumstances the semi-crystalline polymer solution showed signs of crystallisation and became gel-like. Realistically, we cannot

guarantee these points obtained at high polymer concentration as the so-called binodal point due to the occurrence of gelation. They do, however, mark the point after which the solution become thermodynamically unstable and not suitable to be used as a polymer dope. In short, the establishment of these isothermal ternary phase diagrams is especially useful in identifying the extent or boundary to which the high concentration polymer solution remains thermodynamically stable. This information is crucial in the preparation of a stable casting dope for membrane fabrication.

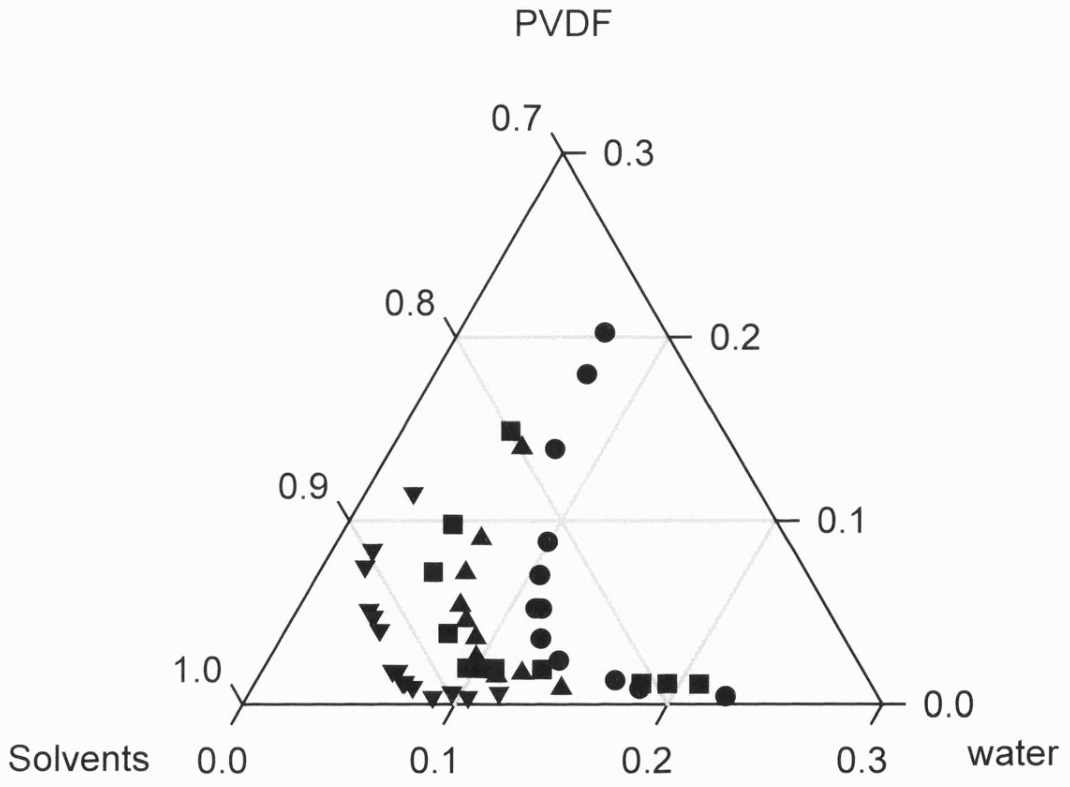

Figure 3.3 Isothermal phase diagram of PVDF K-760 / water / solvents ternary system at 25 °C▼ TEP, ▲ NMP, ● DMAc, ■ DMF

3.5.2 EFFECT OF ADDITIVES ON PVDF / DMAC / WATER PHASE DIAGRAM

The effects of three additives, namely polyvinylpyrrolidone (PVP, M_w=10k), ethanol and lithium perchlorate ($LiClO_4$) on the phase inversion behaviour of PVDF/DMAc system were studied at both 25 °C and 70 °C.

In general, the presence of additive was found to reduce the system's degree of tolerance for water, as shown by the reduction in the width of the one phase miscibility gap in Figure 3.4 (a). It is evident that at 25 °C, the reduction of the envelope of the one phase homogenous region follows the trend of $LiClO_4$ > PVP > ethanol. This is in reverse order with the miscibility of these additives with DMAc. The solvent-additive miscibility follows the trend of ethanol > PVP > $LiClO_4$ which was clearly demonstrated by their ease of dissolution in the solvent. It is evident that the presence of additives lowers the solvent power, due to competitions between polymer molecules and additives in solvent – solute interaction; hence lesser polymer-solvent interactions could take place.

With reference to Figure 3.4(b), it is evident that the system's degree of tolerance for water was greatly enhanced at a solution temperature of 70°C. With the precipitation curves of the PVDF / DMAc / water system shifted towards the right (as compared to Figure 3.4 (a)), a wider region of one phase system continuity was indicated. In addition, it is also interesting to observe that the precipitation curves for various additives collided at higher temperature of 70 °C. This indicates that the presence of additive has limited influence on the phase separation behaviour of PVDF polymer solution and solution stability at elevated temperature. This can be explained based on the greater macromolecular chain movement and chain mobility permissible at higher temperature hence resulting in a weaker polymer-solvent interaction. This is also clearly supported by the lower solution viscosity recorded at higher temperature as will be discussed in section 3.5.4.

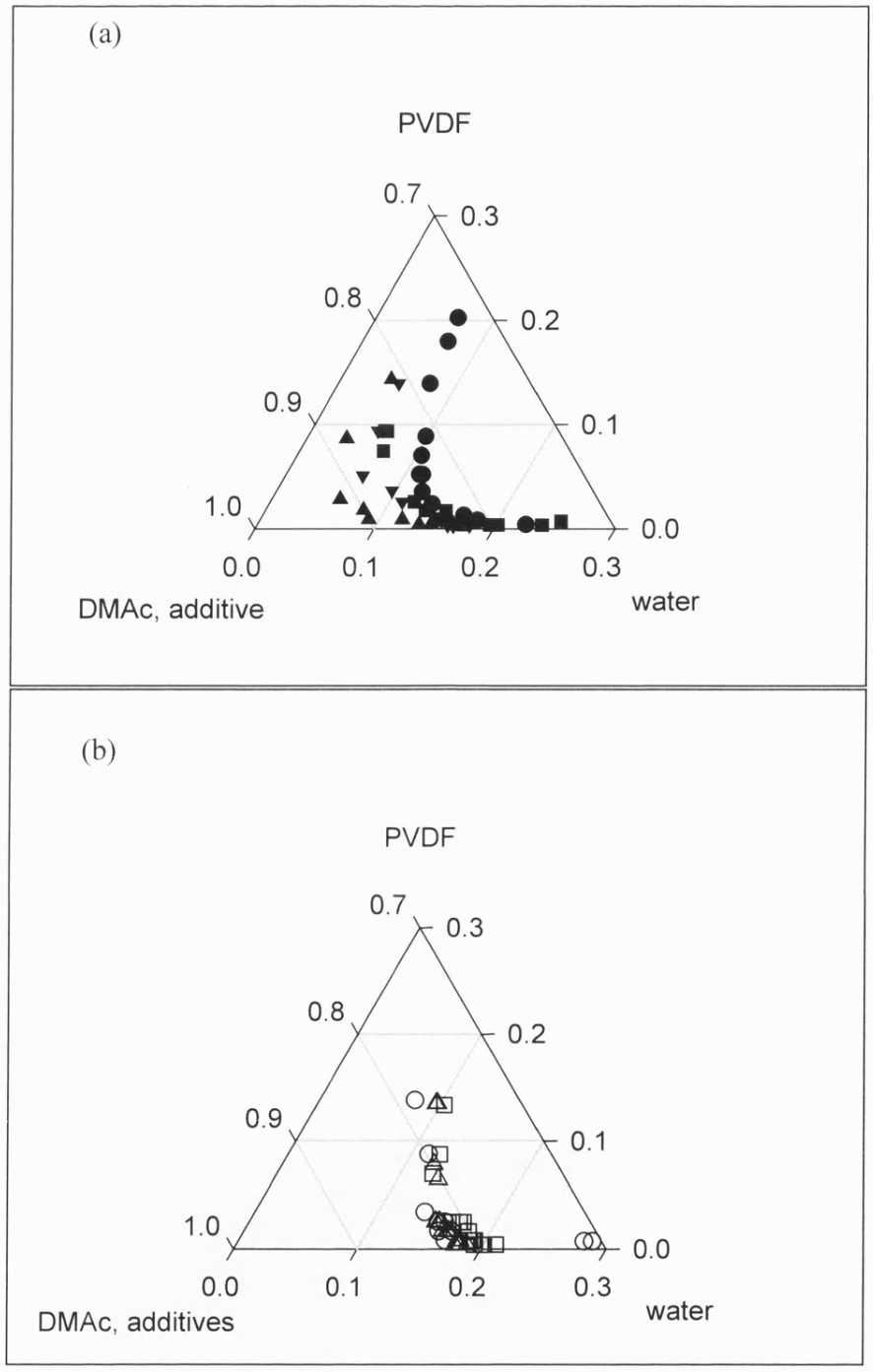

Figure 3.4 Effects of additives on the precipitation curves of PVDF/DMAc/water ternary system at (a) 25 °C : ● no additive, ▼ 6 wt% PVP, ▲ 6 wt% $LiClO_4$ and ■ 6 wt% ethanol; (b) 70°C : ○ no additive, ▽ 6 wt% PVP, △ 6 wt% $LiClO_4$ and □ 6 wt% ethanol

Figure 3.5 shows the isothermal precipitation curves for all three additives used (i.e. PVP (M_w = 10k), $LiClO_4$ and ethanol) in relation to their concentrations (i.e. 2 wt% and 6 wt%) added to PVDF / DMAc system at solution temperature of 25 °C and 70 °C, respectively. Based on experiments carried out at 25 °C, the following observations were recorded: in the case where ethanol was used as additive, the titration end point was noted as when the solution became visibly turbid, and remained in liquid form at isothermal conditions for more than 24 hours. In the case of PVP (M_w = 10k) two different end points were noted. For dilute polymer concentration (PVDF concentration less than 10 wt%), the titration end point was marked by the visually detectable turbidity, with very noticeable precipitates when seen under light. At PVDF polymer concentration greater than 10 wt%, the turbid solution exhibited gelling behaviour after being kept at constant temperature of 25 °C for prolong period of time, i.e. more than 24 hours. As for when $LiClO_4$ was used as the additive, the already cloudy solution showed gelling behaviour similar to that of PVP (M_w = 10k) at PVDF concentration as low as 8 wt%, within a shorter period of time (less than 24 hours). Meanwhile, at higher PVDF concentration (i.e. more than 10 wt%), the solution was found to form transparent gel without any sign of cloudiness / turbidity.

At 70 °C, however, all titration end points were marked by the solution becoming visibly cloudy, without any sign of gelation. Hence, it is proposed that elevated temperature was in fact suppressing polymer crystallisation and enhancing liquid-liquid demixing from amorphous regions. When the solution was removed from the 70°C water bath and maintained at 25 °C, visible precipitates could be seen floating in the already turbid low concentration polymer solutions; meanwhile the already turbid high concentration polymer solutions gelled within a short time span. In conclusion, these results suggest that the presence of additives facilitate polymer crystallisation at a low temperature of 25 °C. However, this effect is restrained at high temperature due to the suppression of crystallisation behaviour at elevated temperature, while phase separation by liquid-liquid demixing dominates.

Regardless of the temperature, it is found that regions occupied by a one phase homogenous solution decreases with the increment in the concentration of additive used, as shown in Figure 3.5(a)-(c). Therefore, it can be said that these additives act

as anti-solvent, reducing the solvent power and system tolerance for water, and hence favouring the phase inversion process of the polymer solution. Similar to the observation made by Cheng (1999), the isothermal precipitation curves obtained at different temperatures were found to shift in a parallel mode. In this study, the curves shifted to the left with increasing quantity of additive used and shifted to the right when the solution temperature was increased, as shown in Figure 3.5(a)-(c).

3.5.3 CLOUD POINT BEHAVIOUR

In this section, discussion will be made on the cloud points of 10 wt%, 15 wt% and 20 wt% PVDF / DMAc system induced with the addition of different non-solvents, i.e. water, ethanol and glycerol, which were investigated over a temperature range of 30 °C to 70 °C. It is evident that the addition of non-solvent 'diluted' the solvent power and eventually resulted in solution cloudiness, i.e. a clear demonstration of the poorer molecular dispersion. The ease of cloud points obtained consistently followed the trend of water > glycerol > ethanol. The amount of non-solvent required to induce the cloud points followed the trend of ethanol > glycerol > water. This demonstrates that water is the strongest non-solvent, while ethanol is the weakest non-solvent of the three studied, as illustrated in Figure 3.6. It is important to note our experimental observation on the overlap between solution cloud point and its gelation behaviour. In some cases, especially at higher concentrations (more commonly at lower temperatures), the cloudy solution turned into a turbid gel after prolong standing. Experimental observations suggested that this gel could be returned to its liquid state by slight elevation of solution temperature, a phenomenon called thermally reversible gelation, which is commonly observed for crystallisable polymer (Domszy *et al.*, 1986). However, crystallisability is not a necessary condition for the formation of quasi-crosslinkages leading to thermal reversible gel networks. The key to the formation of gel lies on the thermodynamic heat of crosslinking (Morawetz, 1975).

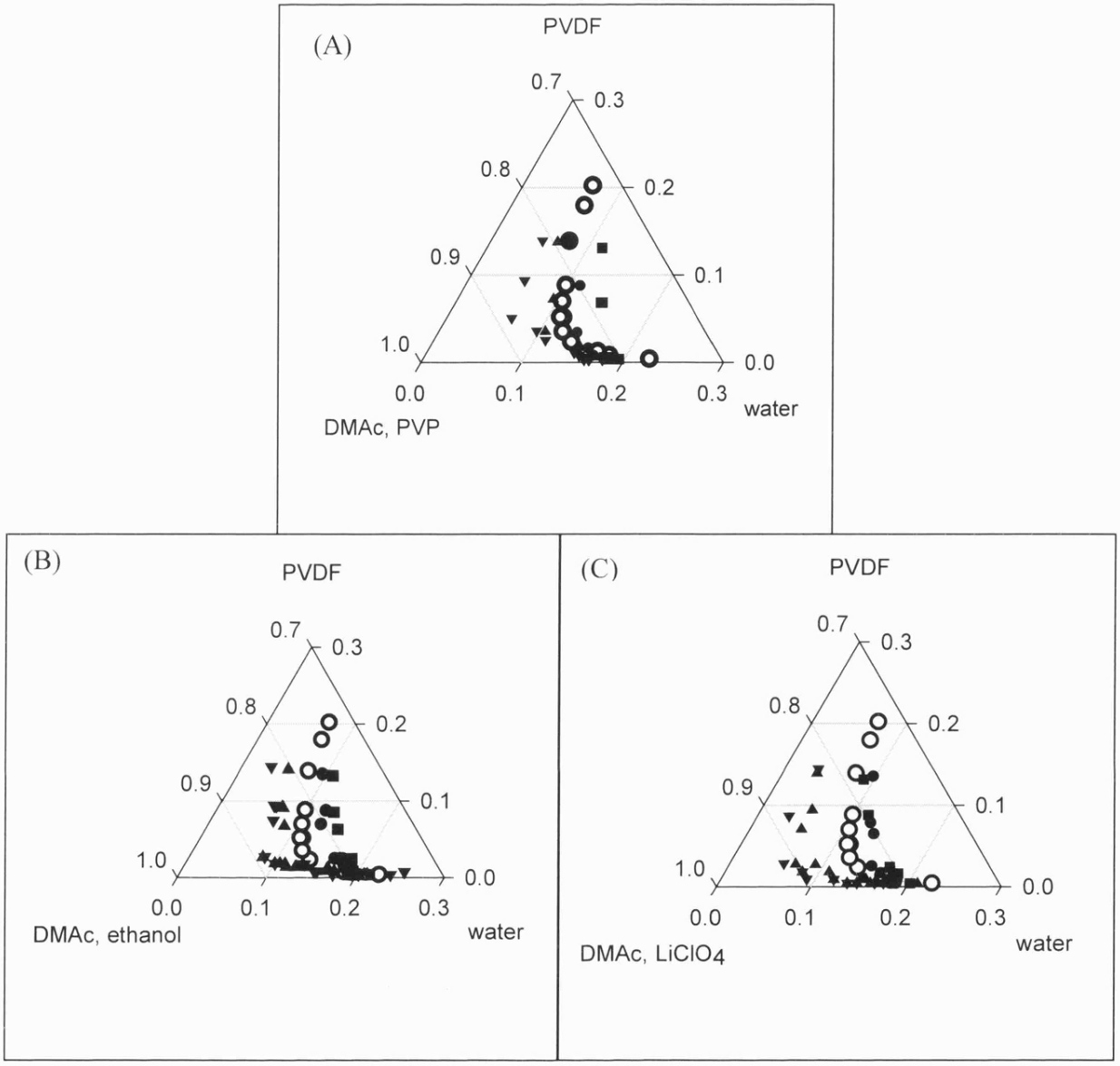

Figure 3.5 Effects of additives concentrations on the precipitation curves of PVDF / DMAc / water ternary system at 25 °C and 70 °C : (A) PVP, (B) ethanol, (C) $LiClO_4$
▲ 2 wt% at 25 °C; ▼ 6 wt% at 25 °C; ● 2 wt% at 70 °C; ■ 6 wt% at 70 °C; ○ no additive at 25 °C

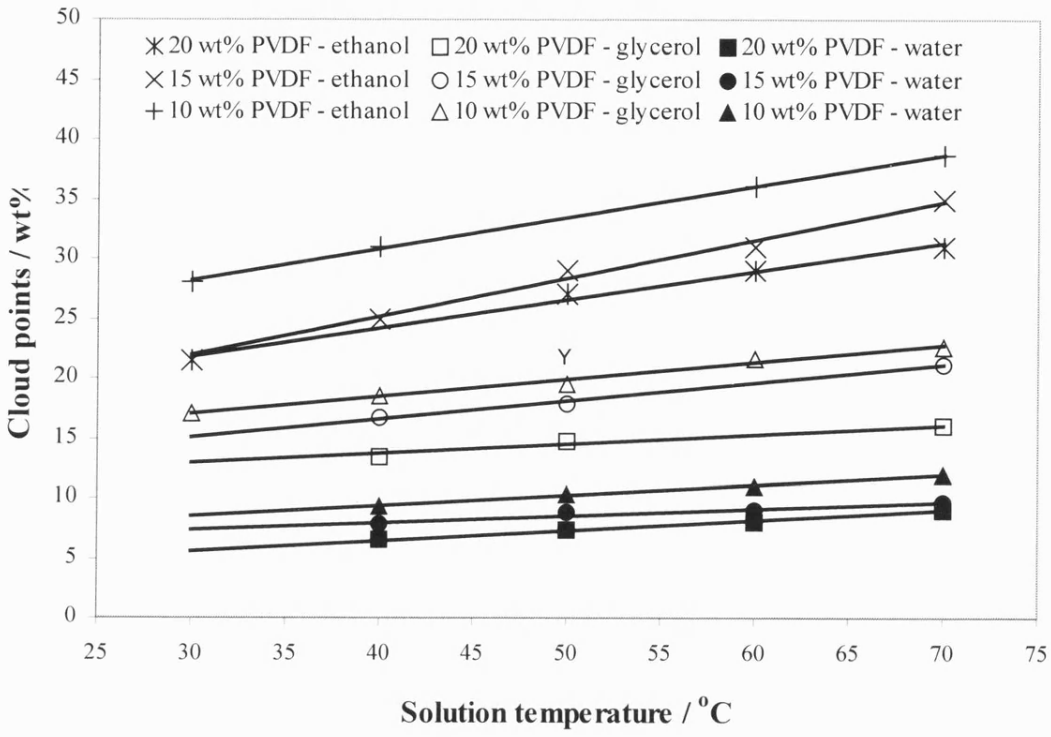

Figure 3.6 The cloud points concentration of water, ethanol and glycerol for 10 wt%, 15 wt% and 20 wt% PVDF / DMAc solutions for temperature range of 30°C – 70°C

3.5.4 Effect of Solvents on Solution Viscosity

Viscosity is a basic parameter in membrane making processes. In the casting of flat sheet membranes, solution viscosity determines the resulting membrane thickness. In the spinning of hollow fibres, solution viscosity is one of the key factors in determining the solution spin-ability, i.e. in the extrusion of hollow fibres, in addition to spinneret size, coagulation medium used, etc. Additionally, solution viscosity has a strong influence on the inter-diffusion of solvent and non-solvent during the phase inversion process, which then controls the kinetic aspect of the membrane formation processes, including the skin formation as well as substructure morphology. Information on solution viscosity is therefore crucial because of its influence on the resulting membrane morphology and performance.

As summarised in Table 3.1, the viscosity of 15 wt% PVDF polymer solution prepared using four different solvents, i.e. DMAc, DMF, NMP and TEP were measured and found to follow the order of TEP (1211 cP) > NMP (1167 cP) > DMAc (619.5 cP) > DMF (488 cP). This is in accordance to their respective formula weights, i.e. TEP (M_w=182.16) > NMP (M_w=99.13) > DMAc (M_w=87.12) > DMF (M_w=73.10). As the molecular size increases, greater restriction was imposed on the intermolecular interactions between polymer-polymer and polymer-solvent and their chain mobility, hence resulted in higher solution viscosity. It is also important to note that homogeneous solution comprises of longer intermolecular chain will precipitate first when there is a change in solution properties, such as a temperature change or addition of non-solvent (Young and Lovell, 1991).

Table 3.1 Solution viscosity of 15 wt% PVDF solution for four different solvents

Molecular formula	**Structural formula***	**Molecular weight* / g.mol^{-1}**	**Density* / g. cm^{-3} at 20°C**	**Solution viscosity** / cP at 30°C**
DMF (C_3H_7NO)	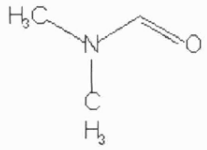	73.10	0.94	488.0
DMAc (C_4H_9NO)	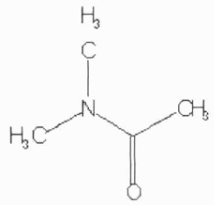	87.12	0.94	619.5
NMP (C_5H_9NO)	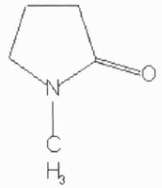	99.13	1.03	1167
TEP ($C_6H_{15}O_4P$)	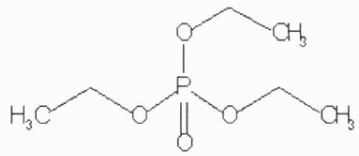	182.16	1.06	1211

(*Source: Sigma Aldrich product catalogue, 2003; ** measured using Bohlin Rheometer Measuring System 4/40)

3.5.5 Effect of Polymer Concentrations on Solution Viscosity

Using DMAc as solvent, the viscosity of 10 wt%, 15 wt% and 20 wt% PVDF / DMAc polymer solutions were measured, as listed in Table 3.2. As expected, solution viscosity increases with increased polymer concentration, i.e. 112.3 cP, 619.5 cP and 2137.5 cP for 10 wt%, 15 wt% and 20 wt% PVDF / DMAc polymer solution, respectively. This is attributed to the increased number of polymer molecules present, resulting in a stronger intermolecular interaction, as more polymer molecules are now present.

Table 3.2 Effect of polymer concentration on PVDF / DMAc solution viscosity (at 30 °C)

PVDF polymer concentration	Solution viscosity /cP
10 wt%	112.3
15 wt%	619.5
20 wt%	2137.5

3.5.6 Effect of Additives On Solution Viscosity

The effect of additives (ethanol, PVP and $LiClO_4$) on the viscosity of 15 wt% PVDF / DMAc system were also investigated at solution temperature of 30°C. For 15 wt% PVDF / DMAc system, the addition of 2 wt% ethanol had little or no impact on the solution viscosity; however, a slight decrement in the solution viscosity was detected with the addition of 6 wt% ethanol, i.e. 584.3 cP, as compared to 613.6 cP for plain 15 wt% PVDF / DMAc polymer solution. In this case, ethanol acts as a weak co-solvent in the PVDF/DMAc system by enhancing the chain mobility and molecular distribution in the PVDF /DMAc system. This is in opposition to its role as a non-solvent in inducing cloud points of PVDF / DMAc system when high concentration of ethanol is present (as shown in Figure 3.6, Section 3.5.3), as ethanol has greater miscibility with DMAc when compared to PVDF polymer.

The addition of either PVP (M_w = 10 kDa) and $LiClO_4$ caused a significant increase in the solution viscosity, as shown in Figure 3.7. Between PVP and $LiClO_4$, the

former could dissolve more easily in DMAc, which suggest its higher affinity and greater chain mobility in DMAc solvent solution. The presence of $LiClO_4$ increases the solution viscosity greatly due to the high affinity of Li^+ with DMAc solvent molecular. As a result of this solvent-solute interaction between DMAc and PVDF polymer were adversely affected.

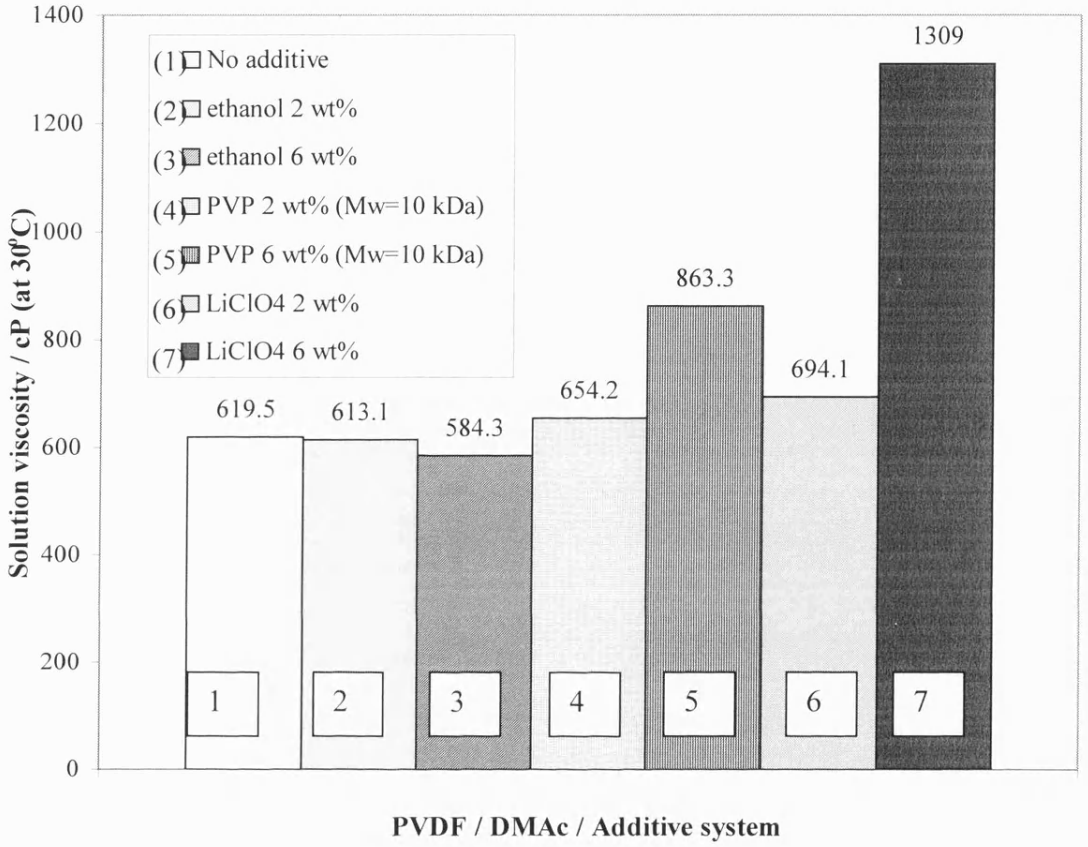

Figure 3.7 Effect of additives (ethanol, PVP (M_w=10 kDa) and $LiClO_4$) on the viscosity of 15wt% PVDF / DMAc solution at 30°C

3.5.7 Effect of Solution Temperature on Viscosity

The effects of temperature on the viscosity of 15 wt% and 20 wt% PVDF solution were studied over the temperature range of 20 °C to 60 °C. As shown in Figure 3.8 solution viscosity generally decreases with the increase in solution temperature. This is primarily due to the increase in polymer-solvent and polymer-polymer chain mobility (and flexibility) at higher temperature. Between the two, it is evident that solution temperature has greater impact on the viscosity of 20 wt% PVDF/DMAc solution as it decreases more sharply with increase temperature. Meanwhile, a near

plateau region with slow decrement in viscosity was observed between 30 °C and 55 °C for 15 wt% PVDF / DMAc solution. This could be explained based on the lower number of polymer-solvent and polymer-polymer interactions present in the latter case. Similar trend f viscosity decrement with the increase in solution temperature was also observe for PVDF / DMAc solution in the presence of various amount of $LiClO_4$ and PVP as additives, as shown in Figure 3.9.

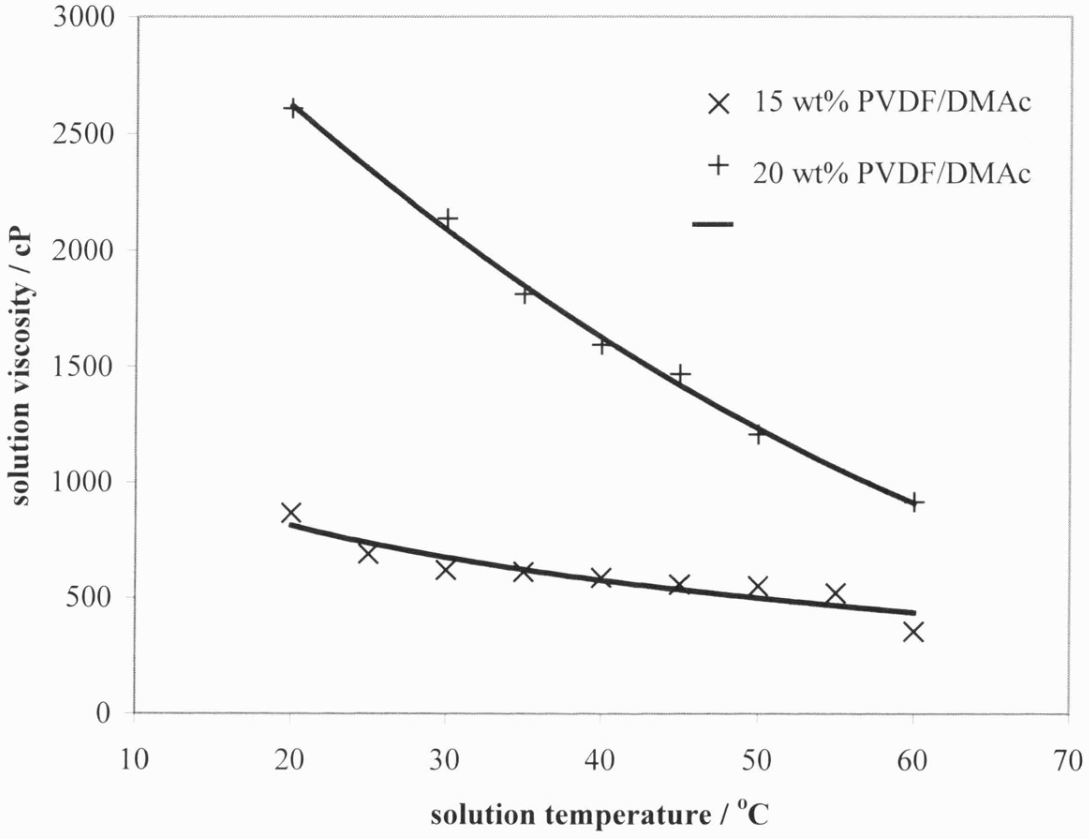

Figure 3.8 Effect of solution temperatures on the viscosity of 15 wt% and 20 wt% PVDF / DMAc solution over a temperature range of 20°C to 60°C

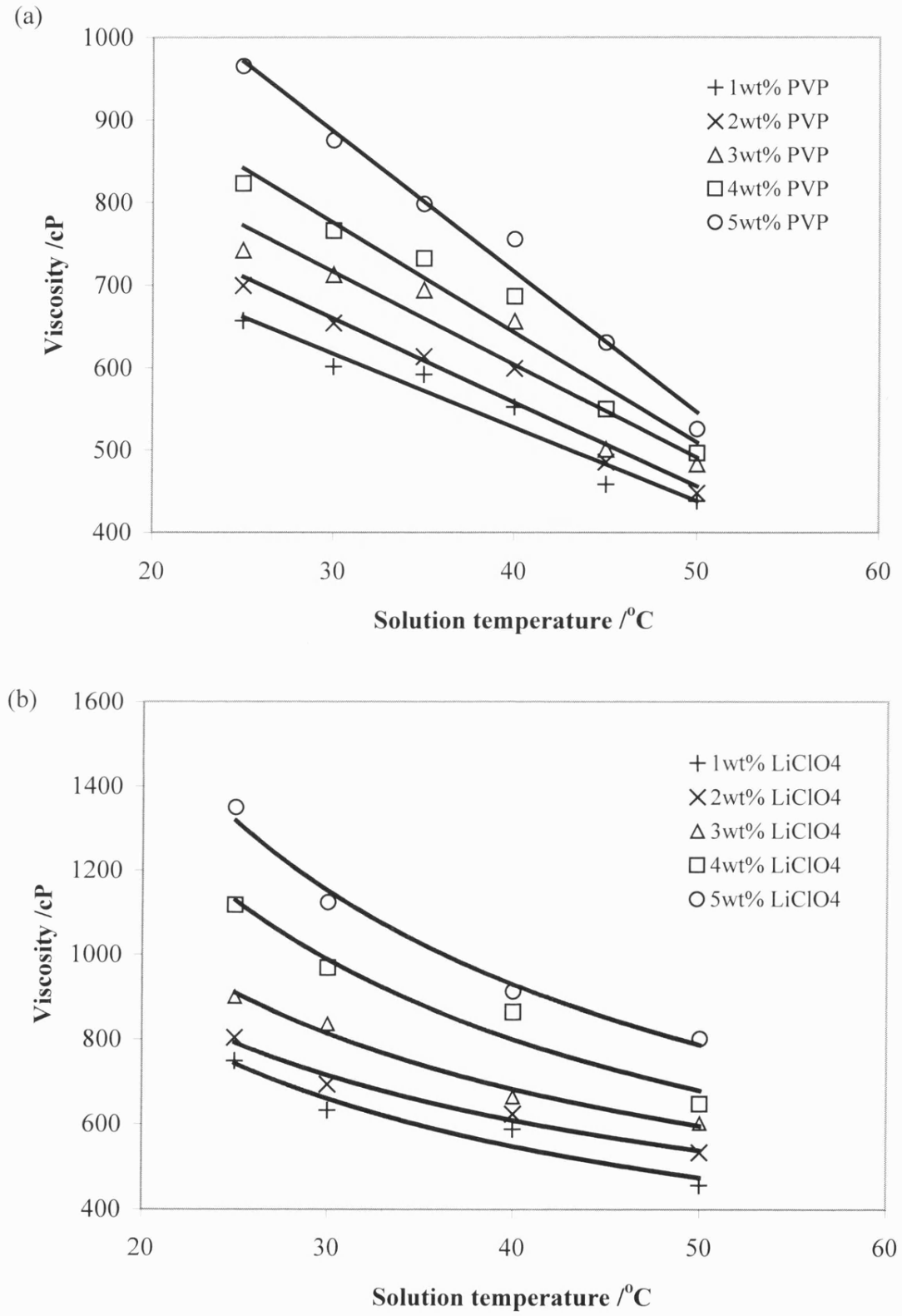

Figure 3.9 Effect of temperatures on the viscosity of PVDF / DMAc solution with the addition of 1 wt% to 5 wt% of non-solvent additives : (a) PVP (M_w = 10kDa) and (b) $LiClO_4$

3.6 CONCLUSIONS

Polymer precipitation curves for poly(vinylidene fluoride) (PVDF) were generated for four different solvent systems, i.e. DMAc, DMF, NMP, and TEP, using water as a non-solvent. Experimental results show solvent strength to be in the order of DMAc > NMP > DMF > TEP. Viscosity measurement showed that solution viscosity increased in accordance to the solvent molecular weight, i.e. TEP > NMP > DMAc > DMF.

Using DMAc as solvent, the presence of additives, i.e., ethanol, $LiClO_4$, and PVP (M_w =10 kDa) decreased the width of the one-phase homogeneous region on PVDF / DMAc / water ternary phase diagram following the trend of $LiClO_4$ > PVP (M_w = 10 kDa) > ethanol at both 25 °C and 70 °C. The presence of $LiClO_4$ and PVP (M_w = 10 kDa) increased the solution viscosity, however the presence of ethanol reduced the solution viscosity, suggesting its role as a weak co-solvent at low concentration. At higher concentration, ethanol was found to be the weakest non-solvent among the three studied, i.e. ethanol < glycerol < water.

In all cases, the effect of additives and their concentrations on the cloud point behaviour was found to be less significant at the higher temperature of 70 °C. Based on the phase separation behaviour observed, experimental results recognised the fact that elevated temperature suppresses gelation and polymer crystallisation and favours liquid–liquid demixing; thus it is expected to result in a more porous membrane structure. A decline in solution viscosity with solution temperature was recorded for all systems studied.

CHAPTER FOUR
MORPHOLOGICAL STUDY OF PVDF ASYMMETRIC MEMBRANES PREPARED VIA IMMERSION PRECIPITATION

4.0 FOREWORD

Asymmetric poly(vinylidenefluoride) (PVDF) membranes were cast using commercial grade Kynar® K760 polymer pellets, using four different solvent systems namely *N, N*-dimethylacetamide (DMAc), *N,N*-dimethylformamide (DMF), 1-methyl-2-pyrrolidone (NMP) and triethyl phosphate (TEP). Focusing on the PVDF / DMAc system, the effects of various additives, such as ethanol, glycerol, lithium chloride (LiCl), lithium perchlorate ($LiClO_4$), polyvinylpyrrolidone (PVP, M_w = 10 kDa, 40 kDa and 130 kDa) and water on the resulting membrane morphology were investigated. The effect of the dope solution temperature on the membrane morphology was also studied for the various additives used. The resulting membrane morphologies were examined using scanning electron microscopy (SEM).

4.1 THE DEVELOPMENT OF PVDF MEMBRANE FABRICATION

As discussed in Section 3.1, the emergence of poly(vinylidene fluoride) PVDF polymer as a popular membrane material is due to its excellent chemical and thermal resistance (Lovinger, 1982; Young and Lovell, 1991). These features are especially important in various industrial applications involving strong and corrosive chemicals. For a successful membrane application, the choice of a compatible membrane material with suitable membrane morphology is crucial. Indeed, membrane properties are very much task specific, i.e. different separation applications require different membrane properties, which are directly related to the membrane structure. Generally, membrane morphology can be controlled by altering the dope composition or by controlling the condition at which the membrane is formed.

As discussed in Sections 2.2 and 2.3, composition pathway of a membrane formation mechanism is a direct result of the combined effect of (a) thermodynamic properties of the dope composition, and (b) diffusional kinetics of the solvent / non-solvent exchange upon immersion in the coagulation bath. Little control can be achieved over the diffusional kinetics of solvent / non-solvent exchange. However, the thermodynamic properties of the polymer dope can be altered by careful formulation of the polymer dope recipe. In this regard, the two main parameters with strong impact on the final membrane morphology are the solvent selection and additive used (Kesting, 1971, 1985). In addition, the temperatures of polymer solution and coagulation bath, as well as the composition of coagulation bath are also frequently considered in attempts to idealise the membrane morphology (Mulder, 1996). Indeed, a desired membrane structure could be engineered and a satisfactory membrane separation performance could be promoted using the *'suitable'* dope composition at *'suitable'* conditions.

In the past, much research on PVDF membrane has been conducted, mainly seeking correlation between membrane morphology and performance with the varying dope compositions (i.e. molecular weight of polymer, solvent and additives used) and preparation parameters (i.e. coagulation medium, quenching bath temperature, evaporation time) (Sugihara *et al.*, 1979; Uragami *et al.*, 1980; 1981; Munari *et al.*, 1983; 1990; Bottino *et al.*, 1981; 1985; 1986; 1988a; 1988b; 1991; Boom *et al.*, 1992; Mulder, 1996; Tomaszewska, 1996; Deshmukh and Li ., 1998; Wang *et al.*, 1999; 2000). In most cases, it is of interest to obtain both good permeability and high mechanical strength of membranes. These are known beneficial properties commonly related to the membrane morphology. As noted in Chapter 3, PVDF polymers exhibited more complex phase separation behaviours primarily due to their semi-crystalline nature, hence making the morphology control process more complicated. In the following sections, effects of dope composition and various preparation parameters on the resulting PVDF membrane morphology and performance will be discussed.

4.1.1 EFFECT OF SOLVENTS ON MEMBRANE MORPHOLOGY

Solvent is undoubtedly the major component in a casting solution, as it typically constitutes of 70-80% of the overall dope content. It plays a very important role in the final membrane properties and performance. Bottino *et al.* (1985, 1986, 1988a, 1988b) and Munari *et al.* (1983, 1990) have done excellent fundamental work providing essential information on PVDF polymer-solvent interaction. Using the Hansen solubility parameter, Bottino *et al.* (1988) identified 8 organic solvents out of forty-six that were screened to be good solvents for the PVDF polymer studied (i.e. Foraflon 1000HD with average molecular weight of 450,000). The eight solvents identified were N,N-dimethylacetamine (DMAc), N-methyl-s-pyrrolidone (NMP), N,N-dimethylformamide (DMF), dimethylsulphoxide (DMSO), hexamethylphosphoramide (HMPA), tetramethylurea (TMU), triethyl phosphate (TEP) and trimethyl phosphate (TMP). Of these solvents, DMAc, DMF, NMP and DMSO have been widely used as the high boiling point strong solvent, accompanied by either acetone or tetrahydrofuran (THF) as the low boiling point weak solvents in the casting of flat sheet membranes (Sugihara *et al.*, 1979; Uragami *et al.*, 1980, 1981a, 1981b; Bottino *et al.*, 1986; 1988a; 1988b; 1991).

Bottino *et al.*, (1991) attempted to correlate the membrane structures with the thermodynamic properties of the casting solution. In their study, the solubility parameters for polymer-solvent and solvent-non-solvent, polymer solvent compatibility, cloud points, solvent-non-solvent excess enthalpy of mixing, casting solution viscosity and solvent-nonsolvent diffusivity were measured and evaluated. Unfortunately, no conclusion could be made on the thermodynamic properties measured. Also, no relationship between the membrane structure and solvent strength could be concluded. However, some distinctions between general membrane structures produced using the eight solvents used were observed, as recapitulated in Table 4.1.

Similar combination of a low boiling point weak solvent (i.e. acetone and THF) with a high boiling point strong solvent (i.e. DMSO, DMF, NMP or DMAc) was used in the making of PVDF membrane (Sugihara *et al.*, 1979; Uragami *et al.*, 1980, 1981a, 1981b). Generally, higher solute rejections and lower permeation rate were recorded

following the increase in the weak solvent concentration. Due to the evaporation of low boiling point solvent during the exposure period, the casting solution became gradually richer in the high boiling point strong solvent, which is believe to have a high capacity of water absorption. The water molecules absorbed acted as the non-solvent, which then result in fast polymer precipitation and the formation of a dense membrane structure, which is responsible for the lower permeation, and higher rejection rate. Concentration polarisation was held responsible for the deviation recorded when tested with higher molecular weight solutes. The effects of various other parameters such as polymer concentration, heat treatment and operating temperature on the membrane performance were also studied. However, the absence of SEM micrographs in the papers makes it impossible to evaluate the relationship between the permeation behaviour with the structural properties of the membranes.

Table 4.1. Effects of solvent on PVDF membrane morphology (Bottino *et al.*, 1988)

Solvent	General membrane structures
TEP	Membrane with honeycomb structure without cavities. Size of alveoli progressively increases from the top to the bottom of the membrane.
DMF	Large number of short finger like cavities beneath the upper layer. The cavities are separated by walls composed of discrete polymer globules.
DMAc TMU TMP	The cavities progressively extend through a considerable fraction of the membrane thickness. Globules near upper layer are larger and more compact.
NMP DMSO	Cavities grow in breadth and length towards the bottom of the membrane without a well-defined shape.
HMPA	Short cavities and isolated voids appear in the porous globular sublayer.

4.1.2 Effect of Additives on Membrane Morphology

It has been reported that the small critical surface tension of PVDF (i.e. about 25 dynes. cm^{-1}) restricts the penetration of coagulant (water) into the nascent membrane (Kong, 2000). With its weak coagulant-polymer interaction and slow coagulation rate, formation of membranes with low permeation rate is inevitable.

Fortunately, this can be overcome by introducing a suitable non-solvent additive (pore former) into the casting solution so as to increase the final membrane porosity.

In brief, additives used in the fabrication of PVDF membranes could be broadly categorised into four groups: (a) polymeric additives such as polyvinylpyrrolidone (PVP) and polyethylene glycol (PEG); (b) weak non-solvents such as glycerol; (c) weak co-solvents such as ethanol and acetone; and (d) small molecular weight inorganic salts such as lithium chloride (LiCl). Effects of additives on the resulting PVDF membrane morphology have been reported in various literatures (Bottino *et al.*, 1985; 1986; 1988; 1991; Uragami *et al.*, 1981; Deskmukh and Li, 1998; Wang *et al.*, 1999; 2000), however the role of different additives will nevertheless vary in different polymer / solvent systems, as will be summarised in the following paragraphs.

The addition of PVP and PEG has been reported to favour macrovoid formation in the fabrication of PVDF membranes (Uragami *et al.*, 1981; Bottino *et al.*, 1988; 1991; Munari *et al.*, 1990; Tomaszewska, 1996; Deshmukh and Li, 1998; Wang *et al.*, 1999). Solution viscosity increases with the addition of either PVP or PEG. This increment is strongly dependent on the molecular weight of PVP and PEG (Uragami *et al.*, 1981; Wang et al., 1999). The increase in solution viscosity reduces the miscibility of casting solution with non-solvent, hence hinders the phase separation kinetics but greatly enhances the thermodynamics for phase separation.

Uragami *et al.* (1981) demonstrated the great improvement of PVDF membrane permeability following the addition of PEG into dope solution containing NMP and THF. With its high affinity for water, the presence of PEG enhances the inflow of water that promotes polymer precipitation, hence resulting in an increase in the size of finger like cavities. It has also been demonstrated that the size of finger like cavities corresponds with the amount or molecular weight of PEG added into the casting solution (Bottino *et al*, 1986). This resulted in membrane with greater permeation flux but a marked decline in membrane rejection and mechanical strength. It should be noted, however, that this is an isolated case; it is absolutely

possible to obtain an increase in membrane rejection, after all, it is down to the pore density and pore size distribution of the membrane prepared.

Shih *et al.* (1990) reported on the usage of glycerol as a non-solvent additive for different solvent systems. Interestingly, for the case where TEP was used as solvent, an increase in glycerol concentration produced membranes with increasing mean pore size and effective porosity, due to thin skin formation. In contrast, for the case where DMSO was used as solvent, an increase in glycerol concentration resulted in a membrane with increased mean pore size, but decreased effective porosity. These differences are attributed to the different affinity of the solvent toward the gelation medium, which can be easily measured using the solubility parameter, which is known to be 8.0 for TEP, 13.0 for DMSO and 23.4 for water. High water affinity of DMSO is believed to be the reason of rapid precipitation rate that leads to the formation of a finger-like structure.

Lithium chloride (LiCl) is another widely used additive in PVDF membrane manufacturing, as it promotes good membrane porosity, smaller average pore and membrane hydrophobicity (Bottino *et al.*, 1988; Wu *et al.*, 1991; Tomaszewska, 1996; Wang *et al.*, 2000; Kong and Li, 2000). Dramatic increase in the dope solution viscosity with the addition of lithium chloride (LiCl) was reported to be the result of the formation of a complex between DMAc and LiCl; as well as macromolecular fluctuating networks between Li+ and the electron donor group of PVDF (Tomaszewska, 1996; Bottino *et al.*, 1988). Also, addition of LiCl has been reported to enhance the membrane permeation performance, but with a reduction in its mechanical strength (Munari, *et al.*, 1990; Tomaszewska, 1996). Wang *et al.*, (2000) however managed to retain the membrane mechanical strength by co-introducing 1-propanol. Due to its good water affinity, the presence of LiCl tends to encourage the water inflow, and enhance the coagulation rate, and hence produce a membrane with good interconnectivity. For an additive that is of weak non-solvent nature such as glycerol, its presence in the dope solution brings the initial composition of the casting solution nearer to the binodal (Boom *et al.*, 1992).

4.1.3 Effect of Polymer Properties on Membrane Morphology

According to Shih *et al.* (1990), membranes cast from high molecular weight polymer have a smaller mean pore size but a higher effective porosity. However, the gas permeability data recorded was found to be considerably lower than membrane cast from low molecular weight polymer, due to the presence of a relatively dense skin layer of 2-3μm. As for the polymer concentration is concerned, it is expected that an increased in polymer concentration would result in a decrease in membrane mean pore size as well as membrane porosity, in accordance with the permeability data reported by Shih *et al.* (1990). Other intrinsic polymer properties such as degree of polymerisation, percentage of crystallinity will inevitably affect the final membrane property. However, correlation between these information and the final membrane properties is yet to be established.

4.1.4 Effect of Coagulation Medium on Membrane Morphology

Coagulation medium is an important preparation parameter in the formation of phase inversion membranes; it is the medium where phase inversion takes place to form the nascent membrane. The formation of top skin layer is known to be a result of the instantaneous polymer precipitation upon immersing in quenching bath (Strathmann, 1971; 1975; 1985; 1986). The formation of finger-like cavities beneath top skin is generally associated with a high rate of polymer precipitation, which increases with the increase in the solvent outflow and non-solvent inflow (Boom *et al.*, 1992). The large macrovoid cavities in the membranes is believed to originate from convective flows formed within the cast fluid solution upon the immersion in the non solvent bath for final precipitation (Frommer and Messalem, 1973). This is mainly due to the high penetration tendency of the non-solvent to mix with the solvent (and therefore it's often described as mixing currents) (Cheng et al., 1999). On the other hand, weak coagulation medium results in slow coagulation rate, hence results in a porous sponge-like structure (Kesting, 1985).

Generally, porous structures with polymeric globules, macrovoids and finger-like cavities tend to disappear with the substitution of water with poor coagulants such as alcohols or organic solvents in the coagulation medium. This results in a slower coagulation rate and hence produces membranes with porous sponge-like structures

without cavities (Kesting, 1985). A lower membrane flux with membrane rejection achieving its climax before declining was reported (Bottino *et al.*, 1985). In some cases, the membranes produced were reported to be very brittle and hard to handle, with no significant Dextran rejection. This is especially true when alcohol content in the coagulation medium exceeded 40% and DMF concentration exceeded 60%. Deshmukh and Li (1998) reported their findings using ethanol (10-50%) in water as coagulation medium, where long finger-like structure near the outer wall of the fiber slowly changed through a short finger-like structure to a sponge-like structure, as the concentration of ethanol in the coagulation medium increases.

In has been reported that an increase in the temperature of coagulation medium tends to enhance both the rate of exchange between casting solvent and coagulant medium, as well as the polymer solubility (Bottino *et al.*, 1985). However, the effect on the former was found to be more dominant. With increasingly rapid precipitation rate (due to a higher non-solvent intrusion rate at higher temperature), the size of macrovoids and finger-like cavities become bigger, and membrane structures were found to shift from having porous structure comprises of polymeric globules to porous alveolar structure as coagulation bath temperature increased from 20°C to 70°C. As a result of this, an increase in membrane flux with increasing coagulation bath temperature was noted (Bottino *et al.*, 1985). Wang *et al.* (2000), however, noted a slight decline in membrane permeability with increased coagulation bath temperature.

4.2 MATERIALS AND METHODS

4.2.1 MATERIALS

Kynar®K760 poly(vinylidene fluoride) (PVDF) polymer pellets used were purchased from Elf Autochem, USA, and were pre-dried at 50°C prior to use. *N,N*-dimethylacetamide (DMAc) [99.9+%, HPLC grade] and 1-methyl-2-pyrrolidone (NMP) [99+%, spectrophotometric grade], *N,N*-dimethylformamide (DMF) [99.8%, ACS reagent garde] and triethyl phosphate (TEP) [99%, GC grade] were used as solvents. Ethanol [reagent grade], glycerol [M_w = 92.09 g. mol^{-1}, 99%], lithium chloride (LiCl) [99+%, ACS reagent grade], lithium perchlorate ($LiClO_4$) [99+%,

ACS reagent grade] and polyvinylpyrrolidone (PVP) [99.9+%, M_w=10 kDa, 40 kDa, 90 kDa and 130 kDa] were used as additives. All chemicals were purchased from Sigma Aldrich and used as received. In all cases, tap water (controlled at desired temperature) was used as the coagulation bath medium.

4.2.2 Preparation of PVDF Polymer Solution

Desired amount of PVDF polymer pellets were weighed and poured into pre-weighted solvents contained in Duran PTFE lined bottles. After subjecting the mixture to vigorous shaking to ensure thorough wetting of polymer pellets, desired quantity of additive (when applicable) was added. The mixture was kept at 60°C isothermal water bath, and was subjected to mechanical shaking [Grant OLS200] so as to assist its dissolution. Once fully dissolved, the mixture was allowed to return to room temperature of 20°C in an isothermal water bath prior to use.

4.2.3 Casting of PVDF Flat Sheet Membranes

The polymer dope solution was cast as a thin film onto glass plates at either 20°C or 50°C and 60±5% RH by use of a 200 μm gap casting knife and immersed into water bath at either 20°C or 50°C, after approximately 10 seconds of evaporation time. The flat sheet membranes formed were kept in a fresh water bath for three days prior to characterisation, to ensure complete removal of residual solvent.

4.2.4 Characterisation of PVDF Flat Sheet Membranes

The cross section structures of the flat sheet membrane were examined using a scanning electron microcscope (SEM) [JEOL JSM-T330 and JEOL JSM-T6310]. The fresh membranes cut into small stripes of approximately 5mm wide and 5cm long for the ease of handling. After half an hour of immersion in pure ethanol, the samples were dipped in liquid nitrogen and then freeze fracture using two forceps. The fractured samples were placed in a petri-dish layered with tissue for the removal of excess moisture. Following that, the membrane sample was adhered on a special aluminium dish using a conductive pad and placed in a silica gel container overnight to ensure thorough removal of moisture from the membrane pores. A thin layer of gold coating was then deposited using [Edwards Sputter Coater S150B] prior to the morphological examination using scanning electron microscope (SEM) [JEOL JSM-

T330]. The pure water flux measurements were carried out in a laboratory-scale test unit. With active membrane area of about 5 cm^2, the water permeation flux was measured using distilled water at room temperature (19-20 ^oC) and a constant working pressure of 1 bar, whereby a stable water flux was obtained after an hour of operation.

4.3 RESULTS AND DISCUSSIONS

In this study, we first compare the morphology of PVDF membranes cast using four different solvents that have been reported to be good solvents for PVDF polymer, i.e. DMAc, DMF, NMP and TEP. Using the PVDF / DMAc system, we sought to compare the effects of different additives (PVP, ethanol, glycerol, LiCl, $LiClO_4$ and water) on the resulting membrane morphology.

4.3.1 EFFECT OF DIFFERENT SOLVENTS ON MEMBRANE MORPHOLOGY

In the preparation of polymer membranes via the phase inversion process, it is crucial that the polymer solution remains in a uniform and stable state (as explicitly discussed in section 2.3). Although one or more solvents may be suitable for a particular polymer, another key consideration is that both the solvent and non-solvent must be completely miscible with one another. In this study, four solvents (DMAc, DMF, NMP and TEP) with different solvent power to PVDF polymer were used to study the morphology of PVDF flat sheet membranes prepared by the immersion precipitation method, whereby pure water was used as the coagulation bath medium. The SEM photographs of these membranes are shown in Figure 4.1.

The relative strength of these four solvents has been discussed based on their respective isothermal ternary phase diagram (Figure 3.3) presented in Section 3.5.1. In short, the solvent strength follows the trend of DMAc > DMF > NMP > TEP. As tabulated in Table 3.1 (Section 3.5.4), solution viscosity of PVDF polymer in these four solvents follows the trend of PVDF / TEP > PVDF / NMP > PVDF / DMAc > PVDF / DMF at 30°C. In both cases, TEP appeared to be the weakest solvent of the four candidates. As shown in Figure 4.1, TEP is a relatively poor solvent among the four used, producing membrane with a symmetrical sponge-like structure through

the whole thickness, and no cavities at all. Due to its weak solvent power, minority presence of non-solvent (i.e. water in this case) was sufficient to disturb the stability of polymer / solvent / non-solvent system. Also, due to the narrow one-phase homogeneous gap of the PVDF / TEP system as shown in Figure 3.3, the system crossed the binodal boundary at an early stage. Another point to consider is the low mutual affinity between TEP and water as compared to NMP, DMF or DMAc (Bottino *et al.*, 1988), hence prohibiting extensive influx of water, and therefore macrovoids could not have developed. This finding is in partial agreement with Bottino *et al.* (1988). In their study, PVDF / TEP membrane exhibited honeycomb structures without cavities, with alveoli size progressively increasing from the top to the bottom of the membrane.

In the case of NMP, irregular macrovoids were observed beneath the skin layer. This structure indicates the formation of a skin layer at an early stage, leaving insufficient time for continuous exchange of solvent and non-solvent to take place. This is in good agreement with the finding of Bottino *et al.* (1988) whereby PVDF / NMP membrane were reported to have cavity growth in breadth and length towards the bottom of the membrane without a well defined shape. With further out-flow of solvent restricted by the presence of early skin formation, macrovoids were formed beneath the skin layer, resulting from the mixture of existing solvent and the penetrated non-solvent. Also, the high hydrophobicity of PVDF material aids in repelling the water entrance. As a result of this, there was not enough water in the substrate phase to induce phase inversion for the formation of a more porous substructure, while the macrovoids developed.

Flat sheet membranes cast using DMF and DMAc as solvents exhibited similar shorter finger-like structure with sponge substrate. These two typical structures indicate slower exchange rate between solvent and non-solvent in the immersion precipitation processes. According to Bottino *et al.* (1988), membranes produced from PVDF / DMF system have large numbers of short finger like cavities beneath the upper layer, which were being separated by walls composed of discrete polymer globules. Meanwhile, membranes produced using the PVDF / DMAc system were

reported to have cavities progressively extending through a considerable fraction of the membrane thickness with large and compact polymer globules near the upper layer.

While studying the effect of these four solvents on membrane morphology, all four membranes were cast using the same casting knife, i.e. with a gap of 200 μm. However, the resulting membrane thickness was found to follow the trend of NMP > TEP > DMF, DMAc. Membrane with the thickness of about 150 μm was obtained using NMP as solvent, was the thickest of all four. In this case, membrane shrinkage caused by out-flow of solvent from the original casting solution was very small due to formation of a membrane skin at an early stage, hence indicating a fast phase inversion process. Membrane cast using TEP as solvent was found to be approximately 60-70 μm and the thickness of the other two membranes cast using DMF and DMAc as solvents were the thinnest, measured at approximately 50 μm. More shrinkage could be caused by greater loss of solvent before the phase inversion process was completed. In order to understand the phase inversion behaviour of PVDF polymer solution, detailed investigation of its diffusional kinetics between solvent and non-solvent exchange is crucial. This, however, is beyond the scope of this study.

As a hydrophobic material, the entrance of water into PVDF casting solution is relatively slow during the immersion precipitation processes. By common sense, a greater amount of non-solvent is needed to induce the phase inversion when a stronger solvent is used. Introduction of non-solvent into the initial casting solution could accelerate this phase inversion process. As discussed in Section 3.5.1, DMAc demonstrated the strongest solvent power to PVDF polymer, as compared to the other three studied. Hence, DMAc was used in our further investigation on the effect of additives and other parameters on the membrane morphology, which will be discussed in the following sections.

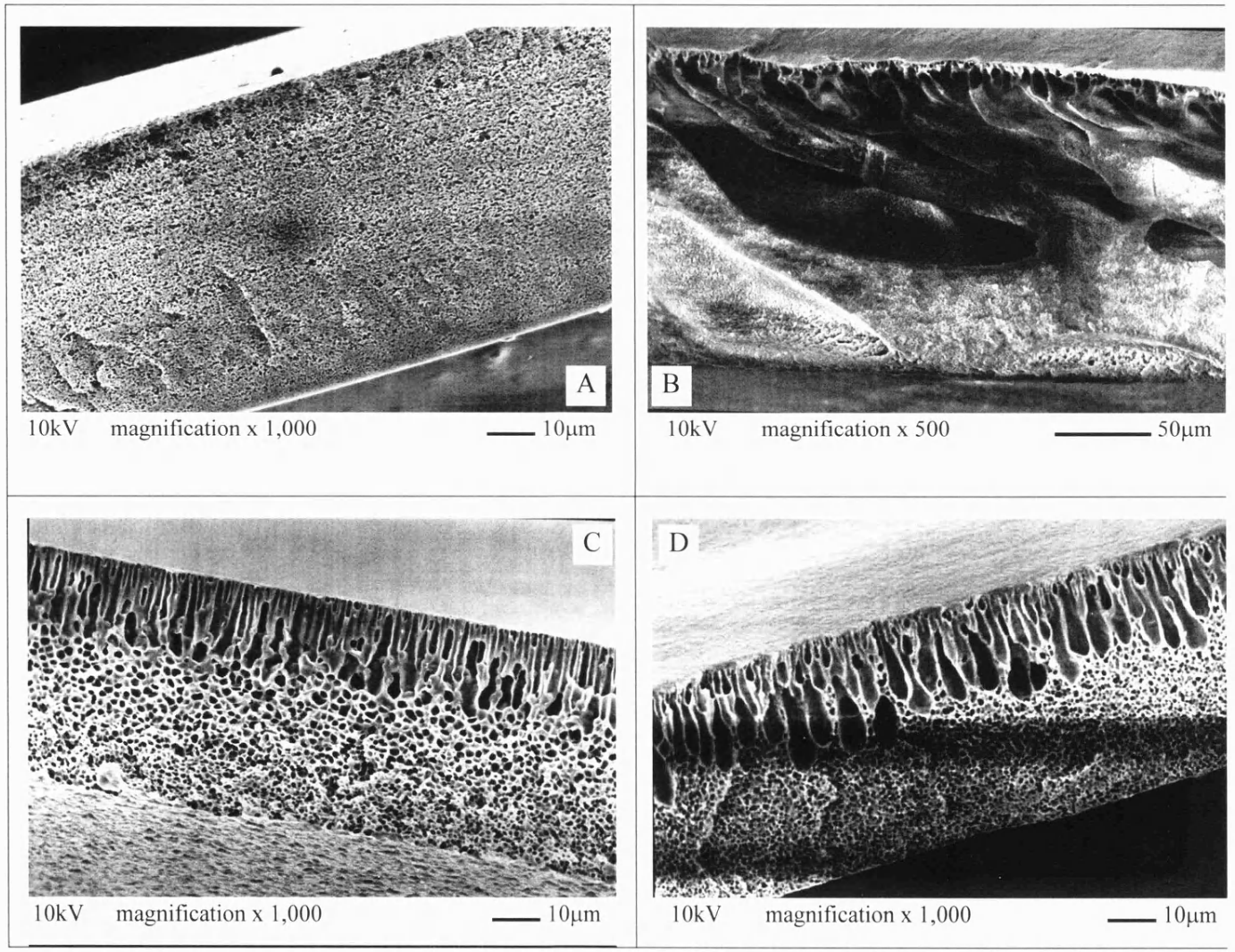

Figure 4.1 Cross sectional structure of membranes cast using 15 wt% PVDF and different solvents: (A) TEP; (B) NMP; (C) DMF and (D) DMAc using water at 25°C as coagulation bath.

4.3.2 EFFECT OF DIFFERENT ADDITIVES ON MEMBRANE MORPHOLOGY

In the following paragraphs, individual as well as combined effects of various additives, namely water, PVP (M_w =10 kDa, 40 kDa and 130 kDa), ethanol, LiCl, $LiClO_4$ and glycerol on membrane morphology will be presented and discussed.

Polyvinylpyrrolidone (PVP)

PVP has been widely used as pore former in membrane fabrication with profound effects on both membrane porosity and permeability (Uragami *et al.*, 1981; Bottino *et al.*, 1988; 1991; Munari *et al.*, 1990; Tomaszewska, 1996; Deshmukh and Li, 1998; Wang *et al.*, 1999). The addition of PVP is accompanied by an increase in the solution viscosity, as discussed in Section 3.5.4.

With reference to Figure 4.2, it is evident that the addition of PVP (M_w = 10 kDa) promotes the formation of macrovoids. This is primarily due to the hydrophilic nature of PVP that enhances the water influx. SEM micrographs also demonstrate the growth in the size of macrovoids as the amount of PVP increases. Extended finger like structure beneath the top skin of PVDF membrane could be clearly seen in Figure 4.2 (A) with the addition of 1 wt% PVP (M_w = 10 kDa). The addition of 3 wt% of PVP resulted in the extensive formation of medium size macrovoids beneath the top skin layer coupled with large macrovoids close to the bottom skin of the membrane, as shown in Figure 4.2 (B). With reference to Figure 4.2 (C), after a further increment in PVP (M_w = 10 kDa) concentration up to 5 wt%, massive macrovoids could be vividly seen extending from beneath the top skin layer throughout the entire membrane thickness. It is important to note that the extensive presence of such macrovoids could be detrimental to membrane mechanical strength (Wang *et al.*, 1999, 2000).

Figure 4.2 Cross sectional structures of 15 wt% PVDF membranes cast with different amounts of PVP (Mw = 10 kDa) as additive: (A) 1 wt% PVP; (B) 3 wt% PVP and (C) 5 wt% PVP using water at 20°C as coagulation bath.

Polyvinylpyrrolidone (PVP) and water

In this section, discussion is focused on the effect of combined addition of PVP (M_w = 10 kDa) and water as non-solvent additive on the membrane morphology and the membrane performance in terms of pure water flux. Cross sectional structures of membranes cast with the addition of water as additive, together with the presence of PVP (M_w = 10 kDa) and PVP (M_w = 90 kDa) in the polymer dope as pore former are as shown in Figure 4.3 (A-D) and Figure 4.4 (A-D) respectively. In both cases, micrographs revealed a reduction in the size of macrovoids as the amount of water added to the polymer dope increased. Also, the macrovoids appeared to be more regular with increasing amount of water added as non-solvent additive.

Table 4.2 summarises the final membrane thickness in relation to the amount of water added into the polymer dope comprises of 15 wt% PVDF / DMAc. For PVP (M_w = 10 kDa), no significant variation in membrane thickness was noted (as shown in Figure 4.3). As for PVP (M_w = 90 kDa), a noticeable increment of 25% in final membrane thickness was recorded when 5.5 wt% of water was added (as shown in Figure 4.4).

Table 4.2 Effect of water content on the final membrane thickness using polymer dope containing 15 wt% PVDF / DMAc at 20°C

10 wt% of PVP (M_w = 10 kDa)		**4 wt% of PVP (M_w = 90 kDa)**	
Amount of water / wt%	**Approx membrane thickness / μm**	**Amount of water / wt%**	**Approx. membrane thickness / μm**
0.0	120	0.0	120
2.0	100	2.0	110
3.7	110	3.6	110
4.6	100	5.5	150

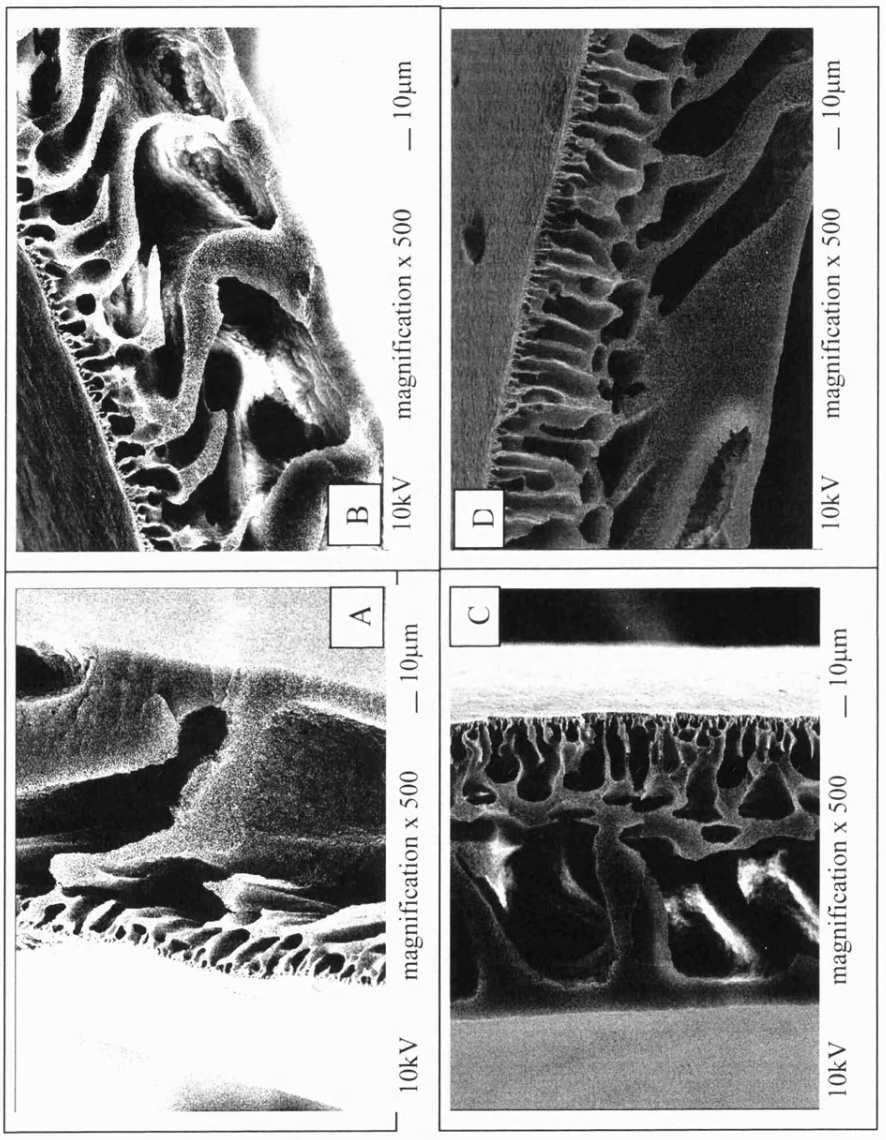

Figure 4.3 Cross sectional structures of 15 wt% PVDF membranes cast using 10 wt% PVP (M_w = 10 kDa) and various amount of water: (A) 0 wt%; (B) 2 wt%; (C) 3.7 wt%; and (D) 4.6 wt% as non-solvent additive using water at 20°C as coagulation bath.

Figure 4.4 Cross sectional structures of 15 wt% PVDF membranes cast using 4 wt% PVP (Mw = 90 kDa) and various amount of water: (A) 0 wt%; (B) 2 wt%; (C) 3.6 wt% and (D) 5.5 wt% as non-solvent additive using water at 20°C as coagulation bath

The effects of combined addition of water and PVP with different molecular weight, i.e. PVP (M_w = 10 kDa) and PVP (M_w = 90 kDa) on the resulting membrane performance in terms of pure water permeation flux are tabulated in Table 4.3 and Table 4.4. Experimental results indicate that the membrane permeation flux increases with the amount of water added.

Table 4.3 Permeation flux of PVDF membranes cast using polymer dope of 15 wt% PVDF, 10 wt% PVP (M_w=10 kDa) and different water content

Amount of water added / wt%	**Water permeation flux / L.m^{-2}.hr^{-1}.bar^{-1}**
Membrane 4.3 (A): 0 wt% of water	Low
Membrane 4.3 (B): 2.0 wt% of water	116
Membrane 4.3 (C): 3.7 wt% of water	980
Membrane 4.3 (D): 4.6 wt% of water	1640

Table 4.4 Permeation flux of PVDF membranes cast using polymer dope of 15 wt% PVDF, 4 wt% PVP (M_w= 90 kDa) and different water content

Amount of water added / wt%	**Water permeation flux / L.m^{-2}.hr^{-1}.bar^{-1}**
Membrane 4.4 (A): 0 wt% of water	145
Membrane 4.4 (B): 2.0 wt% of water	380
Membrane 4.4 (C): 3.6 wt% of water	417

Other additives

The effect of other additives, namely ethanol, glycerol, LiCl and $LiClO_4$ on the resulting membrane morphology were also studied. With reference to Figure 4.5, it is obvious that these additives, i.e. ethanol, glycerol, LiCl and $LiClO_4$ produce very distinctive morphology even at a low concentration of 2 wt%. As illustrated in Figure 4.5(A), the addition of 2 wt% of $LiClO_4$ results in a membrane with massive irregular macrovoids. The addition of LiCl promoted the extension of long finger-like structure to nearly the entire membrane thickness as shown in Figure 4.5B. The presence of glycerol (Figure 4.5C) also resulted in the formation of macrovoids. Meanwhile, the addition of ethanol (Figure 4.5D) demonstrated enhanced asymmetric membrane morphology with short finger like structure beneath the skin.

Figure 4.5 Cross sectional structures of 15 wt% PVDF membrane cast using polymer dope containing 2 wt% of (A) $LiClO_4$; (B) LiCl; (C) glycerol; and (D) ethanol as additives using water at 50°C as coagulation bath.

A series of membranes were also prepared using various additives (namely glycerol, ethanol, $LiClO_4$, and three types of PVP) to study the effect of these additives on the resulting membrane performance based on their water permeation flux. These membranes were cast using casting knife of 200μm gap, using water at 20°C as coagulation medium. Improved water permeation fluxes were recorded for all additives used, as listed in Table 4.5.

Table 4.5 Effect of additives on membrane water permeation flux

PVDF concentration / wt%	**Amount of Additive / wt%**	**Water permeation flux / $L.m^{-2}.hr^{-1}.bar^{-1}$**
15.2	Nil	3.9
15.8	7.7 wt% glycerol	18.6
15.5	8.2 wt% ethanol	82.1
15.7	7.7 wt% $LiClO_4$	91.8
15.4	7.5 wt% PVP (M_w = 10k)	100.8
15.9	8.1 wt% PVP (M_w = 40k)	138.6
15.4	7.5 wt% PVP (M_w = 130k)	846.0

In Figure 4.6, SEM micrographs revealed the morphology of 15 wt% PVDF membrane in the presence of various concentrations of ethanol (Figure 4.6A and Figure 4.6B) and glycerol (Figure 4.6C and Figure 4.6D). The effect of ethanol and glycerol as non-solvent to PVDF / DMAc system have been studied in Section 3.5.3, whereby approximately 18 wt% of glycerol and 29 wt% of ethanol was required to induce cloud point behaviour of 15 wt% PVDF / DMAc system at 50°C (Figure 3.6). Here, the addition of 2 wt% of ethanol does not result in any abnormality in membrane morphology, apart from slightly longer finger-like structure beneath the top skin as shown in Figure 4.6(B). When ethanol concentration was increased to 35 wt%, the resulting membrane exhibited a symmetrical structure composed of uniform nodules as shown in Figure 4.6(A). This phenomenon could be attributed to the occurrence of gelation induced by crystallisation as ethanol can act as non-solvent at sufficiently high concentration (as discussed in Section 3.5.3). A similar phenomenon was reported by Cheng *et al.* (1999) for 1-Octanol / DMF / PVDF and water / DMF / PVDF using a soft coagulation bath to suppress the liquid-liquid demixing process. Between Figure 4.6(C) and Figure 4.6(D), it is evident that the increase in glycerol concentration from 7.7 wt% to 22.5 wt% resulted in more regular finger-like macrovoids, supported by an open porous substrate. The addition of glycerol is therefore believed to have favoured liquid-liquid demixing.

4.3.3 Effect of Coagulation Temperature on Membrane Morphology

According to Wang *et al.* (2000), the increase in coagulation bath temperature has little influence on the PVDF membrane coagulation rate, due to the slow interaction between water and PVDF. In this study, an obvious structural change was noted when both the dope solution and coagulation bath temperatures were increased, especially with the presence of additives. It is believed that at higher dope and coagulation bath temperatures, the diffusional kinetics of solvent out-flux and water in-flux was enhanced (Uragami *et al.*, 1981). Moreover, higher temperatures are known to suppress crystallisation and favour liquid-liquid demixing process. A similar conclusion was also drawn in a PVDF membrane study using 1-Octanol / DMF / PVDF and water / DMF / PVDF ternary systems (Cheng *et al.*, 1999).

Figure 4.7 illustrates the effect of elevated temperature (both coagulation bath and dope) on the resulting membrane morphology. Figure 4.7(A-a) and Figure 4.7(B-b) show the morphology of 15 wt% PVDF membrane with the addition of 2 wt% ethanol and 2 wt% glycerol at 20 °C and 50 °C. The increase in casting temperature to 50 °C shortened the finger-like structures beneath the top skin layer cast with 15 wt% PVDF and 2 wt% ethanol. The massive irregular macrovoids at 20 °C as shown in Figure 4.7(B) due to the presence of glycerol were replaced by more regular longitudinal macrovoids as casting temperature increased to 50 °C (as shown in Figure 4.7(b)), indicating a better inter-component mixing at a higher solution temperature of 50 °C prior to final polymer precipitation. It is important to note that PVDF membranes cast from 15 w% PVDF with 2 wt% of LiCl or $LiClO_4$ were too soft and often curled up in the process of drying, hence making them impossible to be examined using SEM. By increasing PVDF polymer concentration to 20 wt%, the morphology of PVDF membrane with 2 wt% of $LiClO_4$ or 2 wt% LiCl as additives are shown in Figure 4.7(C-c) and Figure 4.7(D-d). In both cases, gelation took place at a low temperature of 20 °C, as clearly shown by the dense matrix across the lower half membrane structure. At higher casting temperature of 50 °C a more open and porous membrane structure took over due to a slower liquid-liquid demixing process.

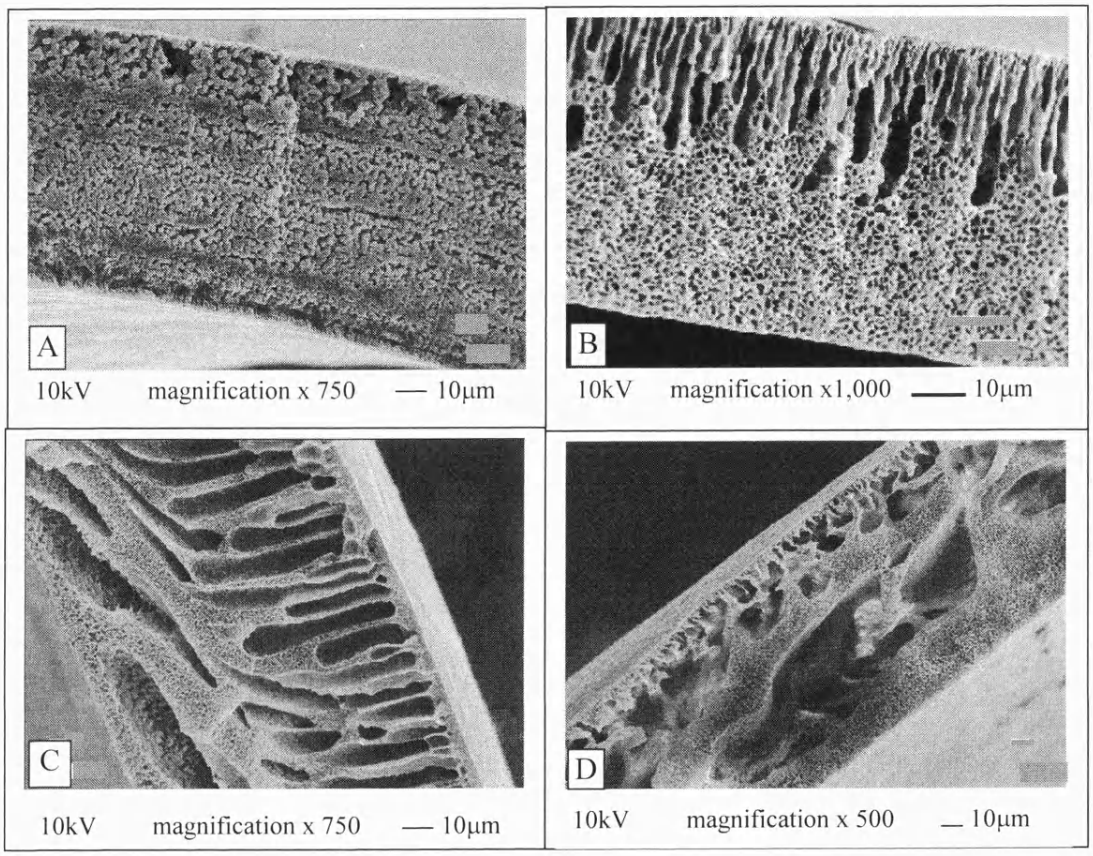

Figure 4.6 Cross sectional structure of flat sheet membranes cast at 50°C using
A) 15 wt% PVDF, 35 wt%ethanol and balance of DMAc;
B) 15 wt% PVDF, 2 wt% ethanol and balance of DMAc;
C) 16 wt% PVDF, 22.5 wt% glycerol and balance of DMAc;
D) 15.4 wt% PVDF, 2 wt% glycerol and balance of DMAc.

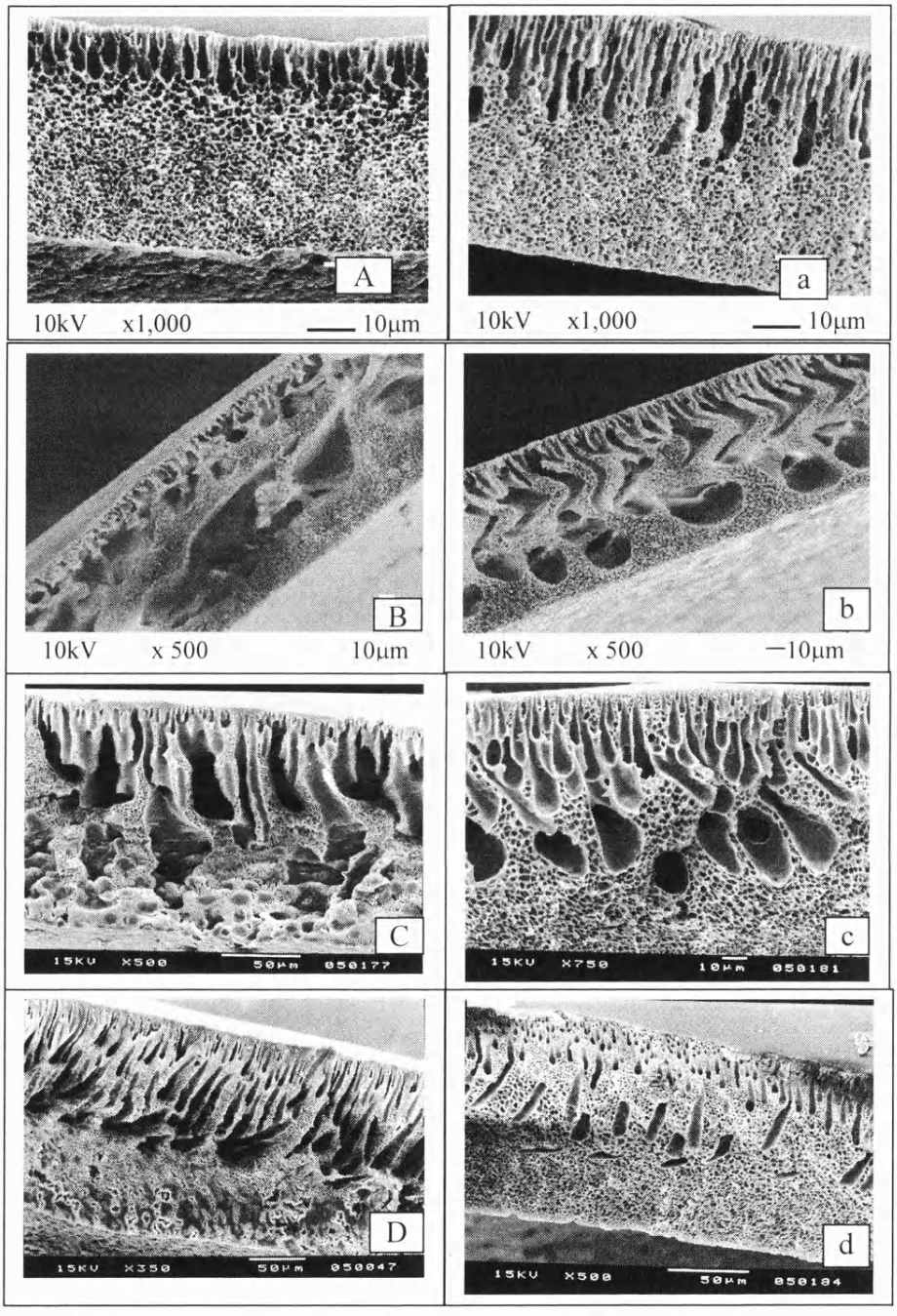

Figure 4.7 Cross sectional structures of PVDF membranes cast at 20°C (A, B, C and D) and 50°C (a, b, c and d) using dope:
(A-a) 15 wt% PVDF, 2 wt% ethanol and balance of DMAc;
(B-b) 15 wt% PVDF, 2 wt% glycerol and balance of DMAc;
(C-c) 20 wt% PVDF, 2 wt% $LiClO_4$ and balance of DMAc;
(D-d) 20 wt% PVDF, 2 wt% LiCl and balance of DMAc.

Figure 4.8 shows the morphology of PVDF membranes cast and coagulated at 20 °C, using combined additives of glycerol with ethanol, LiCl or $LiClO_4$. It can be seen from Figures 4.8(A-a), additive combination of 2.8 wt% glycerol and 1.95 wt% ethanol produced membranes with short finger-like structure beneath the top skin layer, supported by a substructure comprised of intermittent macrovoids and cellular pores. Additive combination of 2.9 wt% glycerol and 2.18 wt% LiCl resulted in extensive longitudal finger-like structure across the entire membrane thickness with evident signs of nodules formation near the bottom end of the membrane, as shown in Figure 4.8(B-b). Globules of approximately 3-5 μm in size could be seen trapped in the membrane matrix, as shown in Figure 4.8b. This could be due to the precipitation of highly localised concentrated PVDF polymer as a result of crystallisation. Meanwhile, additive combination of 3.1 wt% glycerol and 1.99 wt% $LiClO_4$ produced membranes with irregular open and broken macrovoids beneath the top skin layer, supported by porous substructures. The substructure is made of open cellular pores linked with islands of dense polymer matrix, forming a flower-like pattern, as shown in Figure 4.8(c). The presence of dense membrane matrix (Figure 4.8(a) and Figure 4.8(c)) and appearance of nodules (Figure 4.8(b)) are structures associated with membrane precipitation via a crystallisation and nucleation process.

These dense structures were absent in membranes cast using the same dope composition at elevated dope and coagulation temperature of 50 °C, as shown in Figure 4.9. Instead, an ordered finger-like structure was formed beneath the skin layer, supported by a more cellular porous substrate structure for all the three membranes variety. Evidently, the influence of additive becomes less significant at high temperature with little morphological difference between these three membranes despite their variation in the dope recipe. (Their unique membrane morphology produced by the addition of these additives is shown in Figure 4.5). To conclude, elevated temperature dominates the overall membrane formation mechanism by suppressing the process of gelation and crystallisation but favours liquid-liquid demixing. Hence, resulted in well-ordered and regimented finger-like structure beneath the top skin layer with porous cellular morphology in the substrate end.

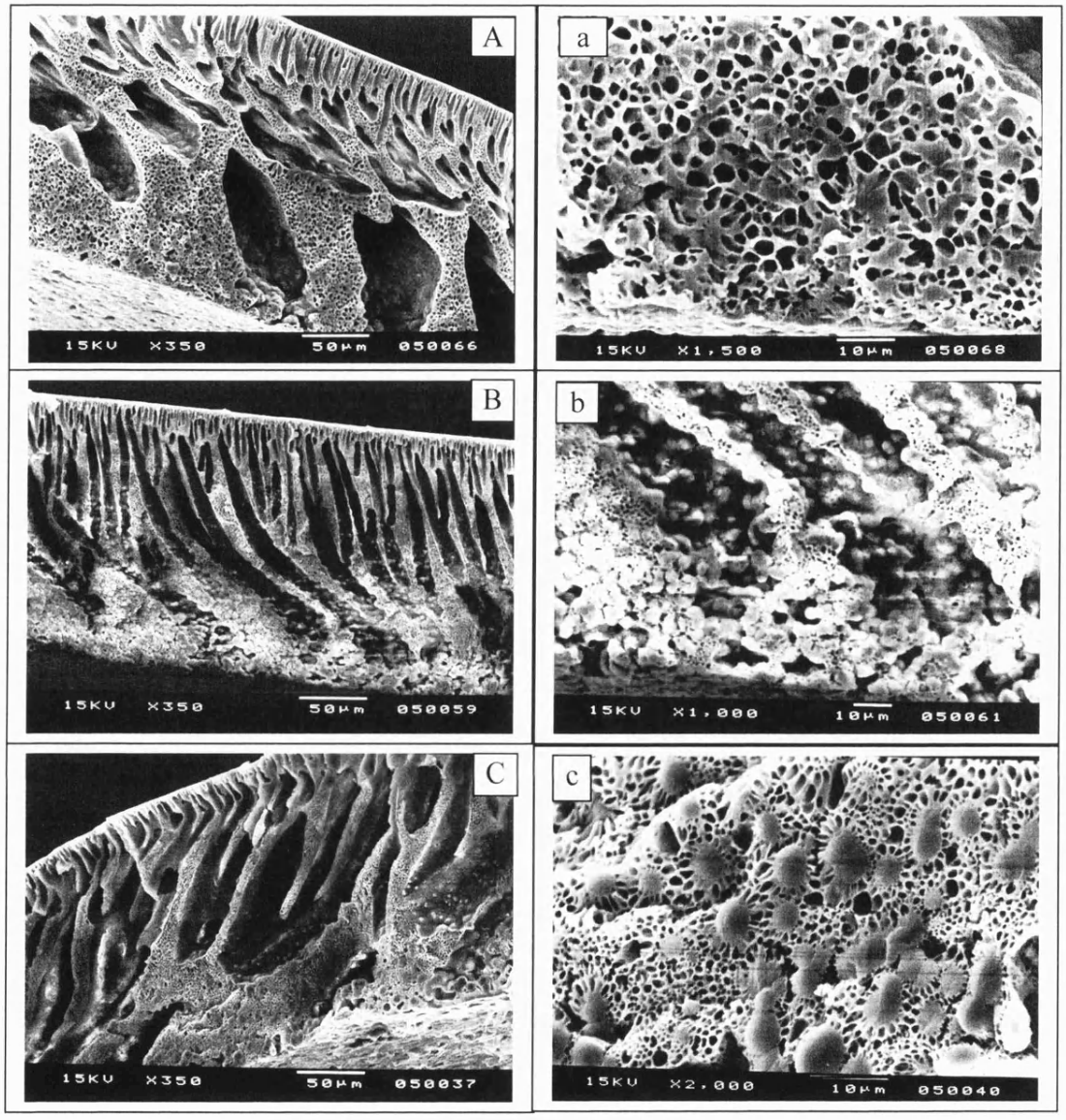

Figure 4.8 Cross section (A, B, C and D) and substrate (a, b, c and d) structures of PVDF membranes cast at 20°C coagulation bath using dope:
A-a) 20 wt% PVDF, 2.8 wt% glycerol, 1.95 wt% ethanol and balance of DMAc;
B-b) 20 wt% PVDF, 2.9 wt% glycerol, 2.18 wt% LiCl and balance of DMAc;
C-c) 20 wt% PVDF, 3.1 wt% glycerol, 1.99 wt% $LiClO_4$ and balance of DMAc.

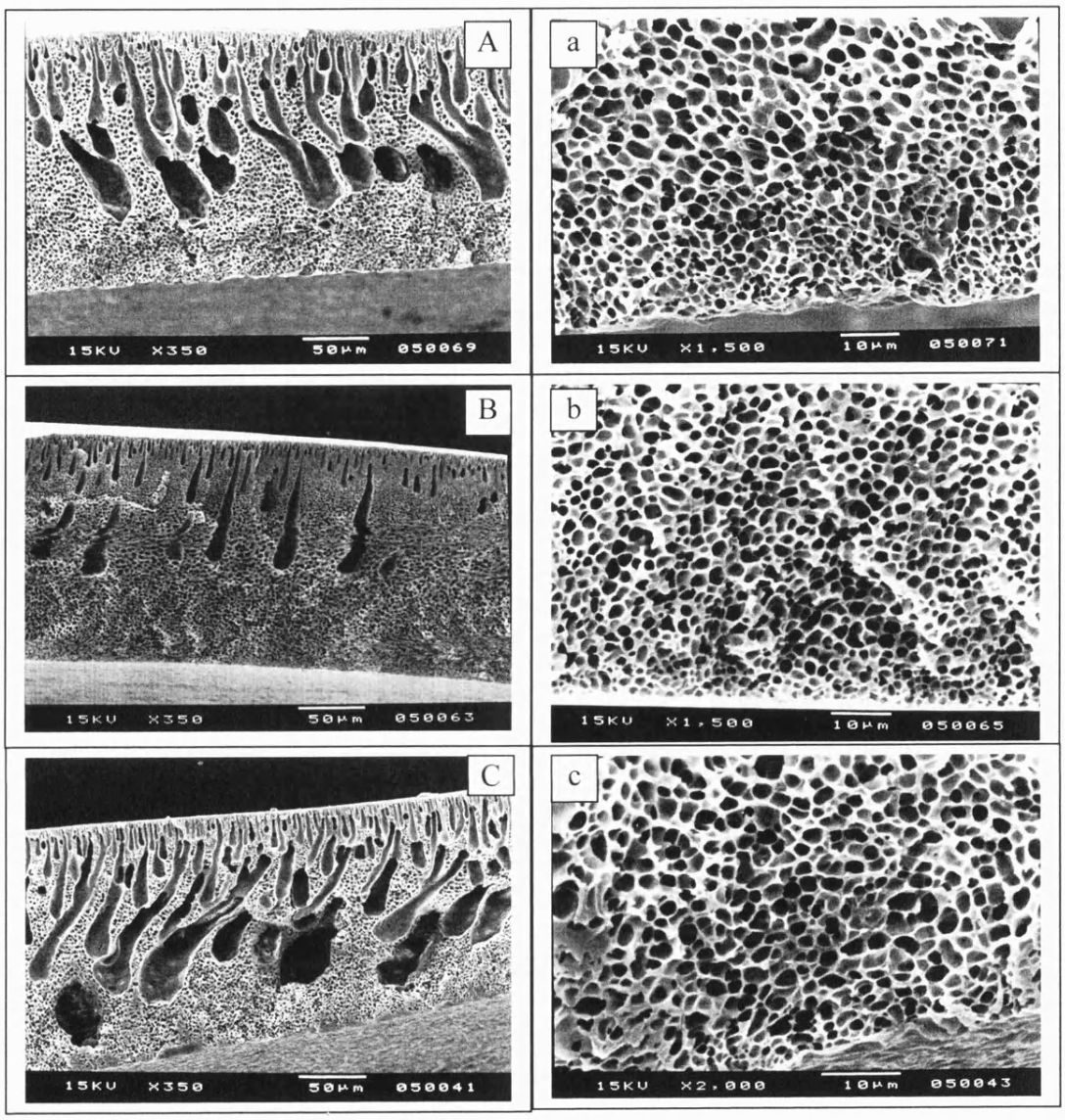

Figure 4.9 Cross-section (A, B, C and D) and substrate (a, b, c and d) structures of PVDF membranes cast at 50 °C coagulation bath using dope:
A-a) 20 wt% PVDF, 2.8 wt% glycerol, 1.95 wt% ethanol and balance of DMAc;
B-b) 20 wt% PVDF, 2.9 wt% glycerol, 2.18 wt% LiCl and balance of DMAc;
C-c) 20 wt% PVDF, 3.1 wt% glycerol, 1.99 wt% $LiClO_4$ and balance of DMAc.

4.4 CONCLUSIONS

The morphology of PVDF membranes produced using four different solvents, i.e. DMAc, DMF, NMP and TEP were studied using SEM. Experimental results revealed the distinctive influence of various solvents on the resulting membrane structure, indicating the importance of solvent choice. In summary, TEP produces symmetrical microporous membrane structures, NMP produces membranes with irregular macrovoids while both DMAc and DMF produce membranes with short finger like structure supported by porous substrates.

Similarly, the influence of various additives (namely ethanol, glycerol, LiCl, $LiClO_4$ and water) on the resulting PVDF membrane morphology was studied. Among the additives studied, PVP was found to promote macrovoid formation, ethanol appeared to induce porous substrates, glycerol was found to suppress gelation induced by crystallisation, while Li^+ salt was found to enhance the gelation behaviour. These characteristic morphologies obtained confirmed their vital role in fine-tuning membrane formation for customised application with specific morphology requirements.

In this study, the addition of additives was found to improve the membrane water permeation flux following the general trend of PVP > glycerol > $LiClO_4$ > ethanol. When combined additives of PVP and water were used, the water permeation flux increased with the amount of water added. When the dope and bath temperature were increased, the distinctive morphology associated with various additives was overwhelmed by the enhanced thermodynamic property of the dope solution. The presence of polymer globules, island of dense polymer matrix and so on in the membrane substructures were replaced by an open cellular pore structure. In conclusion, temperature is the dominating parameter affecting the final PVDF membrane morphology. Elevated temperature in both polymer dope and coagulant was found to suppress crystallisation; while promoting liquid-liquid demixing prior to nucleation or gelation processes.

CHAPTER FIVE

FABRICATION OF POLY(VINYLIDENE FLUORIDE) HOLLOW FIBRE MEMBRANES

5.0 FOREWORD

This chapter focuses on the fabrication of poly(vinylide fluoride) hollow fibre membranes via the phase inversion method, using water as external coagulation medium. The individual and/or combined effects of non-solvent additives such as lithium perchlorate ($LiClO_4$), glycerol and polyvinylpyrrolidone (PVP, M_w = 10 kDa) on the resulting membrane morphology and performance were studied. Also, the effects of coagulation bath temperature and the composition of internal coagulant on the formation of nodules in the final membrane matrix will be presented and discussed based on scanning electron microscopy (SEM) observations. Membrane permeation properties were analysed using nitrogen permeation data, while membrane mechanical strength was assessed based on collapse pressure.

5.1 PVDF AS A COMMERCIAL MEMBRANE MATERIAL

In recent years poly(vinylidene fluoride) (PVDF) has become an increasingly popular polymer choice in membrane fabrication, primarily for its excellent chemical resistance and thermal stability. Benzinger (1980) verified this fact by soaking samples of Pennwalt PVDF (commercial Kynar® grade) membrane in various organic solvents, oxidants, acidic and basic solutions. These desirable properties, coupled with its intrinsic hydrophobicity, make it an outstanding membrane material in many industrial waste treatment applications, such as those involving oily emulsion (Vigo *et al.*, 1984; Kong and Li, 1999), organic/water separations (Jian and Pintauro, 1993; 1996; 1997) gas absorption and stripping (Li *et al.*, 1999) and membrane distillation (Wu *et al.*, 1991; Ortiz de Zarate *et al.*, 1995; Tomaszewska, 1996; Khayet and Matsuura, 2001; 2002).

In comparison with its rivals, having equally attractive chemical and thermal resistance properties, (i.e. polytetrafluoroethylene (PTFE) and polypropylene (PP)), only PVDF can be made into asymmetric membranes using the Loeb-Sourirajan phase inversion

method (Wang *et al.*, 2000). In relation to this, recent studies also revealed that asymmetric PVDF membranes have a much lower mass transfer resistance in soluble gas removal, offering a mass transfer coefficient 2-8 times higher than that of commercial PP membranes (prepared via a thermal stretching method) due to their highly asymmetric structure (Wang *et al.*, 1999). In addition, the organic selective nature of PVDF polymer (as reported by Chabot *et al.,* 1997) is another bonus feature, especially for applications involving the recovery of organic compounds from waste streams. Also worth mentioning here is their ability to withstand prolonged exposure to high temperatures of 200°F, hence allowing them to be autoclaved if necessary (Benzinger, 1980).

5.2 Recent Advances in the Making of PVDF Hollow Fibre Membranes

Early publications on PVDF membrane production focused strongly on the fabrication of flat sheet membranes in relation to their various preparation parameters, and the corresponding membrane permeation performance (Uragami *et al.,* 1980; 1981a; 1981b; Sugihara *et al.*, 1979; Bottino *et al.*, 1985; 1988b; 1991; Munari *et al.*, 1990). Geometrically, hollow fibre is preferred to flat sheet primarily for its high packing density, which is a crucial consideration in industrial operations. The use of hollow fibre cartridges also offers the advantage of easy maintenance and up scaling, with minimum system interruption. Hence, an escalation in PVDF hollow fibre membrane research activities focusing on both membrane fabrication and final application was observed in recent years (Jian and Pintauro, 1997; Deshmukh and Li, 1998; Kong and Li, 1999; 2001; Wang *et al.*, 1999; 2000; Yeow *et al.*, 2002; Khayet and Matsuura, 2002).

Although some of the information obtained from the casting of flat sheet membranes could be useful in the development of hollow fibre membranes, the formation of hollow fibre membranes is universally recognised to be much more complex than of flat sheet membranes. Hence, similar conditions cannot simply be extended to produce hollow fibres with matching morphology. For instance, an essential difference in the dope formulation of flat sheet and hollow fibre membranes lies in their dope viscosity requirement. A flat sheet membrane can be cast from polymer dope with viscosity as low as a few hundred cP, while hollow fibre spinning requires a minimum viscosity of a

few thousand cP (Wang, 1996). In the case of flat sheet membrane casting, the phase inversion process begins from the top surface of a cast film with the bottom surface adhereing to the casting surface, upon immersion in coagulation medium. In the spinning of hollow fibre membranes, however, the phase inversion process takes place from both internal and external surfaces of the hollow fibres. The phase inversion process of the internal skin starts immediately after the polymer is extruded from the spinneret as the polymer dope comes into contact with internal coagulant on the hollow fibre bore side. The phase inversion of the outer surface could take place simultaneously, (i.e. as soon as the polymer dope is extruded from the spinneret), as in the case of wet spinning. Alternatively, this process commences upon immersion in the external coagulant bath after a short period of solvent evaporation, as in the case of a dry jet wet spinning, where the extruded polymer dope is exposed to a designated air-gap.

There are many factors affecting the final membrane morphology and performances of a hollow fibre membrane. These include the basic polymer dope properties such as polymer concentration, additives used and solution viscosity (all of which play a very important role in the final inter- and / or intra- molecular interactions and solvent / non-solvent diffusional exchange). Additionally, the intermediate compositional change due to solvent / non-solvent exchange during phase inversion process is strongly influenced by the composition and temperature of both the internal and external coagulation medium. Meanwhile, engineering aspects of hollow fibre spinning such as polymer extrusion rate, air gap, take up velocity, etc. also require extremely fine adjustment so as not to adversely affect the final membrane formation processes. Fundamental asymmetric membrane formation mechanisms via the phase inversion method (more specifically, via the immersion precipitation process) have been discussed in Section 2.2. Due to the highly complex nature of phase inversion-immersion precipitation processes and the interdependencies of these parameters, correlation between the aforementioned factors and the resulting membrane morphology and performance is yet to be established. Important findings related to the fabrication of PVDF membranes reported in the literature will be compiled and discussed in the following sections.

5.2.1 THE EFFECT OF DOPE COMPOSITIONS

The key to a successful membrane fabrication starts with a thermodynamically stable polymer dope. As discussed in section 2.2.1, a suitable dope formulation produces a solution in a 'metastable' equilibrium state whereby the solution remains indefinitely stable in the absent of external disturbance (which could be the intrusion of non-solvent, solvent loss from the polymer dope, or a change in solution temperature). In this regard, it is important to understand the fundamental role of each component, to maximise its function in the formulation of a stable polymer dope. Polymer and solvent are the two key components in a polymer dope. Polymer concentration is very important in determining the solution viscosity; it will also affect the final membrane strength and pore sizes. Similarly, the choice of a good solvent is extremely important in preparing a stable polymer solution. Often, co-solvents and additives are introduced to sway the macromolecular solution properties, either to increase the solution viscosity, to subtly amend its miscibility gap width or to lower its non-solvent tolerance. Indeed, a proper understanding of the phase separation behaviour requires knowledge of macromolecular chain interactions, chain mobility as well as polymer-solvent and polymer-polymer interaction, which cannot be obtained without understanding the fundamentals of the participating components. With this knowledge in hand, co-solvent and additives could be manipulated so as to produce desireable membrane morphology.

5.2.2 SELECTION OF SOLVENT AND CO-SOLVENT

As noted in Section 2.3, one of the most persistent limitations in membrane preparation is the lack of a predictable and systematic method of solvent selection (Klein and Smith, 1972). Proper selection of solvent is essential in formulating a highly thermodynamically stable polymer dope, which itself is crucial in maintaining high polymer chain mobility and strong polymer-solvent (P-S) interactions. Solubility parameter approach is a good tool in identifying good solvent for non-polar amorphous system, which has also been adopted for crystalline polymer (Bottino *et al.*, 1991). It is the crystallisation energy barrier that hinders the dissolution of crystalline polymer in organic solvent. Poor / weak solvent can only weaken the intermolecular chain bond of macromolecules but unable to break the bond. In contrast, strong solvent will dissolve the macromolecules and will not result in chain aggregates.

A total of 8 organic solvents, namely *N,N*-dimethylacetamide (DMAc), *N, N*-dimethylformamide (DMF) and dimethylsulfoxide (DMSO), hexamethylphosphoramide (HMPA), N-methyl-2-pyrrolidone (NMP), triethyl phosphate (TEP), trimethyl phosphate (TMP), tetramethylurea (TMU) were identified as good solvents for PVDF out of 46 screened (Bottino *et al.*, 1991). Of these, DMAc, DMF, NMP and DMSO have been widely used in the fabrication of PVDF membranes.

In some cases, tetrahydrofuran (THF) and acetone (Ac) were introduced as low boiling point weak co-solvents, alongside DMF and NMP as the core strong solvents (Sugihara *et al.*, 1979; Bottino *et al*, 1991). With the evaporation of low boiling point co-solvent, the polymer concentration in the remaining polymer dope increases and resulted in a dense top layer formation. Strong water affinity of the high boiling point solvent encourages water influx. Hence, the amount of non-solvent reaches the point of phase separation quickly and produces a microporous membrane structure.

5.2.3 The Use of Non-Solvent Additives

The overall aims of using additive are to improve the membrane morphology, to enhance the membrane separation and permeation performance and to reinforce the membrane mechanical strength. This can be achieved via one of the following functions of an additive: (a) as a pore former, (b) increase solution viscosity, (c) acceleration of the phase inversion process.

Polyvinylpyrrolidone (PVP), lithium chloride (LiCl), polyethylene glycol (PEG), various small molecular weight alcohols (namely methanol, ethanol and propanol), organic acids (such as phosphoric and sulfonic acid) and water are among the commonly used additives in the fabrication of PVDF membranes, as will be discussed in the following paragraphs.

PVP has been extensively used and studied in the membrane fabrication as an efficient way of producing highly porous PVDF hollow fibre (Deshmukh and Li, 1998; Wang *et al.*, 1999; 2000). The addition of PVP is known to promote non-solvent influx upon immersion in the coagulation bath (due its hydrophilic nature) hence favouring the formation of macrovoids in PVDF hollow fibre membranes (Deshmukh and Li, 1998).

In general, increased membrane effective porosity, well interconnected pores, higher permeation flux and good solute rejection are among the many positive characteristics associated with the addition of PVP; with membrane mean pore size remains fairly consistent (Wienk *et al.*, 1996; Deshmukh and Li, 1998, Wang *et al.*, 1999). However, it is important to understand that the presence of macrovoids in general, including that of finger-like cavities, may be disadvantageous to membrane permeation, as their skinned configuration could be a self-contained dead volume with no permeable surface available (Kesting, 1985). According to Wienk (1996), a virtual binodal could be postulated to describe the reduction of demixing gap following the addition of PVP. This virtual binodal is only valid for a very short timescale from the beginning of the demixing process, during which the inter-diffusion of the two polymers relative to each other is considered negligible and the membrane formation process is predominantly governed by the diffusion of solvent and non-solvent. As the membrane formation process proceeds, the diffusion of the two polymers with respect to each other becomes more important (Wienk, 1996). The main disadvantage of PVP is the difficulty in complete rinsing, particularly those with higher molecular weights (Deshmukh and Li, 1998; Wang *et al.*, 1999). As a highly hydrosoluble polymer, any residue of PVP has an adverse effect in the final hydrophobicity of PVDF membranes.

The introduction of poly(ethylene glycol) (PEG) has been reported to improve membrane permeability, at the expense of the solute rejection performance; which could be marginally reversed by heat treatment longer than 10 minutes (Uragami *et al.*, 1981b). The authors explained this phenomenon based on membrane shrinkage behaviour after heat treatment. SEM photograph revealed a bigger pore size after 10 minutes heat treatment, which correspond with the lowest rejection and highest permeation recorded. However, no further evidence was provided for the reversed phenomena for heat treatment longer than 10 minutes.

Lithium chloride (LiCl) is another widely used additive in PVDF membrane manufacturing, as it promotes good membrane porosity, smaller average pore and membrane hydrophobicity (Bottino *et al.*, 1988; Wu *et al.*, 1991; Tomaszewska, 1996; Wang *et al.*, 2000; Kong and Li, 2000). In fact, it has been described as a preferred additive to PVP or PEG as a pore former because it can be thoroughly removed to prevent jeopardising the membrane hydrophobicity (Wu *et al.*, 1991). A study

conducted by Tomaszewska (1996) showed that PVDF membrane porosity and permeation flux increased with the amount of LiCl added. However, a major drawback of employing LiCl as non-solvent additive is the decrease in the membrane mechanical strength (Bottino *et al.*, 1988; Tomaszewska, 1996). Wang *et al.* (2000) managed to retain the membrane mechanical strength by introducing LiCl together with small molecular weight alcohol such as methanol, ethanol or 1-propanol.

Membrane effective porosity and pore radius have been reported to increase with the amount of water added as non-solvent additive in the polymer dope (Khayet and Matsuura, 2001). In line with this, gas permeation results showed that the membrane mass transfer resistance of the membrane decreases with increased water concentration, heading towards a plateau. The addition of 1,2-ethaniol resulted in a decrease in membrane liquid entry pressure (LEP_w), primarily due to the increase in maximum pore size that in turn is responsible for the improved pure water flux (Khayet *et al.*, 2002). Their calculations also showed greater membrane porosity in conjunction with the increase in maximum pore size. However, the effective membrane porosity remains apparently independent of the non-solvent additives.

5.2.4 Effect of Coagulation Bath Mediums

Coagulation medium is another important factor in the formation of phase inversion membranes; it is the medium where solvent-non-solvent exchange takes place to form the nascent membrane structure. Wijmans *et al* (1983) explored the effect of coagulation bath composition on the precipitation kinetics and concluded that the addition of solvent to the coagulation bath slows down the precipitation rate, resulting in a membrane morphology change from finger-like to sponge-type structure.

Compositional effect of the coagulation bath on the membrane structure was investigated using pure water, a number of organic compounds (i.e. various alcohols, organic solvents and glycerol) and their mixtures with water as the coagulation bath (Bottino *et al.*, 1985). Macrovoids and fingerlike cavities tended to disappear and were replaced by a porous structure of polymeric globules, as alcohols and organic solvents were introduced into the coagulation bath. A symmetrical membrane morphology with globular structures throughout the whole membrane thickness was observed when pure

alcohol was used. However, the membrane produced became brittle and difficult to handle when the concentration of alcohols (and other organic compounds) in the coagulation bath exceeded 40 vol%, hence this process became impractical. The presence of these organic compounds in the coagulation bath slows the polymer precipitation rate, as they are essentially not only a poor coagulant, but also serve as a weak solvent for the polymer dope; hence resulting in a slow coagulation process which produces porous structures without cavities. In terms of membrane performance, permeation flux was found to decrease with the increased concentration of alcohol in the coagulation bath medium. Membrane rejection exhibited a maximum before declining as the alcohol/organic solvent content in the coagulation bath increased, with no significant Dextran rejection at coagulation bath alcohol content exceeded 40 %, and DMF concentration exceeding 60 % (Bottino *et al.*, 1985).

Similar studies conducted by Deshmukh and Li (1998) in the production of hollow fibre membranes reported a shift in membrane morphology with the addition of ethanol (10 % - 50 %) in coagulation bath. The long finger-like structures near the outer wall of the hollow fiber slowly become a short finger-like structure before finally being substituted by an overall sponge-like structure. The formation of macrovoids could be explained as a result of the rapid growth of the coagulation front. Optical monitoring confirms that three distinctive membrane structures (i.e. large finger-void like, finger-like and sponge-like structures) are related to the strength of the coagulation medium that determines the speed of polymer precipitation, which in turn is a function of the penetration time (Yao *et al.*, 1988). In general, a fast coagulation rate results in the formation of large finger-like macrovoids, whereas a slow coagulation rate results in a porous sponge-like structure, consistent with the conclusion made by Kesting (1985). In addition, the increment in the ethanol content in the external coagulation bath also resulted in a decline in membrane effective porosity, as the number of macrovoids diminished (Deshmukh and Li, 1998).

5.2.5 Effect of Coagulation Bath Temperature

An increase in the temperature of coagulation medium tends to enhance the exchange of casting solvent in the polymer dope with non-solvent in the coagulant medium. With the combined effects of greater non-solvent inflow and higher solvent outflow, a more rapid

polymer precipitation is anticipated, hence resulting in an increase in the size of macrovoids and finger-like cavities. According to Bottino *et al.* (1985), overall membrane structures were found to shift from having porous structures formed by polymeric globules to porous alveolar structure after coagulation bath temperature was increased from 20 °C to 70 °C. This was accompanied by an increase in membrane flux. Wang *et al.* (2000), however, noted otherwise, whereby a slight reduction in membrane permeability was recorded with increased coagulation bath temperature. Similarly, Tomaszewska (1996) reported a near 2-fold nitrogen permeability decrement for flat sheet PVDF membrane prepared at higher temperatures of 293 K (20 °C) (as compared to those prepared at 277 K (4 °C)). However, no detailed explanation to this phenomenon was provided.

5.2.6 Effect of Internal Coagulant

Water has been widely used as a strong internal coagulant in hollow fiber spinning, producing a nicely circular internal skin. In some applications where an internal skin is not required, it can be eliminated by slowing down the polymer precipitation rate, which can be easily achieved by introducing a weak co-solvent into the internal coagulation medium (i.e. by lowering the coagulant strength). A good example of this is the use of ethanol/water mixtures as the internal coagulation medium whereby hollow fibres without internal skin were produced via wet spinning, which showed greatly enhanced permeation properties (Wang *et al.*, 1999). In some cases, however, it produced an undesirable non-circular fibre lumen, which leads to poor fibre integrity. Based on a log-normal pore size distribution curve, bigger membrane pore and nodule sizes near the inner fibre wall were reported when 50vol% ethanol-water mixture was used as both internal and external coagulant (Khayet *et al.* 2002).

5.2.7 Effect of Spinning Conditions

Knowledge of the general effects of various spinning conditions (including air gap, polymer extrusion rate, internal coagulant injection rate, take up velocity) on the resulting membrane morphology and performance are well established (Kim *et al.*, 1995; Wang *et al.*, 1999; 2000). Here, a brief summary of the known effects of the spinning conditions will be provided. Increase in air gap is known to eliminate the formation of an outer skin, often resulting in increased membrane porosity and

permeation properties. Polymer extrusion rate plays an important role in the final membrane dimensions, particularly the outer diameter and the wall thickness. Meanwhile membrane inner diameter is strongly influenced by the injection rate of internal coagulant. Take up velocity needs to be carefully adjusted to match the free falling velocity of the extruded polymer jet. More importantly, it is the combined effects of all these parameters that determine the final membrane morphology, which in turn will affect the membrane separation performance, as none of these parameters could be mutually exclusive of each other at any one time.

In this study, focus is placed on the effects of various parameters (namely types and concentrations of additives, compositions of internal coagulant and temperature) on the resulting PVDF hollow fibre membranes.

5.3 OLEFIN/PARAFFIN SEPARATION

The separation of olefin from hydrocarbon mixtures is one of the most important processes in the petrochemical industry. Following the decline in world petroleum reserves, the need to recover the olefins and paraffins present in the vent gas, has attracted considerable attention primarily for its potential economic revenue, as well as a means of resource conservation. In this regard, light olefins such as ethylene and propylene are important commodity chemicals in terms of sales value and as basic feedstock (Oscar, 1983).

5.3.1 SCENARIO OF CURRENT PETROCHEMICAL INDUSTRIES

A number of chemical and physical processes are employed in petroleum refineries to convert crude oil into marketable products and feedstocks, of which catalytic cracking units is a commonly used process to increase petrol yield from crude oil and hence improve refinery's process economic. Purge gas from this process contains significant amounts of olefin and paraffin that are often used as refinery fuel (Eldridge, 1993). According to the Chemical Economic Handbook (CEH), global ethylene production amounted to 90.4 million metric tons in 2001, with an estimated value of USD$60 billion. This level of production represents an average annual growth of 3.9% from the 1997 level. Meanwhile, global production of propylene amounted to 48 million metric

tons in 1998, with an estimated value of USD$15 billion. Global propylene consumption is expected to grow annually at the rate of 5.4 % from 1998 to 2003 (http://ceh.sric.sri.com/Public/Reports). Furthermore, increasingly stringent emission standard and public awareness regarding sustainable development requires a more environmental friendly treatment method prior to their disposal. For various economic and environmental reasons as mentioned above, it is therefore of interest to study the recovery of olefin from hydrocarbon mixtures.

To date, cryogenic distillation remains the dominant technology utilised in olefin/paraffin separations despite its intensive energy requirement (due to the low relative volatilities of the components) and high capital cost (distillation columns are typically up to 300 feet tall and can contain over 200 trays). Physical adsorption, physical absorption, chemical absorption and membrane separation are among the few feasible alternative technologies available for olefin/paraffin separation (Yang and Hsiue, 1997; Gawronski and Wrzesinska, 2000). Physical adsorption usually requires a complicated regeneration cycle, and therefore is not economically feasible.

Nevertheless, utilisation of a mass-separating agent such as a membrane, instead of an energy-separating agent such as cryogenic distillation, could substantially reduce the process energy requirements. Membrane process has been proven a more efficient and economical separation technology, but conventional membranes usually have low permeability and selectivity for the olefin/paraffin components (Staudt-Bickel and Koros, 2000). Hybrid membrane technology with an olefin-selective facilitator (with large olefin capacity and fast reaction rates) would permit the use of smaller contactors. Owing to its high specific surface area (interfacial area per unit volume), membrane contactors promise higher volumetric mass transfer rates than conventional scrubber, i.e. typically in the range of 500 – 5000 m^3/m^2 for membrane contactors as compared to 20-500 m^3/m^2 in conventional scrubbers (Iversen *et al.*, 1997).

In reality, however, there are very few non-distillation processes being used in the chemical and refinery industry, partly due to the conservative nature of the refinery and petrochemical industry. Also, the presence of contaminants such as H_2O, CO_2, H_2S, COS, AsH_3, CS_2, and NH_3 in the vent gas stream from catalytic cracking unit is problematic to all treatment technologies (Isalski, 1989). Even trace amounts of these

contaminants can seriously jeopardise the performance of metal-based absorption and chemical adsorption process. The addition of feed pre-treatment steps would negatively impact the overall process economics.

5.3.2 OLEFIN/PARAFFIN SEPARATION USING MEMBRANE TECHNOLOGY

Conventional membrane-based gas separation devices have been extensively studied as a means to separate olefin/paraffin mixtures, whereby many of the polymeric materials tested demonstrated some rather low permeability and selectivity were, primarily due to the similar molecular sizes and solubilities between olefin and paraffin, hence resulting in poor separation performance (Koros, 1993; Kovvali, *et al.*, 2002). For instance, poly(dimethylsiloxane) has been reported to have ideal C_3H_6 / C_3H_8 separation factor of 1 at 313 K (40 °C) (Ito and Hwang, 1989) and 1.1 at 323 K (50 °C) (Tanaka *et. al.*, 1996). Cellulose acetate has been reported to have ideal C_3H_6 / C_3H_8 separation factor 3.8 at 313K (40 °C) (Ito and Hwang, 1989). 1,2-polybutadiene exhibited ideal C_3H_6 / C_3H_8 separation factor of 1.7 at 323 K (50 °C) (Tanaka *et. al.*, 1996).

Modified polymeric materials such as polyimide have stood out as more promising polymer choices for plain membrane based olefins/paraffins separation. Tanaka *et al.* (1996) reported ideal C_3H_6 / C_3H_8 selectivity over a range of 8.6 – 27, using various polyimide membranes. Using carbonised polyimide membrane, C_3H_6 / C_3H_8 selectivity up to 56 was reported by Hayashi *et al.* (1996). More impressively is the ideal C_3H_6 / C_3H_8 separation factor of 77 obtained using polyimide resins containing fluorine (Shimazu, 1998). Using 6FDA based polyimide flat membranes, Staudt-Bickel and Koros (2000) reported an ideal C_2H_4 / C_2H_6 selectivity of 3.13, and ideal C_3H_6 / C_3H_8 separation factor of 32.9 at 298 K (25 °C). However, significantly lower selectivities were recorded in mixed gas experiments, i.e. a reduction of 20% in the case of ethylene/ethane and 50% in propylene/propane separation respectively (Staudr-Bickel and Koros, 2000), possibly attributed to plasticisation by propylene. Due to their poor selectivity, the use of non-reacting polymeric membranes in olefin/paraffin separation is thought to be ineffective. In contrast, the concept of introducing a transport facilitator has been proven attractive and will be detailed in the following paragraphs.

5.4 OLEFIN/PARAFFIN SEPARATION VIA π COMPLEXATION

Olefin/paraffin separation using the concept of facilitated transport works on the principles of a strong, specific and yet reversible chemical complexation called π complexation (King, 1987). Firstly, the mixture to be separated is contacted with a second phase containing a complexing agent that reacts reversibly with the solute of interest, in this case olefins. In the second part of the process, the reaction is reversed and the solute is recovered.

5.4.1 THE PRINCIPLE OF π COMPLEXATION

By definition, π complexation pertains to the main group of transition metals in the periodic table. These metals (or their ions) can form the normal σ bond to carbon; additionally, the unique characteristics of the d-orbitals in these metals (or their ions) can form bonds with unsaturated hydrocarbons (olefins) and this bondage is known as the π complexation (Cotton and Wilkinson, 1966). The advantage of chemical complexation is that the bonds formed are stronger than those by van der Waals forces alone, so it is possible to achieve high selectivity and high capacity for the component to be bound. In the meantime, the bonds are still weak enough to be broken by using simple engineering operations such as raising the temperature or decreasing the pressure.

5.4.2 COMPLEXING AGENTS

Two most commonly used metal ions in facilitated transport membranes for olefin/paraffin separation are cuprous (I) and silver ion, i.e. Cu^+ and Ag^+ respectively. Ag^+ and Cu^+ form reversible complexes with π electrons in olefins but not with saturated compounds like paraffins (Beverwijk *et al.*, 1970). Other cations known to form complexes with olefins are Pt(II), Pd(I) and Hg(II). This reversible complex phenomena (under temperature and/or pressure swing) can be utilised in the facilitated transport of the desired olefins from the feed stream across the membrane to the permeate side under proper conditions, thereby resulting in a selective separation (Yang and Hsiue, 1998). The other cations form much stronger bonds hence making the desorption process more complicated (Keller *et al.*, 1992).

Based on comparison made between silver nitrate ($AgNO_3$), silver tetrafluoroborate ($AgBF_4$) and silver perchlorate ($AgClO_4$). Keller *et al.* (1992) concluded that solubility of olefins in aqueous silver solution is dependent on the anion of the salt and the salt concentrations. Below 1 M, olefin solubility per mol of salt decreases in the order of $ClO_4 >> BF_4 > NO_3$. In more concentrated solution, olefin solubility decreases in the order of $BF_4 >> ClO_4 > NO_3$, which is in accordance with the strength of the corresponding acids.

5.4.3 VARIOUS FACILITATED MEMBRANE TECHNOLOGIES

Facilitated-transport membranes for olefin/paraffin separation via π complexation can be further divided into immobilised liquid membranes (ILMs) (Teramoto *et al.*, 2002), solvent swollen, fixed site carrier complex membranes (Yang and Hsiue, 1998), dry complex electrolyte membrane (Pinnau and Toy, 2001), ion exchange membrane (IEMs) (Yamaguchi *et al.*, 1996), and membrane contactor systems (Bessarabov *et al.*, 1999). Each of these will be discussed in the following paragraphs.

Immobilised liquid membranes (ILMs) are also known as supported liquid membranes (SLMs). These membranes are prepared by impregnating a microporous membrane with a solution (typically water) containing the carrier (i.e. silver ion), the carrier solution being held within the pores of the membrane by capillary forces (Hughes, 1986; Teramoto *et al.*, 1986; Cussler, 1994; Tanaka, *et al.*, 1996). These membranes exhibit high olefin/paraffin selectivity, but with poor mechanical stability and relatively short life span due to the loss of solvent (usually water) and carrier over time (Keller *et al.*, 1992; Teramoto *et al.*, 1986). To overcome the problem of moisture loss in ILMs, Teramoto *et al.* (2002) experimented a new system called bulk flow liquid membrane (BFLM). In this system, the carrier solution containing olefin-carrier complex was allowed to permeate through the membrane; at the down stream permeate side, olefin was released as the complex decomposed at lower pressure.

Solvent swollen, fixed site carrier complex membranes are prepared by swelling the membrane matrix with a low volatile carrier liquid such as glycerol, containing Ag^+. These solvent swollen complex membranes can be regarded as another type of liquid membrane with the swelling agent (under low vapor pressure) retained in the membrane

and serving as a solvent for silver ion. Property wise, solvent swollen complex membranes could be regarded as a buffer / transition between IMLs and dry complex membranes. The presence of a low vapour pressure swelling agent helps combating the problem of drying out effect faced by the ILMs. As a result of this, it doesn't require a humidified feed stream which is commonly used in applications involving dry complex membranes (Hsiue and Yang, 1993, 1994; Yang and Hsiue, 1996a, 1996b, 1997, 1998).

Dry complex electrolyte membranes are also known as carrier-polymer blend membranes. As their name implies, the membranes are prepared using a casting solution containing a mixture of carrier (Ag^+) and polymer (Hong *et al.*, 2001; Sunderrajan *et al.*, 2001). Pinnau and Toy (2001) prepared dry complex electrolyte membranes in the form of composite membranes by coating a thin (~5μm) poly(ether oxide)-silver tetrafluoroborate layer onto a microporous poly(etherimide) (PEI) support. The essential feature that distinguishes between the dry complex electrolyte membranes from solvent swollen, fixed site carrier complex membranes is that ionic motions in a solid polymer electrolyte take place without the presence of a solvent or plasticiser. Rather, the ionic transport relies on the local polymer relaxation process of flexible polymer chains (Pinnau and Toy, 2001).

In ion-exchanged membranes (IEMs), the carrier is the counter-ion that is strongly bound by strong electrostatic charges in the membranes; hence it cannot be forced out or washed away. As a result of this, IEMs are claimed to provide longer membrane operating life (le Blanc *et al.*, 1980). However, both dry complex electrolyte membranes and IEMs must be operated continuously in a water vapor saturated environment so that the membranes remain olefin selective. Nafion/$AgBF_4$ membranes prepared by Yamaguchi *et al.* (1996) gradually lost their olefin selectivity over paraffin after 100 minutes of operation due to evaporation, but were regained with the addition of water vapor in the feed stream. It was also found that the membranes were effective only for a very narrow humidity range. In addition, minimum feed stream humidity had to be maintained in order to stabilise the olefin flux and its olefin-facilitating feature (Ericksen *et al.*, 1993; Hong *et al.*, 2001). To avoid the problems associated with the above-mentioned membrane configurations, membrane based gas-liquid and liquid – liquid contactor have been proposed for use in olefin-paraffin separations (Davis *et al.*, 1993; Tsou *et al.*, 1994; Bessarabov *et al.*, 1999).

In this study, a PVDF hollow fibre membrane contactor is designed for use in the separation of olefin/paraffin mixtures with a silver nitrate aqueous solution as the source of silver ion (Ag^+) facilitating agent. The benefits of using a hollow fibre membrane contactor include the absence of emulsions, no flooding at high flow rates, no unloading at low flow rates and no density difference between fluids required. Most importantly, it offers a very high interfacial area, i.e. 30 times more than gas absorber and 500 times more than liquid-liquid extraction column (Gabelman and Hwang, 1999). Details on membrane mass transfer with chemical reaction could be located in various literatures (Goddard *et al.*, 1974; Schultz *et al.*, 1974; Kreulen *et al.*, 1993a; 1993b) and is beyond the scope of this study.

5.5 MATERIALS AND METHODS

5.5.1 MATERIALS

Preparation of PVDF Hollow Fibre Membranes

Kynar®K760 poly(vinylidene fluoride) (PVDF) polymer pellets used were purchased from Elf Autochem, USA, and were pre-dried at 50°C prior to use. *N,N*-dimethylacetamide (DMAc) [99.9+%, HPLC grade] was used as solvents. Glycerol [Fw=92.09, 99%], lithium perchlorate ($LiClO_4$) [99+%, ACS reagent grade] and polyvinylpyrrolidone (PVP) [99.9+%, Mw=10 kDa] were used as additives. 1-methyl-2-pyrrolidone (NMP) [99+%, spectrophotometric grade] and distilled water were used as internal coagulants. All chemicals were purchased from Sigma Aldrich and used as received. In all cases, water was used as the external coagulation bath medium.

Separation of Hexene / Hexane Mixtures via π Complexation with Ag^+

Hexane [99.9+%, HPLC grade] and hexene (hex-1-ene, 100% pure, laboratory reagent grade] were purchased from Fisher Scientific. Silver nitrate 1.0 N [volumetric standard] was purchased from Aldrich Chemical. All chemicals were used as received.

5.5.2 PREPARATION OF PVDF CASTING DOPE

The desired amount of pre-dried (24 hours oven dried at 50°C) PVDF polymer pellets were weighed and poured into pre-weighed solvents contained in 1-liter Duran PTFE lined bottles. It is crucial to subject the mixture to vigorous shaking so as to ensure thorough wetting of polymer pellets, prior to the addition of additive (when applicable).

The polymer dope mixture was then placed in a 50°C isothermal water bath and subjected to continuous stirring using an overhead stirrer [IKA® WERKE] at 500rpm for 48 hours. In all cases, an electronic balance [Precisa 2200C, accuracy ±0.005g] was used. Finally, the fully dissolved polymer solution was filtered and transferred to a stainless steel reservoir. The polymer solution was allowed to stand and degassed for 24 hours at room conditions prior to hollow fibre spinning to ensure complete removal of gas bubbles trapped in the viscous casting solution. The viscosity of spinning solution prepared was measured using Bohlin CS Rheometer [Bohlin Instrument Ltd.] at ambient conditions.

5.5.3 SPINNING OF PVDF HOLLOW FIBRE MEMBRANES

PVDF hollow fibre membranes were spun using PVDF/DMAc/non-solvent/additives casting dope prepared via a dry-wet phase inversion method using the experimental set-up as illustrated in Figure 5.1. The solution tank was pressurised to 2-2.5 bar using purified nitrogen [BOC Gas], polymer extrusion rate was regulated using a needle valve, while internal coagulant was introduced to the inside circle of the spinneret at a controlled flow rate of approximately 2 $ml.s^{-1}$ [Ismatec, REGLO-Z]. The nascent hollow fibre emerged from the tip of the spinneret with/without passing through an air-gap, and was guided through the two water baths before landed in a final collection bath to complete the solidification process. It was important to ensure that the nascent hollow fibre was not subjected to any mechanical dragging when guided through the water bath; this could be achieved by adjusting the take-up velocity [Samsung Electronics, FARA Moscon E5] of the hollow fibre close to its free falling velocity as it left the spinerette and entered the first coagulation bath. Figure 5.2 shows the correlation between the motor take up rotation with the actual take up velocity. The hollow fibres prepared were immersed in the final water bath for a period of three days, with daily change of water, so as to ensure thorough removal of residual solvent and additives prior to final membrane drying in ambient conditions. Table 5.1 summarises the basic hollow fibre spinning parameters.

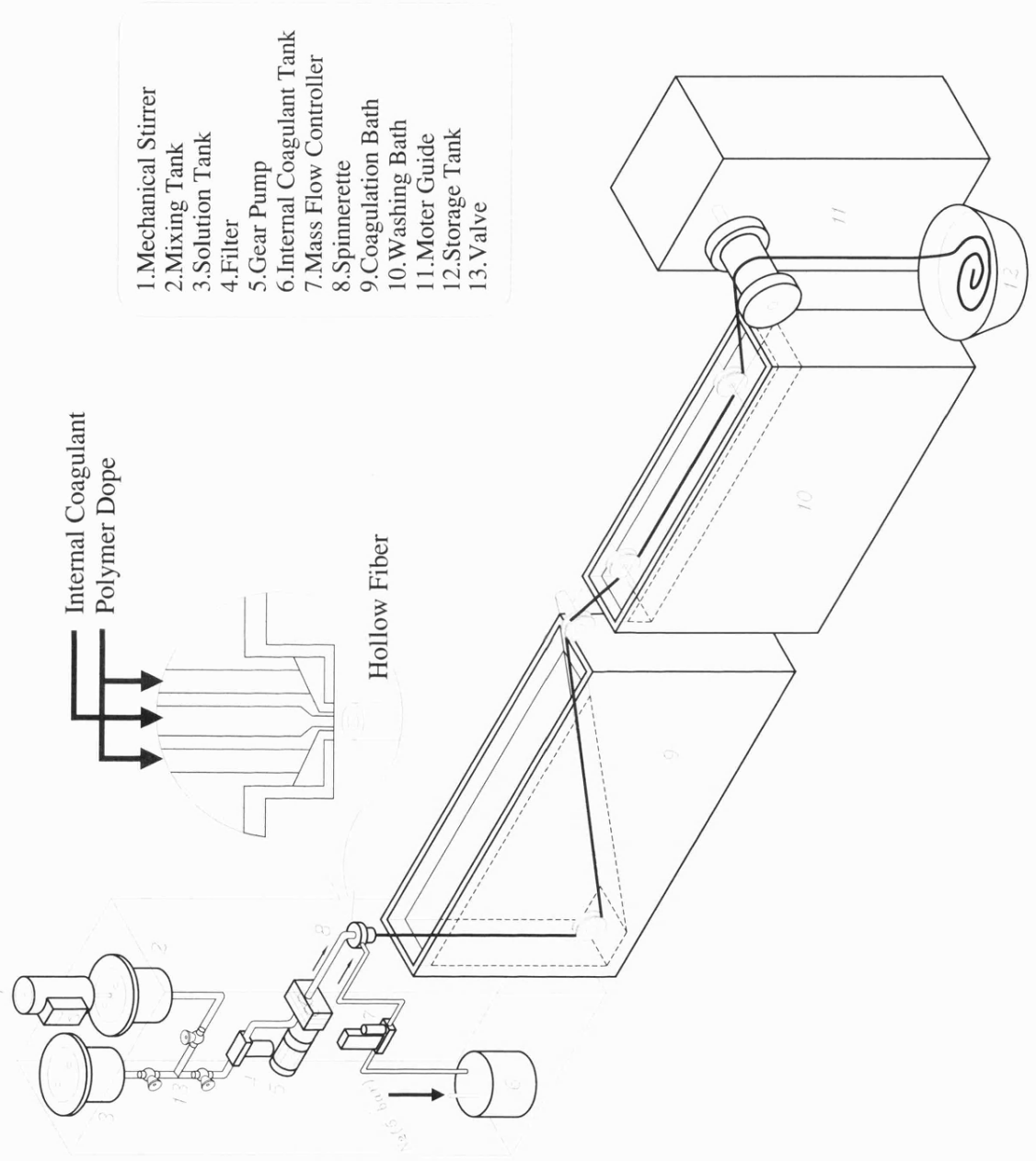

Figure 5.1 Schematic illustration of a hollow fibre membrane spinning apparatus

Table 5.1 Hollow fibre spinning parameters

Spinning conditions	
Internal coagulant injection rate	~ 2.0 ml/min
Polymer extrusion rate	10 – 12 ml/min
Nitrogen pressure	2 – 2.5 bar
Air gap	0 – 2cm
Take-up velocity	~ 4.5 m/min
Room temperature*	20 ±1 °C
Relative humidity*	40 - 60%

*Note: Air-conditioned laboratory environment

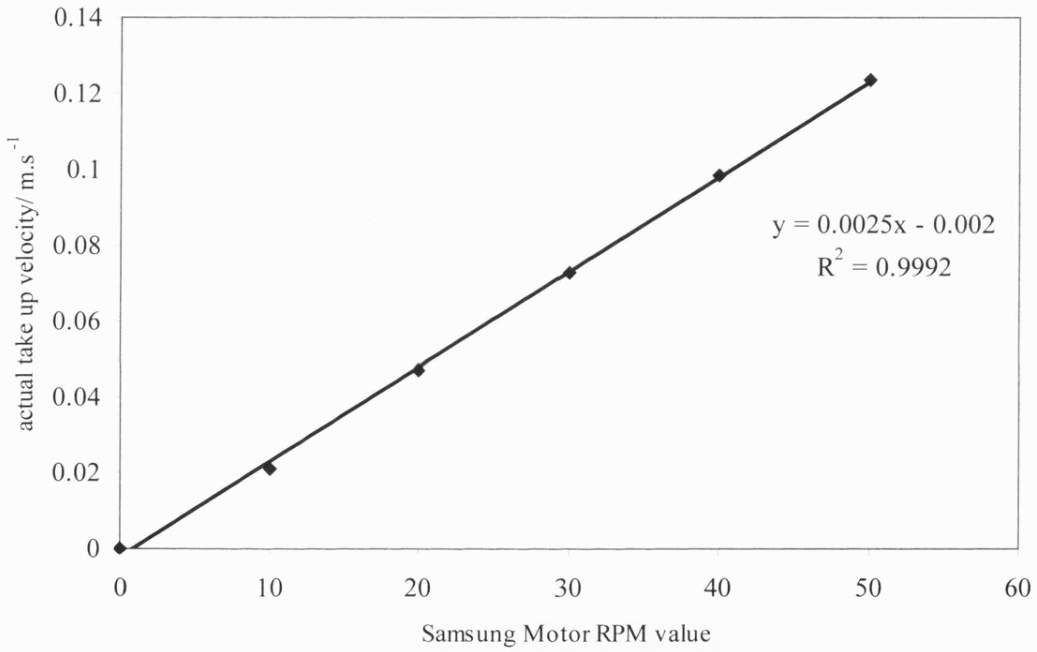

Figure 5.2 Correlations between motor rotations and fibre take up velocity

5.5.4 Gas Permeation Test

Gas permeation properties of the PVDF hollow fibre membranes were studied using apparatus as shown in Figure 5.3, using purified nitrogen [BOC Gas] as the test gas. PVDF hollow fibres were first dried in ambient conditions and then assembled as a test module using PTFE tubing and stainless steel fittings. Both ends of the hollow fibre were potted using epoxy resin [Epotek 605]. Each test module contained 1-2 fibres with length of about 10cm each. Gas permeation rate was measured using a soap-bubble

meter, at 0.5 bar pressure increment interval, up to a maximum 9 bar pressure. Before the membrane collapsed, the gas permeation flux increases in proportion with pressure. A drastic change in the nitrogen permeation rate (either an increment or a decrement) indicates the collapsed of mechanical integrity, without necessarily being accompanied by a visible physical rupture.

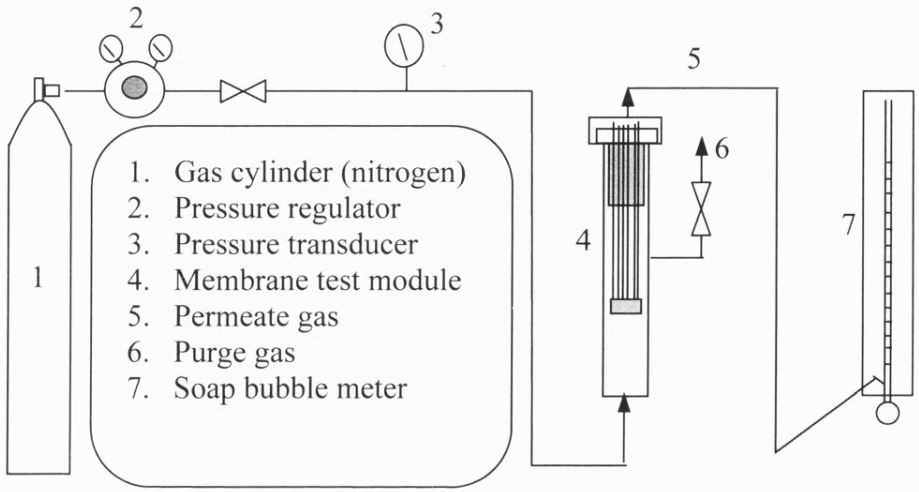

Figure 5.3 Schematic illustrations of gas permeation test apparatus

5.5.5 MORPHOLOGY STUDY

The cross section structures of the PVDF hollow fibre membranes were studied using a scanning electron microscope [JEOL JSM-T330 and JEOL JSM-T6310]. The fresh hollow fibres were cut into small pieces of approximately 5cm for the ease of handling. After half an hour of immersion in pure ethanol, the samples were dipped in liquid nitrogen and then freeze fractured using two forceps. The fractured samples were placed in a petri-dish layered with tissue for the removal of excess moisture. Following that, the sample fibre was adhered on a special aluminium dish using a conductive pad and placed in a silica gel container overnight to ensure thorough removal of moisture from the membrane pores. A thin layer of gold coating was then deposited [using Edwards Sputter Coater S150B] prior to the morphological examination using scanning electron microscope (SEM) [JEOL JSM-T330], images were taken using the attached camera [Mamiya 6x7, 50A-MRH].

5.5.6 MEMBRANE SHRINKAGE BEHAVIOUR

The longitudinal shrinkage (S_l) of a hollow fibre due to direct drying was determined by measuring the length of the hollow fibre before and after the drying, as expressed in the following equation:

$$S_l = \frac{\text{wet length - dry length}}{\text{wet length}} \qquad \text{(Equation 5.1)}$$

A simple one-stage solvent exchange method was then used to study the reduction in membrane shrinkage behaviour. The wet membranes were cut into a measured length of approximately 8cm and immersed in pure ethanol [reagent grade, Sigma Aldrich] for a designated period, after which they were removed from the ethanol bath and allowed to dry in ambient condition.

Assuming the membrane shrinkage in both the radial direction and the wall thickness is equal to that in the longitudinal direction, the total membrane shrinkage (S_t) is calculated by the following equation (Chabot *et al.*, 1997):

$$S_t = 1-(1-S_l)^3 \qquad \text{(Equation 5.2)}$$

5.5.7 HEXENE/HEXANE SEPARATION USING PVDF HOLLOW FIBRE MEMBRANE CONTACTOR

Experimental set-up for Olefin/paraffin separation with a hollow fiber membrane contactor is schematically shown in Figure 5.4. The silver nitrate aqueous solution was circulated [CP Instruments BPV-2] through the hollow fibre lumen while the hexene / hexane mixture was introduced [Vender] counter-currently into the shell side of the membrane contactor, which was fabricated using Swagelok® stainless steel fittings. Basic features of the hollow fibre membrane contactors prepared will be presented Table 5.3 in Section 5.6.6. Unless otherwise specified, hexene/hexane feed mixtures were fed to the contactor shell side at room temperature and 1 bar feed pressure [Norgren gauges]. The hexene removed from hexene/hexane mixtures was recovered with a hot water bath with temperature of 50°C and then collected in a cold trap. The system was drained and purged dry with purified air after each run to prevent permanent deposition of silver nitrate solution in the membrane matrix. Refractometer [Abbe 60] was used to analyse the composition of feed hexene / hexane mixtures and residual hexene concentrations at 20°C.

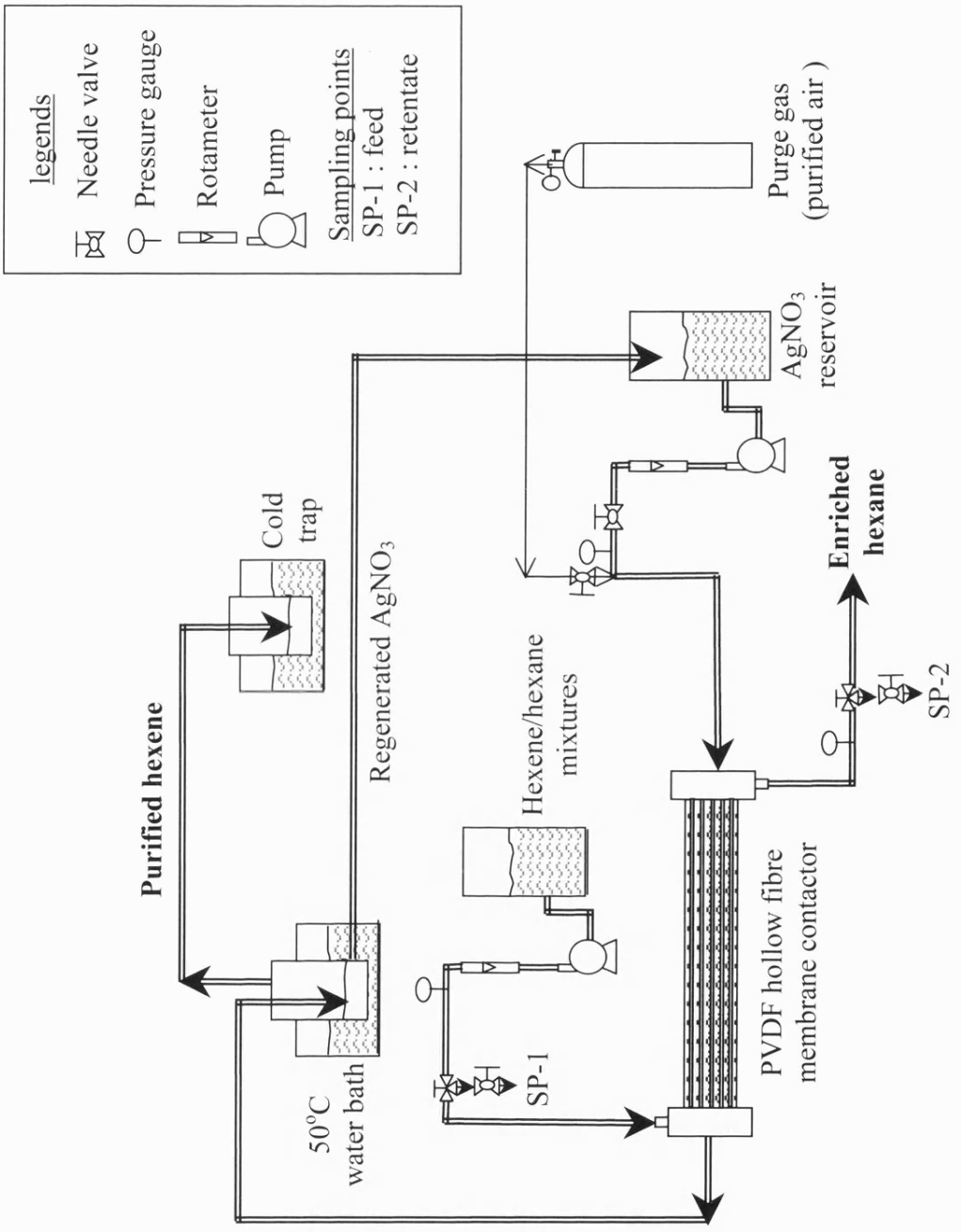

Figure 5.4 Schematic illustration of apparatus arrangement for the separation of hexene / hexane mixtures via π complexation with silver ion using PVDF hollow fibre membrane contactor

5.6 RESULTS AND DISCUSSIONS

In the following sections, variations in the resulting hollow fibre membrane morphology due to the change in the use of non-solvent additives, internal coagulants, and external coagulation bath temperature will be presented and discussed. In addition, effects of the abovementioned parameters on the resulting membrane gas permeation properties, mechanical strength as well as the membrane pore size distribution profile will be presented and analysed.

5.6.1 EFFECT OF NON-SOLVENT ADDITIVES ON MEMBRANE PROPERTIES

Increasing the amount of $LiClO_4$ added to 20 wt% PVDF / DMAc polymer dope (in the presence of 0.5 wt% PVP) has three visible morphological effects: (a) a thicker and denser skin layer; (b) a reduction in the presence of macro cavities beneath the skin layer; and (c) a reduction in the deposition of dense polymer matrix within the porous substructure, as clearly illustrated in Figure 5.5. In addition, viscosity measurements recorded an increase in solution viscosity, i.e. 2358 cP, 3949 cP and 4402 cP in accordance with the amount of $LiClO_4$ present in the polymer dope, i.e. 1 wt%, 2 wt% and 3 wt% respectively. Higher solution viscosity suggests a stronger macromolecular interaction and lower chain mobility, which would result in a lower non-solvent tolerance. Table 5.2 summarises the properties of the polymer solution used in the membrane spinning.

Table 5.2 Effect of $LiClO_4$ content on the viscosity of PVDF polymer dope

Membrane morphology	Dope composition / wt% (in balance of DMAc)			Viscosity / cP	
	PVDF	PVP	$LiClO_4$	at 25°C	at 50°C
Figure 5.5 (a)	20.02	0.40	0.99	2358	1755
Figure 5.5 (b)	19.93	0.50	2.07	3949	2290
Figure 5.5 (c)	19.94	0.50	3.05	4402	3262

With reference to scanning electron micrographs showed in Figure 5.5, thicker skin deposition revealed an instantaneous and localised polymer precipitation upon immersion in the coagulation bath due to low non-solvent tolerance. The skin formed

restricts further non-solvent inflow, it also hinders the solvent outflow from the polymer dope, and therefore a slow overall post-skin formation phase separation could take place within the remaining polymer / solvent / additives / non-solvent mixtures.

Membrane mean pore size calculated using nitrogen permeation data (following the method developed by Kong (2000)) was found to be 0.0156 μm, 0.0288 μm and 0.0467 μm for hollow fibre showed in Figure 5.5 (a), (b) and (c), respectively. Evidently, the growth in the membrane mean pore size is proportional to the increment in the amount of $LiC1O_4$ present in the polymer dope. There is, however, no clear trend between the effective membrane porosity with the amount of $LiClO_4$ added. As listed in Table 5.4, effective membrane porosity was calculated to be $9.2144x10^{-5}$ m^{-1}, 3.6568 $x10^{-6}$ m^{-1} and $1.8918x10^{-5}$ m^{-1} m for hollow fibres shown in Figure 5.4(a), (b) and (c), respectively. This is hardly surprising as the thick skin layer dominates the overall membrane resistance. A thicker hollow fibre skin, however, contributes to a better mechanical strength as shown by the higher collapse pressure. Hollow fibres spun with 1 wt% $LiClO_4$ collapsed when subject to 8.5 bar shell side pressure, followed by hollow fibre spun with 2 wt% $LiClO_4$ showing sign of collapse when subjected to 9 bar shell side pressure. Meanwhile, hollow fibre spun from 3 wt% $LiClO_4$ remained intact even at 9 bar pressure. Pore statistics of the spun hollow fibre membrane is tabulated in the Table 5.3

Table 5.3 Pore statistics and mechanical strength of hollow fibre spun using different amount of $LiClO_4$ as additive

Membrane morphology	**Dope composition / wt % PVDF / PVP / $LiClO_4$** in balance of DMAc	**Mean pore size / μm**	**Effective surface porosity / m^{-1}**	**Collapse pressure / bar**
Figure 5.5 (a)	20.02 / 0.50 / 0.99	0.0156	$9.2144x10^{-5}$	8.5
Figure 5.5 (b)	19.93 / 0.50 / 2.07	0.0288	3.6568 $x10^{-6}$	9.0
Figure 5.5 (c)	19.94 / 0.50 / 3.05	0.0467	$1.8918x10^{-5}$	> 9.0

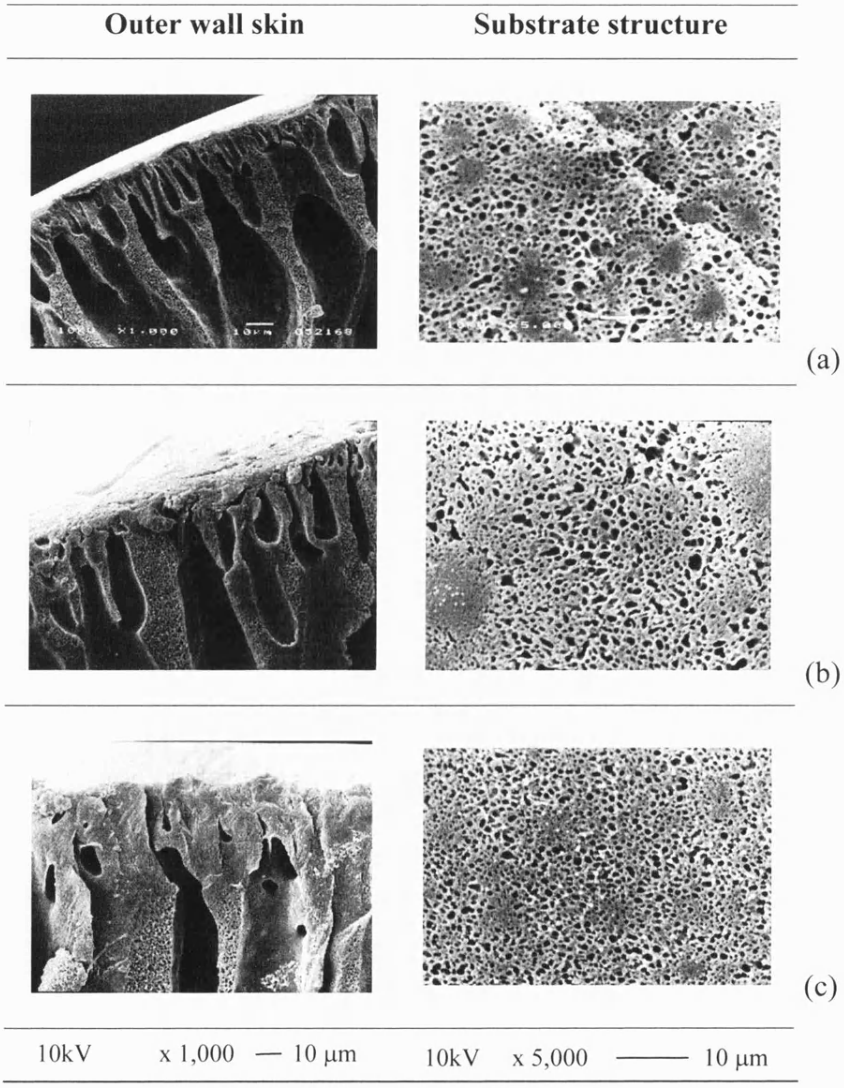

Figure 5.5 Effect of $LiClO_4$ on PVDF hollow fibre membrane morphology using dope containing 20 wt% PVDF, 0.5 wt%PVP (M_w10k) with (a) 1 wt% $LiClO_4$; (b) 2 wt% $LiClO_4$; (c) 3w t% $LiClO_4$; in the balance of DMAc using water as internal and external coagulation medium

.

With reference to Figure 5.6, a distinctive morphological difference between the three hollow fibres could easily be spotted. In general, the addition of 1 wt% glycerol results in a very dense membrane structure. Meanwhile, the presence of 0.5 wt% of PVP produces macrovoids adjacent to both outer and inner membrane skin.

Comparing between the near inner wall structures in Figure 5.6 (a) and (b), the individual globule present in Figure 5.6 (a) is replaced by fused globules in Figure 5.6 (b) indicating a much faster rate of nucleation growth. Glycerol functions as a mild non-solvent that is stronger than ethanol but weaker than water, with the ability to induce gelation (as discussed in section 3.5.3). Meanwhile in Figure 5.6 (c), a more open porous substructure is obtained with no sign of globules at all. This is because the presence of PVP enhances non-solvent inflow due to its hydrophilic nature; the bulk inflow of non-solvent caused a sudden turbulence to the solution thermodynamic equilibrium hence resulted in the formation of macrovoids where the envelope of non-solvent was encapsulated by a region of polymer rich phase. Further liquid-liquid demixing resulted in a membrane with porous substructure. Similar membrane morphology was also obtained with the use of PVP (Munari *et al.*, 1988).

As explained, the addition of glycerol resulted in a more densed polymer deposition while PVP resulted in a more porous morphology. This is also confirmed from calculation with the former having an effective porosity of 8.6248×10^{-7} m^{-1} and membrane mean pore size of 0.0196 μm, while the latter had a much greater effective porosity of 1.8919×10^{-5} m^{-1} and a bigger mean pore size of 0.0467 μm, as summarised in the following Table 5.4.

Table 5.4 Effect of dope compositions on the membrane mean pore sizes

Membrane morphology	**Dope composition / wt% (in balance of DMAc)**			**Mean pore size**
	PVDF	**$LiClO_4$**	**Additional additive**	**/ μm**
Figure 5.6 (a)	20.02	3	Nil	0.0146
Figure 5.6 (b)	19.93	3	1 wt % glycerol	0.0196
Figure 5.6 (c)	19.94	3.05	0.5 wt% PVP	0.0467

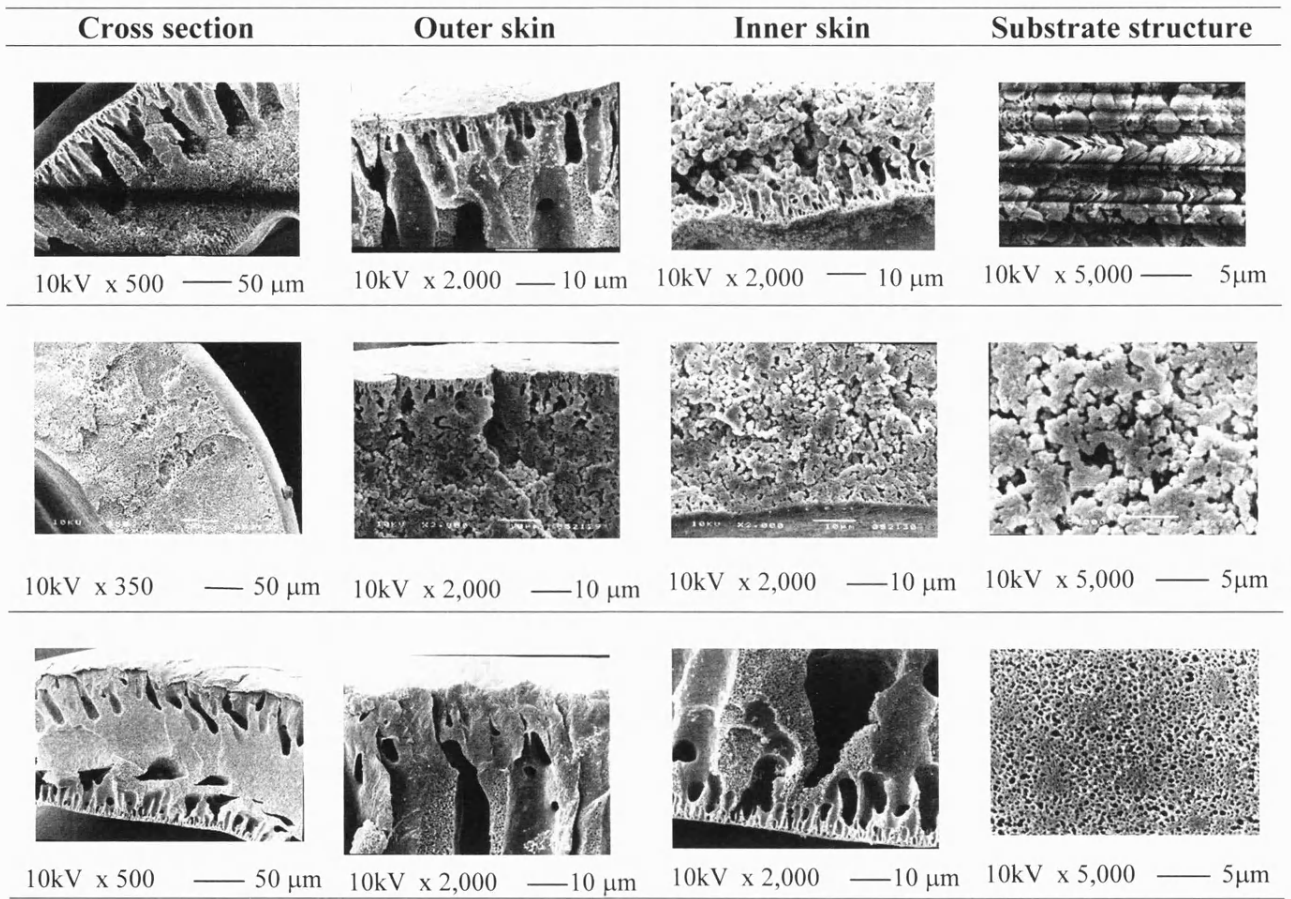

Figure 5.6 Comparison of PVDF hollow fibre morphology spun using dope containing 20 wt% PVDF with (a) 3 wt% $LiClO_4$; (b) 3 wt% $LiClO_4$ and 1 wt% glycerol; (c) 3 wt% $LiClO_4$ and 0.5 wt% PVP in the balance of DMAc using water as internal and external coagulation medium

5.6.2 Effect of Internal Coagulant on Membrane Properties

The effect of internal coagulant on the resulting membrane morphology is clearly demonstrated in Figure 5.7. Deposition of dense polymer matrix is clearly demonstrated due to the change in the internal coagulant used. Increasingly dense polymer matrix was noted when a greater concentration of NMP was used as internal coagulant. In addition, short finger-like structures beneath the inner wall skin were becoming less apparent as the concentration of NMP in internal coagulation medium increased. Membrane cross sectional thickness was measured and a thickness of 140 μm was recorded when water was used as internal coagulant. This thickness was found to increase from 147 μm to 171 μm and 220 μm when 25 vol% NMP, 50 vol% NMP and 100 vol% NMP was used as internal coagulant (Table 5.5). This could be explained based on the slow inner skin formation in the presence of NMP. As mentioned in Section 3.5.1, NMP was found to be a strong solvent for PVDF polymer, just after DMAc. No conclusion, however, could be drawn on the relationship between the ratios of NMP in internal coagulation medium with the membrane pore statistics.

Table 5.5 The effect of internal coagulant composition on the final membrane thickness for hollow fibre spun using dope containing 20 wt% PVDF, 76.5 wt% DMAc, 3.0 wt% $LiClO_4$ and 0.5 wt% PVP

Membrane morphology	Internal coagulant / vol%		Membrane thickness / μm	Mean pore size / μm	Effective surface porosity / m^{-1}
	water	NMP			
Figure 5.7 (a)	100	0	140	0.0319	4.46×10^{-6}
Figure 5.7 (b)	75	25	147	0.0285	2.85×10^{-6}
Figure 5.7 (c)	50	50	171	0.0489	1.15×10^{-5}
Figure 5.7 (d)	0	100	220	0.0467	1.19×10^{-5}

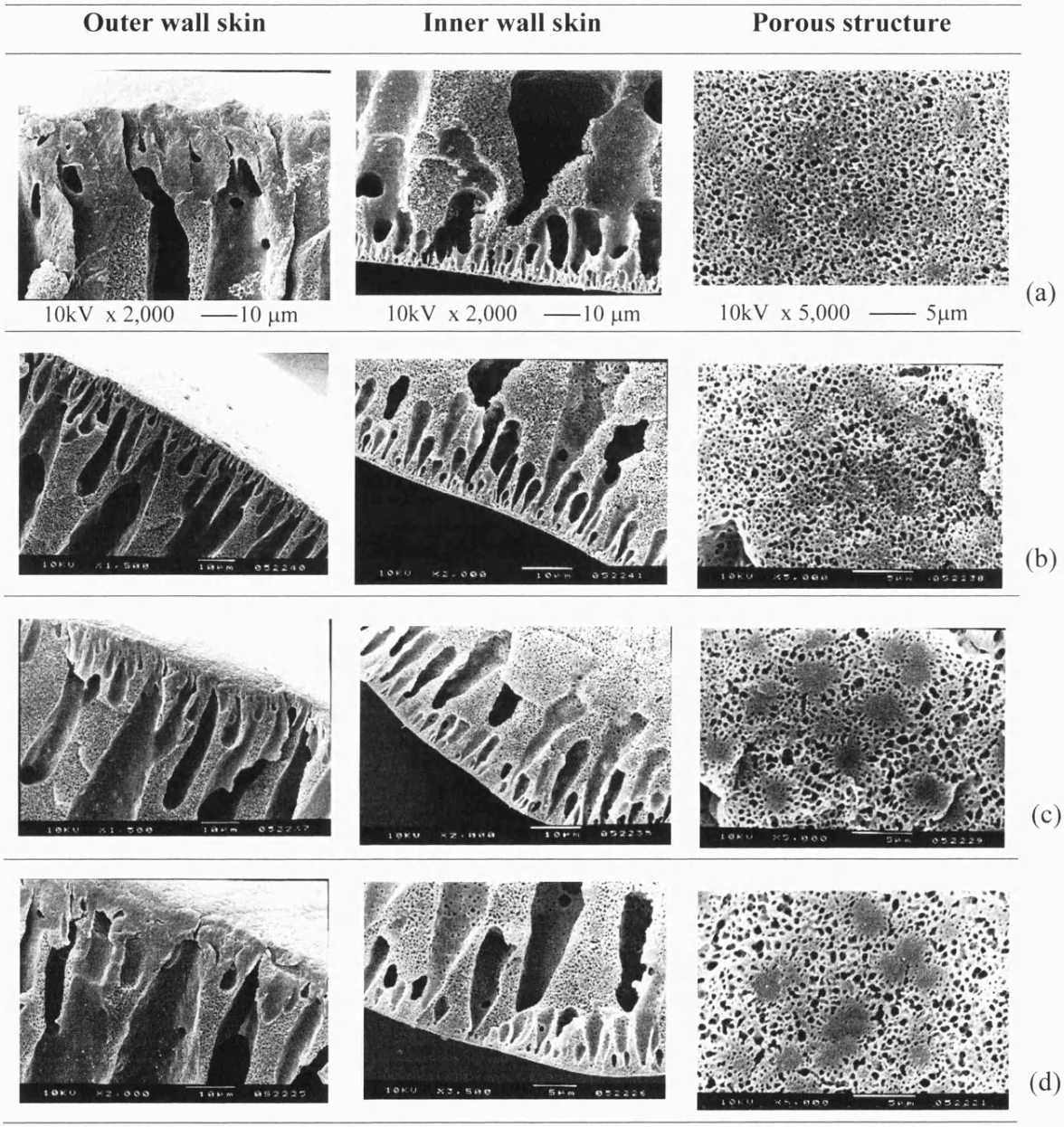

Figure 5.7 Morphology of hollow fibre spun from polymer dope containing 20 wt% PVDF, 76.5 wt% DMAc, 0.5 wt% PVP and 3.0 wt% $LiClO_4$ using (a) water; (b) 25 vol% NMP; (c) 75 vol% NMP; and (d) 100 vol% NMP as internal coagulant, in 25 ^{o}C water coagulation bath.

It is believed that the addition of solvent in the internal coagulant delays the skin formation on the membrane bore side. Absent or incomplete inner skin formation allows continuous exchange between the solvent in the polymer dope and the mixtures of the coagulation medium. Also, the presence of strong solvent such as NMP in the internal coagulation medium can diffuse and penetrate into the polymer dope, thus lowering the polymer precipitation rate due to the sustained high concentration of solvent in the dope. A high concentration of solvent in the polymer dope during the final phase inversion process has been reported to be favourable for the formation of a more porous membrane structures (Espenan and Aptel, 1986).

The effect of internal coagulant on the resulting membrane performance was also examined. Here, the hollow fibre membranes were prepared from dope solution containing 20 wt% PVDF, 76.5 wt% DMAc, 1.0 wt% glycerol and 3.0 wt% $LiClO_4$ using 35°C water as external coagulation bath. Scanning electron micrographs of these hollow fibre membranes are shown in Figure 5.8. In this case, no morphological variation could be visually detected. However, based on gas permeation experiment, membrane effective porosity was found to increase from 8.6248×10^{-7} m^{-1} when water was used to 9.8630×10^{-5} m^{-1} when 25 vol% NMP was introduced as internal coagulant. As for mean pore size, this decreased dramatically from approximately 0.02 μm when 100v ol% water was used as internal coagulant to approximately 0.003 μm when 25 vol% NMP was introduced as internal coagulant. In this study, the use of water as internal coagulant consistently produces hollow fibre with greater mechanical strength due to the rapid skin formation. Membrane collapse pressure drastically declined from 9 bar to 5.5 bar when 25 vol% NMP was used as internal coagulant, despite the increase in the membrane cross sectional thickness in the latter case, as summarised in Table 5.6.

Table 5.6 The effect of internal coagulant on the final membrane thickness for hollow fibre spun using dope containing 20 wt% PVDF, 76.5 wt% DMAc, 1.0 wt% glycerol 3.0 wt% $LiClO_4$ and 0.5 wt% PVP

Membrane morphology	**Internal coagulant / vol%**		**Mean pore size / μm**	**Effective surface porosity / m^{-1}**	**Membrane collapse pressure / bar**
	water	**NMP**			
Figure 5.8 (a)	100	0	0.0197	8.6248×10^{-7}	9
Figure 5.8 (b)	75	25	0.0025	9.8630×10^{-5}	5.5

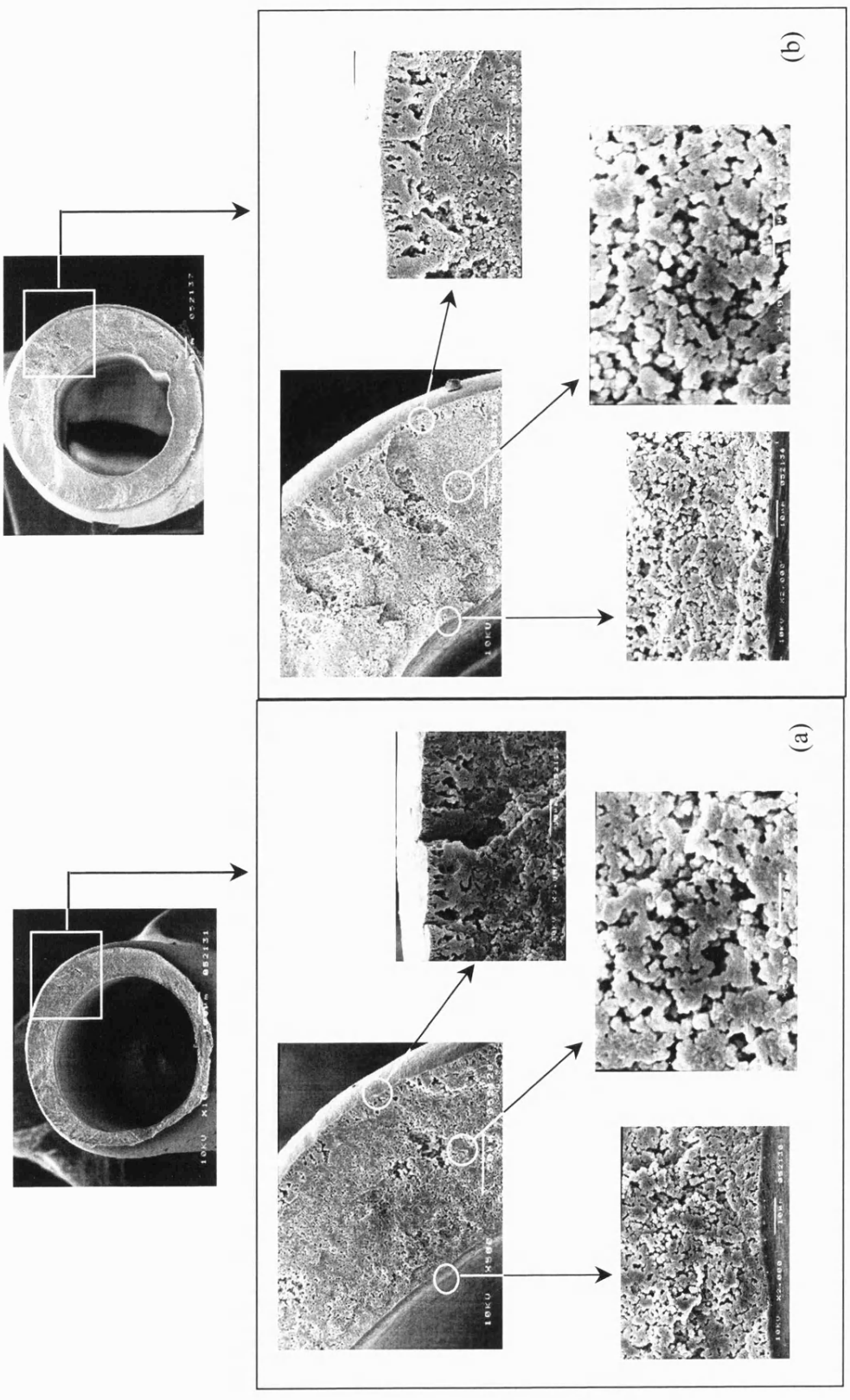

Figure 5.8 Morphology of hollow fibre spun from polymer dope containing 20 wt% PVDF, 77.0 wt% DMAc, 1.0 wt% glycerol and 3.0 wt% $LiClO_4$ using (a) water and (b) 25 vol% NMP as internal coagulant, in 25 °C coagulation bath

5.6.3 EFFECT OF SOLUTION AND COAGULATION BATH TEMPERATURE

The coagulation bath serves as the final quenching bath in which the nascent membrane is allowed to set while the exchange of solvent and non-solvent is actively taking place. Between hollow fibre morphologies illustrated in Figure 5.9 (a) and Figure 5.9 (b), the latter has a more extended longitude finger-like structure beneath both sides of the hollow fibre skin, followed by a more porous middle structure. A similar observation was also made between Figure 5.10 (a) and Figure 5.10 (b). In both cases, deposition of dense spherical nodular structures was abundant throughout the middle section of the hollow fibre, connecting between the cavities beneath the outer and inner skin of the hollow fibre, using low temperature coagulation bath. These visible spherical nodules suggest that the phase inversion process taking place was via an instantaneous liquid-liquid demixing process, i.e. individual nuclei grow until they collide and merge (Broen *et al.*, 1981). The presence of crystalline nodules is not favourable in membrane formation; it is described as dead volume where no permeation could take place for (Kesting, 1985).

A clear transformation of membrane morphology from a dense structure with globular/nodular deposits (Figure 5.9 (a) and Figure 5.10 (a)) to an open porous structure (Figure 5.9 (b) and Figure 5.10 (b)) could be observed when the coagulation bath temperature was increased to 50°C. This is due to a complex combination of enhanced diffusional kinetics at higher bath temperature which results in a more rapid solvent / non-solvent exchange and improved miscibility among all components, coupled with greater non-solvent tolerance capacity of the polymer dope at higher temperature. Similar conclusion was drawn by Jian and Pintauro (1993) whereby a highly microporous asymmetric structure was obtained when cast from polymer solution that was pre-heated to 50 °C. Between Figure 5.9 (a) and Figure 5.10 (a), the former has more individual spherical nodules while the latter exhibits more merged nodules. This could be due to the longer time frame available for nuclei growth as a result of a milder internal coagulant used (i.e. with the presence of 25 vol% NMP). Nodule size in the range of 80 μm – 200 μm was reported by Khayet *et al.* (2002) when 50 vol% ethanol was used as both internal and external coagulation medium, however no photographic evident was provided.

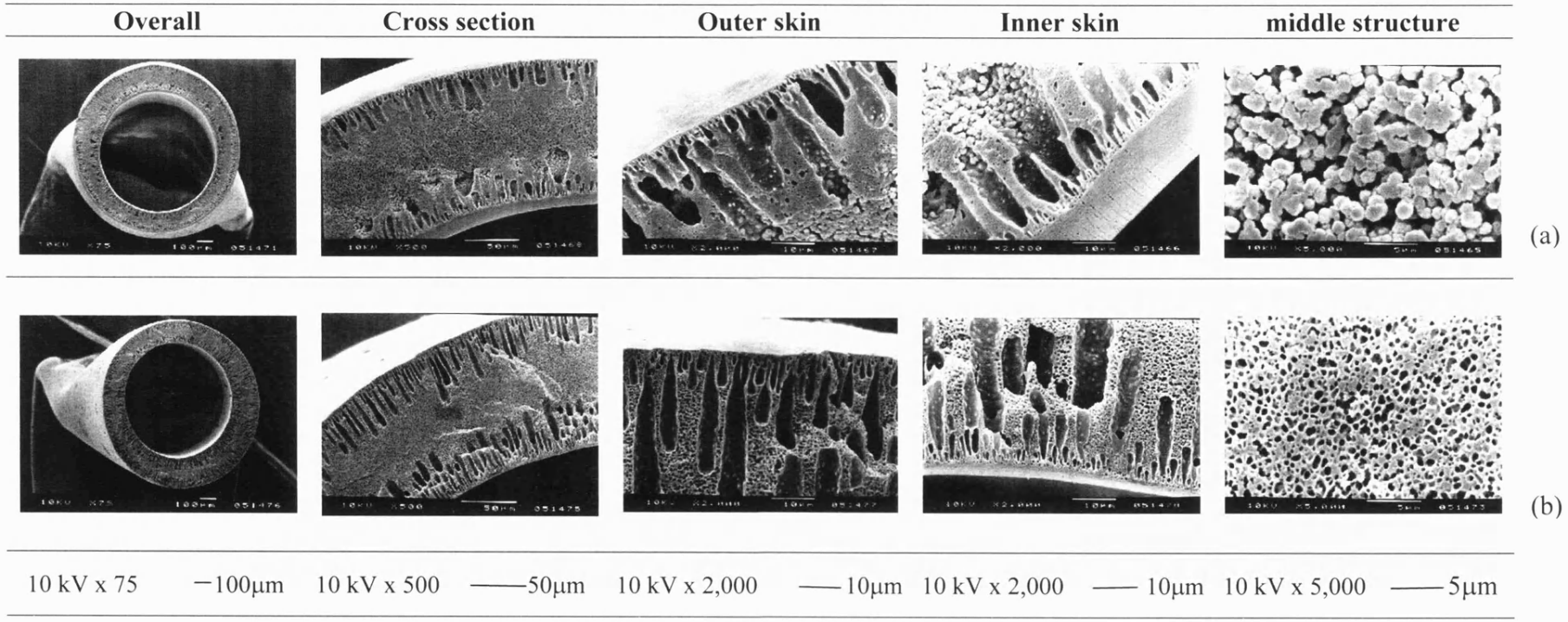

Figure 5.9 Morphology of hollow fibres spun from dope containing 20 wt% PVDF, 74 wt% DMAc, 6 wt% $LiClO_4$ using
(a) water as internal coagulant, 25°C water as coagulation medium
(b) water as internal coagulant, 50°C water as coagulation medium

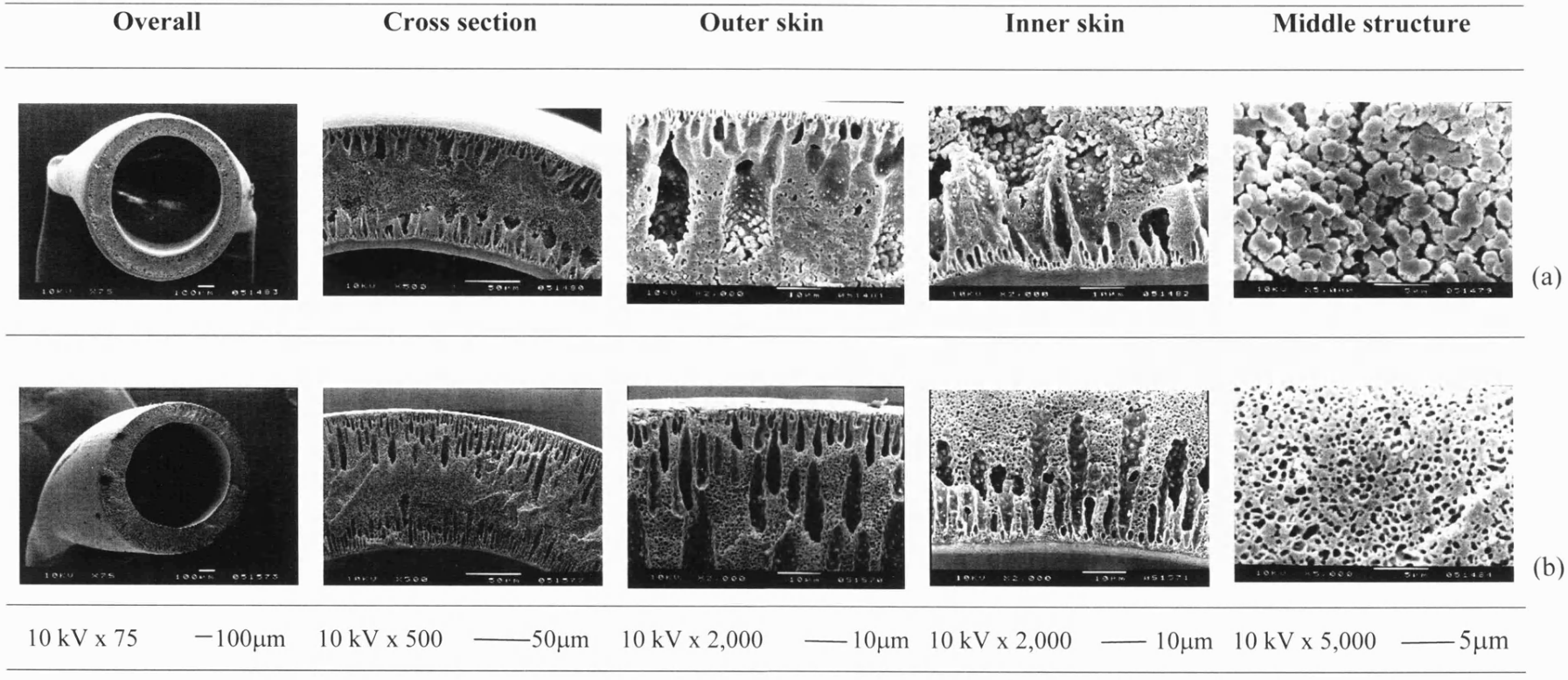

Figure 5.10 Morphology of hollow fibres spun from dope containing 20wt%PVDF, 74wt%DMAc, 6wt%$LiClO_4$ using
(a) 25 vol% NMP/ 75 vol% water as internal coagulant, 25°C water as coagulation medium
(b) 25 vol% NMP/ 75 vol% water as internal coagulant, 50°C water as coagulation medium

The effect of coagulation bath temperatures on the resulting membrane permeation properties were investigated. Membrane pore statistics summarised in table 5.7 clearly demonstrates the benefits of an increased bath temperature in increasing the membrane mean pore size. In line with this, higher permeation rate was also recorded for membrane produced at higher bath temperature, as shown in Figure 5.11.

Table 5.7 The effect of coagulation bath temperature on the final membrane properties for hollow fibre spun using dope containing 20 wt% PVDF, 77.0 wt% DMAc and 3.0 wt% $LiClO_4$ using water as internal coagulant

Bath temperature / °C	**Mean pore size / μm**	**Effective surface porosity / m^{-1}**
25	0.0124	34.04
50	0.0146	41.52

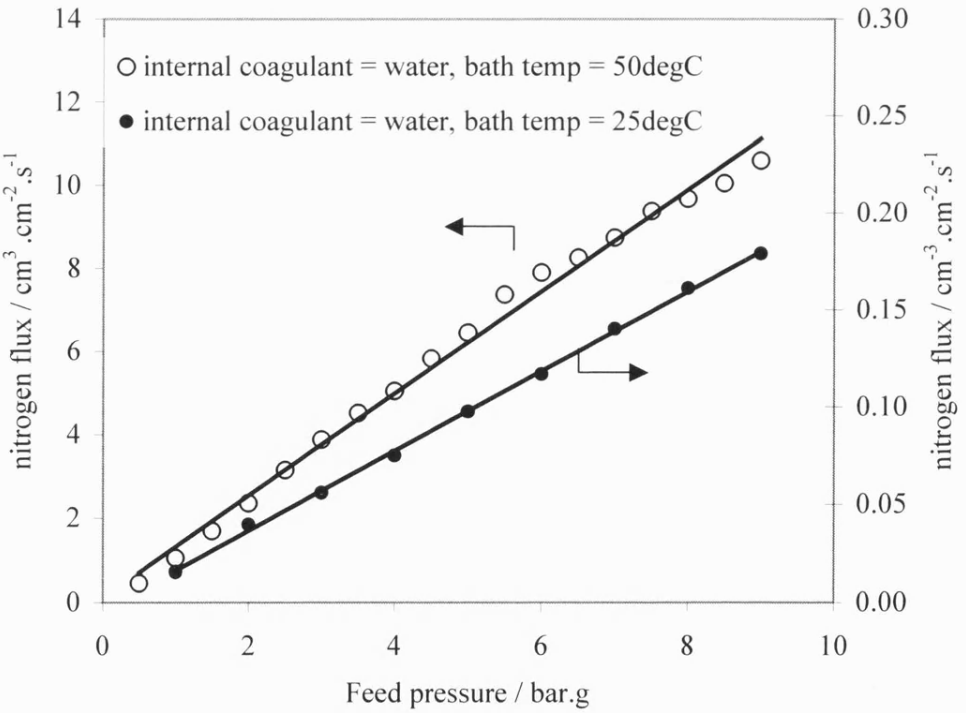

Figure 5.11 Nitrogen gas permeation flux for hollow fibre membrane spun from dope containing 20 wt% PVDF, 77 wt% DMAc and 3 wt% $LiClO_4$ using water as internal coagulant at 25 °C and 50 °C water bath temperature

However, at $LiClO_4$ concentration of 6 wt%, increasing bath temperature resulted in lower nitrogen permeation as shown in Figure 5.12. This trend is consistent for the two different internal coagulants (i.e. 100vol% water and 25 vol% NMP in water) used. The increase in $LiClO_4$ concentration is expected to reduce the solution tolerance for non-solvent, hence it is expected for the mixture to have a narrower demixing gap. This leads to a shorter precipitation pathway, allowing quick instantaneous dense skin formation that results in a lower permeation performance. Scanning electron micrographs of these membranes are shown in Figure 5.9 and Figure 5.10. A decrease in membrane permeation with the increase in coagulation bath temperature was also reported by Tomaszewska (1996), whereby the formation of a thicker skin was thought to be responsible for this finding. However, photographic example presented did not show the difference between two skin layers very clearly.

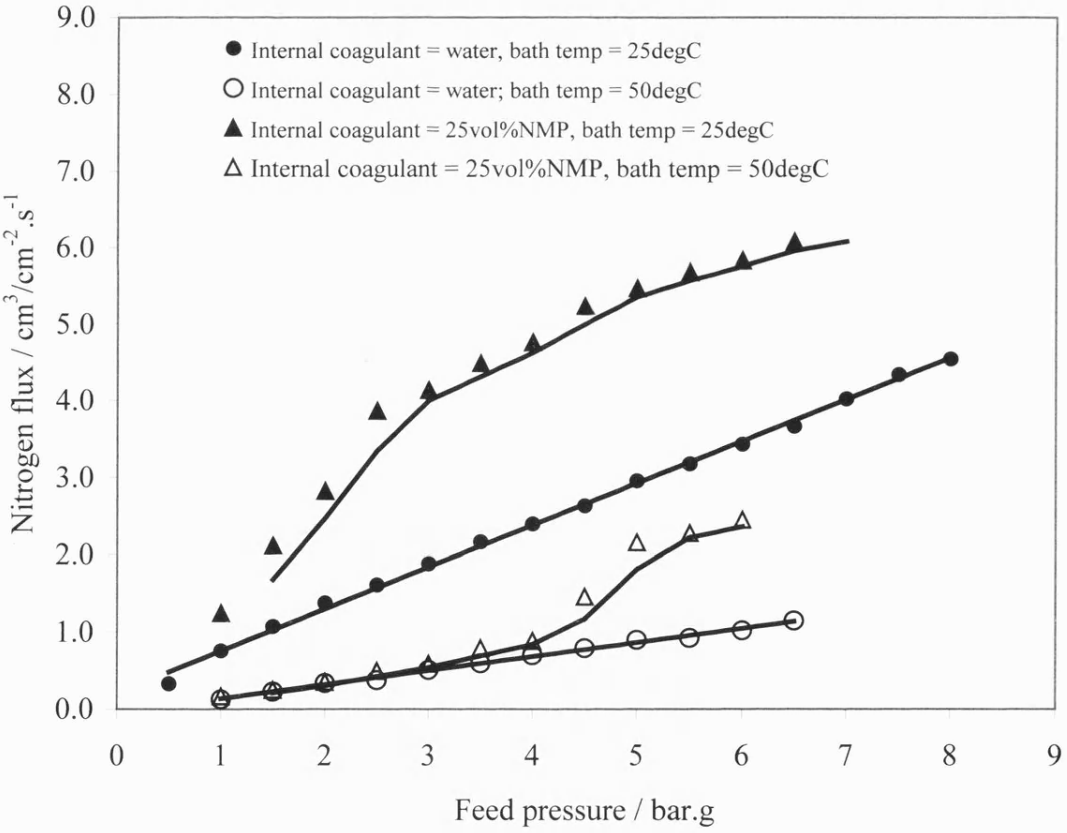

Figure 5.12 Nitrogen gas permeation flux for hollow fibre membrane spun from dope containing 20 wt% PVDF, 74 wt% DMAc and 6 wt% $LiClO_4$ using water and 25 vol% NMP as internal coagulant at 25 °C and 50 °C water bath temperature

5.6.4 COMBINED EFFECTS OF INTERNAL COAGULANT AND BATH TEMPERATURE

In this Section, discussion is based on the effect of combining the changes in internal coagulant composition and coagulation bath temperature on the resulting membrane properties. Experimental results suggest that the effect of internal coagulant is suppressed when higher coagulation bath temperature is used. Figure 5.13 shows the effect of internal coagulant on resulting hollow fibre morphology at higher coagulation bath temperature. The finger like structures from the inner wall diminished when 25 vol% NMP was introduced to the internal coagulant and disappeared as 75 vol% NMP was used as internal coagulant. As discussed in Section 5.6.3, the presence of NMP results in a much slower inner skin formation, as NMP is a very strong solvent for PVDF polymer. This, coupled with the high bath temperature which enhances the miscibility of all components present, resulted in a more homogeneous overall solution extending from the inner skin towards to middle region, prior to final polymer precipitation. Also, membranes formed at higher bath temperature are mechanically weaker, as confirmed by their lower collapse pressures. At 50°C bath temperature, membrane collapse pressure of 7 bar, 6 bar and 5.5 bar was recorded when 100 vol% water, 25 vol% NMP and 75 vol% NMP was used as internal coagulant, respectively. In comparison, membrane collapsed pressure of 8.5 bar 7.0 bar and 6.0 bar was recorded for those fabricated at bath temperature of 25°C using the same internal coagulant.

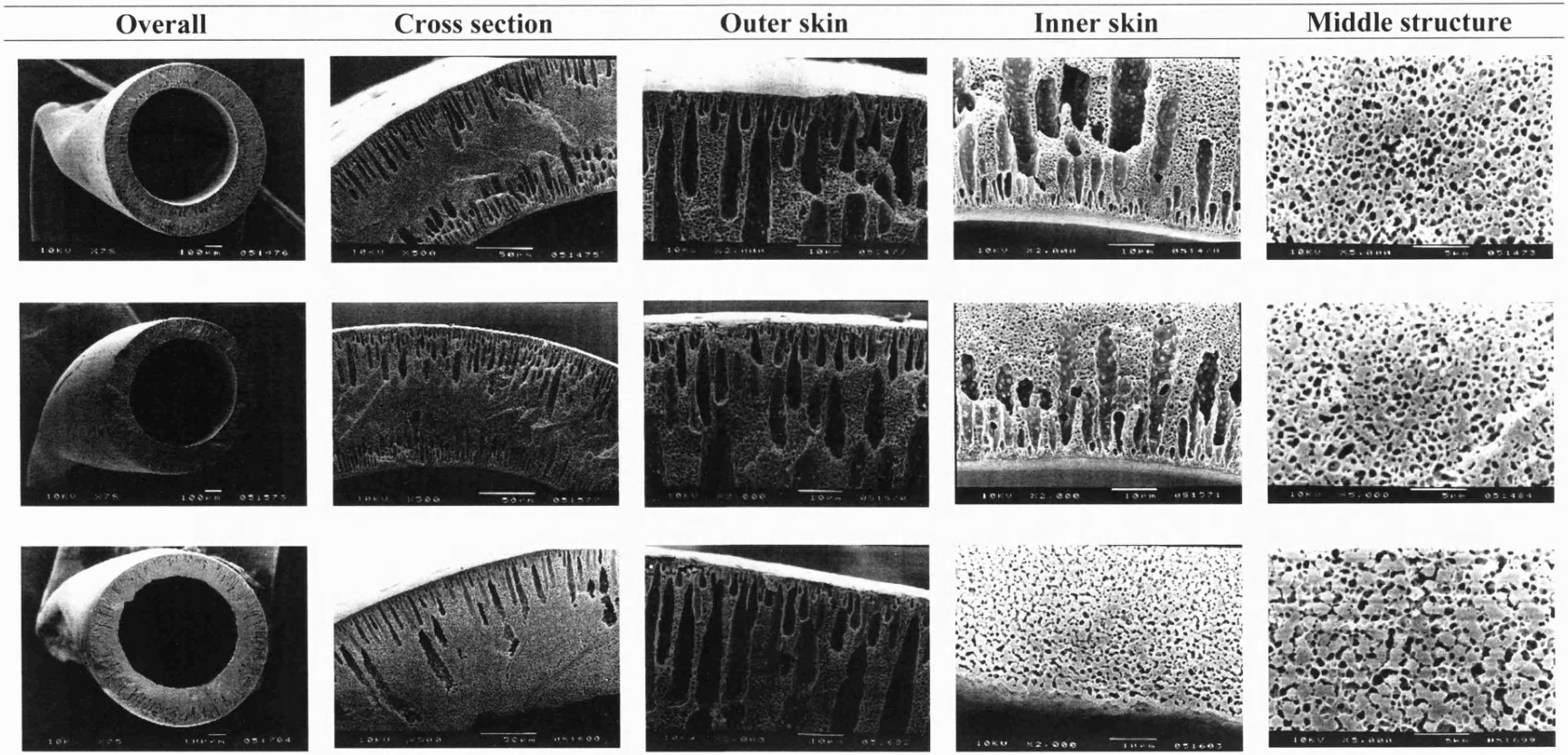

Figure 5.13 Morphology of hollow fibre spun from dope containing 20 wt% PVDF, 74 wt% DMAc, 6 wt% $LiClO_4$ using (a) water (b) 25 vol% NMP / 75 vol% water (c) 75 vol% NMP / 25 vol% water as internal coagulant; 50°C water as coagulation medium

5.6.5 MEMBRANE SHRINKAGE BEHAVIOUR

Using similar Kynar grade PVDF polymer, Benzinger *et al.* (1980) concluded that PVDF membrane could be dried without loss of physical strength, flexibility, flux or retention properties, therefore no treatment with surfactant or humectant was required prior to drying.

In this study, however, membrane longitudinal shrinkage up to 7.19 % was noted for hollow fibre membrane subject to direct air drying without conditioning / treatment. This membrane was spun using dope containing 19.83 wt% PVDF, 0.49 wt% PVP and 0.99 wt% $LiClO_4$ in the balance of DMAc. Degree of shrinkage eased as concentration of $LiClO_4$ increased, i.e. from 7.19 % for 0.99 wt% $LiClO_4$ to 6.58 % for 2 wt% $LiClO_4$ and further down to 5.71% for 3 wt% $LiClO_4$.

Morphologies of these membranes are shown in Figure 5.5, whereby an increase in the outer skin thickness was recorded following the amount of $LiClO_4$ present (as discussed in Section 5.6.1). With thicker skin, the effects of moisture loss during the drying process perhaps occurred more mildly, hence the membrane pore structure was subject to a less abrupt change in surface tension and was able to retain more of its nascent properties. Based on their membrane pore size distribution functions for these membranes as shown in Figure 5.14, it can be concluded that there is an increase in pore size following the amount of $LiClO_4$ added in the polymer dope, i.e. in the order of 3 wt% > 2 wt% > 1 wt%.

Using the same polymer material, shrinkage of dried hollow fibre membrane was only reported in Wang *et al.* (2000), but not in other preceding works (Deshmukh and Li, 1998; Wang *et al.*, 1999; Kong, 2000). In order to combat this shrinkage problem, Wang *et al.* (2000) adopted an organic non-solvent exchange method (by 5 minutes immersion in methanol, ethanol, 1-propanol and in some cases followed by a second stage of immersion in hexane) whereby a reduction of longitudinal shrinkage from 12 % to less than 7 % was achieved. Generally, the degree of shrinkage reduction decreases following the post treatment with 1-propanol > ethanol > methanol. PVDF membrane shrinkage behaviour was also observed on unsupported flat sheet PVDF membranes (Khayet and Matsuura, 2001).

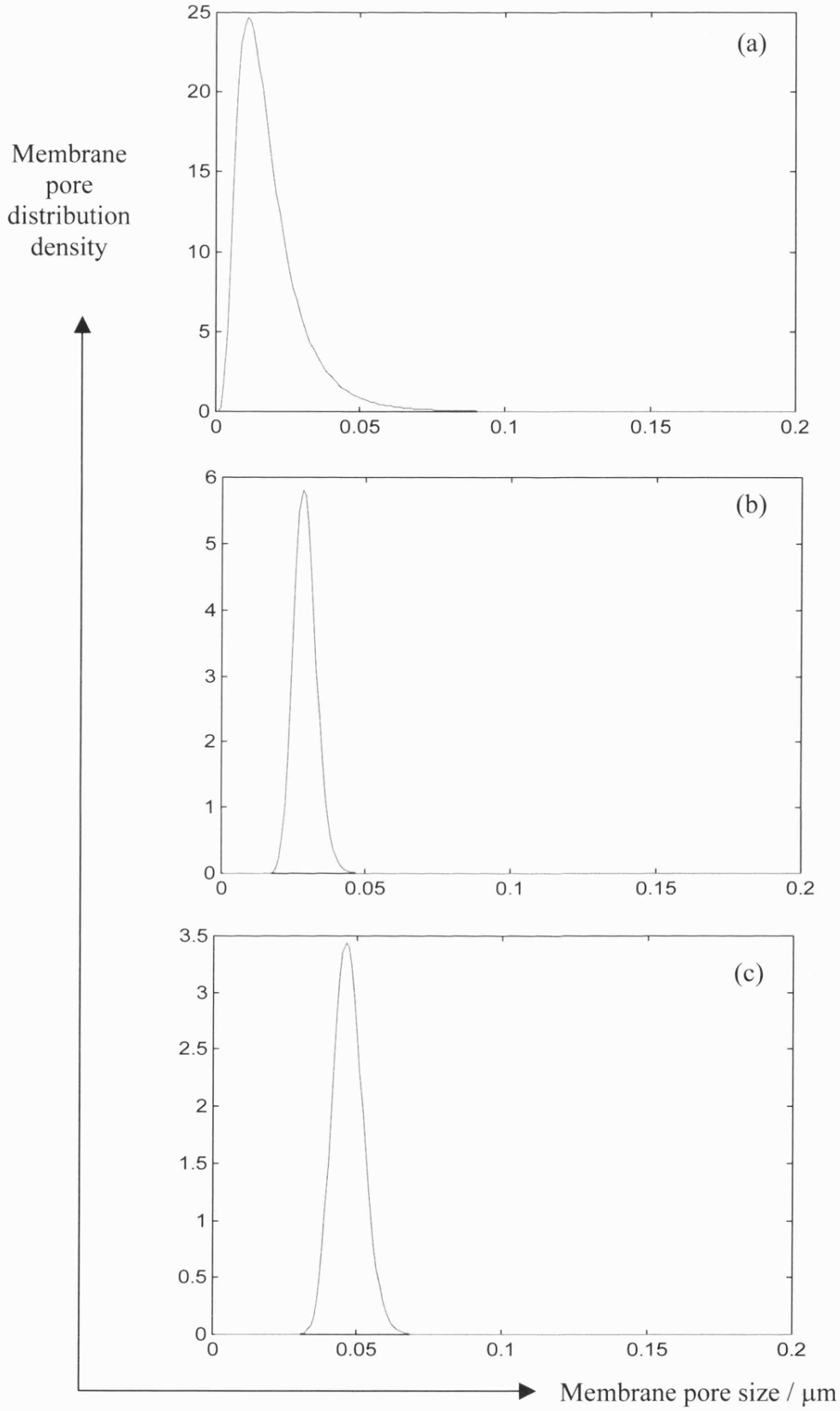

Figure 5.14 Pore size distribution of hollow fibre membrane spun from dope containing 20wt%PVDF, 0.5wt%PVP and (a) 1 wt%; (b) 2 wt% and (c) 3 wt% $LiClO_4$; in the balance of DMAc using 25 vol% NMP / 75 vol% water as internal coagulant, 40°C water as external coagulation medium

In order to overcome this problem, a similar solvent exchange method was used whereby the fresh membrane was immersed in 50 % aqueous ethanol solution for 4 hours and then in pure ethanol for 24 hours prior to final air-drying. It was believed that by replacing water in membrane pores with compounds having lower surface tension (such as low molecular weight alcohols) could eliminate the shrinkage behaviour, which was demonstrated to be successful by Wang *et al.* (2000) but the reverse was reported by Khayet and Matsuura (2001).

In this study, ethanol was used as the replacement solvent in a simple one-stage solvent exchange method to monitor the membrane shrinkage recovery. With reference to Figure 5.15, 10 minutes immersion in ethanol resulted in a maximum reduction in membrane shrinkage for all three batches studied. Interestingly, the shrinkage recovery reduces as the immersion time increases, and finally restored to nearly the same level of shrinkage as those without post treatment after 30 minutes of immersion as illustrated in Figure 5.16 (shrinkage ratio = post treatment shrinkage / original shrinkage).

When subjected to a short period of ethanol immersion (in this case, 10 minutes), sufficient ethanol replacement took place and penetrated the membrane pores; hence the membrane pores were in fact filled with ethanol/water mixtures. As the wet samples were removed and exposed for drying, ethanol that is more volatile presumably evaporated quicker than water. At this stage, the membrane pores were not completely dry at once due to the residual water remaining, hence the membrane drying process occurred in a less drastic way compared to purely water filled pores. Here, the drying process could be described as a 2 stages moisture loss accompanied by a much milder change in surface tension. As the immersion time increased, greater extent of ethanol substitution took place. By considering the case of the other extreme whereby the membrane pores are filled with pure ethanol, due to the higher volatility of ethanol, a rapid moisture loss will take place, hence despite the lower surface tension, membrane pore structures experienced a more intense drying process which is shown by this study to be equally destructive to the prevention of membrane shrinkage.

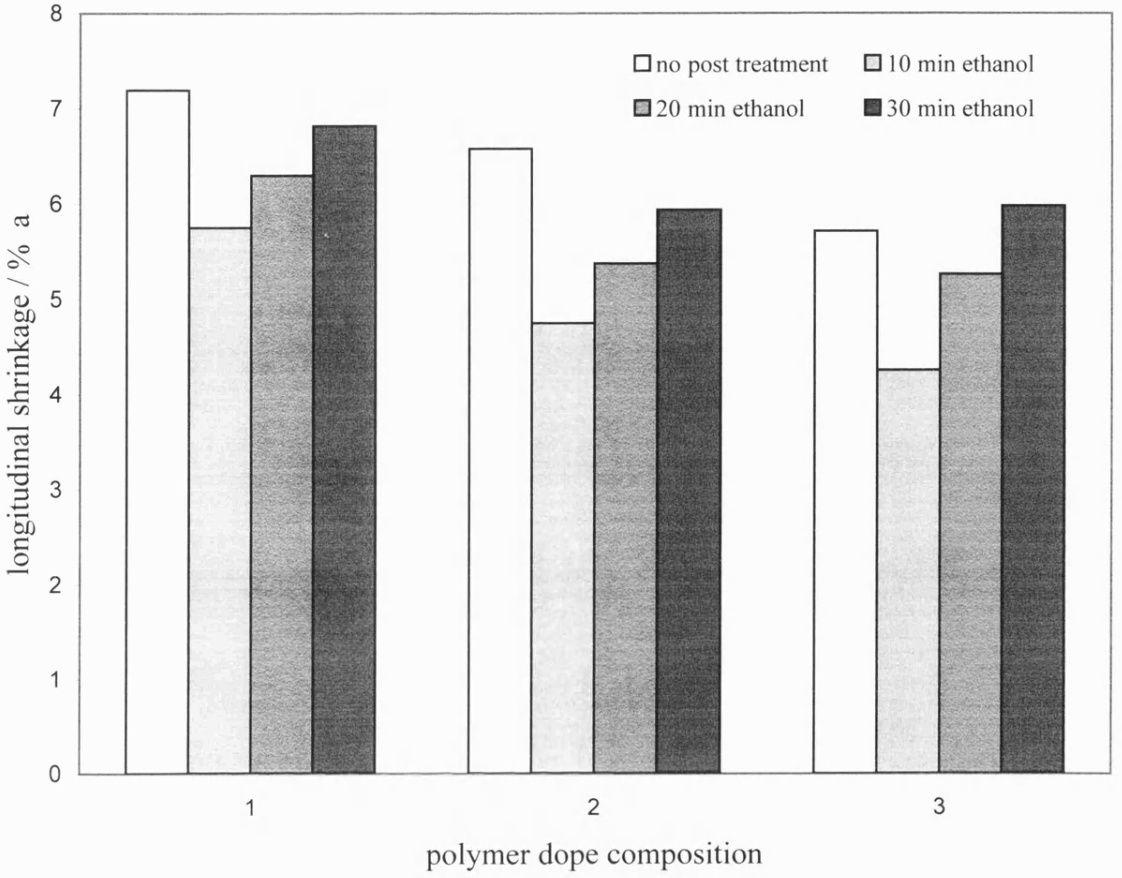

Figure 5.15 Effects of post treatment on shrinkage behaviour of hollow fibre membranes spun from dope containing 20 wt% PVDF, 0.5 wt% PVP with (1) 1wt%; (2) 2wt% and (3) 3wt% $LiClO_4$; in the balance of DMAc using 40°C water as internal and external coagulation medium

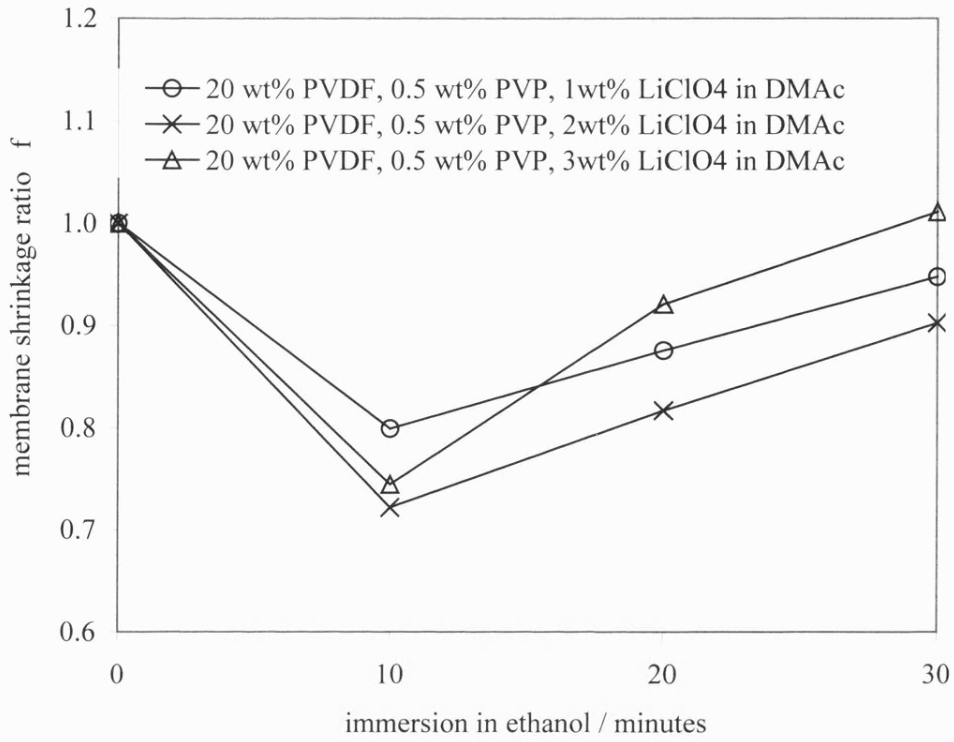

Figure 5.16 Effect of immersion time in ethanol on the ratio of membrane shrinkage

5.6.6 Hexene/hexane Separation via π Complexation with Silver Ions Using PVDF Hollow Fibre Membrane Contactor

Separation of hexene from hexene/hexane mixtures via π complexation with silver ion (Ag^+) using a PVDF hollow fibre membrane contactor was performed using three different hollow fibre membrane contactors previously prepared. 1 M aqueous silver nitrate was used as the carrier solution containing the complexation agent Ag^+ at ambient temperature (approximately 20 °C). Effect of various operating parameters on the resulting hexene / hexane separation performance of the membrane contactor were studied by varying the feed concentrations, feed flow rates, silver nitrate circulation velocities, their respective flow ratios (R = silver nitrate circulation velocity/ hexene-hexane feed velocity) and operating pressures. Cross sectional morphology of these hollow fibre membranes are illustrated in Figure 5.17. Table 5.8 summarises the basic properties of the hollow fibre membranes used as well as the dimensions of the membrane contactors prepared.

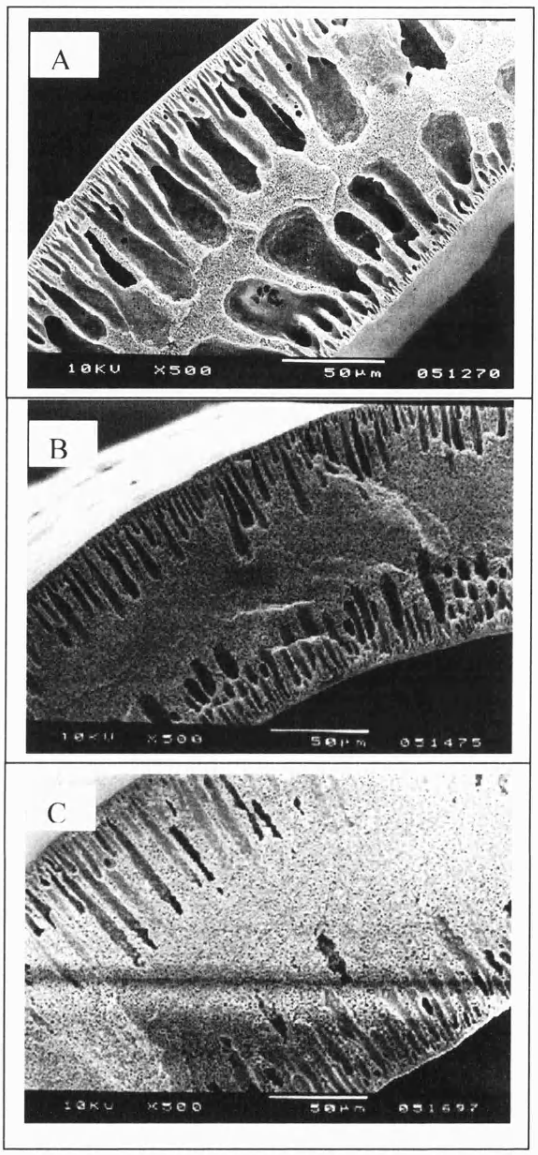

Figure 5.17 Cross sectional structure of membranes used in hollow fibre contactors (HFC-1, HFC-2 and HFC-3) spun using the following dope composition:
A: 20 wt% PVDF, 3 wt% glycerol, 0.42 wt% PVP, 0.46 wt% $LiClO_4$ and 76wt% DMAc at 50°C
B: 20 wt% PVDF, 6 wt% $LiClO_4$ and 74 wt% DMAc at 50°C
C: 20 wt% PVDF, 3 wt% $LiClO_4$ and 77 wt% DMAc at 50°C
using water as internal coagulant, in 50°C water as coagulation medium

Table 5.8 Basic features of PVDF hollow fibre membrane contactors

	HFC-1	HFC-2	HFC-3
length (cm)	28	19	19
Number of fibres	11	20	20
Contact area (cm^2)	67.74	83.57	83.57
Collapse pressure (bar)	5.5	7.0	>9.0
Effective porosity	2.3166×10^2	1.9434×10^2	4.1529×10^3
Mean pore size (μm)	0.0495	0.0181	0.0142

Using hollow fibre membrane contactor HFC-1, feed solution containing 10 vol% hexene and 90 vol% hexane mixture was fed into the contactor shell side at room temperature and 1 bar feed pressure. With $AgNO_3$ flowing counter-currently at the rate of 2.27 $ml.min^{-1}$ (flow velocity of 0.89 $cm.s^{-1}$), Ag^+ was supplied in excess throughout the whole experiment. Preliminary experimental data revealed that residue hexene concentration increases with increased feed velocity as shown in Table 5.9, with hexene reduction of 46 % attainable. This is not a dramatic hexene removal, however it indicates the feasibility of the process design for the intended purpose, i.e. hexene removal via π complexation with Ag+ ion using PVDF hollow fibre membrane contactor.

Table 5.9 Residue hexene concentration at different feed velocities

Feed velocity / cm. min^{-1}	**Residue hexene concentration / vol%**
6.02	5.36
6.62	7.06
9.33	7.54
19.27	7.81

When comparing the separation performance of HFC-2 (effective porosity = 1.9434×10^2) and HFC-3 (effective porosity = 4.1529×10^3), HFC-2 with greater effective porosity demonstrated better hexene removal. When fed with feed stream containing 5 vol% hexene concentration, HFC-3 evidently out performed HFC-2 by

demonstrating higher hexene removal of 93.65%, as summarised in the following Table 5.10.

Table 5.10 Comparison between the hexene removal of HFC-2 and HFC-3

Membrane contactor	Hexene/hexane feed flow rate / ml.s^{-1} A	$AgNO_3$ recirculation rate / ml.s^{-1} B	Flow ratio B/A	Maximum hexene removal / %
HFC-2	0.1154	0.6039	5.23	56.87
HFC-3	0.1293	0.6056	4.68	93.65

In the following paragraphs, discussions will be made based on experimental results obtained using membrane contactor HFC-3, to study the effects of various operating conditions on hexene removal. Using HFC-3, feed solution containing 5 vol% of hexene was fed into the contactor shell side at a controlled flow rate (A) between 0.12-0.13 ml.s^{-1}. Maximum hexene removal was found to decline from 93.65% to 79.89% following the increase in silver nitrate circulation rate from 0.61 ml.s^{-1} to 1.46 ml.s^{-1}, i.e. an increase in flow ratio from 4.7 to 11.2. A further decrement in hexene removal to 44.85% was recorded when the silver nitrate circulation rate was further increased to 2.67 ml.s^{-1} (flow ratio of 22.9). Summary of these experimental results is as tabulated in following Table 5.8.

Table 5.11 Effects of flow ratio on the maximum hexane removal

Hexene/hexane feed flow rate / ml.s^{-1} A	$AgNO_3$ recirculation rate / ml.s^{-1} B	flow ratio B/A	Maximum Hexene removal / %
0.1293	0.6056	4.6835	93.65
0.1307	1.4617	11.1799	79.89
0.1165	2.6695	22.9108	44.85

At constant flow ratio of 4.68 (i.e. by maintaining hexene/hexane feed flow rate at 0.13 ml.s^{-1} and silver nitrate circulation rate at 0.61 ml.s^{-1}), maximum hexene removal was found to increase with the decrement in feed hexene concentration. As

summarised in Table 5.12, hexene removal as high as 93.65 % was attainable when the feed concentration was reduced from 9.97 vol% to 4.85 vol%.

Table 5.12 Effects of feed hexene concentrations on hexene removal

Feed hexene concentration / vol%	**Maximum hexene removal / %**
9.97	33.75
8.21	41.39
4.85	93.65

With reference to Table 5.13, no clear trend in term of hexene removal was noted when the shell side pressure was increased from 1.0 bar to 2.2 bar and then further increased to 3.3 bar. Also, due to the variation in the feed hexene concentration (6.05 vol%, 5.16 vol% and 6.0 vol%) and the flow ratio (5.65, 5.97, 5.82), which could also have impacted the hexene removal efficiency, no conclusive statement can therefore be made.

Table 5.13 Effect of shell side pressure on the removal of hexene

Shell side pressure / bar	**Feed hexene concentration / vol%**	**Hexene/hexane feed flow rate / $ml.s^{-1}$ A**	**$AgNO_3$ circulation rate / $ml.s^{-1}$ B**	**Flow ratio B/A**	**Maximum hexene removal / %**
1.0	6.05	0.1072	0.6056	5.65	37.3
2.2	5.16	0.1017	0.607	5.97	44.64
3.3	6.0	0.1043	0.6067	5.82	32.99

5.7 CONCLUSIONS

In this chapter, the information and understanding obtained from the previous chapters 3 and 4 are utilised in the formulation of a suitable polymer dope. Here, focus is placed on improving the hollow fibre membrane properties. Ideally, membranes with well-connected porous network, good mechanical strength and thin top skin layers are desirable. Another aim is to eliminate morphology associated with gelation and crystallisation.

The use of $LiClO_4$ as an additive is found to be favourable in the production of highly porous hollow fibre membranes. Experimental results revealed that $LiClO_4$ (in the presence of PVP) promoted a better mechanical strength (as confirmed by the higher collapse pressure) and resulted in an increase in membrane mean pore sizes. No conclusion, however, can be drawn regarding the effective surface porosity. With additional 2 wt% of $LiClO_4$ in the polymer dope, a membrane mean pore size increment of nearly 3-fold was noted (i.e. from 0.0156 μm (at 1 wt% $LiClO_4$) to 0.0467 μm (at 3 wt% $LiClO_4$)). Scanning electron micrographs revealed that the addition of glycerol also promoted the formation of macrovoids, similar to those formed by the addition of PVP.

The impact of internal coagulant composition (NMP / water mixtures) on the resulting membrane morphology was clearly documented using scanning electron micrographs. In general, SEMs showed a decline in inner skin structure with the increment in NMP concentrations. Based on gas permeation experiments, the introduction of 25 vol% NMP in the internal coagulant resulted in the following adverse effects, i.e. lower mean pore size and lower effective surface porosity. However, further increment in NMP content to 50 vol% and 75 vol%, resulted in a thicker overall membrane cross sectional thickness with bigger values for membrane mean pore size increase and its effective surface porosity. No significant difference could be detected with further NMP increment to 100 vol% apart from a sharp decline in membrane collapse pressure, which is believe to be a result of the skin elimination.

At 25°C, a variety of dense polymer matrices were found to be abundant in the membrane substrate structures between the inner and outer skin. These structures (which are unique to the additive used) could be eliminated by elevating the temperature of the polymer dope and by using a high temperature coagulation bath. In return, open cellular porous substrate structures were formed. This was accompanied by an increase in membrane mean pore size and effective surface porosity, obtained from gas permeation test data. Hence it can be concluded that thermodynamic properties of the polymer dope could be enhanced which has a vital role in the final membrane morphology by influencing the inter-diffusional properties among all components.

Membrane shrinkage behaviour was believed to be strongly related to the surface tension properties of the quenching bath. Using pure ethanol as a conditioning medium prior to the final membrane drying, a reduction in membrane shrinkage phenomena could be achieved. This, however, is strongly dependent on the duration of immersion. More studies are required before any firm conclusion can be drawn.

Feasibility of the PVDF hollow fibre membrane contactors developed in the separation of hexene / hexane mixtures via π complexation with Ag^+ was clearly demonstrated based on these preliminary experimental results. In brief, an increase in feed concentration and silver nitrate recirculation rate resulted in a decline in maximum hexene removal, while the increase in membrane effective porosity was found to favour the hexene removal, possibly due to a more efficient contact mode. To conclude, data obtained from this preliminary experimental work indicates the feasibility of separating olefin/paraffin mixtures via π complexation with Ag^+ using the PVDF hollow fibre membrane contactor previously developed, with potentially up to 94 % of hexene removed. Indeed, the full potential of these membrane contactors are yet to be revealed. More systematic studies is therefore recommended to further understand the transport properties and separation performance under various operating conditions.

CHAPTER SIX

DEVELOPMENT OF COMPOSITE HOLLOW FIBRE MEMBRANES FOR VAPOUR PERMEATION APPLICATION

6.0 FOREWORD

The emergence and importance of membrane separation technology, especially vapour permeation in the area of solvent recovery has long been recognised, primarily attributed to its environmental and economical implication (Baker *et al.*, 1987; Sander and Janssen, 1991). This chapter focuses on the development of a composite membrane for the removal of volatile organic compounds (VOC) from contaminated air streams.

6.1 VOC EMISSION PROBLEMS

Scientifically, volatile organic compounds (VOC) include all organic compounds; either in gas or vapour form, with vapour pressure less than 760 mmHg (101.3kPa) at 20°C, which are capable of producing photochemical oxidants by reaction with nitrogen oxides in the presence of sunlight.

Emission of these VOC into the atmospheric environment by both natural biogenic and anthropogenic sources, primarily from petroleum and petrochemical related activities, as well as the distribution plus usage of vehicular gasoline, is no longer a new issue. From both environmental and health aspects, many of these chemicals are either known carcinogens or toxic in nature, especially the aromatic and halogenated hydrocarbons, which may seriously harm the biosphere, hydrosphere and atmosphere. Moreover, the vast scale of the petrochemical industries often leads to a very complex waste problem (Simmons, *et al.*, 1994). Increasing public attention together with a better understanding of the adverse effects of these emissions has nevertheless imposed a greater pressure towards more stringent environmental regulations. Numerous epidemiological studies focusing on both occupational and ambient VOC exposure have highlighted the emergence of this problem. From an economic point of view, the presence of valuable hydrocarbon compounds in the waste streams makes its recovery economically appealing. For instance, Peinemann *et al.* (1986) estimated an annual organic solvent emissions of 10 to 15 million tonnes in the United States, of which

naphtha, toluene, xylene, perchloroethylene, trichloroethane, acetone, ethanol and methanol together share almost 80% of the total emissions (Baker *et al.*, 1987). Feng *et al.* (1991) identified solvent-based coating industries as the major contributor. Jansen *et al.* (1994a) presented a quantitative summary on the losses from industrial solvent emission in terms of both monetary as well as energy value, as tabulated in Table 6.1.

Table 6.1 Resale and energy value of solvent emitted (Jansen *et al.*, 1994a).

Country	Emissions (tones/year)	Resale value (million US$/year)	Energy value (GWh/year)
USA	22,000,000	1,300-2,200	18,000-31,000
Germany	2,000,000	120-200	1,700-2,800
Netherlands	300,000	18-30	250-420

Assumptions made:
1. 30-50% of emissions can be recovered.
2. Solvent price = US$200/tonne; energy value = 10,000 $kJ.kg^{-1}$.

Figure 6.1 compares the applicability of various treatment technologies over a wide range of feed VOC concentrations. Operating cost of carbon adsorption generally increases with increasing feed vapour concentrations, whereas the operating cost of membrane process scales with the feed flow rate. As a result of this, carbon adsorption is preferred when dealing with dilute VOC exhaust stream, while membrane technology is preferred when higher VOC concentration is involved, as shown in Figure 6.1, for there is no frequent regeneration required. To conclude, membrane technology offer a promising monetary return in vapour permeation application, particularly for treating small volumes of waste gas with relatively high vapour concentration, (at the emission point where air dilution is minimal), followed by its environmental applications (Jansen, *et al.*, 1994b; Mulder, 1994b).

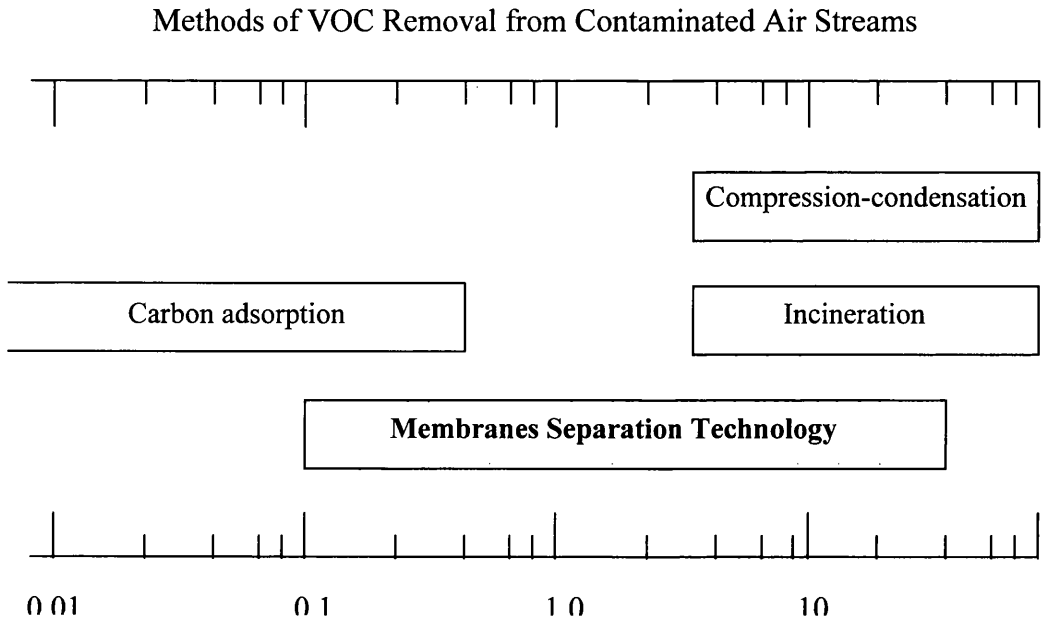

Figure 6.1 Approximate useful ranges of various treatment technologies for the removal of organic vapours from air (Baker and Wijmans, 1994)

In recent years, a growing amount of technical literature has been published by both academic and industrial contributors, namely University of Twente, New Jersey Institute of Technology (NJIT), Membrane Technology Research (MTR), GKSS, Industrial Membrane Research Institute (IMRI), University of Ottawa and so on, as will be discussed in the following sections. Despite extensive research on the basic principles and methodology of membranes, tailor making and optimisation of vapour permeation membranes, however, remains scarce and the commercial market of this application is still immature.

6.2 Basic Principles of Vapour Permeation Technology

Vapour permeation simply speaking is the transport of vapours via a membrane system from a vapourous feed mixture to a vaporous permeate stream, as illustrated in Figure 6.2. The fact that it is fed with a vaporous stream, rather than liquid as in pervaporation, offers an important theoretical advantage in the sense that no heat input is required for the vaporisation of liquid feed streams upon their permeation through the membrane

matrix (Ho and Sirkar, 1992). With the absence of high temperature treatment, the possibility of thermal induced phase and chemical structural change is therefore eliminated.

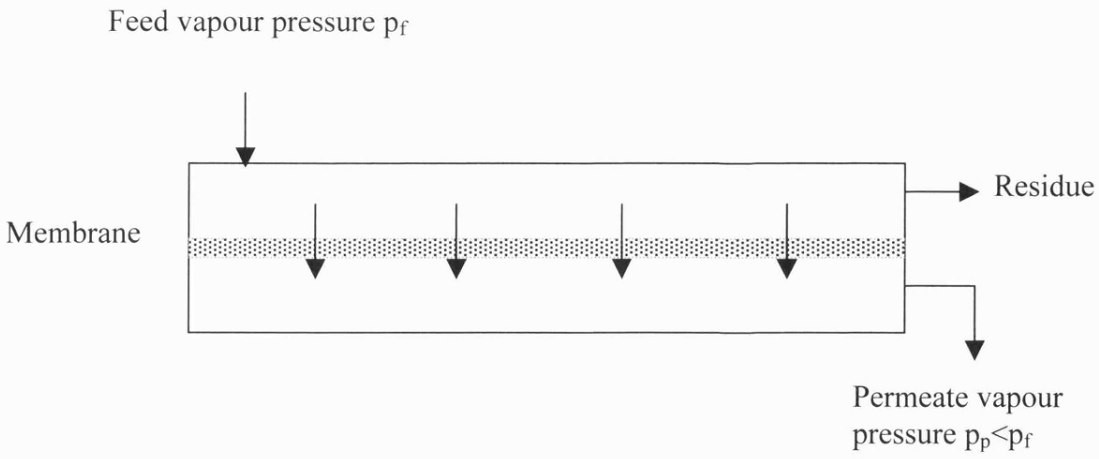

Figure 6.2 Schematic illustration of vapour permeation principle.

Vapour permeation operates on the principle that different components in gaseous/vapourous mixtures have different permeation rates, thus enabling preferential removal of one or more components across the membrane media. In vapour permeation, an external driving force is introduced by applying vacuum at the permeate side, hence, maintaining a pressure difference between the feed and permeate side for trans-membrane diffusion. The degree of separation, however, is governed not only by the differences in the relative transport rates of the feed components via the membrane matrix, but also involves the relative driving force imposed on each component. In short, if the membrane system were permitted to go to equilibrium, permeation would continue to occur until the pressure and composition of gas on both sides of the membrane were equal, with no separation being achieved. In other word, separation is achieved only if the system is maintained away from the equilibrium-state, i.e. by maintaining a lower partial pressure with continuous condensation of permeate stream at the downstream side.

In vapour permeation technology, composite membranes, i.e. porous substrates made of synthetic polymeric material laminated with a thin layer of dense silicone-based material, are often used. Here, the porous substrate provides the required mechanical

strength, allowing the membrane to tolerate both the harsh manufacturing process and pressure differentials imposed during applications. Meanwhile, the silicone coating performs the actual separation by eliminating the possible presence of pinholes, thus enhancing the membrane selectivity. In many cases, this membrane is also being regarded as a solution diffusion membrane in accordance with its transport mechanism .

Vapour permeation differs from membrane gas separation processes, as it requires an extra feature other than high permeability and good selectivity, which is membrane stability against vapour attack. From the literature, vapour permeabilities are expected to be 100–10,000 times higher than nitrogen while membrane selectivity of 100–200 is essential in the recovery of low concentration organic solvents from air stream (Baker *et al*, 1987; Peinemann et al., 1986). In terms of its permeability requirements, it has to be much more permeable to hydrocarbons than air.

Peinemann and Mohr (1989) suggested that a membrane with a permeability of 100 to 10,000 times more permeable to solvent than air is essential in the recovery of low concentration organic solvents from air. Also, in order to serve its purpose in the treatment of the extremely large amount of solvent laden exhaust gas streams, high surface area and packing density are undoubtedly other important criteria to be considered in the selection of membrane systems, thus making hollow fibre membrane modules an ideal choice. On top of that, membrane materials used should also possess excellent chemical stability in order to withstand organic vapour attack. Hence, it has to be able to "adsorb" and "desorb" the solvent without any alteration to its properties. In addition, a membrane's ability to withstand high temperatures – ideally up to 200°C is an additional advantage due to the high temperature involved in the treatment of industrial gaseous waste streams (Baker *et al.*, 1987), and also, to prevent undesirable capillary condensation in the membrane interface.

Currently, flat sheet membranes have been widely employed for vapour permeation regardless of their limited area and low packing density. Leemann *et al.* (1996) commented that the unavailability of commercial membranes with sufficiently high packing density, and insufficient solvent stability of the existing membranes are among the major difficulties encountered in the development of vapour permeation membrane technology. The factors affecting the design of membrane vapour-gas separation system

have been addressed in detail by Baker *et al.* (1998). The viability and applicability of a composite membrane, which combines the separation properties of a coating material and the mechanical strength of a supporting layer, in the area of vapour permeation has gained much attention recently, leading to numerous research attempts (Paul *et al.*, 1988; Kimmerle *et al.*, 1988; 1991; Bume *et al*, 1991; Feng *et al.*, 1991; 1993; Founda *et al.*, 1993; Fritsch *et al.*, 1993; Deng *et al.*, 1998; Polotsky and Polotskaya, 1998; Teng *et al.*, 2000; Yagagishita *et al.*, 2001). In the fabrication of composite hollow fibre membranes, a microporous hollow fibre membrane with good mechanical strength is coated with a thin layer of selective polymer to perform the separation. Ideally, the defect free top layer should be as thin as possible while the support membrane should possess a high porosity with reasonably small pore size. Realistically, the effects of fibre properties, both support and coating layers, on the separation performance are inevitable (Rautenbach *et al.*, 1998).

6.2.1 Recent Development in Vapour Permeation Technology

Despite its relatively short industrial application, vapour permeation has been well recognised for its potential cash inflow, especially when valuable organic vapours such as reusable solvents, aroma and flavour essences are involved (Fouda *et al.*, 1993). To date, recovery of halogenated hydrocarbons, gasoline vapours and organic solvents from air are among the major industrial vapour permeation applications with quite a number of pilot plants being installed worldwide, especially in developed countries like Germany (Peinemann and Ohlrogge, 1994) and the USA (Baker, 1985; Baker and Wijman, 1994).

Among current vapour permeation membranes, silicone coated thin film composite flat sheet membranes are found to be predominant (Baker 1985; Kulkarni *et al.*, 1986; Peinemann *et al.*, 1986; Baker *et al.*, 1987; Behling, 1988; Paul et al., 1988; Pinnau *et al.*, 1988; Behling *et al.*, 1989; Feng *et al.*, 1991; Deng *et al.*, 1992; Feng *et al.*, 1993; Fouda *et al.*, 1993; Fritsch *et al.*, 1993; Baker and Wijmans, 1994; Ito *et al.*, 1995; Ohlrogge, 1995; Petersen and Peinemann, 1997; Singh *et al*, 1998; Teng *et al.*, 2000). Theoretically, this combination is proven to be unsatisfactory from the viewpoint of low packing density of flat sheet membranes, as well as poor chemical stability possessed by silicone rubber (which is highly susceptible to vapour attack) (Leeman *et al.*, 1996).

Thus, more and more studies have been carried out to search for membrane materials with better chemical stability and this will be discussed in greater detail in the following sections.

For practical reasons, MTR incorporates its organic selective flat sheet composite membranes into spiral wound modules for the separation and recovery of volatile organic compounds (VOC). This module design, which is commercially known as the VaporSep^{TM} System, is a membrane envelope wound around a porous central collection pipe, with vapour permeability 10-100 times higher than air (Baker, 1985; Wijmans and Helm, 1989; Wijmans, 1990; Baker and Wijmans, 1994; Baker *et al.*, 1998). Mesh spacer material is used to form channels for the feed air and the permeate vapours of which the feed air is circulated laterally through the module. As the air stream passes across the membrane surface, the organic solvent preferentially passes through the membrane and enters the permeate channel. This permeate vapour spirals inward to the central permeate collection pipe and then passes to the permeate condenser. Briefly, VaporSep^{TM} consists of two steps: compression-condensation and membrane vapour separation. This combination utilises the advantages of both compression-condensation and membrane separation to create an optimised overall process that achieves better separation performance, at higher efficiency, than either method alone (Baker, 1985; Jacobs *et al.*, 1993).

GKSS marketed their plate and frame membrane configuration, commercially known as GS-modules with a hydrocarbon vapour / nitrogen selectivity greater than 10. This membrane consists of three layers of different materials, with an elastomeric permselective top layer coating on a microporous polyetherimide (PEI) substrate and a non-woven fabric to provide the required mechanical strength. Polyetherimide was chosen as the microporous supporting layer instead of the commonly used polysulfone based on the following two reasons, i.e. its high permeability at a defined pore size; and its stability against fuel vapour attack. (Behling, 1988 and Behling *et al.*, 1989; Ohlrogge, et al., 1990; Ohlrogge *et al.*, 1993(a); Ohlrogge, *et al.*, 1993(b); Ohlrogge and Wind, 1994; Peinemann and Ohlrogge, 1994; Ohlrogge, 1996). A number of industrial plants using these GS modules have been installed in Germany for VOC removal, as described in Peinemann and Ohlrogge (1994).

On the other hand, Sourirajan and co-workers from IMRI have done quite an extensive survey on the separation of organic vapour-air mixtures using asymmetric aromatic membranes, both in the form of flat sheet (Feng *et al.*, 1991; Deng *et al.*, 1992; Feng *et al.*, 1993) and hollow fibre (Deng *et al.*, 1995a; Deng *et al.* 1995b; Deng *et al.*, 1998). Asymmetry is introduced to the membrane structure using the phase inversion technique in the membrane preparation in order to reduce the membrane resistance and to increase the permeation rate. It is claimed that both PI and PEI asymmetric membranes showed better vapour permeability than silicone rubber composite membranes. Therefore, the authors concluded that the coating step could be eliminated if the membrane pore size were properly adjusted via control of the membrane preparation conditions (Feng *et al,* 1991 and Feng *et al.*, 1993). Besides, Deng *et al.* (1995a, 1995b) studied the separation performance of asymmetric PEI hollow fiber membrane in the presence and also, the absence of water, which was found to have no effect on the permeability of hydrocarbon or gasoline vapours. In contrast, Fouda *et al.* (1993) reported the effect of water vapour in lowering the permeate benzaldehyde concentration. In line with this, Cha *et al.* (1996) reported successful water vapour removal using dried Cuprophan homogeneous hollow fibre membranes. Another interesting conclusion is that highest benzaldehyde removal efficiency does not necessarily come from membranes with perfectly coated porous substrate (Fouda *et al.*, 1993). However, no further explanation was made on that conclusion. A more recent publication discusses on the development of poly(vinylidene fluoride) (PVDF) hollow-fiber membranes (Chabot *et al.*, 1997). In their study, a thin layer was coated on PEI porous substrate to study its intrinsic organic selective properties, which were found to have resulted in enhanced propanol permeation while suppressing water permeation.

6.2.2 Selection of Membrane Materials

As mentioned, the majority of experimental works reporting on vapour permeation have focused on silicone coated thin film composite membranes. Silicone rubber, in general, posseses high thermal stability because of the high bond energy of its main structure, i.e. 90 kcal.mol^{-1} for -Si-O-; as compared with only 60kcal/mol for –C-C-. However, conventional silicone rubber (PDMS) is found to be rather susceptible to gasoline vapour attack. Hence, it is not expected to be a good choice for the recovery of C_6-C_8 hydrocarbons, which are the main components of gasoline (Billmeyer, 1984).

Moreover, silicones are known to swell due to the vapours sorption. When vapours are sorbed, the attractive chain-to-chain forces decrease, causing the free volume to increase; thus, result in a lower transport resistance for any species diffusing through the swollen polymer. Lately, increasing effort is being placed on the synthesis and modification of silicone rubber coupled with the search for alternative polymeric materials capable of recovering VOC from either gas or liquid streams (Ilinitch *et al.*, 1992; Fritsch *et al.*, 1993; Schultz and Peinemann, 1996; Bennett *et al.*, 1997; Chabot *et al.*, 1997; Cranford *et al.*, 1997; Pinnau *et al.*, 1997).

The selection of an appropriate membrane material for a vapour permeation process follows some common rules covering the physical, mechanical and chemical attributes of the polymeric material. The mechanical properties, as quantified by the polymer's tensile strength and glass transition temperature, will determine the membrane's ability to withstand the conditions of the operating environment. Meanwhile, the chemical properties will determine the membrane's compatibility with the feed organic vapour stream. In vapour permeation application, the separation is governed by differential pressure – the operation can take place over a wide range of temperature and pressure and is restricted only by the membrane's physical limits such as structural constraints. Bell *et al.* (1988) discussed the relationship between molecular dimensions and chemical properties of the permeating components as well as structural properties of polymer and the separation characteristics of pervaporation membranes, which can be extended to the selection of polymer material for vapour permeation applications.

One of the earliest studies on the permeation of organic vapour through various synthetic membrane materials was reported in Baker *et al.* (1987) where separation of various organic vapours from air was conducted using different polymeric films, namely chloroprene (neoprene), chlorosulfonated polyethylene (Hypalon®), fluoroelastomer (Fluorel®), PDMS, polyvinylchloride (PVC), polyacrylonitrile butadiene (nitrile rubber), silicone rubber and silicone polycarbonate. Despite the fact that vapour permeability may vary by 10 to 1000 times for different membrane materials, it does exhibit a common trend in permeability rate as follows: octane > toluene > trichloroethane > acetone >> nitrogen. The author also emphasised the ease of ultra-thin membrane preparation as one of the important criteria in the selection of polymeric

material. In conclusion, silicone rubber is still the preferred choice for the separation of acetone/air, despite the fact that Hypalon® posseses a more attractive permeability-selectivity pair simply because it can be easily fabricated into ultra thin films with a thickness of 0.5 - 2.0 μm.

As the search for better performing VOC compatible membrane material proceeds, Schultz and Peinemann (1996) investigated the separation of higher hydrocarbons from methane by using more than 40 membrane materials, namely imides, amidimides, kaptons, silanes, siloxanes, kraton, fluoroelastomers, butylketones, carbonates, sulfocarbonates and their copolymers. Polyoctylmethylsiloxane (POMS) and polytrimethylsilylpropyne (PTMSP) were found to be the two most promising alternatives with improved selectivity and permeability as compared to conventional silicone rubber (PDMS). Similarly, Nagai *et al.* (1997) reported on Poly-1-trimethylsilyl-1-propyne (PMSP) as a potential alternative to gas separation membranes with O_2 permeability as high as 10^3 Barrer.

With reference to the work done by Pinnau *et al.* (1997), it is evident that the prime attractive feature of PTMSP lies in its extremely high excess free volume, which is approximately 27% as compared with 3-9% for conventional glassy polymers, providing sorption capacity that is 10 times higher than the conventional glassy polymers with a diffusion coefficient that is 3 to 6 order of magnitudes greater than in the glassy polymers. Therefore, resulting in an extremely high gas permeability compared with any known polymer. In fact, this has been reported by a group of researchers from Meiji University, Japan (Nakagawa *et al.*, 1989). It should also be noted, however, that this high permeability is coupled with an extremely low selectivity for permanent gas mixtures, i.e. O_2/N_2 selectivity as low as 1.5. The price, availability and the varying quality of commercially available PTMSP make its current use problematic (Schultz and Peinemann, 1996). Another major problem faced by PTMSP is the ageing effects on its gas permeability and selectivity, as described by Pinnau *et al.*, (1997). In their study , the membrane was continuously exposed to a 2 mol% n-butane/ 98 mol% hydrogen gas mixture over a period of 47 days. Experimental results showed that after 2 days of continuous exposure to the gas mixture, the permeability remained while the selectivity dropped from 33 to 29. Furthermore, the permeation

properties of collapsed/ aged PTMSP membranes could be restored to more than 70 % of the newly cast film permeability value by passing through n-butane for about 6 hours. The authors concluded that the physical aging in PTMSP could be restored, if not stopped, by contacting PTMSP with hydrocarbon vapours, in this case, n-butane. Kim and Hong (2000) in their study on the transport properties of CO_2 and CH_4 using chemically modified polysulfones, concluded that membrane permeability could be increased by introducing a bulky side group. The explanation behind this lies in the greater chain packing distance due to bulky substituents, which in turn weakens the chain stiffness and chain interaction.

The most important goal in gas and vapours separation applications is to develop materials with both high permeabilities and selectivities. As noted by Peinemann *et al.* (1989), less selective membrane materials are found to be too energy intensive, while highly selective membranes, on the other, often require huge membrane area. The problem of low diffusion fluxes as exhibited by highly selective rubbery membrane could be tackled by minimising the effective membrane thickness. This solution, however, is accompanied by the problem of insufficient mechanical strength, together with the difficulty in ensuring zero defects. On the other hand, highly permeable glassy polymers, in most cases, are not suitable for the recovery of organic vapours on a technical scale due to low vapour permeability. Specifically, polymer material suitable for the separation of organic vapours from air should be highly permeable to organic solvents, but relatively impermeable to air. Incorporating the above discussion, this problems could be overcome by using composite membranes, i.e. with a very selective rubbery polymeric material being deposited as a thin layer upon a porous substrate made of glassy polymer, as will be discussed in the following section.

6.2.3 Development of Composite Membranes

In recent years, the focus of membrane research has been extended to the study on the preparation techniques and permeation patterns for composite membranes, to incorporate the advantage of both dense (good selectivity) and porous membranes (good permeability). In composite membranes, the thin dense skin layer laminated on the porous substrate is responsible for the active separation, while the porous substrate is responsible in providing the mechanical support.

Even though composite membranes have been widely used in the study of both pervaporation and vapour permeation application, few publications related on coating and preparation of composite membranes could be found. This area remains inherently immature, especially when hollow fibre is involved. From the author's literature search, dip coating is found to be the most widely employed coating method, primarily due to its ease of operation. However, detailed elaborations on the coating techniques and practices are found to be extremely limited. This is especially true for large-scale industrial membrane system where no literature disclosure on the coating practices could be obtained.

By using composite membranes, combination of both types of materials, i.e. selective rubbery material deposited on highly permeable porous glassy substrate, allows a membrane's properties to be tailored to specific separation problems. More importantly, the fact that it is made up of two different materials enables it to be optimised independently so as to achieve the desired optimum separation performance (Kimmerle *et al.,* 1991). As for the membrane morphology, it is desirable for the substructure to be sufficiently porous with bridgeable pore sizes so as to minimise the transport resistance (Kimmerle *et al.*, 1988) and at the same time to exhibit the separation performance that is close to the intrinsic value of the selective coating layer (Pinnau *et al.*, 1988). To date, the commonly used support membranes include cellulosic membrane, polysulfones (PSf), polyamide-imide (PAI), polyvinylidene fluoride (PVDF), polyetherimide (PEI) and polyethersulfone (PESf).

Ideally, it is desirable to minimise the thickness of this layer as much as possible in order to reduce the mass transfer resistance, which in turn means an increase in membrane permeation flux. The obvious challenge here, then, is to form an extremely thin selective coating layer with zero defects. On the other hand, as noted by Kimmerle *et al.* (1991), it might be advisable to use a slightly thicker dense coating layer such that the overall permeation resistance through the composite membrane will be ultimately governed by the selective layer, i.e. dominated by the presence of sorption/solution coefficient. With this, variation in porous substrate properties, where diffusion transport (not necessary true) is found to be dominant, is no longer influential on the overall mass transfer, thus simplifying the overall separation performance study.

In a study conducted by Kimmerle *et al.* (1988), PDMS coated polysulfone hollow fibre membranes with a theoretical coating thickness of 12.7 μm, and physical coating thickness of 0.5-1.5 μm were used for solvent recovery from air. Nitrogen permeation of the spun substrate could be adjusted between $2.63 \times 10^{-3} - 5.92 \times 10^{-2}$ $cm^3.cm^{-2}.s^{-1}.cmHg^{-1}$ by varying the spinning parameters. A few years later, Fritsch *et al.* (1993) reported on the fabrication of silicone/non-silicone grafted blend composite membrane via one step dip coating and thermal crosslinking process whereby an effective coating thickness of 0.7-15 micron was deposited, which allowed nitrogen gas permeation of greater than 0.09 $cm^3.cm^{-2}.s^{-1}.cmHg^{-1}$. According to the authors, the resulting film thickness could be varied by changing the concentration of the coating solution. In the same year, Fouda *et al.* (1993) cast polyetherimide (PEI) onto flat sheet polyester backing material using automated casting machine, followed by silicone coating. However, no information was reported regarding the coating thickness obtained. Schultz and Peinemann (1996) managed to produce composite membrane with 10μm PDMS coating thickness via dip coating of support membrane in 1-10 % polymer solution, with butane flux of 1.4 $m^3.m^{-2}.hr^{-1}.bar^{-1}$ (equivalent to permeation flux of 0.05 $cm^3.cm^{-2}.s^{-1}.cmHg^{-1}$).

Petersen and Peinemann (1997) described the preparation of interfacial polymerised composite flat sheet membranes using new polyamides. With silicone coating on 1μm active skin, this composite membrane exhibited nitrogen, oxygen, carbon dioxide and methane permeation of 1.03×10^{-5}, 2.25×10^{-5}, 1.10×10^{-4} and 2.0×10^{-5} $cm^3.cm^{-2}.s^{-1}.cmHg^{-1}$, respectively. The authors concluded interfacial polycondensation as a polymer and copolymer design tool with no solubility limits.

In the following year, Singh *et al.* (1998) studied pure and mixed gas acetone/nitrogen permeation using commercial filler free PDMS composite membrane with 28 μm PDMS coating, where nitrogen permeability of 245 Barrers was recorded. In the same study, a gravimetric sorption study was conducted using a 350 μm PDMS dense film to investigate the acetone uptake at 28 °C whereby a pure acetone permeability coefficient of greater than 20,000 Barrers was measured. Also, the sorption isotherm of acetone in PDMS was described using a modified version of the Flory-Huggins model with a concentration-dependent interaction parameter. Acetone/nitrogen selectivity increased

from 85 to 185 following the increase of the feed acetone partial pressures from 0 to 67 % of saturation.

Chern and Wu (1996) reported the fabrication of multilayer alumina oxide composite membranes with polyimides (PI) and poly(amide-imide) (PAI) skins via interfacial condensation for air separation. Experimental results showed that the O_2/N_2 selectivity could be increased with increasing times of coating, i.e. from 2.41 to 3.34, 3.91 and 5.60 after 5-times, 20-times and 40-times of coating, respectively. The authors explained that the high O_2/N_2 selectivity is due to the great chain stiffness of the polyimides formed, which possess higher mobility selectivity from their molecular sieve like behaviour. These improved selectivity values, as expected, were accompanied by a decrement in gas permeation rates. However, oxygen permeation of greater than 100 x 10^{-5} and nitrogen permeation of greater than 20 x 10^{-5} $cm^3.cm^{-2}.s^{-1}.cmHg^{-1}$ are considered as remarkably high when 40 times of coating is taken into consideration. In another study, SEM photograph confirmed a 20 μm carboxymethylated poly(vinyl alcohol) (CMPVA) skin cast on flat sheet polyethersulfone (PESf) support membrane (Nam *et al.,* 1998). This composite membrane was employed for pervaporation study of water-isopropanol mixture and will not be further discussed here.

Cha *et al.* (1997) and Bhaumik *et al.* (2000) published their pilot plant studies using plasma polymerized silicone-coated composite hollow fibre membranes, having active skin thickness close to 1 μm. However, no discussion was made on the coating procedures. At VOC concentration range of 500-51,700 ppm, fed at 0.5-1.2 $cm^3.min^{-1}$ per fibre, 98 % VOC removal was achieved (Cha *et al.*, 1997). Similarly, Teng *et al.* (2000) developed 25-30μm thick aromatic polyimide flat sheet membranes via polymerisation.

It should also be noted that ultra thin nonporous silicone coated membranes with a thickness of ~1 μm are so highly permeable to organic vapours that conventional porous substrates have been found to introduce significant pressure drop in the permeate stream, thus resulting in a great loss in the selectivity between the organic vapours with nitrogen gas. Pinnau *et al.* (1997) employed a much thicker silicone coating so that the entire permeation resistance lies within the selective coating layer. This way, the

substrate becomes merely a mechanical support with no resistance significance. Even though this would lead to a decrease in the vapour permeation flux, the permeation properties however become more predictable and consistent.

In addition to the abovementioned challenge to minimise the coating thickness, equal fibre quality is an essential property in ensuring high separation performance. According to Rautenbach *et al.* (1998b), fibre skin thickness is the most important parameter and its deviation should be kept within 10% of the average value. It is worth mentioning here that in vapour permeation processes that utilise composite membranes, skin thickness could also be referred to as the associate coating thickness.

Equally important with the coating thickness is the O_2/N_2 selectivity for the coated membranes. It has been well accepted that properly coated, defect-free tight membranes will give a permeability ratio (i.e. P_{O2}/P_{N2}) which is synonym to oxygen nitrogen selectivity (i.e. O_2/N_2) of at least 2 (Kimmerle *et al.*, 1988; Nijhuis *et al.*, 1991).

Meanwhile, it has been well recognised that ideal selectivity measured with pure gases seldom predicts the mixed gas behaviour of the polymer accurately. Normally, the mixed gas selectivity is lower than the pure gas selectivity. For instance, based on pure component flux, polyhexadecylmethylsiloxane (PHDMS) exhibited the highest butane over methane selectivity, i.e. $\alpha_{Methane}^{Bu\tan e}$ greater than 200; however, showed a poor selectivity of only 2 in mixed gas test. Similarly, POMS-SSM membranes showed an ideal selectivity of greater than 20 with mixed gas selectivity, $\alpha_{Methane}^{Bu\tan e}$ as low as 12 (Schultz and Peinemann, 1996). This could be easily explained by referring to the interaction between the permeants and also with the polymer matrix. On the other hand, a study conducted by Leeman *et al.* (1996) found that coupling effects such as preferential sorption to be very mild and weak. Similarly, permeability of acetone and nitrogen were reported to be sensibly independent of the presence of the other component (Singh *et al.*, 1998).

The urgency of the VOC emission problem as highlighted in Section 1.1 suggests that it is crucial to have a holistic perspective on the overall problem to be tackled, so as to enable an efficient and yet cost effective emission control. This includes a thorough

understanding of the technology to be used, i.e. everything from its engineering principles down to its microscopic level mass transfer theories are equally important; as well as complete knowledge on the physico-chemistry of the organic vapours to be recovered.

This study aims to develop composite hollow fibre membranes with appropriate membrane substructures and desired coating layers for benzene, toluene and xylene (BTX) removal via a coating method. Polyvinylidene fluoride (PVDF) was chosen as the support membrane material for its excellent thermal and chemical stability, while divinylpolydimethylsiloxane (divinyl-PDMS) was selected as coating material for its good permeation properties for organic vapours (Lau *et al.*, 1997)

6.3 MATERIALS AND METHODS

6.3.1 MATERIALS

Kynar®K760 poly(vinylidene fluoride) (PVDF) polymer pellets used were purchased from Elf Atochem, USA, and were pre-dried at 50°C prior to use. N-methyl pyrrolidone (NMP) [Synthesis grade, Merck], lithium chloride (LiCl) [Reagent grade, Sigma Aldrich], and distilled water were used as internal coagulants, while tap water was used as external coagulation bath medium.

The coating materials used comprised of divinyl-polydimethylsiloxane (divinyl-PDMS) [1000cs, United Chemical Technologies, Inc.], with oligosilylstyrene as crosslinking agent and platinum divinyltetramethyldisiloxane complex as catalyst [United Chemicals Technologies, Inc.] and hexane as solvent [Analytical grade, Fisher Chemicals].

For hydrocarbon recovery experiments, benzene [analytical grade, 99.9% purity] was purchased from J.T. Baker while toluene [analytical grade, 99.9% purity] and xylene [analytical grade, 99.9% purity] were purchased from Merck. All chemicals were used as received.

6.3.2 FABRICATION OF ASYMMETRIC PVDF HOLLOW FIBRE MEMBRANES

PVDF hollow fibre membranes used as the support membrane in this study were spun using the dry-wet phase inversion method, using the following dope compositions: 15 wt.% PVDF in 85 wt.% NMP and 4.0 g of lithium chloride (LiCl) was added in every 100.0 g of PVDF-NMP solution as non-solvent additive. The detailed spinning procedure used in this study has been reported in Section 5.5.3.

6.3.3 PREPARATION OF COATING SOLUTION

A detailed description on the development, preparation and formulation of the divinyl-polydimethylsiloxane (divinyl-PDMS) coating solution used in this study was reported by Lau *et al.* (1997). Basically, this formulation consists of oligosilylstyrene as crosslinking agent, divinyl terminated polydimethylsiloxane as the core coating material, platinum-divinyltetra-methyldisiloxane complex as a Karstedt's catalyst using hexane as solvent. 10wt% PVDMS coating solutions were prepared based on PVDMS:oligomer ratio of 1:4, in the presence of 16 wt/vol % of catalyst concentration (by dissolving 0.16 g of platinum-divinyltetra-methyldisiloxane complex into 1 ml of hexane solvent). In the preparation of 100 ml of 10 wt% PVDMS, 5.8667 g of PVDMS and 1.4667 g of oligomer were poured into two separate volumetric flasks containing 50 ml hexane each. After 2 hours of mechanical shaking at 150 $ml.min^{-1}$ [Certomat® shaker], a total of 835.21 µl of 16 wt/vol % catalyst was added into the well-mixed PVDMS-hexane solution. Again, this catalyst-PVDMS-hexane mixture was subjected to another 30 minutes of mechanical shaking so as to ensure homogenous mixing; followed by the addition of 50 ml oligomer-hexane solution to form the final 100ml oligomer-catalyst-PVDMS-hexane solution mixture. This final mixture was then subjected to another 24 hours of mechanical shaking before it is ready to be used.

6.3.4 PREPARATION OF COMPOSITE MEMBRANES VIA DIP COATING METHOD

In this study, composite hollow fibre membranes were prepared via dip coating method. The overall coating procedure comprises of four steps, i.e. pre-treatment with hexane or coating solution, heat treatment at 50 °C, vacuum coating and finally post-crosslinking at 50 °C. Briefly, the spun hollow fibres were cut and assembled into test bundle with a length of 10-15 cm. In the pre-treatment step, the hollow fibre bundles were immersed in either hexane or coating solution for 60 seconds at room condition (25 °C, 60 % RH),

followed by heat treatment at 50 °C for 4 hours. After that, the treated hollow fibres were allowed to cool to room temperature, followed by vacuum coating whereby it was immersed in the coating solution with vacuum pressure applied at the fibre lumen side for an intended duration, ranging from 30 seconds to 4 minutes. This was followed by post- crosslinking at 50 °C for 24 hours. The temperatures and treatment durations adopted in the above procedure were determined from preliminary experimental studies.

6.3.5 Characterisation of Composite Hollow Fibre Membranes

The cross-sectional structure of the coated hollow fibre was first examined using a microscope [Olympus SZ-ET and Olympus TL2] to determine its overall integrity and uniformity, followed by a more detailed examination using scanning electron microscopy (SEM) [Hitachi S-4100]. The sample hollow fibres were fractured after immersion in liquid nitrogen for one minute using forceps. The fractured fibre was adhered on a special aluminium stud dish using a conductive pad and placed in a silica gel container overnight to ensure thorough removal of moisture from the membrane pores. After that, the dried fibre samples were coated with a thin layer of gold using ion-sputtering device [JEOL, JFC-1100E] before a detailed morphology examination using SEM. Under magnification of 500 times or more, the thickness of the coating layer could be clearly seen and measured from the SEM photograph taken, as will be disclosed in Section 6.4. For membranes with no visible coating layer, a gravimetric method was used, weight difference before and after the coating procedures were measured using an electronic balance [Mettler Toledo AE 160] with accuracy of 0.0001 g. With known fibre dimension, mass gained after the coating was then converted into the theoretical coating thickness.

Gas permeation tests were also carried out using an apparatus as described in Section 5.5.4. A total of 11 different composite membranes were prepared and tested using purified oxygen and nitrogen [BOC]. The coating conditions for these eleven membranes together with their permeation results will be presented in Section 6.4 (Table 6.3).

6.3.6 HYDROCARBON RECOVERY SYSTEM

The hydrocarbon recovery system employed in this study comprised of three main components: (a) feed stream consisting of a solvent pool bubbled with nitrogen gas of known flow rate; (b) membrane separation unit consisting of a membrane module housed in a constant temperature box; and (c) low pressure down stream with vacuum pump maintaining a pressure of less than 10 mbar. Table 6.2 summarises the basic features of the hollow fibre membrane modules used in BTX recovery experiment, where 11 coated fibres (i.e. fibre number 7 in Table 6.3) were mounted and packed inside a stainless steel tube, with epoxy seals applied at both ends.

Table 6.2 Basic features of the hollow fibre membrane modules used

Properties	Dimension
No of fibres	15
Fibre length / m	0.40
ID / μm	458
OD / μm	770
Membrane Area / cm^2	145.2
Housing inner diameter / mm	7.40

Experimental set up for the separation of individual BTX (benzene, toluene and xylene) from nitrogen is as illustrated in Figure 6.3. In the separation experiments, nitrogen gas was bubbled through a solvent pool containing benzene, toluene or xylene creating solvent laden stream and fed into the PVDMS-PVDF membrane unit, housed in an isothermal box. The mixture was fed into the shell side of the hollow fibre membrane module. A vacuum pump [Diaphragm Vacuum Pump MZ 2C, Vacuumbrand] was used to maintain downstream pressure of about 10 mbar, with a condensation unit attached at the downstream side for the collections of permeate condensates. Perkin Elmer 8700 gas chromatography was used to analyse the sample concentrations taken from the feed and retentate streams using a FID detector.

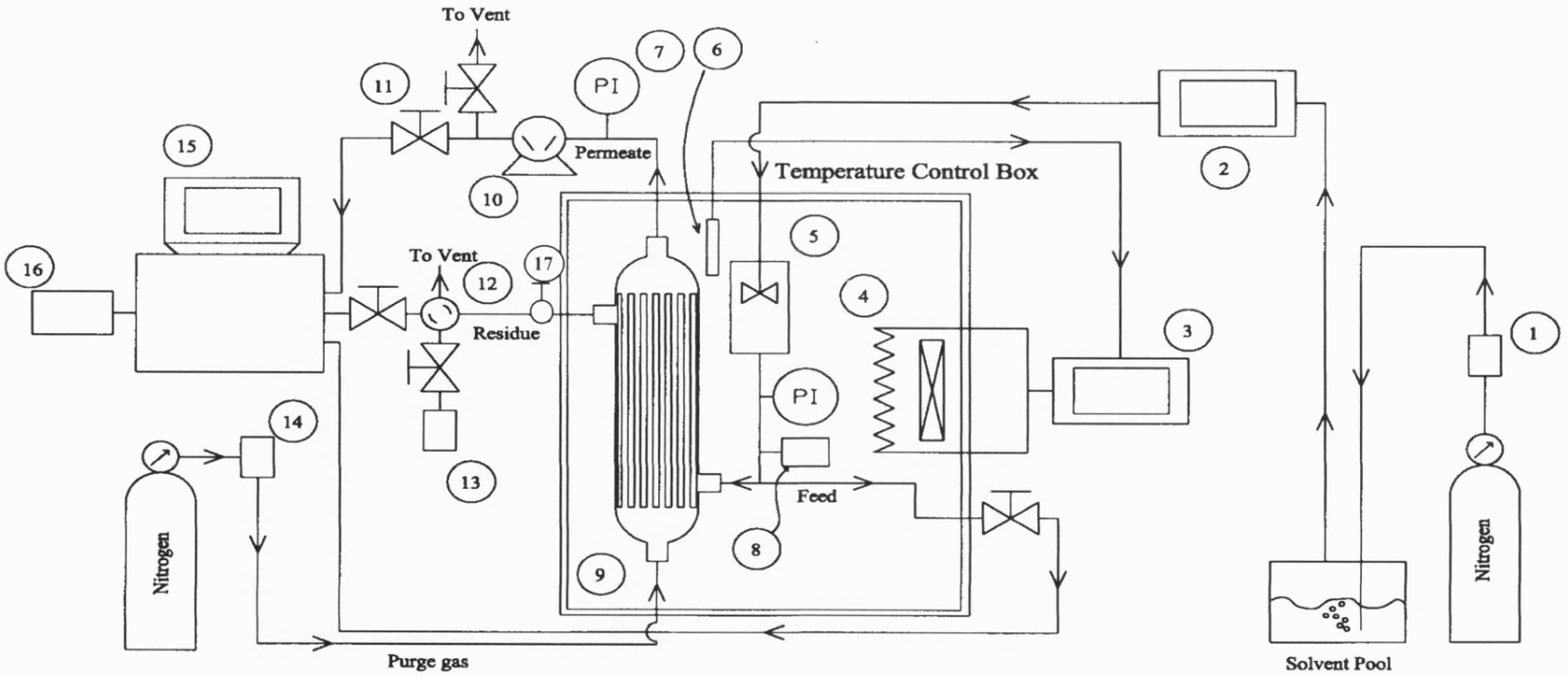

Figure 6.3 Schematic diagram for BTX recovery system

1. Mass flow controller, 2. Flow rate display unit, 3. Temperature display unit, 4. Heating element and circulating fan, 5. Gas mixer, 6. Temperature sensor, 7. Pressure gauge, 8. Flow meter, 9. Hollow fibre membrane module, 10. Vacuum pump and display unit, 11. Two-way valve, 12. Four-way valve, 13. Bubblemeter, 14. Rotameter, 15. Gas Chromatograph, 16. Printer, 17. pressure regulator

6.4 RESULTS AND DISCUSSIONS

6.4.1 MORPHOLOGY OF DIVINYL-PDMS-PVDF COMPOSITE HOLLOW FIBRE MEMBRANES

In this study, a coating procedure involving pre-treatment, heat treatment, vacuum coating and post-crosslinking was studied. Each of these steps plays an important role in the successful fabrication of a desired composite membrane. Pre-treatment is useful in order to form a durable coating layer on the surface of the substrate. Heat treatment is to enhance the strength of the bondage between the pre-coated layer and the substrate. The thickness and uniformity of the coating layer depend critically on the duration and other conditions applied during the vacuum coating process. Finally, post-crosslinking is to further ensure a stable and durable bond between the coated layer and the substrate. The morphological examination of fibre integrity, uniformity and coating layer thickness was carried out using scanning electron microscopy, and correlations of these properties with the preparation conditions will be discussed below.

6.4.2 EFFECT OF PRE-TREATMENT

The effects of two different pre-treatment methods, i.e. pre-wetting in hexane or in the coating solution itself, are studied. Experimental results obtained for the pre-treated membranes reveal a drop in nitrogen fluxes after pre-treatment particularly for the membrane pre-treated with the coating solution. As can be seen in Table 6.3, for example, the nitrogen flux of 2.42 $cm^3/cm^2.s$ for a raw asymmetric PVDF (Fibre 1) was reduced to 1.58 $cm^3/cm^2.s$ for membrane pre-treated with hexane (Fibre 2), and $4.07x10^{-2}$ $cm^3/cm^2.s$ for that pre-treated with 10wt% DIVINYL-PDMS coating solution (Fibre 3). However, with reference to the SEM photographs, there is no visible difference among the three, as shown in Figure 6.4.

Table 6.3 Effect of coating practice on resulting coating thickness, nitrogen permeation and permance ratio of O_2/N_2.

Fibre No	Pretreatment	Vacuum coating (minutes*freq)	Coating thickness (μm)	Nitrogen flux ($cm^3/cm^2/s$)	Nitrogen permeance ,P/ *l* ($cm^3/cm^2.cmHg.s$)	Permance ratio O_2/N_2
1	Nil	Nil	-	2.4168	1.59E-02	0.91
2	Sol	Nil	-	1.5827	1.04E-02	0.92
3	CS	Nil	-	4.07E-02	2.68E-04	1.08
4	Nil	4*1	20.31[#]	1.51E-02	9.91E-05	1.21
5	Sol	4*1	15.23[#]	3.16E-02	2.08E-04	0.99
6	CS	4*1	12.13[@]	9.75E-04	6.42E-06	2.81
7	CS	2*2	7.02[@]	2.04E-03	1.34E-05	2.24
8	CS	2*1	6.66[@]	2.17E-03	1.43E-05	2.6
9	CS	1*2	5.33[@]	2.40E-03	1.58E-05	2.48
10	CS	1*1	3.33[@]	8.24E-03	5.42E-05	1.08
11	CS	0.5*2	2.66[@]	1.52E-02	9.97E-05	1.21

Note: freq = frequency; Sol = solvent; CS = coating solution
[#]Coating thicknesses was calculated using constant weight method
[@]Coating thicknesses were measured from SEM photographs

Operating condition: upstream pressure (gauge pressure) = 2 atm, downstream pressure = atmospheric pressure

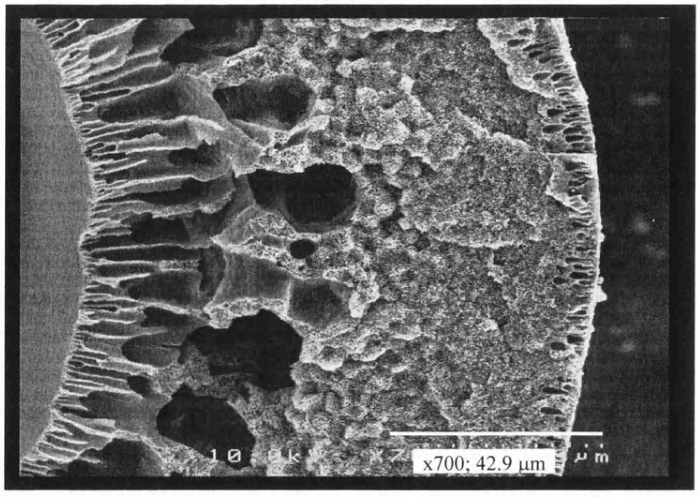

(a)

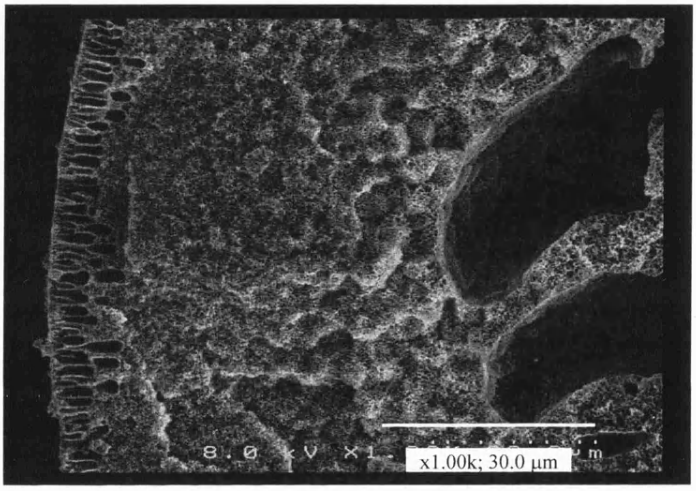

(b)

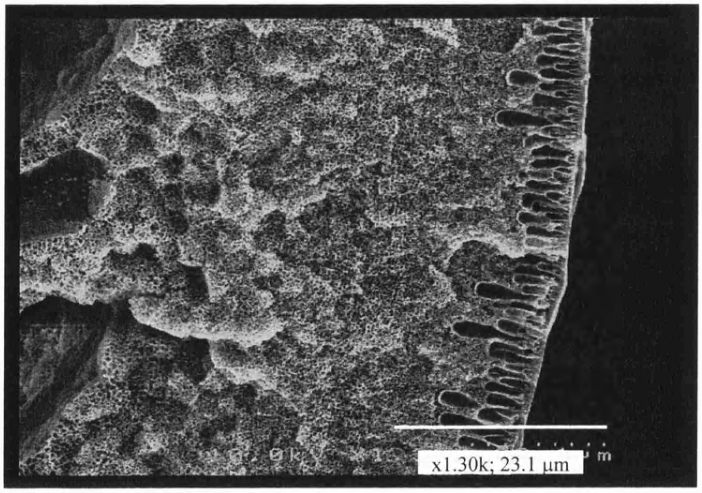

(c)

Figure 6.4 Scanning electron micrographs of asymmetric PVDF hollow fibre membrane:
(a) raw PVDF without pretreatment;
(b) pre-treated with hexane
(c) pre-treated with 10 wt% divinyl-PDMS solution.

SEM photographs for the vacuum coated divinyl-PDMS composite membranes (prepared with and without pre-treatment) are shown in Figure 6.5. There is no clear inner boundary of the coating layer for the composite membranes prepared without pre-treatment (Figure 6.5(a)) and the pre-treated with hexane (Figure 6.5(b)). Rather, clogged pores can be clearly seen in these photographs. Based on the gravimetric method and dimension of the supporting hollow fibre, their weight gain suggests that coating layers with thickness of 20.31 μm for the fibre without pre-treatment and 15.23 μm for the fibre pre-treated with hexane should be formed. Hence, it is fairly obvious that intrusion of coating materials into the surface pores of the substrate hollow fibres during vacuum coating has occurred, therefore resulting in clogged pores. For the fibre pre-treated with coating solution, on the other hand, a uniform coating layer surrounding the substrate hollow fibre could be clearly seen as illustrated in Figure 6.5(c).

6.4.3 Effect of Vacuum Coating Duration and Time

Preliminary experimental observations have shown that a suitable pressure drop across the coating substrate must be applied in order to form a stable coating layer of a desired thickness. In this respect, vacuum was applied in the fibre lumen side to create a driving force for the adherence of the coating layer. A suitably limited extent of intrusion of coating solution into the surface pores of the substrate may help to reduce the size and quantity of surface pores as well as to provide anchorage for the formation of a stable coating layer. Ultimately, the thickness of the coating layer is controlled by the duration of the vacuum coating, where coating thickness increases with increased coating duration. For example, the coating layer thickness of 3.33 micron with one-minute coating increases to 6.66 or 12.13 microns when the coating duration is increased to 2 or 4 minutes respectively, as shown in Table 6.3. In comparing the effect of single-stage and two-stage coating, experimental results suggest that repeated short vacuum coatings favour the formation of a thinner dense coating layer, as compared to single long vacuum coating. As shown in Figure 6.6, a thinner coating layer of 7.02 μm was obtained for composite membrane prepared via a two-stage 2 minute vacuum coating as compared to 12.13 μm (Figure 6.5c) for a single 4 minute vacuum coating.

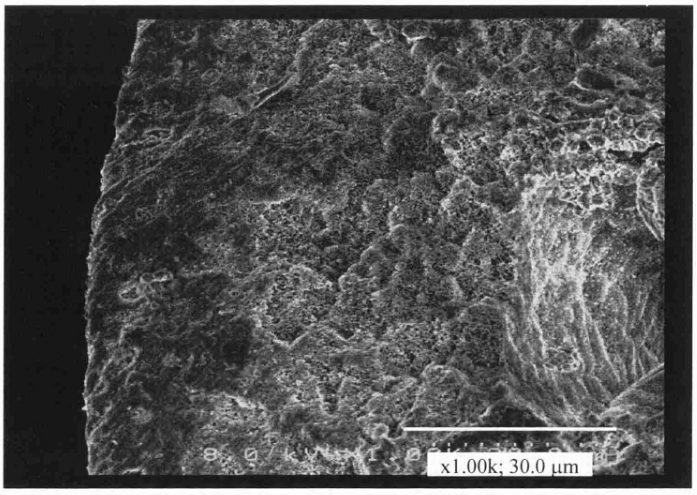

(a)

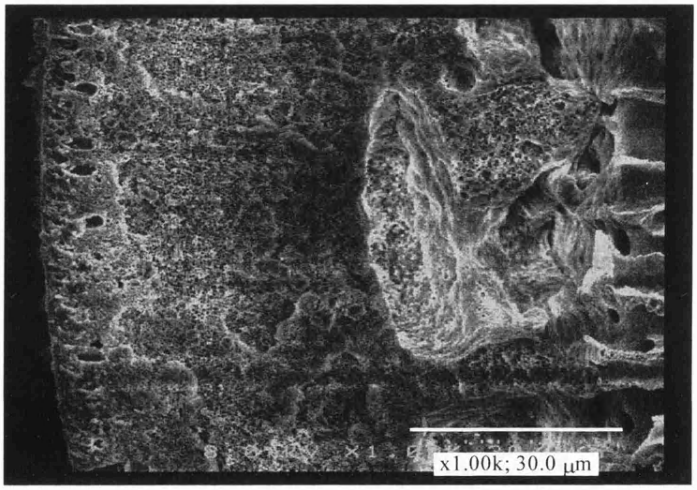

(b)

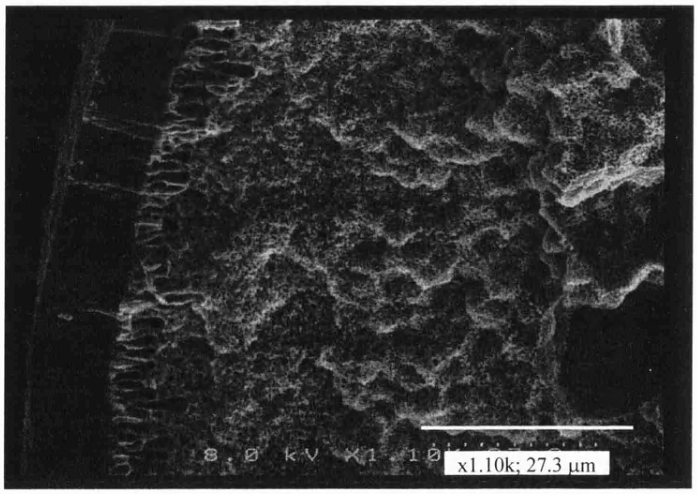

(c)

Figure 6.5 Cross sectional structures of coated divinyl-PDMS-PVDF composite hollow fibre membranes: (a)no pretreatment, but with 4x1 minutes vacuum coating, fibre no. 4; (b)pretreated with hexane and 4x1 minutes vacuum coating, fibre no. 5; (c) pretreated with 10wt% divinyl-PDMS solution and 4x1 minutes vacuum coating, fibre no. 6.

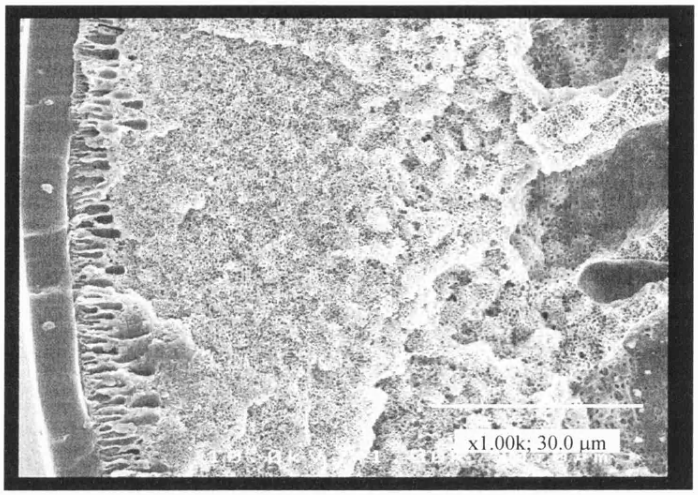

Figure 6.6 Scanning electron micrographs of coated divinyl-PDMS-PVDF composite hollow fibre membrane: pretreated with 10wt% divinyl-PDMS and 2x2minutes vacuum coating (fibre no.7 in Table 6.3).

During the fabrication of composite membranes, it is desirable to have a minimum coating thickness with as little resistance as possible. The experimental results in Table 6.3 indicate that the coating thickness could be further reduced with a one-minute coating (both single- and two- stage coating). However, the coated fibres are no longer defect-free, as the selectivity of O_2/N_2 of the coated fibres approach to unity (fibres 10 and 11 in Table 6.3).

6.4.4 Effect of Coating on Membrane Surface Texture

Apart from the measurable effects of coating on the permeation and selectivity properties of the resulting composite membranes, a much smoother membrane surface was observed on the coated PVDF hollow fibre (Figure 6.7(b)) as compared to the coarse surface of the non-coated membranes (Figure 6.7(a)), due to the deposition of a thin layer of dense crosslinked coating material. Similar observations have also been reported for composite membranes prepared via the interfacial condensation method (Cher and Wu, 1997; Petersen and Peinemann, 1997).

6.4.5 Recovery of BTX

Experimental results for BTX recovery are shown in Figure 6.8. It can be seen that a higher recovery rate is obtained for component with higher molecular weight, i.e. in the sequence of xylene > toluene > benzene. This could be explained in terms of their relative condensability, which increases with increasing molecular weight. Higher molecular weight generally result in lower diffusivity, as diffusion tends to decrease with increasing molecular weight (and permeant diameter) as larger molecule interact with more segment of the polymer and are thus becoming less mobile. In fact, the effects of increasing permeant size on permeability is a balance between the opposing effects of the diffusion coefficients, which decreases with increasing size, and the solubility, which increases with increasing size. In addition, the solubility coefficient of gases/vapours increases with increasing condensability. In the case of simple gases, theses two effects are comparable, however, when vapours are concerned, the sorption becomes the dominating factor (Baker *et al.*, 1987), hence the degree of xylene recovery in this study is higher than those of toluene and benzene.

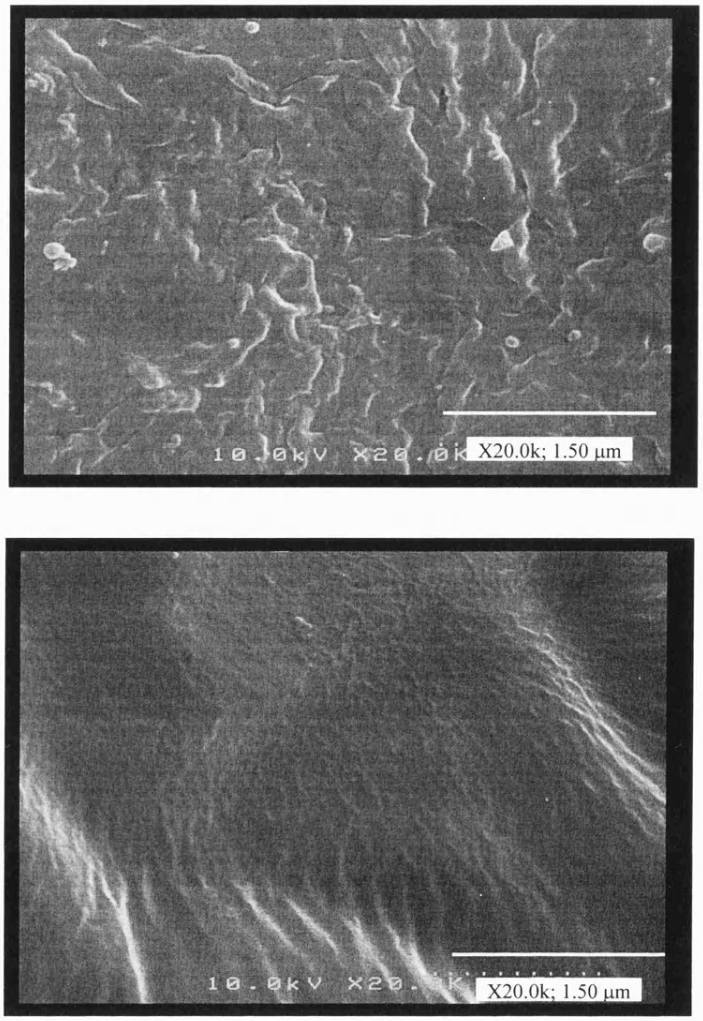

(a)

(b)

Figure 6.7 Scanning micrograph showing the surface structure of
(a) raw asymmetric PVDF hollow fibre membrane
(b) divinyl-PDMS-PVDF composite hollow fibre membrane (fibre no.7 in Table 6.3)pre-treated with 10wt% divinyl-PDMS and 2x2 minutes vacuum coating.

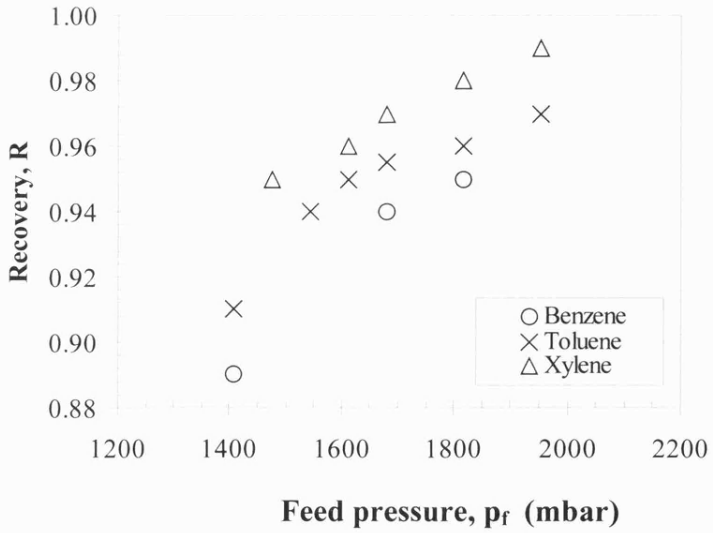

Figure 6.8 BTX recoveries at various operating pressures, using feed containing 5 vol% BTX, at 50 ml.min^{-1} feed flow rate, 40^{o}C operating temperature

6.5 Conclusions

Divinyl-PDMS coating layer with the thickness in a few microns was successfully coated on a PVDF hollow fibre membrane. Experimental results clearly indicate that the undesirable intrusion during the vacuum coating stage could be avoided via pre-treatment using the coating solution. This could be attributed to the formation of a thin coating layer after pre-treatment and heat treatment steps, which successfully reduce the pore size and quantity of surface pores on the substrate membranes; thus, enhances the permselectivity of the resulting composite membranes. Also, with the coating solution pre-treatment, a stable coating layer could be laminated with its thickness remains controllable by controlling the duration and frequency of the vacuum coating. The ability of the prepared divinyl-PDMS-PVDF composite membrane in selectively separating the BTX from nitrogen is clearly demonstrated with recovery greater than 95%, therefore, putting forward its potential of being a substitution of conventional silicone rubber due to its overall chemical stability.

CHAPTER SEVEN

CONCLUSIONS AND RECOMMENDATIONS

7.0 CONCLUSIONS AND RECOMMENDATIONS

In this study, some important aspects of the development of asymmetric PVDF membranes via the phase inversion – immersion precipitation technique were studied. Some important features in the development of composite membranes were also investigated. The membranes developed were tested in waste treatment applications involving organic compound removal, i.e. hexene / hexane separation using hollow fibre membrane contactor and benzene, toluene and xylene (BTX) recovery using composite PVDF hollow fibre membranes developed during the study.

Based on both qualitative and quantitative data presented, the importance of solvent choice and additives used on the resulting membrane properties were demonstrated. It is believed that elevated temperature is advantageous in the fabrication of PVDF membranes because of the following reasons: In the preparation of a polymer solution, the increase in solution temperature aids the polymer and additive dissolution, while encouraging component miscibility. In terms of solution properties, the increase in solution temperature boosts the system thermodynamic properties and enhances its non-solvent tolerance. From cloud point data obtained, the effect of additives and their concentrations on the cloud point behaviour was found to be less significant at the higher temperature of 70 °C. In membrane fabrication (via the phase inversion immersion precipitation process), the distinctive morphologies associated with different additives were replaced by an open porous cellular substrate structures at higher dope and bath temperature. It can be concluded that elevated temperature suppresses polymer crystallisation and gelation but favours liquid–liquid demixing; hence the increase in solution temperature resulted in the formation of a porous cellular substrate structure which could potentially offer better permeation properties.

With the high level of complexity involved in the phase inversion process, and the preliminary nature of the phase separation studies carried out during these experiments, it is feasible to perform further research into the various basic aspects of PVDF polymer phase separation behaviour, which is essentially the precursor to membrane formation via the phase inversion process. This can be achieved using more advanced analytical techniques and tools such as Differential Scanning Colorimetry which were beyond the scope of this study, and unavailable during the course of this work.

A 4-step coating procedure (involving pre-treatment, pre-crosslinking, vacuum coating, and finally post-crosslinking) has been developed in this study. Composite hollow fibre membranes with coating of a few microns thick were successfully produced without any sign of adverse intrusion into the substrate pores. An enhanced oxygen/nitrogen selectivity was demonstrated by these composite membranes due to the selective nature of the divinyl-PDMS rubbery coating material. Further studies, however, is necessary to examine the transport resistance originate by the additional dense coating layer.

The feasibility of the PVDF hollow fibre membranes in waste treatment applications was tested using the example of hexene/hexane separation via π complexation with silver ion. The viability of the PVDF composite hollow fibre membranes developed was clearly demonstrated using the example of BTX recovery. Both case studies were found to be successful, however further study is required to investigate the microscopic transport phenomena in order to have a thorough understanding of the separation processes. Combining the knowledge of the membrane formation, as well as the intended separation processes, the possibility of a process specific tailor made membrane separation device can be anticipated.

REFERENCES

Bailey, J.L. and R.E. McCune. Microporous vinylidene fluoride polymer and process of making same. United States Patent 3.642,668, Feb. 15, 1972.

Baker, R.W. Process for recovering organic vapors from air. United States Patent 4,553,983, Nov. 19. 1985.

Baker, R.W. and J.G. Wijmans. Membrane separation of organic vapors from gas streams. In: Polymeric Gas Separation Membranes, D.R. Paul and Y.P. Yampol'skii [Eds]. CRC Press Inc., New York, pp. 353-397, 1994.

Baker, R.W., J.G. Wijmans and J.H. Kaschemekat. The design of membrane vapor-gas separation systems, Journal of Membrane Science, 151: 55-62, 1998.

Baker, R.W., N. Yoshioka, J.M. Mohr and A. J. Khan. Separation of organic vapors from air, Journal of Membrane Science, 31: 259-271, 1987.

Beck, T.W. and Lee, M.B. Method of making polyvinylidene fluoride membrane. United States Patent 5,489,406, Feb. 6, 1996.

Beckman, I.N., D.G. Bessarabov and R.D. Sanderson. Phenomenological theory of the facilitated diffusion of gases in fixed site carrier membranes at non-steady state. In: Proceedings of Euromembrane '95 Vol. II. W.R. Bowen, R.W. Field and J.A. Howell [Eds]. Pp. II-182-185, 1995.

Behling, R.-D. Separation of hydrocarbon vapors from air. In Proceedings of the 6th Annual Membrane Technology / Planning Conference. Leading Edges, Major Developments and New Applications in Membrane Technology, Nov. 1-3, 1988, Session V-4, Cambridge, Massachusetts, pp.7-23, 1989.

Behling, R.-D., K. Ohlrogge, K.-V. Peinemann, and E. Kyburz. The separation of hydrocarbons from waste vapor streams. In: Membrane Separations in Chemical Engineering, AIChE Symposium Series 272, Vol. 85. A. E. Fouda, J. D. Hazlett, T. Matsuura, and J. Johnson [Eds]. AIChE, New York, pp. 68–73, 1989.

Bell, C.-M., F.J. Gerner and H. Strathmann. Selection of polymers for pervaporation membranes. Journal of Membrane Science, 36: 315-329, 1988.

Bennett, M., B.J. Brisdon, R. England, R.W. Field. Performance of PDMS and organofunctionalised PDMS membranes for the pervaporative recovery of organics from aqueous streams. Journal of Membrane Science, 137: 63-88, 1997.

Benzinger, W.D., B.S. Parekh and J.L. Eichelberger. High temperature ultrafiltration with kynar poly(vinylidene fluoride) membranes. Separation Science and Technology, 15(4): 1193-1204, 1980.

Benzinger, W.D., and D.N. Robinson. Porous Polyvinylidene Fluoride Membrane and Process for Its Preparation. United States Patent 4,384,047, 1982

Berg, L. Separation of 1-hexene from hexane by extractive distillation. United States Patent 5,460,700, Oct. 24, 1995.

Bessarabov, D.G. Phenomenological analysis of ethylene transport in a membrane contactor containing solution of silver nitrate. Desalination, 115: 265-277, 1998.

Bessarabov, D.G., A.V. Vorobiev, E.P. Jacobs, R.D. Sanderson and S.F. Timashev. Separation of olefin/paraffin gaseous mixtures by means of facilitated transport membranes based on metal conducting perfluorinated carbon-chain copolymers. In: Proceedings of Euromembrane '95 Vol. II. W.R. Bowen, R.W. Field and J.A. Howell [Eds]. Pp. II-186-189, 1995.

Bessarabov, D.G., J.P. Theron and R.D. Sanderson. Novel application of membrane contactors: solubility measurements of 1-hexene in solvents containing silver ions for liquid olefin/paraffin separations. Desalination, 115: 279-284, 1998.

Bessarabov, D.G., J.P. Theron, R.D. Sanderson, H.-H. Schwarz, M. Schossig-Tiedemann and D. Paul. Separation of 1-hexene/n-hexane mixtures using a hybrid membrane/extraction system. Separation and Purification Technology, 16: 167-174, 1999.

Bessarabov, D.G., R.D. Sanderson, E.P. Jacobs and I.N. Beckman. High efficiency separation of an ethylene/ethane mixture by a large-scale liquid membrane contactor containing flat sheet non-porous gas separation membranes and a selective flowing liquid absorbent. Industrial Engineering and Chemistry Research, 34:1769-1778, 1995.

Bessarabov, D.G., R.D. Sanderson, V. V. Valuev, Y. M. Popkov and S.F. Timashev. New Possibilities of electroinduced membrane gas and vapor separation. Industrial Engineering and Chemistry Research, 36: 2487-2489, 1997.

Bessieres, A., M. Meireles, R. Coratger, J. Beauvillain and V. Sanchez. Investigations of surface properties of polymeric membranes by near field microscopy. Journal of Membrane Science, 109: 271-184, 1996.

Bhaumik, D., S. Majumdar and K.K. Sirkar. Pilot-plant and laboratory studies on vapor permeation of VOCs from waste gas using silicone coated hollow fibers. Journal of Membrane Science, 167: 107-122. 2000.

Billmeyer, F.W. Jr. Textbook of Polymer Science. John Wiley & Sons Inc., New York, USA, pp. 8, 151-185, 578, 1984.

Bottino, A., G. Capannelli, A. Imperato and S. Munari, Ultrafiltration of hydrosoluble polymers. Effect of operating condition on the performance of the membranes. Journal of Membrane Science, 21: 247-267, 1984.

Bottino, A., G. Capannelli, S. Munari, A. Turturro. Solubility parameters of poly(vinylidene fluoride). Journal of Polymer Science: Part B: Polymer Physics, 26: 785-794, 1988a.

Bottino, A., G. Capannelli, S. Munari, A. Turturro. High performance ultrafiltration membranes cast from LiCl doped solutions. Desalination, 68:167-177, 1988b.

Bottino, A., G. Camera-Roda, G. Capannelli and S. Munari. The formation of microporous polyvinylidene difluoride membranes by phase separation. Journal of Membrane Science, 57: 1-20, 1991.

Bottino, A., G. Capannelli, S. Munari, Permeation characterictics of poly(vinylidene fluoride) membranes. Polymer, 21: 21-30, 1980.

Bottino, A., G. Capannelli, S. Munari. Effect of coagulation medium on properties of sulphonated polyvinylidene fluoride membranes. Journal of Applied Polymer Science, 30: 3009-3022, 1985.

Bottino, A., G. Capannelli, S. Munari. Factors affecting the structure and properties of asymmetric polymeric membranes. In: Membrane and Membrane Processes. E. Drioli, M. Nakagaki [Eds]. Plenum Press, New York, pp. 163-178, 1986.

Broens, L., F.W. Altena, C.A. Smolders and D.M. Koenhen. Asymmetric membrane structures as a result of phase separation phenomena. Desalination, 32: 33-45, 1980

Burke, J. http://palimpsest.stanford.edu/byauth/burke/solpar/ 1984.

Cabasso, I., E. Klein and J.K. Smith. Polysulfone hollow fibers. I. Spinning and Properties. Journal of Applied Polymer Science, 20: 2377-2394, 1976.

Cabasso, I., E. Klein and J.K. Smith. Polysulfone hollow fibers. II. Morphology. Journal of Applied Polymer Science, 21: 165-180, 1977.

Cantrell, C.J. Vapor recovery for refineries and petrochemical plants. Chemical Engineering Progress, 78(10): 56-60. 1982.

Capanneli, G., F. Vigo and S. Munari. Ultrafiltration membranes – Characterisation methods. Journal of Membrane Science, 15: 289-313, 1983.

Castro, E.F., E.E. Gonzo and J.C. Gottifredi. The analysis of sorption data of organic vapors ion polymeric membranes through novel theories. Journal of Membrane Science, 113: 57-64. 1996.

Cha, J.S., R. Li and K. K. Sirkar. Removal of water vapor and VOCs from nitrogen in a hydrophilic hollow fiber gel membrane permeator. Journal of Membrane Science, 119: 139-153. 1996.

Cha, J.S., V. Malik and D. Bhaumik, R. Li and K. K. Sirkar. Removal of VOCs from waste gas streams by permeaion in a hollow fiber permeator. Journal of Membrane Science, 128: 195-211. 1997.

Chabot, S., C. Roy, G. Chowdhury and T. Matsuura. Development of poly(vinylidene fluoride) hollow fiber membranes for the treatment of water/organic vapor mixtures. Journal of Applied Polymer Science, 65 : 1263-1270. 1997.

Chahboun, A., R. Coratger, F. Ajustron, J. Beauvillain, P. Aimar and V. Sanchez. Comparactive study of micro and ultrafiltration membranes using STM, AFM and SEM techniques. Ultramicroscopy, 41: 235- 242, 1992.

Cheng, L.P. Effect of temperature on the formation of microporous PVDF membranes by precipitation from 1-octanol/DMF/PVDF and water/DMF/PVDF systems. Macromolecules, 32: 6668-6674, 1999.

Cheng, L.P., T.H. Young, L. Fan and J.J. Gau. Formation of particulate microporous poly(vinylidene fluoride) membranes by isothermal immersion precipitation from the 1-octanol/dimethylformamide/poly(vinylidene fluoride) system. Polymer, 40: 2395-2403, 1999.

Chern, Y.T. and B.S. Wu. Preparation of composite membranes with polyimides and poly(amide-imide)s skin via interfacial condensation for air separation, Journal of Applied Polymer Science, 63: 693-701. 1997.

Cheryan, M. Ultrafiltration Handbook. Technomic Publication Co.Inc., Lancaster, USA, 1986.

Cho, I.H., D.L. Cho, H.K. Yasuda and T.R. Marrero. Solubility of propylene in aqueous silver nitrate. Journal of Chemical Engineering Data, 40: 102-106, 1995a.

Cho, I.H., H.K. Yasuda and T.R. Marrero. Solubility of ethylene in aqueous silver nitrate. Journal of Chemical Engineering Data, 40: 107-111, 1995b.

Cotton, F.A. and G. Wilkinson, Advanced Inorganic Chemistry, 2nd edition. Chapters 25 and 28, Interscience, New York, 1966.

Cranford, R.J., C. Roy and T. Matsuura. Vapour permeation applied for the separation of water from organic compounds and gases using asymmetric polyetherimide / polyvinylpyrrolidone capillary tubes. Canadian Journal of Chemical Engineering, 75(2): 471-475. April 1997.

Crowder, M.L. and C.H. Gooding. Spiral wound, hollow fiber membrane modules: A new approach to higher mass transfer efficiency. Journal of Membrane Science, 137: 17-29. 1997.

Crowder, R.O. and E.L. Cussler. Mass transfer in hollow fiber modules with non-uniform hollow fibers. Journal of Membrane Science, 134: 235-242. 1997.

Crowder, R.O. and E.L. Cussler. Mass transfer resistances in hollow fiber pervaporation. Journal of Membrane Science, 145: 173-184. 1998.

Cussler, E.L. Facilitated and active transport. In: Polymeric Gas Separation Membranes. D.R. Paul and Y.P. Yampol'skii [Eds]. CRC Press, Boca Raton, Florida, pp. 274-300, 1994.

Damszy, R.C., R. Alamo, C.O. Edwards and L. Mandelkern. Thermoreversible gelation and crystallization of homopolymers and copolymers. Macromolecules, 19: 310-325, 1986.

Davies, J.C., R.J. Valus, R. Eshraghi and A. Velikoff. Facilitated transport membrane hybrid systems for olefin purification. Separation Science and Technology, 28(1-3): 463-476, 1993.

Deng, S., S. Sourirajan, T. Matsuura and B.A. Farnand. Volatile hydrocarbon emission control by polymeric membranes. In: Proceeding of the 6th Conference on Pervaporation Processes in the Chemical Industries, Sept. 27-30, 1992, Ottawa, Canada. pp. 504-513, 1992.

Deng, S., S. Sourirajan, T. Matsuura and B.A Farnand. Study of volatile hydrocarbon emission control by an aromatic poly(ether imide) membrane. Industrial Engineering and Chemistry Research, 34: 4494-4500, 1995a.

Deng, S., T. Liu, S. Sourirajan, T. Matsuura and B.A. Farnand. A study of volatile hydrocarbon emission control by polyetherimide hollow fiber membranes. Journal of Polymer Engineering, 14(4): 219-235, 1995b.

Deng, S., A. Tremblay and T. Matsuura. Preparation of hollow fibers for the removal of volatile organic compounds from air. Journal of Applied Polymer Science, 69: 371-379. 1998.

Deschamps, A., R. Dick and C. Lecomte. Development of gaseous permeation membranes adapted to the purification of hydrocarbons. In: Future Industrial Prospects of membrane Processes, L. Cecille and J.-C. Toussaint [Eds]. Elsevier Applied Science, London, pp. 153-162, 1989.

Deshmukh, S.P. and K. Li. Effect of ethanol composition in water coagulation bath on morphology of PVDF hollow fibre membranes. Journal of Membrane Science, 150: 75-85, 1998.

Doi, D. M. Introduction to Polymer Physics. Clarendon Press, Oxford, pp. 120, 1996.

Domszy, R.C., R. Alamo, C.O. Edwards and L. Mandelkern. Thermoreversible gelation and crystallization of homopolymers and copolymers. Macromolecules, 19: 310-325, 1986.

Eldridge, R.D. Olefin/paraffin separation technology: A review. Industrial Engineering and Chemistry Research, 32: 2208-2212, 1993.

Elias, H.G. Macromolecules, Vol 2: Synthetis, Materials, and Technology. 2nd eds. Plenum Press, New York, pp. 1342, 1984.

Erickson, O.I., E. Aksnes, I.M. Dahl. Facilitated Transport of ethylene through nafion membranes, Part II: Glycerine treated water swollen membranes. Journal of Membrane Sceince, 85: 99-108, 1993.

Espenan, J.M. and P. Aptel. Outer skinned hollow fibre spinning and properties. In: Membrane and Membranes Process, E. Drioli and M. Nakagaki [Eds]. Plenum Press, New York, pp. 151-161, 1986.

Farnand, B.A. and T.M. Giddings. Membrane processing of petroleum fractions,

. In: Proceedings of the 6th Conference on Pervaporation Processes in the Chemical Industries, Sept. 27-30, 1992, Ottawa, Canada, pp. 403-410, 1993.

Feng, X., S. Sourirajan, H. Tezel, and T. Matsuura. Separation of organic vapor from air by aromatic polyimide membranes. Journal of Applied Polymer Science, 43: 1071-1079, 1991.

Feng, X., S. Sourirajan, F.H. Tezel, T. Matsuura and B.A Farnand. Separation of volatile organic compound/ nitrogen mixtures by polymeric membranes. Industrial Engineering and Chemistry Research, 32: 533-539, 1993.

Ferguson, F.D. and T.K. Jones. The Phase Rule. Butterworth, London, pp.112, 1966.

Field, R.W. Mass transport and the design of membrane systems. In: Industrial Membrane Separation Technology. K. Scott and R. Hughes [Eds]. Blackie Academic & Professional, London, pp. 67-112, 1996.

Flory, P.J. Principles of Polymer Chemistry. Cornell University Press, New York, pp. 672, 1953.

Flory, P.J. Structural regularity and crystallinity in macromolecules. In: Structural Order in Polymers. Ciardelli, F. and P. Giusti [Eds]. Pergamon Press, Oxford, pp. 3-9, 1981.

Fouda, A., Y. Chen, J. Bai and T. Matsuura. Wheatstone bridge model for laminated polydimethylsiloxane/polyethersulfone membrane for gas separation. Journal of Membrane Science, 64: 263-270, 1991.

Fouda, A., J. Bai, S.Q. Zhang, O. Kutowy and T. Matsuura. Membrane separation of low volatile organic compounds by pervaporation and vapour permeation. Desalination, 90: 209-233, 1993.

Freeman, H.M., T. Harten, J. Springer, P. Randall, M.A. Curran and K. Stone. Industrial pollution prevention: a critical review. Journal of Air and Waste Management Association, 42(5): 616-656, 1992.

Friesen, D.T., D.B. Newbold, S.B. McCray, and R. Roderick J. Hollow fiber vapor permeation membranes and modules. European Patent Application EP 0 753 337 A2, Jan. 15, 1997.

Fritsch, D., K.-V. Peinemann and R.-D. Behling. Silicone/ non-silicone grafted composite membranes for air vapor separation. Desalination, 90: 235-247, 1993.

Fritzche, A.K., A.R. Arevalo, A.F. Connolly, M.D. Moore, V. Elings and C.M. Wu. The structure and morphology of the skin layer of poly(ether sulfone) ultrafiltration membranes: a comparative atomic force microscope and scanning electron microscope study. Journal of Applied Polymer Science, 45: 1945-1953, 1992.

Frommer, M.A. and R.M. Messalem. Mechanisl of membrane formation. VI. Convective flows and large void formation during membrane precipitation. Industrial. Engineering Chem. Prod. Res. Develop., 12(4): 329-333, 1973.

Frommer, M.A., I. Feiner, O. Kedem and R. Bloch. The mechanism for formation of 'skinned' membranes II. Equilibrium properties and osmotic flows determining membrane structure. Desalination, 7: 393-402, 1980.

Fuji, T.N. and T.Y. Kawasaki. Polyvinylidene fluoride type resin hollow filament microfilter and process for producing the same. United States Patent 4,399,035. Aug. 16, 1983.

Gabelman, A., S.T. Hwang. Hollow fibre membrane contactors. Journal of Membrane Science, 159: 61-106, 1999.

Gekas, V. Terminology for pressure-driven membrane operations. Desalination, 68: 77-92, 1988.

Gienger, J.K. and R.J. Ray. Membrane-based hybrid processes. In: New Membrane Materials and Processes for Separation, AIChE Symposium Series 261, Vol 84. K. K. Sirkar and D. R. Lloyd [Eds], pp.168-177, New York, AIChE, 1988.

Goddard, J. D., J. S. Schultz, S.R. Suchdeo. Facilitated transport via carrier mediated diffusion in membranes, Part II. Mathematical aspects and analyses. AIChE Journal, 20: 625-642, 1974.

Hansen, C.M. Some answered and unanswered questions about the solubility parameter. Macromolecular Solutions. In: Solvent-Property Relationships in Polymers. Seymour, R.B. and G. A. Stahl [Eds]. Pergamon Press, New York, pp. 233, 1982.

Hayama, A., F. Kohori and K. Sakai. AFM observation of small surface pores of hollow fibre dialysis membrane using highly sharpened probe. Journal of Membrane Science, 197: 243-249, 2002.

Hayashi, J.-I., H. Mizuta, M. Yamamoto, K.Kusakabe, S. Morooka. Separation of ethane.ethylene and propane/propylene system with carbonised BPDA-pp'ODA

polyimide membranes, Industrial Engineering and Chemistry Research, 35: 4176-4182, 1996.

Hedley, W.H., S.M. Menta, C.M. Moscowitz, R.B. Reznik, G.A. Richardson and D.C. Zanders. Potential Pollutants from Petrochemicals Processes. Technomic Publishing Co., Inc., Westport, Connecticut, USA, 1975.

Henis, J.M.S. and M.K. Tripodi. Multicomponents membranes for gas separations. United States Patent 4,230,463, Oct. 28, 1980.

Henis, J.M.S. and M.K. Tripodi. Composite hollow fibre membranes for gas separation: resistance model approach. Journal of Membrane Science, 8: 233-242. 1981.

Ho, C-C. and A.L. Zydney. Measurement of membrane pore interconnectivity. Journal of Membrane Science, 170: 101-112, 2000.

Ho, W.S. and K.K. Sirkar. Membrane Handbook. Van Nostrand Reinhold, Amsterdam. pp. 163-215, 1992.

Hong, P.D. and C.M. Chou. Phase separation and gelation behaviors in polyvinyl(fluoride)/tetra(ethylene glycol) dimethyl ether solutions. Polymer, 41: 8311-8320, 2000.

Hong, S.U., J.Y. Kim and Y.S. Kang. Effect of water on the facilitated transport of olefins through solid polymer electrolyte membranes. Journal of Membrane Science, 181: 289-293, 2001.

Hsiue, G. H. and J. S. Yang, Novel methods in separation of olefin/paraffin mixture by functional polymeric membranes. Journal of Membrane Science, 82: 117-, 1993.

Hsiue, G. H. and J. S. Yang, Ag^{+} contained complex membranes for the separation of C4 olefin paraffin mixture. Journal of Polymer Research, 1: 35-40, 1994.

Hughes, R. Applications in gas and vapour phase separations. In: Industrial Membrane Separation Technology. K. Scott and R. Hughes [Eds]. Blackie Academic & Professional, London. pp. 114-150, 1996.

Hughes, R.D., J.A. Mahoney, E.F. Steigelmann. Olefin separation by facilitated transport, In: Recent Developments in Separation Science Vol. 9. N.N., Li and J.M. Calo [Eds]. CRC Press, Boca Raton, Florida. pp. 173-195, 1986.

Hughes, T.W., D.R. Tierney and Z.S. Khan. Measuring fugitive emissions from petrochemical plants. Chemical Engineering Progress, 7 (8): 35-39, 1979.

Ilinitch, O.M., C.L. Semin, M.V. Chertova and K.I. Zamaraev. Novel polymeric membranes for separation of hydrocarbons. Journal of Membrane Science, 66: 1-8, 1992.

Isalski, W.H. Separation of Gases. Clarendon Press, Oxford, pp. 189, 1989.

Ito, A., K. Adachi and Y. Feng. Separation of aromatics by vapor permeation through solvent swollen membrane. Journal of Chemical Engineering of Japan, 28(6): 679-683, 1995.

Ito, A., S.-T. Hwang, Permeation of propane and propylene through cellulosic polymer membranes. Journal of Applied Polymer Science, 38: 483-490, 1989.

Iversen, S.B., V.K. Bhatia, K. Dam-Johansen, G. Jonsson. Characterisation of microporous membrane for use in membrane contactor. Journal of Membrane Science, 130: 205-217, 1997.

Jacobs, M. L., R. W. Baker, J. Kaschemekat and V. L. Simmons. Industrial applications for membrane vapor recovery systems. In: Proceedings of the 86th Annual Meeting and Exhibition, Volume 4A, 93-TP-31B.07, June 13-18, 1993, Denver, Colorado. pp. 1-12, 1993.

Jansen, A.E., P.H.M. Feron, J.J. Akkerhuis, B. Ph. ter Meulen. Vapour recovery from air with selective membrane absorption. In: Separation Technology, Proceedings of the Third International Symposium on Separation Technology. E.F. Vansant [Ed]. Elsevier Science B.V., Amsterdam, pp. 583-598, 1994a.

Jansen, A.E., R. Klaassen, P.H.M. Feron, J.H. Hanemaaijer, B. Ph. Ter Meulen. Membrane gas absorption processes in environmental applications. In: Membrane Processes in Separation and Purification. J.G. Crespo and K.W. Böddeker [Eds]. Kluwer Academic Publishers, Amsterdam. pp. 343-356, 1994b.

Jian, K. and P.N. Pintauro. Integral asymmetric poly(vinylidene fluoride) (PVDF) pervaporation membranes. Journal of Membrane Science, 85: 301-309, 1993.

Jian, K., P.N. Pintauro and R. Ponangi. Separation of dilute organic/water mixtures with asymmetric poly(vinylidene fluoride membranes. Journal of Membrane Science, 117: 117-133, 1996.

Jian, K. and P.N. Pintauro. Asymmetric PVDF hollow fiber membranes for organic/water pervaporation separations. Journal of Membrane Science, 135: 41-53, 1997.

Jones, A.L. Fugitive emissions of volatile hydrocarbons, Chemical Engineer, 406: 12-15, 1984.

Kamide, K., Manabe, S., Nohmi, T., Mokino, H., Narita, H. and Kawai, T. Mechanism of gas permeation through porous polymeric membrane. In: Polymeric Separation Media. A. R. Cooper [Ed]. Plenum Press, New York, pp. 35-74, 1982.

Kang, Y.S., H. J. Kim and U. Y. Kim. Asymmetric membrane formation via immersion precipitation method. I. Kinetic effect. Journal of Membrane Science, 60: 219-232, 1991.

Karode, S.K., V.S.Patwardhan and S. S. Kulkarni. An improved model incorporating constriction resistance transport through thin film composite membranes. Journal of Membrane Science, 114: 157-166, 1996.

Karode, S.K. and S. S. Kulkarni. Analysis of transport through thin film composite membrane using an improved Wheatstone bridge resistance model. Journal of Membrane Science, 127: 131-140, 1997.

Karode, S.K. and A. Kumar. Formation of polymeric membranes by immersion precipitation: an improved algorithm for mass transfer calculations. Journal of Membrane Science, 187: 287-296, 2001.

Keller, G.E., A.E. Marcinkowsky, S.K. Verma, K.D. Williamsonm. In: Separation and Purification Technology. N.N. Li, J.M. Calo [Eds]. Marcel Dekker, New York, pp. 59-83, 1992.

Kesting, R.E. Synthetic Polymeric Membranes. McGraw-Hill Book Co., New York, pp. 307, 1971.

Kesting, R.E. Synthetic Polymeric Membranes: A Structural Perspective. 2nd. Ed. John Wiley & Sons, Inc., New York, pp. 348, 1985.

Khayet, M. and T. Matsuura. Preparation and characterisation of polyvinylidene fluoride membranes for membrane distillation. Industrial Engineering and Chemistry Research, 40: 5710-5718, 2001.

Khayet, M., C.Y. Feng, K.C. Khulbe and T. Matsuura. Study on the effect of a non-solvent additive on the morphology and performance of ultrafiltration hollow fibre membranes. Desalination, 148: 321-327, 2002

Kim, H.J and Hong S.I. The transport properties of CO_2 and CH_4 for chemically modified polysulfones. Journal of Applied Polymer Science, 76: 391-400, 2000.

Kim, J.-H., Y.-I. Park, J. Jegal and K.-H. Lee. The effects of spinning conditions on the structure formation and the dimension of the hollow fiber membranes and their relationship with the permeability in dry-wet spinning technology. Journal of Applied Polymer Science, 57: 1637-1644, 1995.

Kim, K. J., A.G. Fane, R. Ben Aim, M. G. Liu, G. Jonsson, I. C. Tessaro, A.P. Broek and D. Bargeman. A comparative study of techniques used for porous membrane charaterisation: pore characterization. Journal of Membrane Science, 87: 35-46, 1994.

Kimmerle, K., C. M. Bell, W. Gudernatsch and H. Chmiel. Solvent recovery from air, Journal of Membrane Science, 36: 477-488. 1988.

Kimmerle, K., T. Hofmann and H. Strathmann. Analysis of gas permeation through composite membranes. Journal of Membrane Science, 61: 1-17. 1991.

King, C.J. Separation processes based on reversible chemical complexation. In: Handbook of Separation Process Technology, Chapter 15. R.W. Rousseau [Ed]. Wiley, New York, pp. 760-774, 1987.

Klausener, P. and D. Woermann. Structure and transport properties of cation exchange gel membranes: facilitated transport of ethane with silver ions as carriers. Journal of Membrane Science, 168: 17-27, 2000.

Klein, E. and J.K. Smith. Asymmetric membrane formation. Solubility parameters for solvent selection. Industrial and Engineering Chemistry Products Research and Developement, 11(2): 207-210, 1972.

Kong, J.F. and K. Li. Oil removal from oil-in-water emulsions using PVDF membranes. Journal of Membrane Science, 16: 83-93, 1999.

Kong, J.F. Fabrication of Polyvinylidene Fluoride Membranes For Waste Treatment. PhD. Thesis. National University of Singapore, 2000.

Kong, J.F. and K. Li. An improved gas permeation method for characterizing and predicting the performance of microporous asymmetric hollow fibre membranes used in gas absorption. Journal of Membrane Science, 182: 271-281, 2001.

Koros, W.J. Membrane based gas separation. Journal of Membrane Science, 83: 1-80, 1993.

Kovvali, S.A., H. Chen and K.K. Sirkar. Glycerol-based immobilized liquid membranes for olefin-paraffin separation. Industrial Engineering and Chemistry Research, 41: 347-356, 2002.

Kreulen, H., C.A. Smolders, G.F. Versteeg and W.P.M. van Swaaij. Microporous hollow fibre membrane module as gas-liquid contactors. Part 1. Physical mass transfer processes. A specific application: mass transfer in highly viscous liquids. Journal of Membrane Science, 78: 197-216, 1993a.

Kreulen, H., C.A. Smolders, G.F. Versteeg and W.P.M. van Swaaij. Microporous hollow fibre membrane module as gas-liquid contactors. Part 2. Mass transfer with chemical reaction. Journal of Membrane Science, 78: 217-238, 1993b.

Kulkarni, S. S., E. W. Funk and N. N. Li. Hydrocarbon separations with polymeric membranes. In: Recent Advances in Separations Techniques III, AIChE Symposium Series 250, Vol 82. N.N. Li, T.A. Hatton, S-T. Hwang, D.M. LaRue, S.A. Leeper and D.L. Roberts [Eds]. AIChE, New York, pp. 78-84, 1986.

Lau, W.W.Y, M.D. Guiver and T. Matsuura. Phase separation in polysulfone/solvent/water and polyethersulfone/solvent/water systems. Journal of Membrane Science, 59: 219-227, 1991.

Lau, W. W. Y., Finlayson, J., Dickson, J. M., Jiang, J. and Brook, M. A. Pervaporation performance of oligosilylstyrene-polydimethylsiloxane membrane for separation of organics from water, Journal of Membrane Science, 134: 209-217, 1997.

Lee, Y., J. Jeong, I. J. Youn and W. H. Lee. Modified liquid displacement method for determination of pore size distribution in porous membranes. Journal of Membrane Science, 130: 149-156, 1997.

Leeman, M., G. Eigenberger and H. Strathmann. Vapour permeation for the recovery of organic solvents from waste air streams: separation capacities and process optimization. Journal of Membrane Science, 113: 313-322, 1996.

Lemanski, J., B. Liu and G.G. Lipscomb. Effect of fiber variation on the performance of cross-flow hollow fiber gas separation modules. Journal of Membrane Science, 153: 33-40, 1999.

Lemanski, J. and G.G. Lipscomb. Effect of fiber variation on the performance of countercurrent hollow fiber gas separation modules. Journal of Membrane Science, 167: 214-252, 2000.

Li, K., J.F. Kong, D. Wang and W.K. Teo. Tailor-made asymmetric PVDF hollow fibers for soluble gas removal. AIChE Journal, 45(6): 1211-1219, 1999.

Liu, T., S. Xu, D. Zhang, S Sourirajan and T. Matsuura. Pore size and pore size distribution on the surface of polyethersulfone hollow fibre membranes. Desalination, 85: 1-12, 1991.

Lonsdale, H.K. The growth of membrane technology. Journal of Membrane Science, 10: 81-, 1982.

Lora, M., J.S. Lim and M.A. McHugh. Comparison of the solubility of PVF and PVDF in supercritical CH_2F_2 and CO_2 and in CO_2 with acetone, dimethyl ether and ethanol. Journal of Physical Chemistry B, 103: 2818-2822, 1999.

Lovinger, A.J. Poly(vinylidene fluoride). In: Development in Crystalline Polymers, Vol. 1. D.C. Bassett [Ed]. Applied Science, London, pp. 195-273, 1982.

Masaharu, S. Polyvinylidene fluoride hollow fiber membrane and its production. Japanese Patent 08,299,770, Nov. 19, 1996.

Matsuyama, H., M. Teramoto, R. Nakatani and T. Maki. Membrane formation via phase separation induced by penetration of non-solvent from vapor phase. I. Phase diagram and mass transfer process. Journal of Applied Polymer Science, 74: 159-170, 1999.

Matsuyama, H., M. Teramoto, R. Nakatani, T. Maki. Membrane formation via phase separation induced by penetration of non-solvent from vapor phase. II. Membrane morphology. Journal of Applied Polymer Science, 74: 171-178, 1999.

Merry, A.J. Membrane equipment and plant design. In: Industrial Membrane Separation Technology. K. Scott and R. Jughes [Eds]. Blackie Academic & Professional, London, pp. 32-66, 1996.

Mohamed, K. and T. Matsuura. Preparation and characterisation of polyvinylidene fluoride membranes for membrane distillation. Industrial Engineering and Chemistry Research, 40: 5710-5718, 2001.

Morawetz, H. Macromolecules In Solution. 2nd. Ed. John Wiley & Sons, Inc., New York, pp. 33-95, 1955.

Mulder, M.H.V., J.O. Hendrikman, J.G. Wijmans and C.A. Smolders. A rationale for the preparation of asymmetric pervaporation membranes. Journal of Applied Polymer Science, 30: 2805-2820, 1985.

Mulder, M. Energy requirements in membrane separation processes. In: Membrane Processes in Separation and Purification. J.G. Crespo and K.W. Böddeker [Eds]. Kluwer Academic Publishers, Amsterdam, pp. 445-475, 1994a.

Mulder, M. The use of membrane processes in environmental problems: an introduction. In: Membrane Processes in Separation and Purification. J. G. Crespo and K. W. Böddeker [Eds]. Kluwer Academic Publishers, Amsterdam, pp. 229-262, 1994b.

Mulder, M. Basic Principles of Membrane Technology. 2nd edition. Kluwer Academic Publishers, Dordrecht, pp. 564, 1996.

Munari, S., A Bottino, G. Camera Roda and G, Capannelli. Preparation of ultrafiltration Membranes. State of the Art. Desalination, 77: 85-100, 1990.

Munari, S., A. Bottino and G. Capannelli. Casting and performance of polyvinylidene fluoride based membranes. Journal of Membrane Science, 16: 181-193, 1983.

Nakao, S-I. Review: Determination of pore size and pore size distribution 3. Filtration membranes. Journal of Membrane Science, 96: 131-165, 1994.

Newbold, D.B., S.B. McCray, D.T. Friesen and R. Roderick J. Membrane-based removal of condensable vapors. Europen Patent Application 0532368 A2, Sept. 14, 1992.

Nijhuis, H.H., M.H.V.Mulder and C.A.Smolders. Removal of trace organics from aqueous solutions. Effect of membrane thickness. Journal of Membrane Science, 61: 99-111. 1991.

Ohlrogge, K. Membranes for dewpointing of gas streams. In: Proceedings of the 1995 Membrane Technology / Separation Planning Conference, Newton, Massachusetts, Oct. 23-25, 1995. Business Communications Company Inc., USA, pp. 284-295, 1995.

Ohlrogge, K. and J. Wind. Small scale applications to separation organic vapors by means of membranes. In: Separation Technology. Proceedings of the Third International Symposium on Separation Technology. E.F. Vansant [Ed]. Elsevier Science B.V., Amsterdam, pp. 903-908, 1994.

Ohlrogge, K., J. Brockmöller, J. Wind and R.-D. Behling. Engineering aspects of the plant design to separate volatile hydrocarbons by vapor permeation. Separation Science and Technology, 28(1-3): 227-240, 1993b.

Ohlrogge, K., J. Wind and R.-D. Behling. Industrial applications of membrane systems to separate hydrocarbon vapors from gas stream. In: 3rd International Conference on Effective Membrane Process. R. Patterson [Ed]. Mechanical Engineering Publication Ltd. , London, pp. 385-390, 1993(a).

Ohlrogge, K., K. –V. Peinemann, J. Wind and R.-D. Behling. The separation of hydrocarbon vapors with membranes. Separation Science and Technology, 25(13-15): 1375-1386, 1990.

Ohlrogge, K., K. Sturken. The separation of organic vapors from gas streams by means of membreanes. In: Membrane Technology in the Chemical Industry. S.P. Nunes and K.-V. Peinemann [Eds]. Weinheim, Wiley-VCH, pp. 71-94, 2001.

Okamoto, K., S. Kawamura, M. Yoshino, H. Kita, Y. Hirayama, N. Tanihara and Y. Kusuki. Olefin/paraffin separation through carbonized membranes derived from an asymmetric polyimide hollow fibre membrane. Industrial Engineering and Chemistry Research, 38: 4424-4432, 1999.

Ortiz de Zarate, J.M., L. Pena, J.I. Mengual. Characterisation of membrane distillation membranes prepared by phase inversion. Desalination, 100: 139-148, 1995.

Oscar, G.F., R.P. Ouellette, R.C. Kuehnel, M.A. Muradaz and P.N. Cherenmisinoff. Ethylene Basic Chemical Feedstock Material. Ann Arbor Science Publisher Inc., Michican, pp. 103, 1983.

Osswald. T.A. and G. Menges. Materials Science of Polymers for Engineers. Hanser Publishers, Munich, pp. 475, 1995.

Passant, N.R. Source inventories and control strategies for VOCs. In: Volatile Organic Compounds in the Atmosphere. R.E. Hester and R.M. Harrison [Eds]. The Royal Society of Chemistry, Cambridge, pp. 51-64, 1995.

Paul, H., C. Philipsen, F.J. Gerner and H. Strathmann. Removal of organic vapor from air by selective membrane permeation. Journal of Membrane Science, 36: 363-372. 1988.

Peinemann, K.-V. and K. Ohlrogge. Separation of organic vapors from air with membranes. In: Membrane Processes in Separation and Purification. J.G. Crespo and K.W. Böddeker [Eds]. Kluwer Academic Publishers, Amsterdam, pp. 357-372, 1994.

Peinemann, K.-V., J. M. Mohr and R. W. Baker. The separation of organic vapors from air. In: Recent Advances in Separations Techniques - III, AIChE Symposium Series 250, Vol. 82. N.N. Li, T.A. Hatton, S-T. Hwang, D.M. LaRue, S.A. Leeper and D.L. Roberts [Eds]. AIChE, New York, pp. 19-26, 1986.

Petersen, J. and K.-V. Peinemann. Novel polyamide composite membranes for gas separation prepared by interfacial polycondensation. Journal of Applied Polymer Science, 63: 1557-1563, 1997.

Piatkiewicz, W. S. Rosinki, D. Lewinska, J. Bukowski and W. Judycki. Determination of pore size distribution in hollow fibre membranes. Journal of Membrane Science, 153: 91-102, 1999.

Pinnau, I., C.G. Casillas, A. Morisato and B.D. Freeman. Long-term permeation properties of Poly(1-trimethylsilyl-1-propyne) membranes in hydrocarbon-vapor environment. Journal of Polymer Science Part B – Polymer Physics, 35(10): 1483-1490, 1997.

Pinnau, I., J.G. Wijmans, I. Blume, T. Kuroda and K.-V. Pienemman. Gas permeation through composite membranes. Journal of Membrane Science, 37: 81-87, 1988.

Pinnau, I., L.G. Toy. Solid polymer electrolyte composite membranes for olefin/paraffin separation. Journal of Membrane Science, 184: 39-48, 2001.

Poddar, T.K. and K.K. Sirkar. A hybrid of vapor permeation and membrane-based absorption-stripping for VOC removal and recovery from gaseous emissions. Journal of Membrane Science, 137: 229-233, 1997.

Ponangi, R.P. and P.N. Pintauro. Separation of volatile organic compounds from dry and humidified nitrogen using polyurethane membranes. Industrial Engineering and Chemistry Research, 35: 2756-2765. 1996.

Qi., Z. and E.L. Cussler. Hollow fibre gas membranes. AIChE Journal, 31(9): 1548-1553, Sept. 1985.

Rautenbach, R. Vapor permeation of a water organic mixtures. Module and process design. In: Proceeding of the 3^{trd} Conference on Pervaporation Processes in the Chemical Industries, Nancy, France, Sept. 19-22, 1988, pp. 287-303, 1988.

Rautenbach, R., A. Struck, T. Melin and M.F.M. Roks. Impact of operating pressure on the permeance of hollow fibre gas separation membranes, Journal of Membrane Science, 146: 217-233, 1998a.

Rautenbach, R., A. Struck and M.F.M. Roks. A variation in the fiber properties affects the performance of defect-free hollow fiber membrane modules for air separation. Journal of Membrane Science, 150: 31-41. 1998b.

Reichelt, G. Bubble point measurements on large areas of microporous membranes. Journal of Membrane Science, 60: 253-259, 1991.

Rege, S.U., J. Padin and R.T. Yang. Olefin/paraffin separation by adsorption: π-complexation *vs* kinetic separation. AIChE Journal, 44(4): 799-809, April 1998.

Reuvers, A.J., J.A.W. van den Berg and C.A. Smolders. Formation of membranes by means of immersion precipitation, Part I. A model to describe mass transfer during immersion precipitation. Journal of Membrane Science, 34: 45-66, 1987.

Reuvers, A.J. and C.A. Smolders. Formation of membranes by means of immersion precipitation, Part II. The mechanism of formation of membranes prepared from the system cellulose acetate-acetone-water. Journal of Membrane Science, 34: 67-86, 1987.

Rogers, C.E. Permeation of gases and vapours in polymers. In: Polymer Permeability. J. Comyn [Ed]. Elsevier Applied Science Publishers, London, pp. 11-73, 1985.

Encyclopedia of Separation Technology Volume 1. D.M. Ruthven [Ed]. John Wiley & Sons, New York, pp. 828, 1997.

Encyclopedia of Separation Technology Volume 2. D.M. Ruthven [Ed]. John Wiley & Sons, New York, pp. 1661, 1997.

Safarik, D.J. and R.B. Eldridge. Olefin/paraffin separations by reactive absorption: a review. Industrial Engineering and Chemistry Research, 37: 2571-2581, 1998.

Schultz, J. S., J. D. Goddard and S.R. Suchdeo. Facilitated diffusion via carrier-mediated diffusion in membranes, Part I. Mechanistic aspects, experimental systems, and characteristic regimes. AIChE Journal, 20: 417-445, 1974.

Schultz, J. and K. -V.Peinemann. Membranes for the separation of higher hydrocarbons from methane. Journal of Membrane Science, 110: 37-45, 1996.

Scott, K. Membrane Separation Technology Industrial Applications and Markets. Scientific and Technical Information, Oxford, pp. 30-38, 1990.

Seymour, R. B. Applications of the solubility parameter concepts in polymer science. Macromolecular Solutions. In: Solvent-Property Relationships in Polymers. R.B. Seymour and G. A. Stahl [Eds]. Pergamon Press, New York, pp. 233, 1982.

Shih, H-C, Y.-S. Yeh and H. Yasuda, Morphology of microporous poly(vinylidene fluoride) membrane studied by gas permeation and scanning electron microscope. Journal of Membrane Science, 50: 299-317, 1990.

Shishatskii, A.M., Y.P. Yampol'skii and K.-V.Peinemann. Effects of thickness on density and gas permeation parameters of glassy polymers. Journal of Membrane Science, 112: 275-285. 1996.

Simmons, V., J. Kaschemekat, M. L. Jacobs and D. D. Dortmundt. Membrane systems offer a new way to recover volatile organic air pollutants. Chemical Engineering, Sept: 92-94, 1994.

Singh, A., B.D. Freeman and I. Pinnau. Pure and mixed gas acetone/nitrogen permeation properties of Polydimethylsiloxane (PDMS). Journal of Polymer Science Part B – Polymer Physics, 36(2): 289-301. 1998.

Singh, S., K.C. Khulbe, T. Matsuura, P. Ramamurthy. Membrane characterisation by solute transport and atomic force microscopy. Journal of Membrane Science 142: 111-127, 1998.

Siversten, B. Estimation of diffuse hydrocarbon leakages from petrochemical factories. Journal of the Air Pollution Control Association, 33 (4): 323-327. 1983.

Shimazu, A., K. Ikeda, H. Hachisuka. Method of selectively separating unsaturated hydrocarbons. United States Patent 5,749, 943, 1998.

Smolders, C.A. and E. Vugteveen. New characterization methods for ultrafiltration membranes. In: Material Science of Synthetic Membranes, ACS Symposium Series 269. D.R. Llyod [Ed]. American Chemical Society, Washington D.C., pp. 327-338, 1985.

Soh, Y.S., J.H. Kim and C.C. Gryte. Phase behaviour of polymer/solvent/non-solvent systems. Polymer, 36 (19): 3711-3717, 1995.

Staudt-Bickel, C. W.J. Koros. Olefin paraffin separation with 6FDA-based polyimide membranes. Journal of Membrane Science, 170: 205-214, 2000.

Strathmann, H. Production of microporous media by phase inversion processes. In: Materials Science of Synthetic Membranes, ACS Symposium Series 269. D.R. Llyod [Ed]. American Chemical Society, Washington D.C., 1985.

Strathmann, H., C. M. Bell and K. Kimmerle. Development of synthetic membranes for gas and vapor separation. Pure Applied Chemistry, 58: 1663-1670, 1986.

Strathmann, H., K. Kock, P. Amar and R.W. Baker. The formation mechanism of asymmetric membranes. Desalination, 16: 179-203, 1975.

Strathmann, H., P. Scheible amd R.W. Baker. A rationale for the preparation of Loeb-Sourirajan type cellulose acetate membranes. Journal of Applied Polymer Science, 15: 811-828, 1971.

Stropnik, Č., V. Musil, M. Brumen. Polymeric membrane formation by wet phase separation; turbidity and shrinkage phenomena as evidence for elementary processes. Polymer, 41: 9227-9237, 2000.

Sugihara, M., M. Fujimoto and T. Uragami. Effect of casting solvent on permeation characteristic of polyvinylidene fluoride membranes. Polym. Prepr., Am. Chem. Soc. Div. Polym. Chem., 20: 999-1001, 1979.

Sunderrajan, S., B.D. Freeman, C.K. Hall and I. Pinnau. Propane and propylene sorption in solid polymer electrolytes based on poly(ethylene oxide) and silver salts. Journal of Membrane Science, 182: 1-12, 2001.

Sungpet, A., J.D. Way, P.M. Thoen and J.R. Dorgan. Reactive polymer membranes for ethylene/ethane separation. Journal of Membrane Sceince, 136: 111-120, 1997.

Tam, C.M., M.M. Dal-Cin, C.E. Capes and T.A. Tweddle. Important considerations in the selection and use of membrane separation processes. . In: Separation Technology, Proceedings of the Third International Symposium on Separation Technology. E.F. Vansant [Ed]. Elsevier Science B.V., Amsterdam, pp. 681-701, 1994.

Tanaka, K., A. Taguchi, J. Hao, H. Kita, K. Okamoto. Permeation and separation properties of polyimide membranes to olefins and paraffins. Journal of Membrane Science, 121: 197-207, 1996.

Tanihara, N., K. Tanaka, H. Kita, K-I. Okamoto, A. Nakamura, Y. Kusuki and K. Nakagawa. Vapor-permeation separation of water ethanol mixtures by asymmetric

polyimide hollow-fiber membrane modules. Journal of Chemical Engineering of Japan, 25(4): 388-396. 1991.

Tanihara, N., H. Shimazaki, Y. Hirayama, S. Nakanishi, T. Yoshinaga and Y. Kusuki. Gas permeation properties of asymmetric carbon hollow fiber membranes prepared from asymmetric poluimide hollow fiber. Journal of Membrane Science, 160: 179-186. 1999.

Teng, M-Y., K-R. Lee, S-C. Fan, D-J. Liaw, J. Huang and J-Y. Lai. Development of aromatic polyamide membranes for pervaporation and vapor permeation. Journal of Membrane Science, 164: 241-249. 2000.

Teramoto, M. H. Matsuyama, T. Yamashori, Y. Katayama. Separation of ethylene from ethane by supported membranes containing silver nitrate as carrier. Journal of Chemical Engineering of Japan, 19: 419-424, 1986.

Tomaszewska, M. Preparation and properties of flat sheet membranes from polyvinylidenefluoride for membrane distillation. Desalination, 104: 1-11, 1996.

Tsou, D.T. M.W. Blachman and J.C. Davies. Silver-facilitated olefin/paraffin separation in a liquid membrane contactor system. Industrial Engineering and Chemistry Research, 33: 3209-3216, 1994.

Uragami, T., M. Fujimoto and M. Sugihara. Studies on syntheses and permeabilities of special polymer membranes. 24. Permeation characteristics of poly(vinylidene fluoride) membranes. Polymer, 21: 1047-1051, 1980.

Uragami, T., M. Fujimoto and M. Sugihara. Studies on syntheses and permeabilities of special polymer membranes. 27. Concentration of poly(styrene sulphonic acid) in various aqueous solutions using poly(vinylidene fluoride) membranes. Polymer, 22: 240-244, 1981a.

Uragami, T., Y. Naito and M. Sugihara. Studies on syntheses and permeability of special polymer membranes. 39. Permeation characteristics and structure of polymer blend membranes from poly(vinylidene fluoride) and poly(ethylene glycol). Polymer Bulletin. 4: 617-622, 1981b.

Wagner, J. Membrane Filtration Handbook. Practical Tips ad Hints. 2nd edition. Osmonics, Inc., pp. 127, 2001.

Wall, L.A. Fluoropolymers. Wiley-Interscience, New York, pp. 550, 1972.

Wang, B.G., Y. Miyazaki, T. Yamaguchi and S. Nakao. Design of a vapor permeation membrane for VOC removal by the filling membrane concept. Journal of Membrane Science, 164: 25-35. 2000.

Wang, D. Polyethersulfone Hollow Fibre Gas Separation Membranes Prepared from Solvent Systems Containing Non-solvent Additives. Ph.D Thesis. National University of Singapore, 1995.

Wang, D., K. Li and W.K. Teo. Preparation and characterization of polyvinylidene fluoride (PVDF) hollow fiber membranes. Journal of Membrane Science, 163: 211-220, 1999.

Wang, D., K. Li and W.K. Teo. Porous PVDF asymmetric hollow fiber membranes prepared with the use of small molecular additives. Journal of Membrane Science, 178: 13-23, 2000a.

Wang, I-F., Ditter, J.F. and Zepf, R. Process of making polyvinylidene fluoride membrane. United States Patent 6,110,309, Aug. 29, 2000b.

Wienk, I.M., R.M. Boom, M.A.M. Beerlage, A.M.W. Bulte, C.A. Smolders, H. Strathmann. Recent advances in the formation of phase inversion membrane from amorphous or semi-crystalline polymers. Journal of Membrane Science, 113: 361-371, 1996.

Wijmans, J.G. Membrane process and apparatus for removing vapors from gas streams. United States Patent 5,071,451, Dec. 10, 1990.

Wijmans, J.G., J.P.B. Baaij and C.A. Smolders. The mechanism of formation of microporous or skinned membranes produced by immersion precipitation. Journal of Membrane Science, 14: 263-274, 1983.

Wijmans, J. G., and V. D. A. Helm. A membrane system for the separation and recovery of organic vapors from gas streams. In: Membrane Separations in Chemical Engineering, AIChE Symposium Series 272, Vol 85. A. E. Fouda, J. D. Hazlett, T. Matsuura, and J. Johnson [Eds]. AIChE, New York, pp. 74-79, 1989.

Wijmans, J. G., H.D. Kamaruddin, S.V. Segelke, M. Wessling and R.W. Baker. Removal of dissolved VOCs from water with an air stripper/membrane vapor separation system. Separation Science and Technology, 32 (14): 2267-2287, 1997.

Wise, H.E. Jr. and P.D. Fahrenthold. Predicting priority pollutants from petrochemicals processes. Environmental Science and Technology, 15(11): 1292-1296, 1981.

Wlosek-Szydlowska, A. and J. Straśzko. Diffusion and permeation of gas mixtures through polymeric membranes: mechanism of diffusion. In: Synthetic Polymeric Membranes, Proceedings of the 29th Microsymposium on Macromolecules Pragus, Czechoslovakia, July 7-10, 1986. B. Sedláček and J. Kahovec [Eds]. pp. 341-353, 1987.

Wu, Y., Y. Kong, J. Liu, J. Zhang and J. Xu. An experimental study on membrane distillation – crystallisation for treating waste waster in taurine production. Desalination, 80: 235-242, 1991.

Yamaguchi, T., C. Baertsch, C.A. Koval, R.D. Noble, C.N. Bowman. Olefin separation using silver impregnated ion-exchange membranes and silver/polymer blend membranes. Journal of Membrane Science, 117: 151-158, 1996.

Yang, M.-C. and E.I. Cussler. Designing hollow fibre contactors. AIChE Journal, 32(11): 1910-1916, 1986.

Yang, J. S. and G. H. Hsiue. C4 olefin/paraffin separation by poly[(1-trimethylsilyl)-1-propyne]-graft-poly(acrylic acid)-Ag^+ complex membranes. Journal of Membrane Science, 111: 27-38, 1996a.

Yang, J. S. and G. H. Hsiue. Novel dry poly[(1-trimethylsilyl)-1-propyne]-$AgClO_4$ complex membranes for olefin/ paraffin separations. Journal of Membrane Science, 120:69-76, 1996b.

Yang, J. S. and G. H. Hsiue. Selective olefin permeation through Ag(I) contained silicone rubber-graft-poly(acrylic acid) membranes. Journal of Membrane Science, 126: 139-149, 1997.

Yang, J. S. and G. H. Hsiue, Swollen polymeric complex membranes for olefin/paraffin separation, Journal of Membrane Science, 138: 203-211, 1998.

Yao, C.W., R.P. Burford, A.G. Fane and C.J.D. Fell. Effect of coagulation conditions on structure and properties of membranes from aliphatic polyimides. Journal of Membrane Science, 38: 113-125, 1988.

Yasuda, H. and J.T. Tsai. Pore size of microporous polymer membranes. Journal of Applied Polymer Science, 18: 805-819, 1974.

Yilmaz, L. and A.J. McHugh. Analysis of nonsolvent- solvent-polymer phase diagram and their relevance to membrane formation modeling. Journal of Applied Polymer Science, 31: 997-1018, 1986.

Yilmaz, L. and A.J. McHugh. Modelling of asymmetric membrane formation. I. Critique of evaporation models and development of a diffusion equation formalism for the quench period. Journal of Membrane Science, 28: 287-310, 1986.

Yilmaz, L. and A.J. McHugh. Modeling of asymmetric membrane formation. II. The effects of surface boundary conditions. Journal of Applied Polymer Science, 35: 1967-1979, 1988.

Young R.J. and P.A. Lovell. Introduction to Polymers. 2nd edition. Chapman & Hall, London. pp. 443, 1991.

Young, T.H., L.P. Cheng, D.J. Lin, L. Fane and W.Y. Chuang. Mechanism of PVDF membrane formation by immersion precipitation in soft (1-octanol) and harsh (water) non-solvents. Polymer, 40: 5315-5323, 1999.

Zeman, L. and Tkacik, G. Characterisation of porous sublayers in UF membranes by thermoporometry. Journal of Membrane Science, 32: 329-337, 1987.

Zryd, J.L. and Burghardt, W.R. Phase separation, crystallization, and structure formation in immiscible polymer solutions. Journal of Applied Polymer Science, 57: 1525-1537, 1995.

Zydney, A. L., P. Aimar, M. Meireles, J. M. Pimbley and G. Belfort. Use of the log-normal probability density function to analyse membrane pore size distributions: functional forms and discrepancies. Journal of Membrane Science, 91: 293-298, 1994.

PUBLICATIONS AND AWARDS

JOURNAL PUBLICATIONS

1. **M. L. Yeow**, R.W. Field, K. Li and W. K. Teo, Preparation of PVDMS/PVDF Composite Hollow Fibre Membranes for BTX Removal. Journal of Membrane Science, 203:1-2 (2002) 137-143.
2. **M.L. Yeow**, Y.T. Liu and K. Li, Isothermal phase diagrams and phase inversion behaviour of poly(vinylidene fluoride)/solvents/additives/water systems. Journal of Applied Polymer Science, 90 (8): 2150-2155, 2003.
3. **M.L. Yeow**, Y.T. Liu and K. Li, Morphological study of poly(vinylidene fluoride) asymmetric membrane - Effects of solvent, additive and dope temperature. Journal of Applied Polymer Science, 92(3): 1782-1789, 2004.
4. **M.L. Yeow,** Y.T.Liu and K. Li. Development of PVDF hollow fibre membrane via phase inversion – immersion precipitation method using lithium perchlorate ($LiClO_4$) as non-solvent additive. Submitted to Journal of Membrane Science, 2004.

CONFERENCE PUBLICATIONS

1. **M.L. Yeow**, W.M. Wan Hashim, K.Li. "Olefin/Paraffin Separation via *pi* Complexation with silver ion using PVDF hollow fibre membrane contactor" (Paper presented at the 3rd International Symposium on Multifunctional Reactors and 18th Collaqium on Chemical Reaction Engineering. 27 - 29 August, 2003, Bath, UK).

AWARDS

1. Awarded **First Prize** in the ***Crystal Faraday Partnership Award*** for the best paper by a young researcher in the area of green chemical technology at the 3rd International Symposium of Multifunctional Reactors and 18th Colloquium on Chemical Reaction Engineering, 27 – 29 August, 2003, Bath, UK.

OTHER CONFERENCE PUBLICATIONS:

1. M. Ellis, **M.L.Yeow**, K. Li, J. Beresford and J. Chaudhuri. "Development of a biodegradable polymer scaffold to mimic cortical bone in a clinically-relevant bioreactor" (Paper presented at the 2nd Annual Meeting at the European Tissue Engineering Society. 3-6 Sept, 2003, Genoa, Italy.

2. M. Ellis, **M.L. Yeow**, H. Shearer, K. Li, J. Beresford and J. Chaudhuria. "A Novel Biodegradable Scaffold To Minimise Mass Transfer Limitations In Tissue Culture To Aid Healing of Non-Union Bone Injuries" (Paper presented at the Tissue and Cell Engineering Society Conference, 8-10 Sept, 2003, Cardiff, UK.